INTEGRATED MODELLING OF GLOBAL CHANGE IMPACTS IN THE GERMAN ELBE RIVER BASIN

Dissertation

zur Erlangung des akademischen Grades
doctor rerum naturalium (Dr. rer. nat.)
in der Wissenschaftsdisziplin Geoökologie

eingereicht an der
Mathematisch-Naturwissenschaftlichen Fakultät
der Universität Potsdam

durch Dipl.-Geoökol. Fred Fokko Hattermann

September 2005

Gutachter:

1. Gutachter: Prof. Dr. Axel Bronstert (Universität Potsdam)
2. Gutachter: Prof. Dr. Nicola Fohrer (Universität Kiel)
3. Gutachter: Dr. Valentina Krysanova (Potsdam Institut für Klimafolgenforschung)

Danksagung

An dieser Stelle möchte ich insbesondere Valentina Krysanova danken, der Hauptbetreuerin meiner Arbeit, die die Idee zu dieser Studie hatte und mich während meiner Tätigkeit immer mit großem Interesse unterstützte. Ohne Ihre umfassende Unterstützung und fachliche Begeleitung wäre diese Arbeit nicht möglich gewesen.

Weiter gilt mein Dank Axel Bronstert, der mir mit fachlichem und freundschaftlichem Rat immer zur Seite stand und unbürokratisch die Betreuung meiner Arbeit an der Universität übernahm.

Mein Dank gilt auch Nicola Fohrer, die, wenn auch aus der Ferne, meinen "wissenschaftlichen Werdegang" von Anfang an begleitete.

Danken möchte ich Frank Wechsung, der immer für eine interessante Diskussion zu haben war.

Weiter möchte ich meinen Kollegen am Potsdam Institut für Klimafolgenforschung danken, ohne die die Arbeit in dieser Form nicht entstanden wäre.

Wolfgang Cramer möchte ich für seine Unterstützung und seinen freundschaftlichen Rat danken, Alfred Becker für die schönen Stunden im Büro und auf den Dienstreisen.

Alison Schlums und Stephen Sitch danke ich für die Korrekturen und Anregungen.

Nicht zuletzt sondern vor allen Dingen gilt mein Dank meinen Eltern und Claudia, die mir mit nie nachlassender Geduld immer liebevoll zur Seite standen.

Summary

The scope of this study is to investigate the environmental change in the German part of the Elbe river basin, whereby the focus is on two water related problems: having too little water and having water of poor quality.

The Elbe region is representative of humid to semi-humid landscapes in central Europe, where water availability during the summer season is the limiting factor for plant growth and crop yields, especially in the loess areas, where the annual precipitation is lower than 500 mm. It is most likely that water quantity problems will accelerate in future, because both the observed and the projected climate trend show an increase in temperature and a decrease in annual precipitation, especially in the summer. Another problem is nutrient pollution of rivers and lakes. In the early 1990s, the Elbe was one of the most heavily polluted rivers in Europe. Even though nutrient emissions from point sources have notably decreased in the basin due to reduction of industrial sources and introduction of new and improved sewage treatment facilities, the diffuse sources of pollution are still not sufficiently controlled.

The investigations have been done using the eco-hydrological model SWIM (Soil and Water Integrated Model), which has been embedded in a model framework of climate and agro-economic models. A global scenario of climate and agro-economic change has been regionalized to generate transient climate forcing data and land use boundary conditions for the model. The model was used to transform the climate and land use changes into altered evapotranspiration, groundwater recharge, crop yields and river discharge, and to investigate the development of water quality in the river basin. Particular emphasis was given to assessing the significance of the impacts on the hydrology, taking into account in the analysis the inherent uncertainty of the regional climate change as well as the uncertainty in the results of the model.

The average trend of the regional climate change scenario indicates a decrease in mean annual precipitation up to 2055 of about 1.5 %, but with high uncertainty (covering the range from -15.3 % to +14.8 %), and a less uncertain increase in temperature of approximately 1.4 K. The relatively small change in precipitation in conjunction with the change in temperature leads to severe impacts on groundwater recharge and river flow. Increasing temperature induces longer vegetation periods, and the seasonality of the flow regime changes towards longer low flow

spells in summer. As a results the water availability will decrease on average of the scenario simulations by approximately 15 %. The increase in temperatures will improve the growth conditions for temperature limited crops like maize. The uncertainty of the climate trend is particularly high in regions where the change is the highest.

The simulation results for the Nuthe subbasin of the Elbe indicate that retention processes in groundwater, wetlands and riparian zones have a high potential to reduce the nitrate concentrations of rivers and lakes in the basin, because they are located at the interface between catchment area and surface water bodies, where they are controlling the diffuse nutrient inputs. The relatively high retention of nitrate in the Nuthe basin is due to the long residence time of water in the subsurface (about 40 years), with good conditions for denitrification, and due to nitrate retention and plant uptake in wetlands and riparian zones.

The concluding result of the study is that the natural environment and communities in parts of Central Europe will have considerably lower water resources under scenario conditions. The water quality will improve, but due to the long residence time of water and nutrients in the subsurface, this improvement will be slower in areas where the conditions for nutrient turn-over in the subsurface are poor.

Zusammenfassung

Ziel der vorliegenden Arbeit ist die Untersuchung der Auswirkungen des Globalen Wandels auf den Wasserkreislauf im deutschen Teil des Elbeeinzugsgebietes. Der Fokus liegt dabei auf Wassermengen- und Wasserqualitätsproblemen.

Die Elbe liegt im Zentrum Europas im Übergangsbereich zwischen ozeanischen und kontinentalen Klimaten, wo die Wasserverfügbarkeit in den Sommermonaten den limitierenden Faktor für das Pflanzenwachstum und die landwirtschaftlichen Erträge bildet. Dies gilt insbesondere für die Lössgebiete im Lee des Harzes, wo die jährlichen Niederschläge unter 500 mm liegen. Es ist sehr wahrscheinlich, dass sich die Wassermengenprobleme in Zukunft noch verstärken werden, denn sowohl das beobachtete als auch das für die Zukunft projizierte Klima in der Region zeigen höhere Temperaturen und fallende Niederschläge, besonders im Sommer. Ein weiteres Problem ist die hohe Nährstoffbelastung der Flüsse und Seen im Elbeeinzugsgebiet. Anfang der neunziger Jahre war die Elbe eine der am stärksten belasteten Flüsse in Europa. Obwohl die Einträge besonders aus Punktquellen durch den Rückgang der Industrie und den Bau von neuen Kläranlagen seitdem gefallen sind, gelangen trotzdem noch große Nährstoffmengen aus diffusen Quellen in die Gewässer.

Die Untersuchungen wurden unter Anwendung des ökohydrologischen Modells SWIM (Soil and Water Integrated Model) durchgeführt, welches über Schnittstellen mit Klimamodellen und agroökonomischen Modellen verbunden wurde. Ein globales Szenario des Klimawandels und des landwirtschaftlichen Wandels wurde regionalisiert, um so die geänderten Randbedingungen für den Szenarienzeitraum zu erhalten. Simulationen mit SWIM dienten dann dazu, die geänderten Randbedingungen in Änderungen im Wasserhaushalt und in den landwirtschaftlichen Erträgen zu transformieren. Außerdem wurde das Langzeitverhalten von Nährstoffen im Untersuchungsgebiet modelliert. Besonderer Wert wurde dabei darauf gelegt, die Unsicherheit der Szenarienergebnisse zu quantifizieren.

Der mittlere Szenarientrend zeigt eine Reduzierung der mittleren jährlichen Niederschläge bis zum Jahre 2055 um ungefähr 1.5 %, wobei die Ergebnisse mit einer großen Unsicherheit behaftet sind: die Spannweite der Niederschläge in den Szenarienrealisationen liegt zwischen -15.3 % und +14.8 %. Die Erwärmung unter Szenarienbedingungen mit ungefähr 1.4 K ist weniger unsicher. Diese relativ geringen Änderungen habe starke Auswirkungen auf den Wasserhaushalt im El-

begebiet: durch die steigenden Temperaturen wird die Vegetationszeit verlängert, und die Niedrigabflussperiode im Sommer wird sich in den Herbst ausdehnen. Insgesamt wird unter dem mittleren Szenarientrend die Wasserverfügbarkeit um ca. 15 % abnehmen. Außerdem werden sich durch die steigenden Temperaturen die Anbaubedingungen für wärmeliebende Ackerfrüchte in der Landwirtschaft verbessern. Die Unsicherheit des Klimatrends ist dort am größten, wo auch die lokalen Änderungen am größten sind.

Die Simulationsergebnisse für das Nuthe-Teileinzugsgebiet der Elbe zeigen, das Retentionsprozesse im Untergrund und in den Feucht- und Auengebieten einen starken Einfluss auf die Wasserqualität und die Nitratkonzentration der Oberflächengewässer haben, da sie durch ihre Lage im Einzugsgebiet eine Schnittstelle zwischen dem umliegenden Einzugsgebiet und den Flüssen und Seen bilden. Die relativ hohe Umsetzung von Nitrat im Einzugsgebiet der Nuthe kann dadurch erklärt werden, dass Nitrat eine relativ lange Aufenthaltszeit im Grundwasser (im Mittel 40 Jahre) mit einer hohen Nitratumsetzungsrate hat, und durch die guten Denitrifizierungsbedingungen in den Feucht- und Auengebieten. Dazu kommt noch, dass große Nitratmengen durch die Pflanzen in den Feuchtgebieten aus dem Grundwasser aufgenommen werden.

Zusammenfassend kann man sagen, das sich die Ökosysteme und die Gesellschaft im Elbeeinzugsgebiet unter Szenarienbedingungen auf niedrigere Wasserverfügbarkeit einstellen müssen. Die Wasserqualität wird sich grundsätzlich zwar weiter verbessern, aber aufgrund der langen Verweilzeit der Nährstoffe im Grundwasser wird dies insbesondere in den Teileinzugsgebieten, in denen die geochemischen Bedingungen für einen hohen Nährstoffumsatz nicht gegeben sind, noch relativ lange dauern.

Contents

1 Introduction **1**

1.1 Integrated water resources management and river basin modeling 3

1.1.1 Why integrated water resources management? 3

1.1.2 Why integrated modeling? 4

1.1.3 Why river basins? 5

1.1.4 Why the Elbe river basin? 6

1.2 The Model 9

1.2.1 Spatial disaggregation 13

1.2.2 Hydrology 16

1.2.3 Vegetation 19

1.2.4 Nitrogen cycle 22

1.3 The Elbe river basin 26

1.3.1 Basin characteristics 26

1.3.2 Natural and socio-economic changes in the region 29

2 Runoff simulations on the macroscale with the eco-hydrological model SWIM in the Elbe catchment - validation and uncertainty analysis **35**

2.1 Introduction 36

2.2 Method and data 40

2.2.1 The model 40

2.2.2 The basin under study 43

2.2.3 Input data and data pre-processing 46

2.2.4 Modelling strategy 49

2.3 Results and discussion 50

2.3.1 Calibration using river discharge dynamics 50

2.3.2 Spatial validation using water table dynamics 55

2.3.3 Validation for meso- and macroscale catchments 56

2.4 Sensitivity and uncertainty analysis 57

2.4.1 Sensitivity analysis 58

2.4.2 Uncertainty analysis 60

2.5 Summary and conclusions 63

3 Integrating groundwater dynamics in regional hydrological modeling 65
3.1 Introduction . . . 66
3.2 Method and data . . . 69
3.2.1 The Model . . . 69
3.2.2 Description of the study area and the data . . . 75
3.2.3 Modeling procedure . . . 77
3.3 Results and discussion . . . 78
3.3.1 Model comparison . . . 78
3.3.2 River discharge . . . 80
3.3.3 Water table dynamics . . . 82
3.3.4 Water table trends in the north-eastern lowland of the Elbe basin . . . 85
3.4 Summary and conclusions . . . 89

4 Integrating wetlands and riparian zones in river basin modeling 91
4.1 Introduction . . . 92
4.2 Material and methods . . . 95
4.2.1 The study area and data . . . 95
4.2.2 The model SWIM . . . 98
4.2.3 Model extensions . . . 100
4.3 Results and discussion . . . 108
4.3.1 Hydrology . . . 108
4.3.2 Nitrogen dynamics . . . 112
4.4 Conclusions . . . 117

5 Assessing uncertainty of water availability in a Central European river basin (Elbe) under climate change 119
5.1 Introduction . . . 120
5.2 Material and methods . . . 124
5.2.1 The modeling strategy . . . 124
5.2.2 The SWIM model . . . 127
5.2.3 The basin under study . . . 129
5.2.4 Input data and data pre-processing . . . 131
5.3 Results and discussion . . . 133
5.3.1 Reference period . . . 133
5.3.2 Scenario period . . . 136
5.4 Summary and conclusions . . . 148

6 Summary and key findings 151
6.1 Validation of the SWIM model for hydrological processes at the macroscale . . . 153
6.2 Implementation of groundwater dynamics at the hydrotope level . 155

6.3 Integration of retention processes in groundwater, wetlands and riparian zones in the SWIM model 157
6.4 Assessing uncertainty of water availability and crop yields in a Central-European river basin under climate change 158

7 Discussion and conclusions **161**

Bibliography **171**

I Appendix **189**

List of Figures **IV**

List of Tables **VI**

II Appendix **VII**

A List of variables. **IX**

B Parameter distributions. **XIII**

C Land use classes. **XVII**

Chapter 1

Introduction

Long term observations have shown that climate and land use intensity are changing on historical time scales (IPCC, Part I, 2001). They are the two main boundary conditions influencing the water and matter balance of a landscape (Kabat et al., 2004). Model experiments and trends from long term observations indicate that the change in both mean climate and climate variability will accelerate in the near future. Increasing climate variability and higher temperatures may lead to an intensification of the hydrological cycle in terms of evapotranspiration and rainfall (IPCC, Part I, 2001). In some regions an increase in magnitudes and frequencies of extreme events are already being observed (Kabat et al., 2002). The vulnerability of certain regions and communities to changes in the hydrological cycle will rise as a consequence of climate change, and foresight management practices will be needed to cope with and to adapt to these changes (IPCC, Part II, 2001). In many parts of the world, water demand is increasing, while concurrently the availability and quality of water resources are decreasing, mainly due to human activities in connection with the growing population, ongoing urbanization, industrialization and the intensification of agriculture. This is often associated with general reductions in environmental quality and it endangers sustainable development (Kabat et al., 2002).

Integrated approaches are required to identify and analyze such unfavorable and undesirable developments to allow sustainable systems to be designed that integrate human society with its natural environment for the benefit of both. One possible adaptation to Global Change is sustainable land and water use and management to mitigate the impacts of the altering boundary conditions (Fohrer,

2002). It is therefore vital to investigate the impacts of climate and land use changes on the water and nutrient balance and to find alternative management options. The basis of such investigations has to be the understanding of historical trends and developments and their impact on the environment (see Krysanova et al., 2005b; Habets et al., 1999a).

Modeling studies generally consider the impacts of either climate or land use changes on the water cycle of a certain region, rarely do they consider both in an integrated model framework. Typically hydrological models do not integrate other important features like vegetation and nutrients, and even when the combined effect of changes in climate and land use are included, interactions and feedbacks are usually not considered (Varis et al., 2004). However, a change in climate will most likely also have an impact on land cover (especially vegetation, Bronstert et al., 2005). Bronstert (2004) discusses the new challenges in hydrological modeling in the context of climate and land use changes, which are summarized in the following four points:

1. The standard calibration methods of hydrological models need to be adjusted or extended to have an adequate representation of altered internal dynamics of the hydrological system if the boundary conditions change. The calibration process should be multi-criteria and multi-site.

2. The development of the scenario of changed boundary conditions should be done considering feedbacks to derive consistent scenarios for land use and climate changes.

3. The uncertainty related to input data, parameters and model processes has to be quantified and, what is new, also the uncertainty in the scenario conditions should be estimated.

4. It is necessary and important to adjust the climate or land use scenarios for extremes such as floods or droughts.

In adopting these challenges, this study aims:

- to improve our understanding of eco-hydrological processes in meso- to macroscale river basins under climate and land use change,

- to find conceptual solutions to describe the relevant processes in a single model framework, and based on it

- to estimate the combined impacts of changing climate and land use on water and nutrient fluxes in a large scale river basin considering the uncertainty of the input data and model parameters.

To fulfill the requirements of integrated river basin modeling at the macro- scale, a first step is to validate the model SWIM (Soil and Water Integrated Model, Krysanova et al., 1998) for the hydrological processes of the Elbe basin. To achieve this SWIM was applied over nested sub-basins typical of the main sub-regions in the Elbe basin. New methods for climate data interpolation, model validation, sensitivity and uncertainty analyzes were developed and implemented. An important finding was that water and nutrient retention processes are particularly important in lowlands and especially in wetlands and riparian zones. After implementation of new model descriptions for wetland processes and the development of special interfaces to climate and agro-economic models, the final step was to apply the validated model over the entire German part of the Elbe basin to assess the possible impacts of Global Change.

1.1 Integrated water resources management and river basin modeling

1.1.1 Why integrated water resources management?

Changes in precipitation and its intensity resulting in severe droughts and disastrous floods and increasing contamination of surface water bodies and groundwater have raised the awareness of the public to environmental change (Kundzewicz et al., 2002). Water is essential for human food production and water supply, for industrial and energy production, fishing and river navigation. Ecosystems are uniquely adapted to the water cycle of river basins, and land use and climate changes may lead to often unfavorable changes in ecosystem structure (Kabat et al., 2002). However, river basins are very complex systems formed and influenced by many different land and water users (natural and anthropogenic), and it is often difficult to trace back changes in the water cycle to one single measure or intervention. Observed trends are often the result of a variety of interacting measures and interventions. Climate change represents only one such intervention. In most parts of the world, the environmental character of catchments, their veg-

etation and soil patterns, water bodies and flow regime, have been significantly altered by humans with their regionally-specific water and land use management (see Chapter 1.3.2).

The complexity of the problem makes it necessary to consider all different land and water users in a river basin using an integrated approach, taking into account dependencies and feedbacks (Bronstert et al., 2005). This is the core of integrated water resources management (IWRM), which tries to consider the catchment and its different users as a whole, where interventions in the water cycle will most likely affect all user, especially those downstream. According to van Beek et al. (2002), IWRM is the encompassing paradigm for adaptation to contemporary climate variability, and it is the prerequisite for coping with the still uncertain consequences of global warming and other related changes in climate and their repercussions on the water cycle. In accordance with recent understanding, IWRM has been defined by the Technical Advisory Committee of the Global Water Partnership as follows (TAC, 2000):

"IWRM is a process, which promotes the co-ordinated development and management of water, land and related resources, in order to maximize the resultant economic and social welfare in an equitable manner without compromising the sustainability of vital ecosystems."

One of the earliest attempts to define an appropriate methodology for integrated river basin management is the scheme of Driving forces - Pressures - States - Impacts - Responses (DPSIR) as suggested by the European Environment Agency (OECD, 1994; UNCSD, 1996). The scheme describes a natural system subject to anthropogenic pressure, where the driving forces (e.g. land use, climate) generate a pressure (e.g. global change, land use change) on the system (the river basin), thus altering the state of the system (e.g. from oligotrophic to eutrophic conditions). This alteration represents an impact, i.e., an effect upon the environment and society, for example a decrease in water availability or quality. When this affects society in an unfavorable way, society reacts by devising and implementing responses (e.g. adapted water and land use management) that can target either the drivers, the pressures or the state so that undesired or threatening impacts are avoided or compensated (Soncini-Sessa, 2004).

1.1.2 Why integrated modeling?

The complexity of integrated water resources management makes it necessary to have a model representation of the internal system dynamics in a river basin, which is able to reproduce the state of a river basin, the pressures generated by driving forces and the impacts induced by changes in these driving forces (Bronstert, 2004).

In the past, much of the emphasis in IWRM and therefore also in integrated river basin modeling has been on predicting the impacts of anticipated changes like land use and water management (Cuddy and Gandolfi, 2004). These pressures on the river system are often referred to as 'internal boundary conditions' and can be controlled and adapted to a certain extend by the local people (users). Over the last decade, public awareness for possible changes in climate and their impacts on the water cycle has grown. These pressures are often referred to as external boundary conditions and are not under the control of the local people. Here, models can support decision makers working in environmental or water management agencies to find solutions for sustainable use of water resources under changing boundary conditions (Varis et al., 2004). Models allow to investigate and test in a cost effective way different planning alternatives, which target the management problem. In recent times, the growing use of integrated catchment models has facilitated discussions and consultation between the various stakeholders in integrated water resources management. Whereas the traditional investigation of impacts focused on more technical indicators like river flow and water quality, today a more open approach to river basin management is taken which also considers the human dimension of the impacts in a participatory way (Pahl-Wostl, 2005).

1.1.3 Why river basins?

Varis et al. (2004) point out that integrated river basin modeling at the regional scale is the most challenging field in climate change research. The most important driving forces of climate change are located at the regional level, where also political decisions and technical measures to adapt to climate change take place.

The river basin is a very suitable spatial unit to investigate impacts of environmental changes because it allows balancing the water and matter fluxes over

entire landscapes (Krysanova et al., 2005b). Natural boundaries of watersheds (considered as a semi-closed system) integrate practically all natural water and biogeochemical fluxes in their catchment area, and thus can be used by the modeler to validate simulation results against observed data at the basin outlet. In addition, water and nutrient flows in rivers are very sensitive to climate variability and large scale changes in land use. Often only a small fraction of rainfall and of the fertilizers originally applied in a basin reach the surface water system; evapotranspiration, plant uptake and retention (translocation and transformation) count for the rest. As a result, relatively small changes in inputs (precipitation, fertilizers) can lead to significant changes in outputs (river discharge and nutrient concentrations and loads), and observations at the basin outlet are accurate indicators for long term changes in climate and land use, which are altering the state of the river system. In addition, river basins combine all relevant environmental processes in a landscape, and therefore all these processes need to be taken into account to find management solutions for sustainable development in a certain region (Fohrer, 2002).

1.1.4 Why the Elbe river basin?

The Elbe river basin was selected because it combines many different aspects, which are of interest to the scientific community as well as for the people living in river basin. Some important hydrological characteristics of the basin and challenges for scientists are:

- The Elbe basin is located in Central Europe at the transition zone between marine and continental climates, with annual precipitation between 900 mm a^{-1} in the northwest and 500 mm a^{-1} in the central part of the basin (see Figure 1.1a).

- The annual per capita water availability is only 680 m^3 a^{-1} in the Elbe catchment (and only 280 m^3 a^{-1} in the Spree subbasin), which is the second lowest of the large rivers basins in Central Europe (in comparison, the Rhine basin and the German Danube basin have rates of 1370 m^3 a^{-1} and 4300 m^3 a^{-1}, (see Stanners and Bourdeau, 1995). As a result, only small changes in land use, water management and in climate variables have large

impacts on the water availability in the catchment, and therefore the Elbe river basin is likely to be highly sensitive to any future changes in climate.

- Recent trends in precipitation differ markedly over large areas within the basin from the anticipated global trend with a decreasing trend in annual precipitation across the central part of the basin (Gerstengarbe and Werner, 2005) (see Figure 1.1b).

- Large parts of the Elbe basin are located in lowland areas having shallow groundwater, and the specific hydrological processes in riparian zones and wetlands are very important for the water and nutrient cycle in the catchment. Until now such processes have either been ignored or are considered secondary in most recent hydrological models.

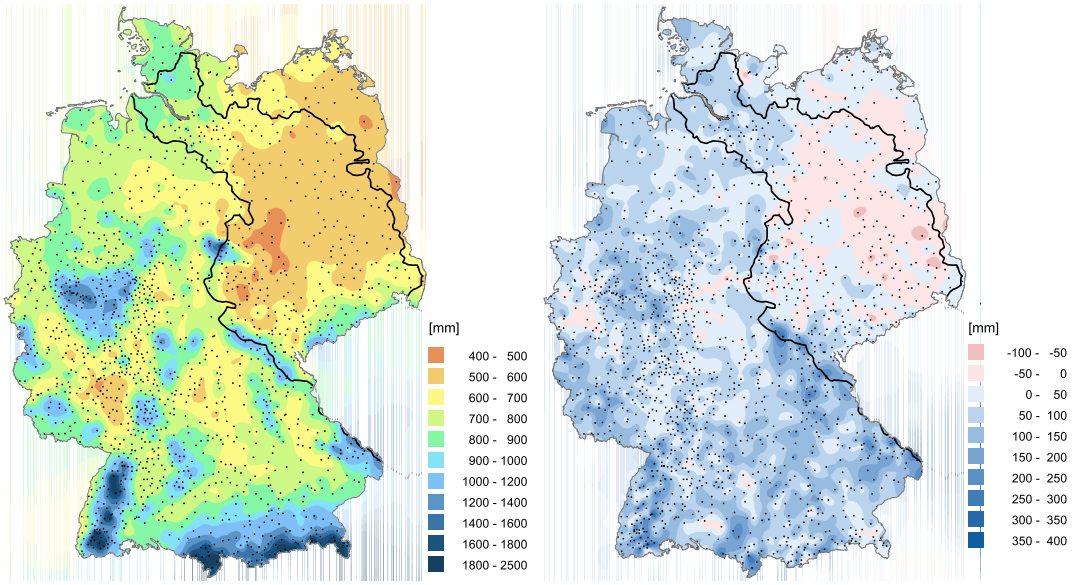

(a) Precipitation (b) Trend

Figure 1.1. Average precipitation 1951-2003 and trend in precipitation 1951-2003 (in black the borders of the German part of the Elbe basin).

The largest part of the catchment area is located in the Czech Republic and in the former German Democratic Republic. Political changes and their influence on land use and water management during the last decades as well as their impacts on water quality and quantity can serve as an example for the possible changes which are ongoing or will take place in other East European countries

(Krysanova et al., 2005b). Examples are basin-wide implementation of improved sewage water treatment, changes in the intensity of agricultural management and climate change.

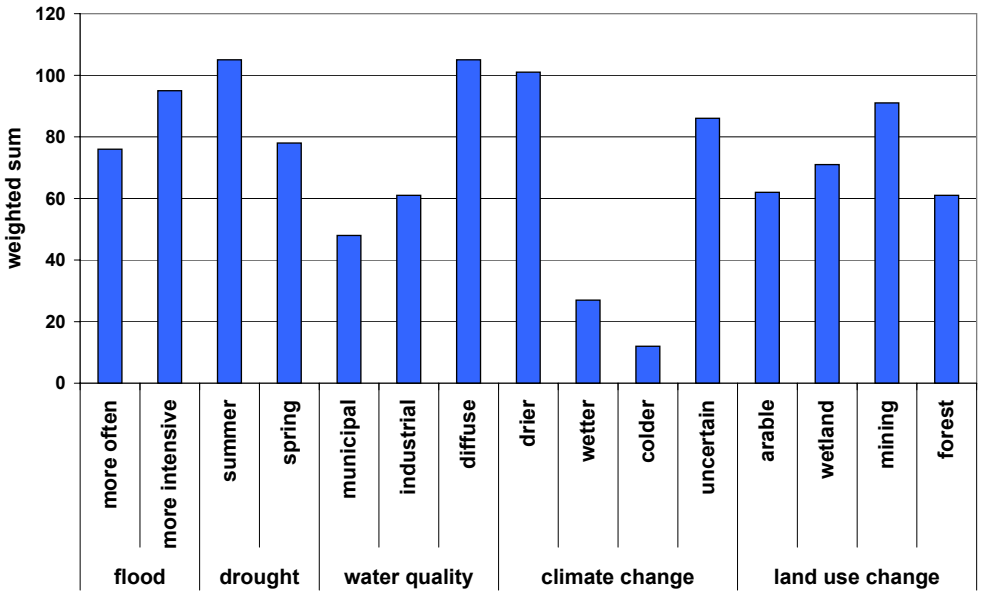

Figure 1.2. Result of a questionnaire compiled in the framework of the German GLOWA Elbe project (Wechsung et al., 2005a) and the EC NEWATER project (Pahl-Wostl et al., 2005). The answers have been weighted according to the importance indicated by the water experts.

Interestingly the people living in the Elbe basin are aware of the environmental change in the catchment: Figure 1.2 gives the result of a questionnaire, where in total 88 persons working in environmental agencies and private firms and involved in water and land use management affairs in the Elbe basin were asked their opinions on the main water related environmental problems in the catchment. They identified summer droughts, diffuse contamination of surface water bodies, followed by climate change (to drier conditions) and the increasing severity of flood events. Another problem associated with climate change to be taken seriously is the uncertainty in future climate variability. The need for scientific support to address the water related problems in the Elbe basin under environmental change is the motivation behind the choice of this basin for the study.

1.2 The Model

Over the last decades, many hydrological models with different degree of physical background have been developed, having different approaches to reproduce the spatial heterogeneity and the hydrological processes in a catchment. According to Bronstert (2003), these models can be classified into three main types: The first type are the so called lumped models (also "black box models"), where the spatial heterogeneity of the landscape is represented only by average characteristics, for example the lumped version of the HBV model (Bergström, 1995). They operate with a minimum of functions, which describe the response of a variable of interest (e.g. of river flow) to a driver (e.g. precipitation). The advantage of the lumped conceptual models is that they are easy to apply at different scales with only a minimum of input data. However, the reliability and transferability of these models is restricted due to the fact that the physical background of the model formulations is limited (Krysanova et al., 1999a).

The second type are fully spatially-distributed physically based models. Examples are the SHE model family (Refsgaard and Storm, 1995) and more sectoral models like groundwater models (Kinzelbach and Rausch, 1995), where the processes of each element (often grid cells) of the landscape are influenced by the processes of the neighboring elements. The advantage of these models (provided that all input data are available) is that they allow to reproduce the lateral flow and transport processes in a river basin from spatial element to spatial element and therefore to consider feedbacks if the physical status of the neighboring element changes. Their disadvantage is the large data demand to identify the model parameter structure and the high computation time to solve the non-linear equations numerically for each single model element. Therefore, they are mostly applied at the plot scale, in small scale watersheds or at hill-slopes, where data support is sufficient, or in benchmarking experiments to compare their model performance against the results of simpler models (see Chapter 3.3.1, Hattermann et al., 2004).

SWIM (Soil and Water Integrated Model, Krysanova et al., 1998) belongs to the third type of hydrological models, to the so called hydrological models of intermediate complexity (HYMIC, Bronstert, 2003), sometimes also called process oriented models, where physically based formulations to describe the variables are combined with more empirical approaches to provide essential input infor-

mation. SWIM is based on two previously developed models, SWAT (Soil and Water Assessment Tool, Arnold et al., 1993, 1994) and MATSALU (Krysanova and Luik, 1989; Krysanova et al., 1989). The hydrological module (see Chapter 1.2.2) and the vegetation module (Chapter 1.2.3) are basically the same as in SWAT, the nitrogen module has been taken from the model MATSALU (Chapter 1.2.4, Krysanova and Luik, 1989; Krysanova et al., 1989). The model history of SWIM and the major differences to SWAT are described in Krysanova et al. (2005a). Figure 1.3 gives a summary of the processes at the hydrotope level and their integration in the model and the feedbacks, and Figures 1.6, 1.7 and 1.8 show these processes in more detail.

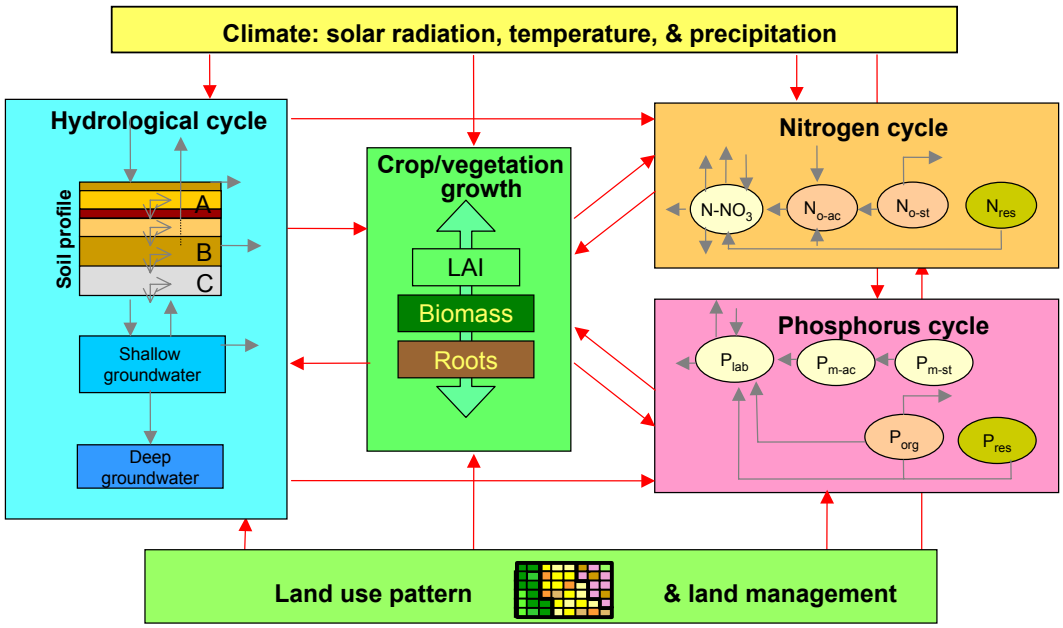

Figure 1.3. Processes included in the model SWIM on the hydrotope level and the feedbacks ($N_{o\text{-}ac}$ = active organic N, $N_{o\text{-}st}$ = stable organic N, N_{res} = fresh organic N, P_{lab} = labile P, $P_{m\text{-}ac}$ = active mineral P, $P_{m\text{-}st}$ = stable mineral P, P_{org} = organic P, P_{res} = fresh organic P).

SWIM is a continuous-time semi-distributed watershed model, which integrates hydrological processes, vegetation, erosion and nutrient dynamics at the river basin scale (Krysanova et al., 1998, 2000). The combination of empirical and physically based descriptions in one model code allows to apply the model on a daily time step at the regional scale, considering the spatial heterogeneity of the landscape and possible feedbacks between vegetation, hydrological processes

and nutrient transport and retention (see Figure 1.3). According to Bronstert et al. (2005) (page 173), these feedbacks are the most important in hydrological modeling of environmental changes. The hydrological cycle influences practically all other processes in SWIM (vegetation growth, nutrient cycling and transport), whereas vegetation has also a strong feedback on the hydrological processes (e.g. evapotranspiration, see Equation 1.12) and nutrient uptake (see Chapter 1.2.3).

Another advantage of the SWIM model is that the model code, written in the FORTRAN programming language, is publicly available and can easily be modified or extended to incorporate new modules as required. An interface implemented in the GRASS Geo-information System (GIS) supports the data pre-processing (Dassau, 2005).

SWIM was chosen for this study, because it integrates the hydrological and plant growth processes relevant for the integrated investigation of global change impacts, and has a spatial disaggregation scheme which allows to incorporate and analyze different land use and water management strategies. During this study, the model was extended to adapt it to the specific environmental characteristics of the Elbe river basin, and to allow its application at the macroscale in the integrated framework of the GLOWA Elbe project (Wechsung et al., 2005a). The main developments in the framework of this work are:

- Implementation of a methodology for sensitivity and uncertainty investigations (Hattermann et al., 2005a,b, see Chapters 2.4 and 4.3) to estimate the reliability of the simulation results.

- Interfaces to regional climate and land use models, whereby new methods for climate data interpolation and crop rotation were developed and implemented (Hattermann et al., 2005c in Chapter 5.2.1, and Wechsung et al., 2005b). They allow to regionalize the climate information from the 369 weather stations and land use information of the 112 counties located in and around the border of the German part of the Elbe basin.

- Implementation of daily groundwater table dynamics (Hattermann et al., 2004, Chapter 3.2.1) at the level of hydrological response units (the so called hydrotopes, see the next Chapter) in order to model the hydrological characteristics of wetlands and their interaction with groundwater in the model run.

- Implementation of water and nutrient retention processes in groundwater, wetlands and riparian zones (Hattermann et al., 2005b, Chapter 4.2.3) to estimate the buffering effects of these areas for water quality and quantity.

An important goal has been to adapt the model developments for application in macroscale basins with commonly available data.

The model extensions listed above have been introduced to overcome some shortcomings of the model, which are relevant for the modeling task of this thesis. Other, which were not particularly important for the objectives of this work are:

- The SWIM model was not designed to investigate flood events. The model simulates on a daily time step, and some processes, especially those which are important for flood generation (like surface flow generation), are represented in the model by conceptual formulations (for example the curve number method, see Equation 1.2), because the physical approaches (e.g. the Green-Ampt method, see Maidment, 1993) would require a much shorter time step, and, as a result, the computation time would increase. The use of the conceptual approaches in combination with the physical ones in this thesis is justified by the fact that it aimed at the investigation of the long-term changes of the water balance and crop yields in the Elbe basin, and not at the investigation of short-term events like floods.

- The hydrotope concept discussed in the next chapter guarantees a spatial resolution of the modeling results (e.g. evapotranspiration, groundwater recharge), which corresponds to the resolution of the spatial input data (the hydrotope level). However, this is only true for the vertical flows. The model concept, where lateral flows are calculated using retention functions, does not allow to follow lateral flows in form of a "particle tracking" (Kinzelbach and Rausch, 1995). The model extensions discussed in Chapter 4.2.3 (Hattermann et al., 2005b) have been introduced to overcome this bottleneck.

- Climate and the hydrological cycle have only a one-way coupling, with climate being the most important driver for the hydrological processes. The impact of the local hydrological status (especially of soil moisture) on the local climate can also be important (Bronstert et al., 2005) and is subject of intensive investigations (Kabat et al., 2004). However, the influence of

hydrological processes and land cover on climate was not the scope of this study.

A full description of the basic version of the model can be found in Krysanova et al. (1998, 2000). An extensive hydrological validation of the model in the Elbe basin including sensitivity and uncertainty analysis of the hydrological processes in the main subregions of the Elbe basin is described in Hattermann et al. (2005a). A brief introduction to the basic model components is given in the following sections. This gives the reader a comprehensive overview of the main model modules and the regionalization concept. The descriptions of the model extensions are presented in the papers (Chapters 2, 3, 4 and 5).

1.2.1 Spatial disaggregation

River basins are a composite of many different geographical features, which are influencing the water and nutrient balance of a landscape (Becker and Braun, 1999).

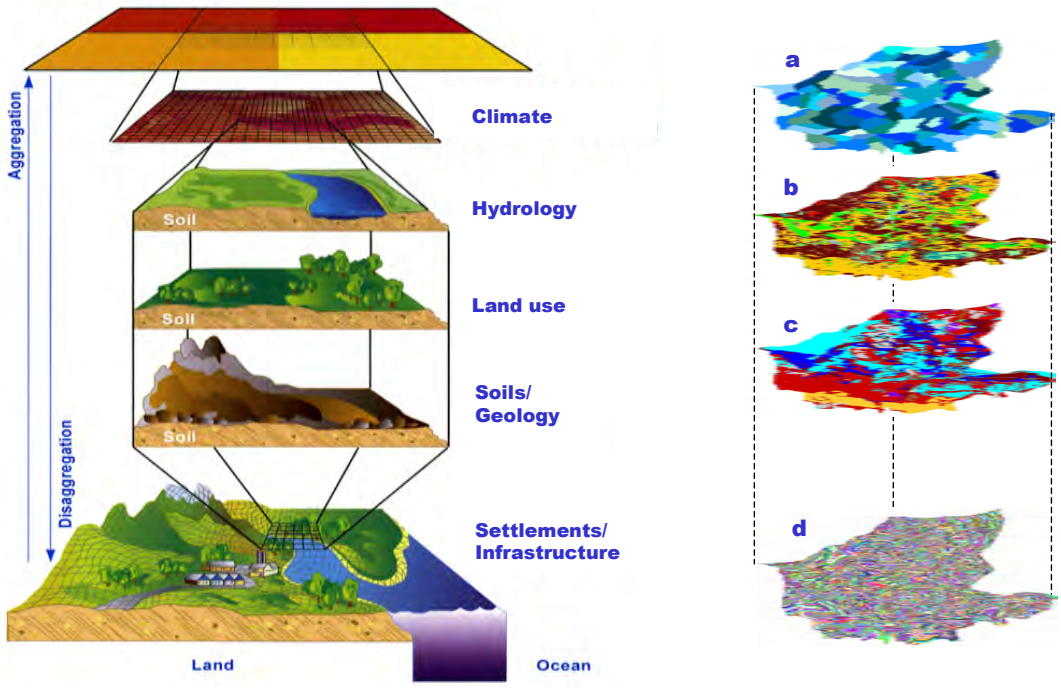

Figure 1.4. Left: aggregation, disaggregation and layers of information in hydrological modeling (Viner and Hume 1997, changed). Right: disaggregation in SWIM: different layers of information are combined to derive hydrological response units (hydrotopes) (a: subbasins, b: landuse, c: soils, d: hydrotopes).

The most important are the topography (e.g. altitude, slope), vegetation (e.g. leaf area index, biomass and root depth), soils (e.g. permeability, fertility), geology (e.g. porosity, hydro-chemical conditions) and land use pattern (e.g. land cover, fertilizer application, surface roughness). Because of their importance for the local water and nutrient cycle, these features have to be represented in the model description of the river basin, if the aim of the study is to investigate environmental changes in a catchment.

Figure 1.4 summarizes the most important layers of information, which are generally needed to mirror the spatial heterogeneity of a landscape in a hydrological model.

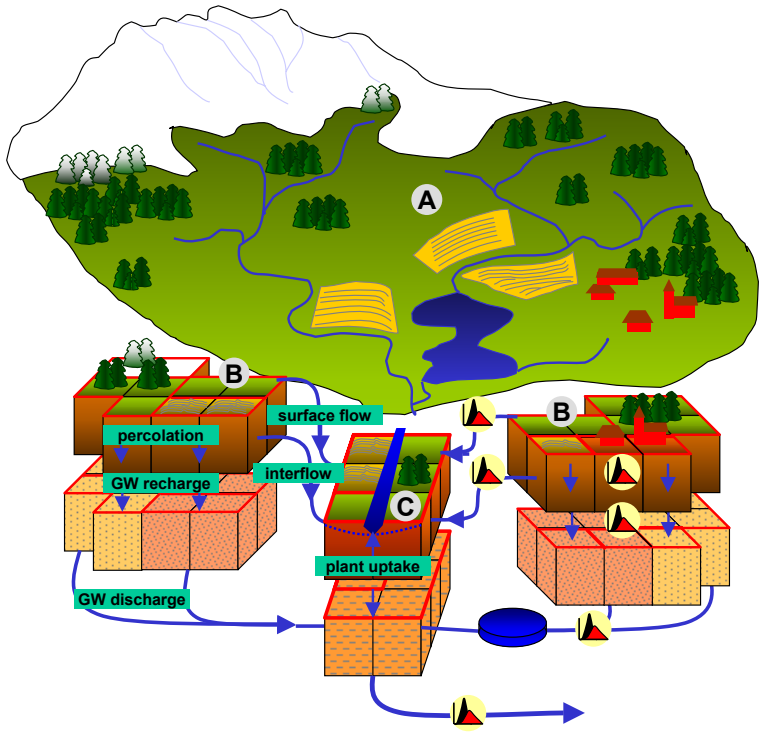

Figure 1.5. Flow generation processes considered in SWIM. The vertical flows at the hydrotope level (B) are aggregated at the subbasin level (A), with the wetlands and riparian zones of the extended model as an interface between catchment area and surface water bodies (C). Black lines delineate grid elements (the basic spatial information), which are aggregated to hydrotopes (red lines).

A three-level scheme of lateral spatial disaggregation from basin to subbasins and to hydrotopes is used, whereby the hydrotopes form the finest disaggregation level. A hydrotope in SWIM is a set of elementary units, which have the same

geographical features like land use and soil type, and which belong to the same subbasin (Figure 1.4). Therefore, it can be assumed that they behave in a hydrologically uniform way. If necessary, it is also possible to apply the hydrotopes as spatially explicit (this can be important for lateral flow processes or for coupling with other models). Hydrotopes are delineated using GIS by overlaying the corresponding spatial map layers (Figure 1.4). The spatial scale of the map with the finest resolution determines the spatial heterogeneity which is represented in the hydrotopes and therefore also in the model description of the river basin.

The flow generation processes which are considered in SWIM are illustrated in Figure 1.5. Water fluxes, plant growth and nitrogen dynamics are calculated for every hydrotope, where up to 10 vertical soil layers can be considered. Soil water and nutrients reach the groundwater surface after percolation through the unsaturated geological layers between soil and groundwater table, whereby a delay function controls the timing of the recharge. Fast lateral flow components in the model framework are surface flow and interflow. A slow lateral flow component is formed by groundwater discharge, due to the normally low hydraulic transmissivity of the aquifer sediments. Lakes are a special form of hydrotopes, where the actual evapotranspiration reaches the potential evapotranspiration. In the extend model, wetlands and riparian zones form an interface between catchment area and rivers and lakes (Chapter 4.2.3, Hattermann et al., 2005b). After reaching the river system, lateral fluxes of water and nutrients are routed over the river network, taking transmission losses into account. The subbasin borders used in the model applications are defined using the GIS GRASS and the digital elevation model DEM), or provided by the local authorities.

1.2.2 Hydrology

The validation of the hydrological processes in a river basin is the fundamental first step of model applications of the SWIM model, because nearly all other processes in SWIM, such as vegetation growth and nutrient transport, are controlled by or connected to water flow and availability (see Figure 1.3). The simulated hydrological system is schematically illustrated in Figure 1.6. It is, with some minor differences, identical to the one of the SWAT model.

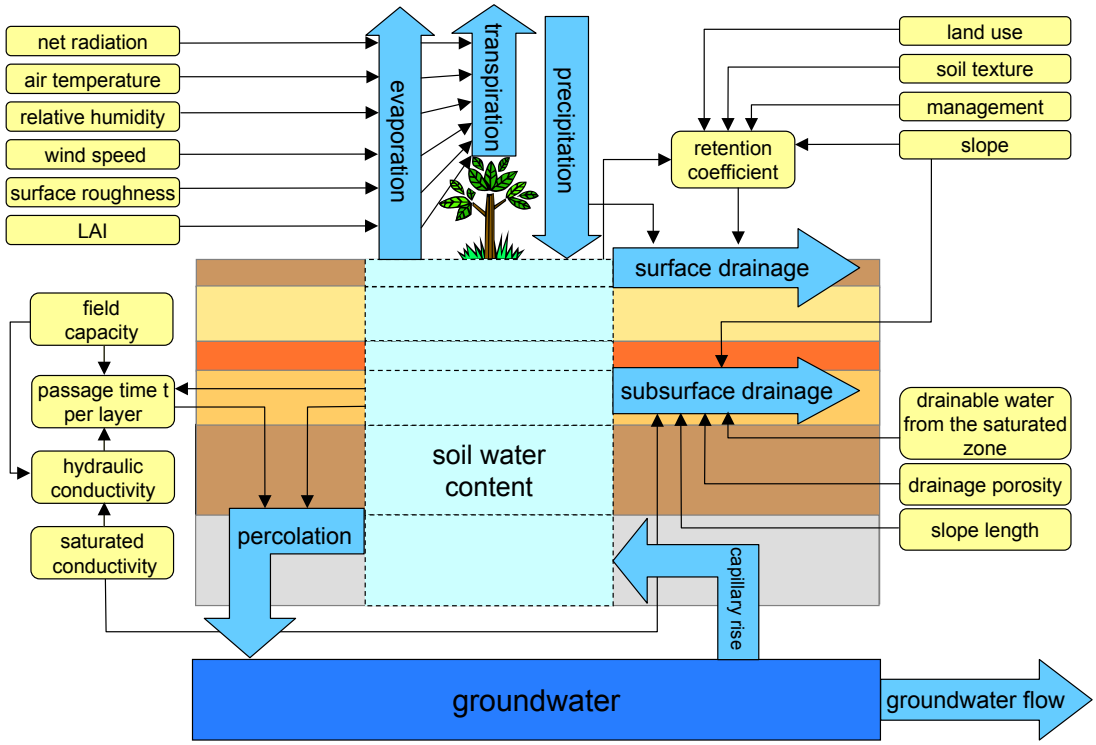

Figure 1.6. The hydrological processes (blue) of the model SWIM including the parameter demand (yellow). These parameters are partly taken from tables and partly calculated by the model (e.g. passage time per soil layer and hydraulic conductivity.)

The Priestley and Taylor (1972) method is used to estimate the potential evapotranspiration E_P $[mm\ d^{-1}]$, where only net radiation R_a $[MJ\ m^{-2}]$ and air temperature are needed as inputs at time step t:

$$E_{P_t} = 1.28 \cdot \left(\frac{R_{a_t}}{H_t}\right) \cdot \left(\frac{\delta}{\delta + \gamma}\right). \tag{1.1}$$

The latent heat of vaporization H $[MJ\ kg^{-1}]$ is calculated as a function of the mean daily air temperature, δ is the slope of the saturated vapor pressure $[kPa\ K^{-1}]$ and γ the psychrometer constant $[kPa\ K^{-1}]$. Soil evaporation and plant transpiration are calculated using the approach of Ritchie (1972), where they are functions of the dynamic leaf area index LAI (see Equations 1.13 and 1.14).

Surface runoff is calculated using a modification of the Soil Conservation Service (SCS) curve number technique (Arnold, 1990; King et al., 1999), where daily surface runoff Q $[mm\ d^{-1}]$ at time step t is estimated from daily precipitation P $[mm\ d^{-1}]$ taking into account a dynamic retention coefficient S_X by using the SCS curve number equation:

$$Q_t = \frac{(P_t - 0.2 \cdot S_X)^2}{P_t + 0.8 \cdot S_X} \qquad P > 0.2 \cdot S_X, \tag{1.2}$$

$$Q_t = 0 \qquad P \leq 0.2 \cdot S_X. \tag{1.3}$$

The retention coefficient S_X $[mm]$ varies spatially depending on different soils, land use and slope, and in time because of changing water content. S_X is related to the curve number C_N by the SCS equation:

$$S_X = 254 \cdot \left(\frac{100}{C_N} - 1\right). \tag{1.4}$$

The parameter C_N is defined for three moisture conditions from dry to wet, and can be calculated or used as a tuning parameter (USDA, 1972).

Water, which has infiltrated into the soil, percolates through the soil layers using a storage routing technique (Arnold, 1990), where $W_{S_{(t)}}$ and $W_{S_{(t+1)}}$ are the water contents of the soil layer at the beginning and end of the day t in mm respectively, and P_{erc} is the amount of percolated water per day from the layer in mm:

$$P_{erc_t} = W_{S_{(t+1)}} - W_{S_{(t)}} = W_{S_{(t)}} \left[1 - exp\left(\frac{-\Delta t}{T_T}\right)\right]. \tag{1.5}$$

T_T is the travel time through each layer in hours and is calculated with the linear storage equation

$$T_T = \frac{W_S - F_C}{K(\Theta)} = \frac{W_S - F_C}{K_S \cdot \left(\frac{W_S}{U_L}\right)^{\beta}}, \tag{1.6}$$

where $K(\Theta)$ is the hydraulic conductivity $[mm\ h^{-1}]$, K_S $[mm\ h^{-1}]$ is the saturated hydraulic conductivity (calculated with a pedotransfer function using the texture classes of each soil layer), U_L denotes the soil water content at saturation $[mm\ mm^{-1}]$, $ß$ is a shape parameter, and F_C is the tabulated field capacity water content of the layer in mm. The soil parameters, as provided by the regional authorities for the so-called 'leading profiles', are normally imprecise and sometimes incorrect or have to be calculated using pedotransfer functions (e.g. for saturated conductivity), so that it is often necessary to calibrate the value of K_S. Lateral subsurface flow or interflow is calculated simultaneously with percolation using a kinematic storage model developed by Sloan et al. (1983). Interflow occurs in a given soil layer if the soil layer below is saturated so that the amount of base flow increases with increasing values of saturated soil conductivity.

The equations for groundwater flow and groundwater table depth were derived from Smedema and Rycroft (1983), assuming that the variation in return flow q $[mm\ d^{-1}]$ at time step t is linearly related to the rate of change in water table height h $[m]$:

$$q_t = q_{t-1} \cdot e^{(-\alpha \cdot \Delta t)} + Rc_{\Delta t} \cdot \left(1 - e^{(-\alpha \cdot \Delta t)}\right), \tag{1.7}$$

$$h_t = h_{t-1} \cdot e^{(-\alpha \cdot \Delta t)} + \frac{Rc_{\Delta t}}{0.8 \cdot S \cdot \alpha} \cdot \left(1 - e^{(-\alpha \cdot \Delta t)}\right). \tag{1.8}$$

Here Rc is the groundwater recharge in mm per day and S the specific yield $[m^3\ m^{-3}]$ or drainable porosity. The reaction factor α is a function of the hydraulic transmissivity T $[m^2\ d^{-1}]$ and the slope length L $[m]$:

$$\alpha = \frac{10 \cdot T}{S \cdot L^2} \tag{1.9}$$

At the macroscale, the basic geo-hydrological input data (transmissivity, specific yield) are usually not available, and therefore the value of α has to be calibrated. The approach has been further developed in the thesis to calculate the groundwater dynamics at the hydrotope level on a daily time step (see Hattermann et al., 2004 in Chapter 3).

The flow routing from subbasin to subbasin is calculated using the Muskingum flow routing method (Maidment, 1993), where a continuity equation is assumed:

$$\frac{d\,(S_R)}{dt} = Q_{i_t} - Q_{0_t} \tag{1.10}$$

Here S_R is the water volume within a certain reach in $[m^3]$, Q_{i_t} $[m^3\ s^{-1}]$ is the inflow rate into the reach and Q_{0_t} $[m^3\ s^{-1}]$ is the outflow rate at time t. The idea of the Muskingum method is to facilitate a variable discharge storage equation:

$$S_{R_t} = K_R \cdot [X \cdot Q_{i_t} + (1 - X) \cdot Q_{0_t}] \tag{1.11}$$

where X is a dimensionless weighting factor in river reach routing. The storage time constant K_R is estimated using the reach length and the wave celerity.

The four main calibration parameters used to adjust the hydrological processes in SWIM are tuning factors for soil percolation (Equation 1.6), groundwater discharge and height (Equations 1.7 and 1.8), flow routing (Equation 1.11) and net radiation (Equation 1.12). Soil percolation, river routing and groundwater height and discharge are adjusted by simply multiplying them with global correction factors (*sccor* for soil percolation, with $0 < sccor < 10$; *rcor* for river routing, with $1 < rcor < 40$; and α for groundwater height and discharge, with $0.05 < \alpha < 0.7$). Total net radiation is adjusted by changing the long wave emission. Since long wave emission is negative in the radiation term and is directly adjusted by a correction factor (*rad*), total net radiation will decrease with increasing values of *rad* (with $-0.3 < rad < 0.3$). The correction of net radiation was used to adjust evapotranspiration. It has to be mentioned that the correction of net radiation became less important in the extended model with the wetland module included. The overall sensitivity of the model results to the tuning parameters for the different subregion in the Elbe basin is described in Hattermann et al. (2005a) in Chapter 2.4.1.

1.2.3 Vegetation

In contrast to most other hydrological catchment models, vegetation processes (plant growth, water and nutrient uptake) are simulated dynamically on a daily time step in SWIM, whereby it is possible to distinguish between 72 different plant types. They are simulated using a simplified EPIC approach (Williams et al., 1984), which is basically the same as implemented in the SWAT model.

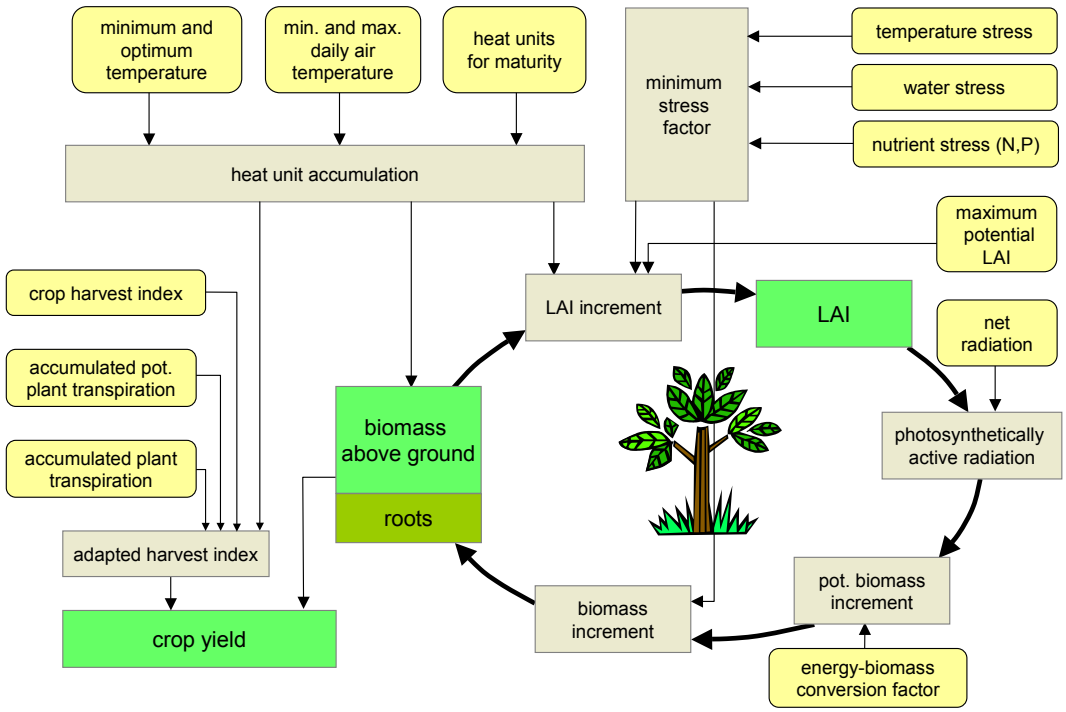

Figure 1.7. The vegetation module in SWIM and its parameter demand (yellow). The parameters are partly taken from tables (e.g. the crop harvest index, maximum potential LAI, biomass energy ratio and the crop specific minimum and optimal temperature for growth), and partly calculated daily (e.g. the heat units and the temperature, water and nutrient stresses).

The advantage of having a dynamic representation of plant processes in the model is the possibility to take into account their type and age specific response to land use management and climate variability, which gives a more realistic feedback on environmental change in the river basin (Bronstert et al., 2005). Typical examples are winter wheat and most other cereals cultivated in Europe (mostly C3 plants), which have their temperature optimum between 12 °C and 15 °C and therefore are not promoted by the anticipated change in temperatures, and maize, which has its temperature optimum around 20 °C and will benefit from the increase in temperature (see Hattermann et al., 2005c in Chapter 5.3.2). Two vegetation types are considered in the module:

- annual vegetation (altogether 42 different arable crops like wheat, barley, rye, maize, potatoes etc., and cover crops) and
- perannual aggregated vegetation types (like e.g. 'mixed forest', 'meadow',

and 'heather'), using specific parameter values for each crop/vegetation type.

The basic processes responsible for plant growth are the interception of energy in terms of net radiation and phenological development of the plants based on accumulation of daily heat units (see Figure 1.7).

The intercepted photosynthetic active solar radiation P_{ar} $[MJ\ m^2]$ is estimated following Beer's law (Monsi and Saeki, 1953):

$$P_{ar} = 0.02092 \cdot R_{ad} \cdot [1 - exp\,(-0.65 \cdot LAI)]\,, \tag{1.12}$$

where R_{ad} is the solar radiation in Ly and LAI the leaf area index. The potential increase in biomass is afterwards adjusted by multiplying P_{ar} with a plant specific biomass-energy ratio B_e $[kg\ ha^{-1}\ d^{-1}]$ (Monteith, 1977).

The potential increase is adjusted further, if one of the plant stress factors for water availability, nutrient availability or temperature is lower 1. The water stress factor is calculated by comparing water supply in soil and water demand, assuming that about 30 % of the total water comes from the top 10 % of the root zone. The approach reflects the observation that plants satisfy their water demand from different layers at the same time, with a maximum from the top layers, and allows roots to compensate for water deficits in certain layers by using more water in other layers with adequate supply. Nutrient uptake by plants is estimated using a supply and demand approach (see Chapter 1.2.4).

The leaf area index LAI in $[m^2\ m^{-2}]$ used in Equation 1.12 is calculated as a function of heat units and biomass, and is different for two phases of the growing season:

$$LAI = \frac{LAI_{max} \cdot B_{ag}}{B_{ag} + exp\,(9.5 - 0.0006 \cdot B_{ag})} \qquad if I_{hun} \leq D_{LAI}, \tag{1.13}$$

$$LAI = 16 \cdot LAI \cdot (1 - I_{hun})^2 \qquad if I_{hun} > D_{LAI}. \tag{1.14}$$

LAI_{max} is the plant specific maximum leaf area index, B_{ag} the aboveground biomass in $[kg\ ha^{-1}]$, and D_{max} is the crop specific fraction of the growing season before LAI starts declining. I_{hun} is the heat unit index ranging from 0 to 1 at physiological maturity:

$$I_{hun} = \frac{\sum_d D_{hun}\,(t)}{P_{hun}}, \tag{1.15}$$

where P_{hun} is the number of potential heat units required for the maturity of the crop. D_{hun} is the value of heat units accumulated per day t, and is calculated using the maximum and minimum daily temperature T_{min} and T_{max} in $^\circ C$:

$$D_{hun}(t) = \left(\frac{T_{max} + T_{min}}{2}\right) - T_b, \quad T_b \geq 0, \tag{1.16}$$

with T_b being the plant specific base temperature in $^\circ C$ below which the plant does not grow.

The daily plant nitrogen demand is calculated as a function of the optimal nitrogen concentration in the crop biomass, and already accumulated nitrogen in biomass. Three parameters are specified for every crop in the crop database to calculate the optimal crop nitrogen concentration as a function of growth stage (see Chapter 1.2.4). The crop is allowed to take nitrogen from any soil layer that has roots, or in the extended version from groundwater, if the roots have access to it (Chapter 4.2.3, Hattermann et al., 2005b). Uptake starts at the upper layer and proceeds downwards until the daily demand is met or until all nitrogen has been depleted.

1.2.4 Nitrogen cycle

The nutrient balance of river basins and most landscapes in Europe has been and still is strongly influenced by human interventions. As a result, the nutrient concentrations in most groundwater and surface water bodies are considerably higher than before, and many surface waters suffer from eutrophication. The reasons are high rates of fertilizer application on farmland and forests, increased atmospheric deposition of nitrogen, and point sources like waste water discharge. However, water of good or sufficient quality is one of the basic demands not only of the society but also of riverine ecosystems. The impacts of land use and climate changes on the nutrient cycle in a river basin can only be investigated using an integrated approach, where changes in temperature, seasonal precipitation and fertilization regimes have feedbacks on plant growth and plant nutrient uptake and therefore also on water quality in groundwater, lakes and river flow (see Bronstert et al., 2005). The model SWIM considers two nutrient cycles, of which the nitrogen module is further described in this section because nitrate has been used in Hattermann et al. (2005b) to investigate the impacts of wetlands and

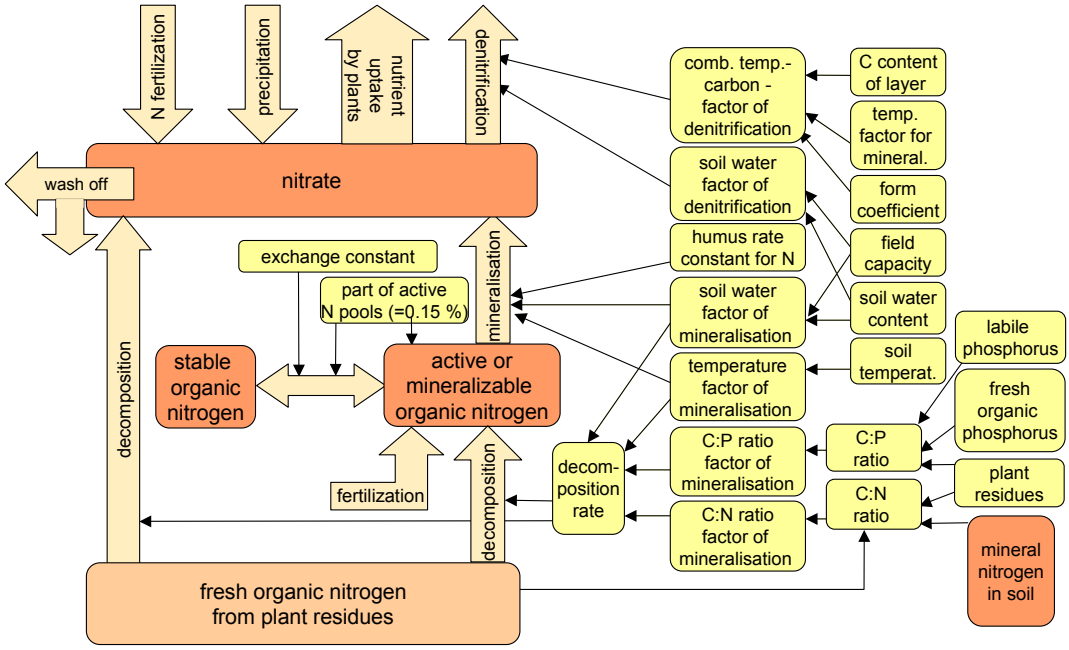

Figure 1.8. The nitrogen module in SWIM with the parameters demanded in yellow, which are partly taken from tables and partly simulated by SWIM (see Krysanova et al., 2000).

riparian zones on the water and nutrient flows.

The nitrogen and phosphorus processes in SWIM are both connected to plant growth and hydrology. They include pools for nitrate nitrogen, active and stable organic nitrogen, organic nitrogen in the plant residue, labile phosphorus, active and stable mineral phosphorus, organic phosphorus, and phosphorus in the plant residue, and the flows of fertilization, input with precipitation, mineralization, denitrification, plant uptake, leaching to groundwater, uptake from groundwater, losses with surface runoff, interflow and erosion (the nitrogen module is shown in Figure 1.8). The model considers two sources of nitrate mineralization (Seligman and van Keulen, 1981):

- the fresh organic nitrogen pool, associated with crop residue, and
- the active organic nitrogen pool, associated with the soil humus.

Organic nitrogen is divided into two pools, the active and readily mineralizable organic nitrogen AN_{or} $[kg\ ha^{-1}]$ and the stable organic nitrogen SN_{or} $[kg\ ha^{-1}]$. Organic nitrogen flow AN_{sflow} in $kg\ ha^{-1}$ between the active and stable pools is

described using an equilibrium approach, assuming that the active pool fraction at equilibrium is 15 %:

$$AN_{sflow} = NC_{as} \cdot \left(\frac{AN_{or}}{AN_{fr}} \right) - SN_{or}, \tag{1.17}$$

where NC_{as} is the rate of flow in 10^{-4} d^{-1}, and AN_{fr} is the active pool fraction.

Decomposition of plant residue and fresh organic nitrogen pools and mineralization flow from fresh organic nitrogen to plant available nitrogen are calculated daily using first order equations. The decomposition rate N_{dec} is a function of C:N ratio, C:P ratio, temperature and water content in soil (Seligman and van Keulen, 1981):

$$N_{dec} = 0.5 \cdot min\left(C_N, C_P\right) \cdot \sqrt{T_f \cdot W_f}, \tag{1.18}$$

where C_N and C_P are exponential functions of the C:N and C:P ratios, T_f is a function of soil temperature and W_f is the relation of soil water to field capacity.

The mineralization from active organic nitrogen is a function of temperature and water content in soil:

$$N_{aom}(i) = N_{hum} \cdot \sqrt{T_f(i) \cdot W_f(i)} \cdot AN_{or}(i), \tag{1.19}$$

where $N_{aom}(i)$ is the mineralization rate in $kg\ ha^{-1}\ d^{-1}$ for the active organic pool in layer i, N_{hum} is the humus rate constant for nitrogen (0.0003 d^{-1}), and $T_f(i)$ and $W_f(i)$ are the temperature and water factors for the layer i.

Denitrification causes nitrate to be volatilized from soil. It occurs only in the conditions of oxygen deficit, which usually is associated with a high water content in soil. Besides, as one of the microbial processes, denitrification is a function of soil temperature and carbon content. The soil water factor considers total soil water and is represented by an exponential function, which reaches 0.5 at 0.7 of field capacity and approaches 1.0 close to field capacity.

The amount of nitrogen (in form of nitrate) transported by water from layer to layer in $kg\ ha^{-1}\ d^{-1}$, and the amount of nitrogen loss by groundwater recharge, interflow and surface flow can be estimated by multiplying the weight of the percolated water in $kg\ ha^{-1}\ d^{-1}$ with the concentration of nitrogen in the water volume. In the same way, the concentration of nitrogen in a soil layer can be estimated by dividing the weight of nitrogen in the layer by the water storage in

the layer.

Nitrogen uptake by plants is estimated using a supply and demand approach, where the daily demand N_{dpl} in $kg\ ha^{-1}\ d^{-1}$ is:

$$N_{dpl}(t) = P_{CN}(t) \cdot P_b(t) - P_{CN}(t-1) \cdot P_b(t-1), \tag{1.20}$$

with $P_{CN}(t)$ being the optimal nitrogen concentration in the plant biomass per day t, and P_b being the accumulated biomass in $kg\ ha^{-1}$. The optimal nitrogen concentration is a function of growth stage using the following equation:

$$P_{CN} = (B_{n1} - B_{n2}) \cdot \left[1 - \frac{I_{hun}}{I_{hun} + exp\,(S_{p1} - S_{p2} \cdot I_{hun})}\right] + B_{n3}, \tag{1.21}$$

where B_{n1-3} are plant specific parameters which describe the fraction of nitrogen in plant biomass including seed at emergence, at 50 % maturity and at maturity. S_{p1} and S_{p2} are shape parameters, and I_{hun} is the heat unit index (see equation 1.15).

Lateral nutrient retention during the passage from the hydrotope to the surface water is calculated using a linear equation and considering the residence time of the nutrients in the subcatchment, the nutrient turn-over and the plant uptake in riparian zones and wetlands. The lateral flow module is described in detail in Hattermann et al. (2005b) in Chapter 4.2.3.

1.3 The Elbe river basin

1.3.1 Basin characteristics

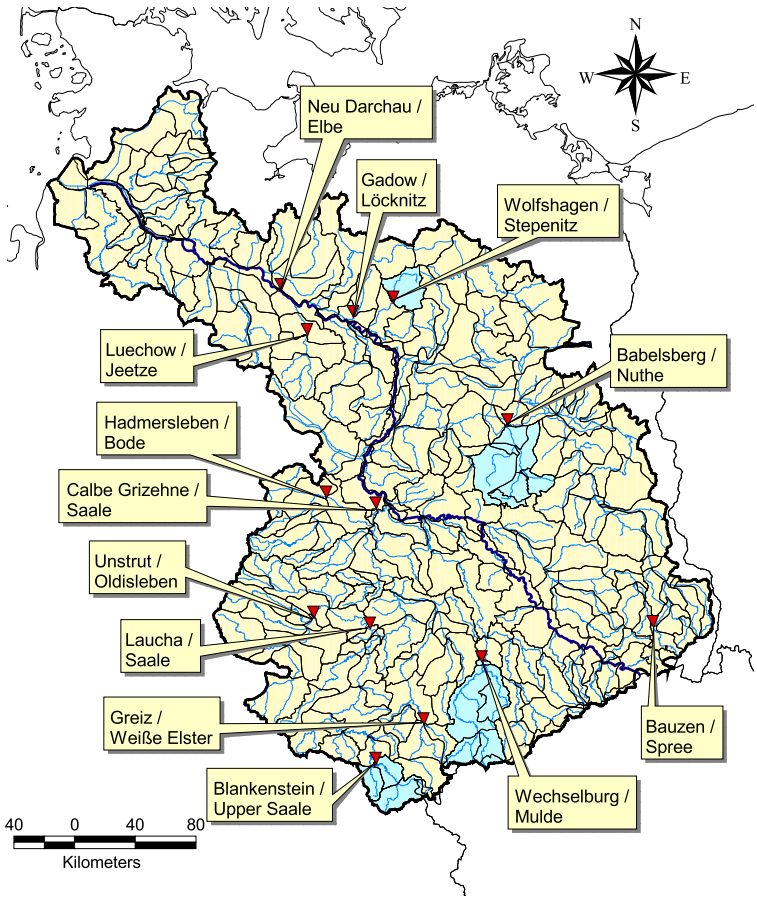

Figure 1.9. Subbasins and 13 gauge stations (right) in the German part of the Elbe basin used in the study. Light blue indicates the nested subbasins which were used in the sensitivity and uncertainty analysis in Chapter 2.4 (Hattermann et al., 2005a) and the Nuthe basin, where the implementation of the riparian zone and wetland module has been evaluated (Chapter 3, Hattermann et al., 2005b).

The Elbe basin is located in Central Europe in the transition zone between marine and continental climates and covers a large part of the former German Democratic Republic. About 25 million inhabitants live in the basin, therein 76 % in Germany. The total Elbe basin, including the Czech part and some small areas in Austria and Poland, has a catchment area of 148,268 km^2. The German part of the Elbe, where the model was applied, covers approximately 80,256 km^2 from

the Czech border to Neu Darchau, the lowest gauge station not influenced by the tide of the North Sea (see Figure 1.9), and in addition 16,148 km^2 in the inter-tidal zone, drained by rivers influenced by the tide or regulated by the local authorities. The total length of the Elbe river is 1092 km, 728 km of that is in Germany (ATV-DVWK, 2000).

Climatically, the central part of the Elbe basin is one of the driest regions in Germany, with mean annual precipitation below 500 mm a^{-1} in the lee of the Harz mountains (western part of the basin, see Figure 1.1). This is important because this area contains the most fertile soils and hence highest agricultural productivity in the basin. The long-term mean annual precipitation over the whole basin is 659 mm a^{-1}, and the long-term mean discharge at the estuary is 877 m^3 s^{-1} with an average inflow from the Czech Republic of 315 m^3 s^{-1} (ATV-DVWK, 2000).

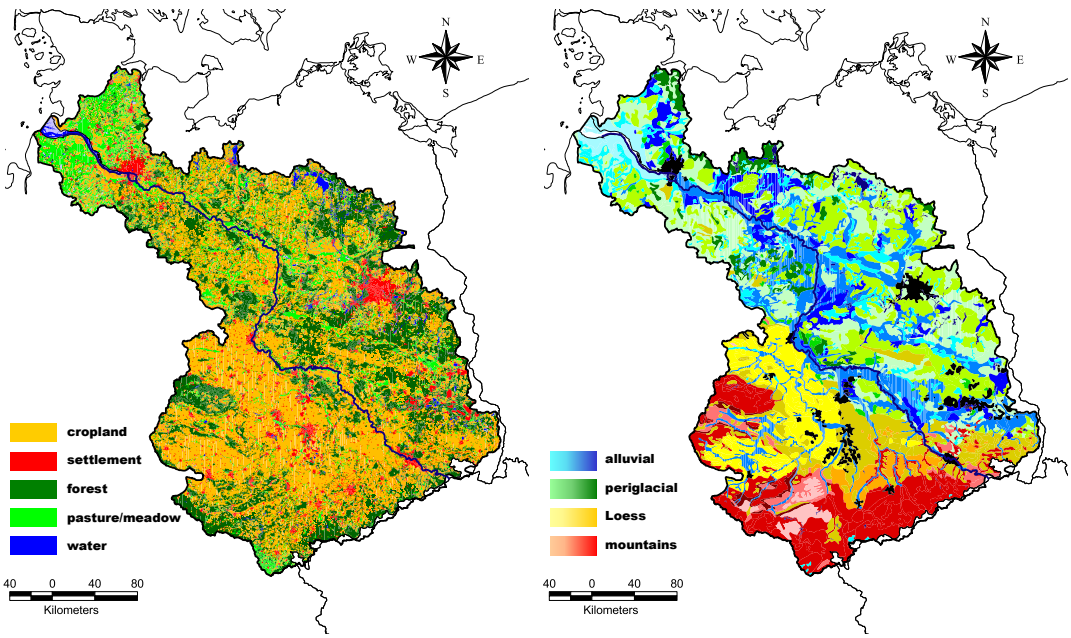

(a) Land use (b) Soils

Figure 1.10. Land use and soils in the German part of the Elbe basin. SWIM distinguishes 15 land use classes (see Annex C), and 52 soil types are located in the catchment.

The Elbe and its estuaries are regulated by 273 dams for flood protection and freshwater supply. As a result of river management measures like river regulation, flood protection and land drainage, the eastern tributaries have lost their natural flow regime (flooding in winter and early spring and low water levels in summer

and autumn). Despite flood protection measures, several extreme floods have occurred over the last decades in the region, culminating in the disastrous August 2002 flood in the Elbe basin. The flood was caused by a low pressure system called Vb ('five b'), a circulation pattern that is known to produce heavy and intensive rainfall, especially across Central Europe (Becker and Grünewald, 2003).

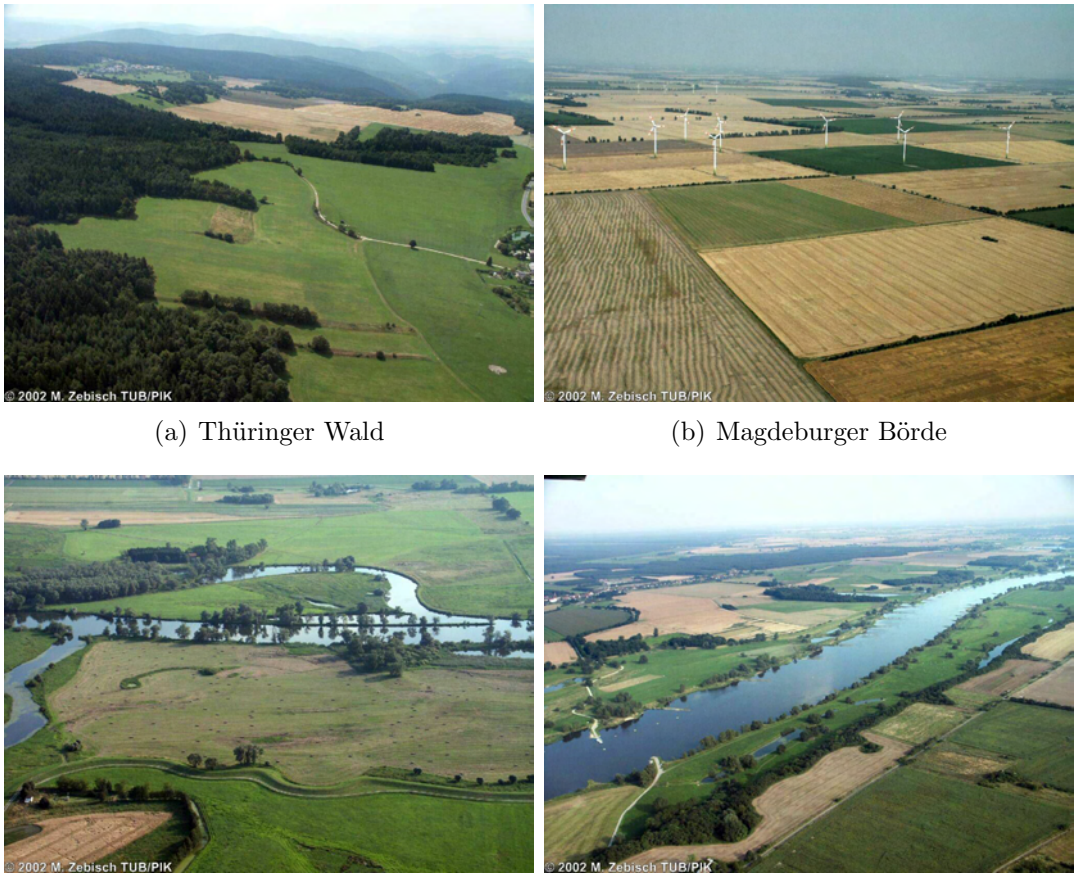

(a) Thüringer Wald (b) Magdeburger Börde

(c) Havelland (d) Elbe

Figure 1.11. The main natural landscapes in the German part of the Elbe basin and the Elbe river. a) the mountainous area in the south and southwest of the catchment: relatively steep slopes and high annual precipitation, the land is mainly covered by forests and grassland. b) the loess plains adjacent to the mountains: relatively flat, low annual precipitation, the land is mainly covered by arable land. c) the northern lowland: bright valleys, river systems in Pleistocene watercourses, shallow groundwater and relatively low amounts of annual precipitation (500-650 mm a^{-1} per year). The land is covered by grassland and riparian forest along the rivers and depending on soil fertility by arable land and forest elsewhere. d) The Elbe river at Wittenberge.

Hydrologically, the area of the German part of the basin can be subdivided into three main subregions (mainly following the soil classes, see Figures 1.10b and 2.2): (1) the mountainous subregion in the south, representing approximately 20 % of the total area, (2) the mountain foothills, predominantly covered by loess soils (approximately 28 %), and (3) the undulating northern lowlands, comprising approximately 52 % of the total area (see Figure 1.11).

The topography of the northern lowland formed during the last ice age (which is called the "Weichsel" ice age in North Germany). The Elbe river is located in an ancient Pleistocene watercourse, where the melted water of the ice sheets coming from the north drained into the North Sea (Wagenbreth and Steiner, 2002). Hence the northern part of the basin comprises mostly sandy glacial sediments transported by ice and is drained by slowly flowing streams with broad river valleys. The higher elevation sites with deeper water tables are covered by sandy, highly permeable soils and predominantly pine forests; the valleys often have loamy riparian soils with very shallow groundwater. Valleys are covered by grassland and forests in areas with shallow groundwater, and arable land is located where drainage systems are implemented and where the fertility of the soils is high (see Figure 1.11c).

The finer deposits, which sedimented in the melting zone of the ice sheets, have been further transported by wind erosion and finally accumulated in the foothills of the mountains (their dominant texture class is silt, the sediments are called "loess" after accumulation). Soils in the loess region, chernozems and luvisols, are therefore mostly loamy and tend to have layers with low water permeability so that in areas with steep slopes floods are generated, namely in the Saale and the Mulde tributaries. These sediments normally have high field capacities and nutrient supply, and the loess subregion is an area with very intensive agricultural land use (see Figure 1.11b).

Mountain soils are mainly thin cambisols, which are formed by weathering products and redeposited rocky materials. The mountainous areas are often covered by forests and grassland.

1.3.2 Natural and socio-economic changes in the region

The region of Central and Eastern Europe, where the Elbe basin is located, has witnessed significant socio-economic changes during the last two decades

(Krysanova et al., 2005b). Fundamental changes started in the German Democratic Republic (GDR) and in the Socialistic Republic of Czechoslovakia (CSSR), resulting in the reunification of Germany which occurred on the 3rd of October 1990, while the people in the former SRC chose to form two independent states, the Czech and the Slovac Republic. The GDR adopted the economic system of the Federal Republic of Germany already on July 1, 1990.

German reunification enabled Eastern Germany to become a part of the European Union already in 1990, while the Czech Republic joined the EU on the 1st of May of 2004. As already mentioned (1.3.1), about 87 % of the Elbe basin area are covered by the former GDR and the Czech part of the CSSR. This is important, because the political changes in the countries have resulted in an overhaul of the sometimes outdated, ineffective, and often highly polluting industries, which were energy and raw materials (including water) intensive (ATV-DVWK, 2000). The socio-economic changes in the region, which led to a collapse of much of the old industry and collective agriculture, have considerably influenced conditions of water availability, water demand and quality in the region. This is illustrated in Krysanova et al. (2005b), where the natural and socio-economic induced changes in the Elbe and in the neighbouring Warta river (the largest tributary of the Oder river), are presented and analysed. Following their discussion, large-scale changes in the socio-economic system in the study area have been superimposed on the global environmental change, and particular, climate change. Rising temperatures, increases in winter precipitation (but decrease of snow cover) and a drop in summer precipitation have been observed in many areas in the Central and Eastern European region (Gerstengarbe and Werner, 2005).

Change in climate and socio-economics have altered the hydrological state of the Elbe river, whereby three basic water-related regional problems can be identified, all have manifested themselves in different regions of the basin: having too much, too little and too polluted water (see Figure 1.12).

Some important indicators of change in Elbe river hydrology are the decreasing water levels in rivers and groundwater observed in large areas of the eastern and lowland parts of the basin (see Chapter 3.3.4). Groundwater recharge, especially, is extremely sensitive to changing boundary conditions like climate and land use, since it represents the residual of the water balance (Gehrels and Peters, 2001). Decreasing precipitation and higher variability (climate pressures) on the

one hand, and river canalization and land melioration (land use pressures) on the other, may cause water depletion, making the development of comprehensive strategies and tools to investigate such complex problems increasingly important (see Hattermann et al., 2004 in Chapter 3).

(a) Tangermünde (b) Spreewald

(c) Fläming (d) Havelland

Figure 1.12. Water related problems in the Elbe basin. a) Too much water: the Elbe close to Wittenberge during the catastrophic summer 2002 flood, causing extensive damage, especially in the southern part of the basin and along the main Elbe stream. A similar flood event occurred only five years earlier in 1997 in the neighboring Oder river basin. b) Too little water: the Spree tributary of the Elbe river in the summer 2002 at Lübbenau, just one week before the Elbe flood. One can see that there is insufficient water for tourist boats. c) Too little water: maize field close to Jüterbog (Nuthe subbasin) in the summer of 2003 (front: without irrigation, back: with irrigation). d) Too poor quality: the Nuthe subbasin close to Berlin.

This is also illustrated in Figure 1.13, where the Havel river, one of the largest

tributaries of the Elbe river, shows a decreasing water level over the last decades, while the Elbe river at Neu Darchau, close to the basin outlet, has no significant trend. Simulation results indicate that the water depletion in the Havel river is the result of two overlaying pressures, where one is climate change (lower precipitation), and another the cut back of the open pit mining in the Spree subbasin, where the pits are flooded and therefore river runoff decreases (Wechsung et al., 2005a).

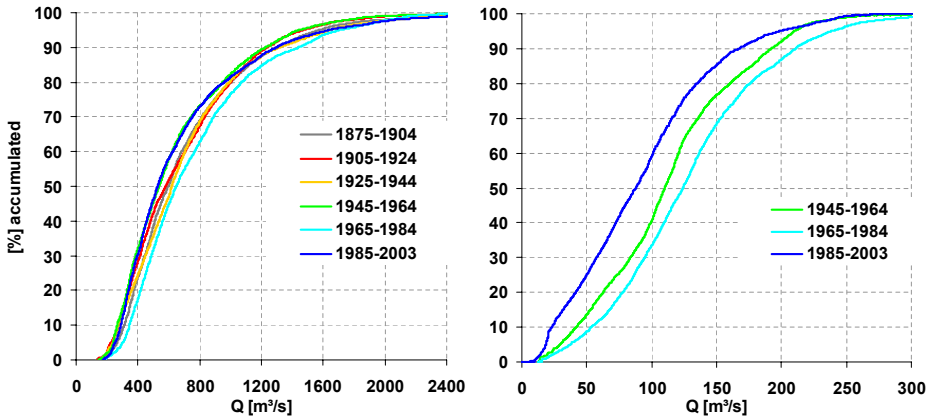

Figure 1.13. Discharge frequency distributions for subsequent 20 year averages starting in 1904 for the Elbe river flow at gauge Neu Darchau ($A_{E0} \approx 80{,}000$ km^2) (left) and the most eastern tributary of the Elbe, the Havel river at gauge Havelberg ($A_{E0} \approx 16{,}000$ km^2) (right). Notable is the significant trend to low flow conditions in the Havel basin during the last two decades, whereas the Elbe flow does not show a significant trend.

Another indicator of change in Elbe river hydrology is the increase in nutrient concentrations (nitrogen and phosphorous) in the Elbe. In 1989 the Elbe was one of the most heavily polluted rivers in Europe (UBA, 2001, page 25). Pollution of surface waters and groundwater caused by the high intensity of water use, discharge of insufficiently treated domestic and industrial wastes and excessive application of fertilizers and pesticides in agriculture represent serious problems in the basin. Nutrient pollution is one of the most widespread forms of water pollution in the region. Even though emissions from point sources have notably decreased in the basin since the 1990s due to reduction of industrial sources and introduction of new and improved sewage treatment facilities (visible in the orthophosphate concentrations), the diffuse sources of pollution still represented

mainly by agriculture, are still not sufficiently controlled (visible in the nitrate concentrations). Nitrate concentrations in the main Elbe tributaries remain high, partly due to the long retention time of nutrients in the subsurface. Figure 1.14 illustrates the development of phosphate and nitrate concentrations in the Elbe river at gauge Schmilka (south of the German part of the Elbe basin) and gauge Zollenspieker (outlet of the basin).

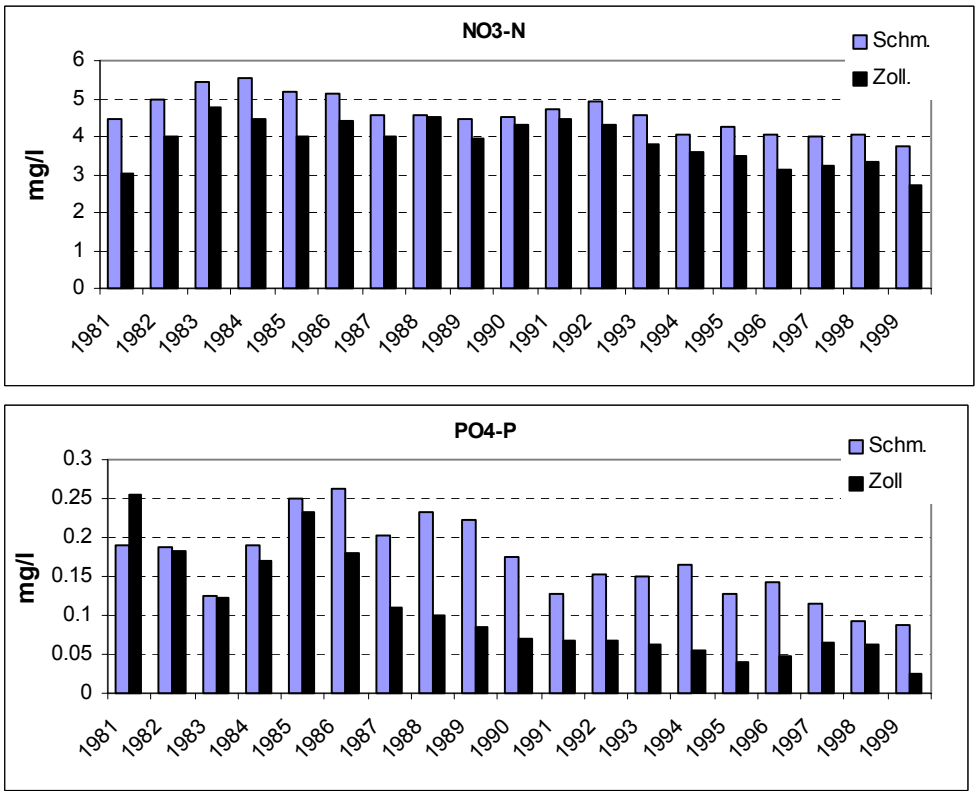

Figure 1.14. Comparison of the average annual concentrations of major nutrients (nitrate N and orthophosphate P) in the Elbe, gauges Zollenspieker and Schmilka from 1981 to 1999 (data source: ARGE Elbe (IKSE, 2001), see also Krysanova et al., 2005b).

This is why the third paper (Chapter 4, Hattermann et al., 2005b) deals with retention processes in the Nuthe subbasin of the Havel river, one of the Elbe largest tributaries, where the nutrient pollution was very high in the 1980s and dropped during the 1990s to a much lower level (see Table 4.1).

HYDROLOGICAL PROCESSES 19, 693–714 (2005)

Chapter 2

Runoff simulations on the macroscale with the eco-hydrological model SWIM in the Elbe catchment - validation and uncertainty analysis

Short title: macroscale hydrological validation

Keywords: macroscale hydrological validation, eco-hydrological model, groundwater dynamics, sensitivity, uncertainty.

Hattermann, FF*, Krysanova, V, Wattenbach, M, Wechsung, F
Potsdam Institute for Climate Impact Research
* Full address of the corresponding author:
Dipl.-geoecol. Fred Fokko Hattermann
Global Change and Natural Systems Department
Potsdam Institute for Climate Impact Research
P.O. Box 601203, Telegrafenberg
14412 Potsdam
Germany
Fax: +49 331 288 2600, Tel. +49 331 288 2649
E-mail: fred.hattermann@pik-potsdam.de

Runoff simulations on the macroscale with the eco-hydrological model SWIM in the Elbe catchment - validation and uncertainty analysis

Abstract This study presents an example where the hydrological processes of the eco-hydrological model SWIM (Soil and Water Integrated Model) are thoroughly analyzed. The model integrates hydrology, vegetation, erosion and nutrient dynamics. It is process based and has to be calibrated. The hydrological validation of the model is of prime importance, because all other ecological processes are related to the water cycle. On the other hand, these ecological processes influence the water cycle in turn, and therefore they where considered in the modeling process and in the sensitivity and uncertainty analysis. The validation was multi-scale, multi-site and multi-criteria: the validation strategy followed a bottom-up approach in which the model was firstly calibrated for 12 mesoscale subbasins, covering the main subregions of the German part of the Elbe basin, and the information gained from the mesoscale was then used to validate the model for the entire macroscale basin. Special attention was paid to the use of spatial information (maps of water table) to validate the model in addition to commonly used observations of water discharge at the basin outlet. One main result was that investigations in smaller catchments have to accompany macroscale model applications in order to understand the dominant hydrological processes in the different areas of the entire basin and at different scales.

The validation was carried out in the German part of the Elbe river basin (≈80,258 km^2). It is representative of semi-humid landscapes in Central Europe, where water availability during the summer season is a limiting factor for plant growth and crop yield.

2.1 Introduction

Models have become a common tool to understand the hydrological processes in river basins and the impacts of human activities on them. It is commonly agreed that a comprehensive model validation has to be the fundamental first step when applying a model (Klemes, 1986; Abbott and Refsgaard, 1996; Refsgaard and Knudsen, 1996; Beven, 1997; Güntner et al., 1999). In particular, prediction of the impacts of land use and climate changes on regional hydrological processes and flow regimes at present requires an understanding of the response of these factors to climate variability in the past (Habets et al., 1999a). Klemes (1986) concluded that hydrological models for prediction should fulfill two basic require-

ments: the first is that the model structure must have a sound physical foundation and each of the structural components should permit a separate validation, and the second is that the model must be geographically transferable, and its parameters be capable of being derived from observations of real-world characteristics. Refsgaard et al. (1996) describe the different validation requirements for lumped conceptual and distributed physically-based models, placing emphasis on the importance of multi-criteria and multi-scale validation methods for the latter model type. But modeling at the meso- (100-10,000 km^2) to macroscale ($\geq$ 10,000 km^2, Becker and Braun, 1999) implies various uncertainties (Bergström and Graham, 1998; Habets et al., 1999b). One reason is that process-based models (the model type normally used on the macroscale) combine physically-based mathematical descriptions and conceptual formulations. Another source of uncertainty is that the available data normally have a rough resolution in time (climate data, groundwater data) and space (maps of soils and land use data) and have to be interpolated to cover the entire region. The level of uncertainty often increases if the model integrates processes of hydrology, agriculture, and geomorphology, where different data sampling protocols may apply. But modeling of physically related processes integrated in one model (e.g. plant growth and changes in soil moisture), also allows to reduce uncertainty, if there are observations to validate both processes separately, because a certain parameter combination, physically possible to describe one process, might result in unreliable results for another. This additional information can serve as a criteria to reduce the parameter space and the uncertainty in the model results. An important issue is therefore the determination of the model sensitivity to the input data and model parameters and the quantification of uncertainty in the simulation of the hydrological processes in order to assess the reliability and robustness of the model results (Tarantola, 2000; Richter et al., 1996). A comprehensive validation will help to reduce the uncertainty of the model results and improve the reliability of the outcome. In our case study a multi-scale, multi-site and multi-criteria validation was performed, namely:

- Model applications in meso- to macroscale subbasins of the basin and in the entire basin to analyze the scale dependency of the model performance (multi-scale validation).
- Investigations in several catchments, located in different subregions, to un-

derstand the overall pattern of the hydrological processes (multi-site validation), in this study the mountainous subregion, the loess area and the lowland.

- Multi-criteria validation, e.g. using a combination of point data like water discharge at the basin outlet (as an integral characteristic for the whole basin), and spatially distributed data, like contour maps of the water table, to improve the reliability of results, e.g. of the simulated flow components (Arnold et al., 1993; Refsgaard and Knudsen, 1996; Andersen et al., 2001).

The use of spatially distributed data at the macroscale to validate simulated hydrological processes is still at an early stage. Validation is usually carried out on the basis of a single-criteria approach which uses exclusively observed river discharge of the main outlet for comparison (Kite and Haberlandt, 1999), or includes in addition observed river discharge in a number of subbasins (Abdulla and Lettenmaier, 1997; Krysanova et al., 1999a; Andersen et al., 2001). In some special applications such as combined hydrological / climatological models, measured soil water saturation is taken as an additional characteristic to evaluate the model results (Habets et al., 1999a), but such data are normally sparse and not available for an entire region. A new source to validate hydrological processes is remote sensing data, which can be used, e.g., to evaluate the spatial distribution of simulated evapotranspiration (Mauser and Schädlich, 1998). However, the use of remote sensing data in hydrological modeling still involves a lot of uncertainty, because while the data have a better spatial resolution, their absolute values are often imprecise (precipitation, soil water content). Sophocleous et al. (1999) and Arnold et al. (2000) used groundwater observations as a second criteria to validate hydrological processes; the former authors coupled the groundwater model MODFLOW and the eco-hydrological model SWAT to simulate the water resources of a mesoscale basin, and the latter used observed groundwater discharge at the river basin outlet in addition to river flow to estimate base flow and groundwater discharge on a monthly time step in the upper Mississippi river basin. Both are promising applications with the constraint that groundwater models like MODFLOW are not applicable on the meso- to macroscale due to the extensive data demands and computation time of the groundwater model, and because groundwater data observed at the basin outlet as used in the second example normally include only limited information about local hydrological dynamics in the basin.

2.1 Introduction

This study focuses on validation of the hydrological module of the eco - hydrological model SWIM (Soil and Water Integrated Model, Krysanova et al., 1998). SWIM was developed on the basis of two previously developed models, SWAT (Arnold et al., 1993, 1994) and MATSALU (Krysanova and Luik, 1989; Krysanova et al., 1989). It was chosen because it combines all major eco-hydrological processes at the meso- to macroscale which are important for land use and climate change impact studies, like hydrology, vegetation, erosion and nutrient dynamics. The approach allows simulation of all interrelated processes within a single model framework using regionally available data. In contrast to meso- and macroscale hydrological models like HBV (Bergström, 1995), SLURP (Kite and Haberlandt, 1999), ISBA (Habets et al., 1999b), MIKE SHE (Refsgaard and Storm, 1995) and INCA (Wade et al., 2002), SWIM is not limited to hydrology or water quality issues, but also dynamically calculates plant growth and takes into account agricultural management practices. The AGNPS model (USDA, 2001) has a similar process-integrating approach and the same roots as SWIM (the CREAMS model, Leonard et al., 1987), but it was designed for mesoscale applications and investigation of single events. The main difference between the macroscale hydrological model SWAT and SWIM is that the former focuses mainly on water quality in rural areas, while SWIM was specifically developed to provide a comprehensive tool to investigate the impacts of land use and climate changes at the regional scale (Krysanova et al., 2005b). Nevertheless, the hydrological module of SWIM is very similar to that of SWAT, and the validation results described in this paper are to a large extent applicable also to SWAT.

The model structure, the main hydrological algorithms and the spatial aggregation scheme are presented in Chapter 2.2.1. Chapter 2.2.2 describes the main geohydrological features of the German part of the Elbe basin, where the validation was conducted. A description of the preprocessing and evaluation of climate input data is given in Chapter 2.2.3. Modelling procedures are described in Chapter 2.2.4, and Chapter 2.3.1 presents the model results for 12 subbasins of the Elbe with an area of 280 to 23,690 km^2 from different subregions of the basin and for the whole basin (80,258 km^2). The model results in Chapter 2.3.2 demonstrate how basin-integral characteristics like water discharge in rivers can be used in combination with maps of the groundwater table as spatial information to cal-

ibrate and validate the model. The robustness of the model results is tested by a comprehensive sensitivity and uncertainty analysis (Chapter 2.4), where the modeling experience gained in Chapter 2.3 is used to define the subregion-dependent parameter distributions.

2.2 Method and data

2.2.1 The model

A brief description of the main processes in SWIM, which are related to the hydrological processes, is given in this section. The main equations and model calibration options are also provided here so that the reader can follow the sensitivity and uncertainty analysis and the discussion of the results later in the paper. A full description of the model can be found in Krysanova et al. (1998, 2000). The calibration parameters discussed in this study are physically based and reflect the regional characteristics of the catchments studied, although it is usually difficult to measure these in a large basin. The model is conventually calibrated using four main global parameters to correct river flow routing, saturated soil conductivity, base flow and solar net radiation in a physically meaningful range. Daily precipitation is corrected using the empirical method developed by Richter (1995), where the systematic error in observed precipitation is adjusted by monthly changing weighting factors. Precipitation is not subject to calibration.

A three-level scheme of spatial disaggregation from basin to subbasin and to hydrotopes is used in SWIM. A hydrotope is a set of elementary units in a subbasin, which have the same geographical features like land use, soil type, and average water table dynamics, and are therefore uniform in their hydrological behavior. Water fluxes, plant growth and nitrogen dynamics are calculated for every hydrotope, where vertically up to 10 soil layers can be considered. The outputs from the hydrotopes are aggregated at the subbasin scale and routed from subbasin to subbasin, taking into account transmission losses.

The Priestley and Taylor (1972) method is used estimate the potential evapotranspiration E_P $[mm\ d^{-1}]$, where only net solar radiation R_a $[MJ\ m^{-2}]$ and

air temperature are needed as inputs at time step t:

$$E_{P_t} = 1.28 \cdot \left(\frac{R_{a_t}}{H_t}\right) \cdot \left(\frac{\delta}{\delta - \gamma}\right) \tag{2.1}$$

The latent heat of vaporization H $[MJ\ kg^{-1}]$ is calculated as a function of the mean daily air temperature, δ is the slope of the saturated vapor pressure $[kPa\ C^{-1}]$ and γ the psychrometer constant $[kPa\ C^{-1}]$. Soil evaporation and plant transpiration are calculated using the approach of Ritchie (1972), where they are functions of the dynamic leaf area index LAI. Radiation is only measured in a few stations and in others not measured directly but calculated using regression methods (using e.g. daily sunshine in hours as input). The uncertainty in the reconstruction of radiation is the reason why radiation is corrected in a physically sound moderate range in the modeling process (Quaschning et al., 2002). The sensitivity of model results to the incoming solar radiation is shown in the sensitivity analysis. The snowmelt component of SWIM is a simple degree-day equation (Knisel, 1980).

Surface runoff is calculated using a modification of the Soil Conservation Service (SCS) curve number technique (Arnold, 1990; King et al., 1999), where daily surface runoff Q $[mm\ d^{-1}]$ at time step t is estimated from daily precipitation P $[mm\ d^{-1}]$ taking into account a dynamic retention coefficient S_X by using the SCS curve number equation:

$$Q_t = \frac{(P_t - 0.2 \cdot S_X)^2}{P_t + 0.8 \cdot S_X} \quad P > 0.2 \cdot S_X, \tag{2.2}$$

$$Q_t = 0 \quad P \leq 0.2 \cdot S_X, \tag{2.3}$$

The retention coefficient S_X $[mm]$ varies spatially depending on different soils, land use and slope, and in time because of changing water content. S_X is related to the curve number C_N by the SCS equation:

$$S_X = 254 \cdot \left(\frac{100}{C_N} - 1\right) \tag{2.4}$$

The parameter C_N is defined for three moisture conditions from dry to wet, and can be calculated or used as a tuning parameter. In the sensitivity analysis the correlation of the model results to changing values of C_N is shown.

Water, which has infiltrated into the soil, percolates through the soil layers using a storage routing technique (Arnold, 1990), where $W_{S_{(t)}}$ and $W_{S_{(t+1)}}$ are the water contents of the soil layer at the beginning and end of the day t in mm respectively, and P_{erc} is the amount of percolated water per day from the layer in mm:

$$P_{erc_t} = W_{S_{t+1}} - W_{S_t} = W_{S_t} \left[1 - exp\left(\frac{-\Delta t}{T_T}\right)\right] \tag{2.5}$$

T_T is the travel time through each layer $[h]$ and is calculated with the linear storage equation

$$T_T = \frac{W_S - F_C}{K\left(\Theta\right)} = \frac{W_S - F_C}{K_S \cdot \left(\frac{W_S}{U_L}\right)^{\beta}} \tag{2.6}$$

where $K(\Theta)$ is the hydraulic conductivity $[mm\ h^{-1}]$, K_S $[mm\ h^{-1}]$ is the saturated conductivity (calculated with a pedotransfer function using the texture classes of each soil layer), U_L denotes the soil water content at saturation $[mm\ mm^{-1}]$, where $ß$ is a shape parameter, and F_C is the tabulated field capacity water content of the layer in mm. The soil parameters, as provided by the regional authorities for the so-called 'leading profile', are normally imprecise and sometimes incorrect or have to be calculated using pedotransfer functions (e.g. saturated conductivity), so that it is often necessary to calibrate the value of saturated conductivity K_S by multiplying it using a correction factor ($sccor$, with $0 < sccor < 10$, 1 for no change). Lateral subsurface flow or interflow is calculated simultaneously with percolation using a cinematic storage model developed by Sloan et al. (1983). Interflow occurs in a given soil layer if the soil layer below is saturated, so that the amount of base flow increases with increasing values of saturated soil conductivity.

The equations for groundwater flow and groundwater table depth were derived from Smedema and Rycroft (1983), assuming that the variation in return flow q $[mm\ d^{-1}]$ at time step t is linearly related to the rate of change in water table height h $[m]$:

$$q_t = q_{t-1} \cdot e^{(-\alpha \cdot \Delta t)} + Rc_{\Delta t} \cdot \left(1 - e^{(-\alpha \cdot \Delta t)}\right) \tag{2.7}$$

$$h_t = h_{t-1} \cdot e^{(-\alpha \cdot \Delta t)} + \frac{Rc_{\Delta t}}{0.8 \cdot S \cdot \alpha} \cdot \left(1 - e^{(-\alpha \cdot \Delta t)}\right) \tag{2.8}$$

Here Rc is the groundwater recharge $[mm]$ per day and S is the specific yield $[m^3\ m^{-3}]$. The reaction factor α is a function of the hydraulic transmissivity T

$[m^2\ d^{-1}]$ and the slope length L $[m]$:

$$\alpha = \frac{10 \cdot T}{S \cdot L^2} \tag{2.9}$$

At the macroscale, the basic geo-hydrological input data (transmissivity, specific yield) are usually not available, and therefore the value of α has to be calibrated.

The flow routing from subbasin to subbasin is calculated using the Muskingum flow routing method (Maidment, 1993), where a continuity equation is assumed:

$$\frac{d\,(S_R)}{dt} = Q_{i_t} - Q_{0_t} \tag{2.10}$$

Here S_R is the water volume $[m^3]$ within a certain reach, Q_{i_t} $[m^3\ s^{-1}]$ is the inflow rate into the reach and Q_{0_t} $[m^3\ s^{-1}]$ is the outflow rate at time t. The idea of the Muskingum method is to derive a variable discharge storage equation:

$$S_{R_t} = K_R \cdot [X \cdot Q_{i_t} + (1 - X \cdot Q_{0_t})] \tag{2.11}$$

where X is a dimensionless weighting factor in river reach routing. The storage time constant K_R is estimated using the reach length and the wave celerity. In SWIM, K_R is multiplied by a correction factor $rcor$ $(1 < rcor < 40)$ to tune the model, where the ratio of storage to discharge increases with increasing routing factors.

The sensitivity of the model results to the four main tuning parameters used to adjust the hydrological processes in SWIM by correcting global radiation (Equation 2.1), soil percolation (Equation 2.6), groundwater height and discharge (Equations 2.7 & 2.8) and flow routing (Equation 2.11) is described in Chapter 2.4.1. While soil percolation, groundwater height and discharge are adjusted by simply multiplying them with global correction factors, SWIM uses a different concept to correct net radiation. Total net radiation is adjusted by changing the most uncertain part of the net radiation Ra, which is the long wave emission. Since long wave emission is negative in the radiation term and is directly adjusted by the correction factor (rad), total net radiation will decrease with increasing values of rad (with -0.3 $< rad <$ 0.3).

2.2.2 The basin under study

The total Elbe basin has an area of 148,268 km^2. The German part of the Elbe, where the model was applied, covers 80,256 km^2 from the Czech border to Neu Darchau, the lowest gauge station not influenced by the tide of the North Sea (see Figure 2.1). The total length of the Elbe river is 1092 km, 728 km of that is in Germany. The Elbe and its estuaries are regulated by 273 dams for flood protection and freshwater supply. As a result of river management measures like river regulation, flood protection and land drainage, the eastern tributaries have lost their natural flow regime (flooding in winter and early spring and low water levels in summer and autumn). Despite flood protection measures, several extreme floods occur during the last decades in the region, culminating in the disastrous August 2002 flood in the Elbe basin. The flood was caused by a low pressure system called Vb ("five b"), a circulation pattern that is known to produce heavy and intensive rainfall, in special in Central Europe (Becker and Grünewald, 2003).

Climatically, the Elbe basin is one of the driest regions in Germany, with mean annual precipitation below 600 mm in the lee of the Harz mountains (western part of the basin). The long-term mean annual precipitation over the whole basin is 659 mm, and the long-term mean discharge at the estuary is 877 m^3 s^{-1} with an average inflow from the Czech Republic of 315 m^3 s^{-1} (ATV-DVWK, 2000).

Over the last two decades, decreasing water levels in rivers and groundwater have been observed in the lowland parts of the basin. Groundwater recharge, especially, is extremely sensitive to changing boundary conditions like climate and land use changes, since it represents the residual of the water balance (Gehrels and Peters, 2001). Decreasing precipitation and higher variability (climate impacts) on the one hand, and river canalization and land melioration (land use impacts) on the other, may be some of the reasons for water depletion, making the development of comprehensive strategies and tools to investigate such complex problems increasingly important.

Hydrologically, the area can be subdivided into three main subregions: (1) the mountainous area in the south, approximately 20 % of the total area, (2) the hilly mountain foreland, predominantly covered by loess soils, and (3) the undulating northern lowlands, approximately 52 % of the total area (see Figure 2.2).

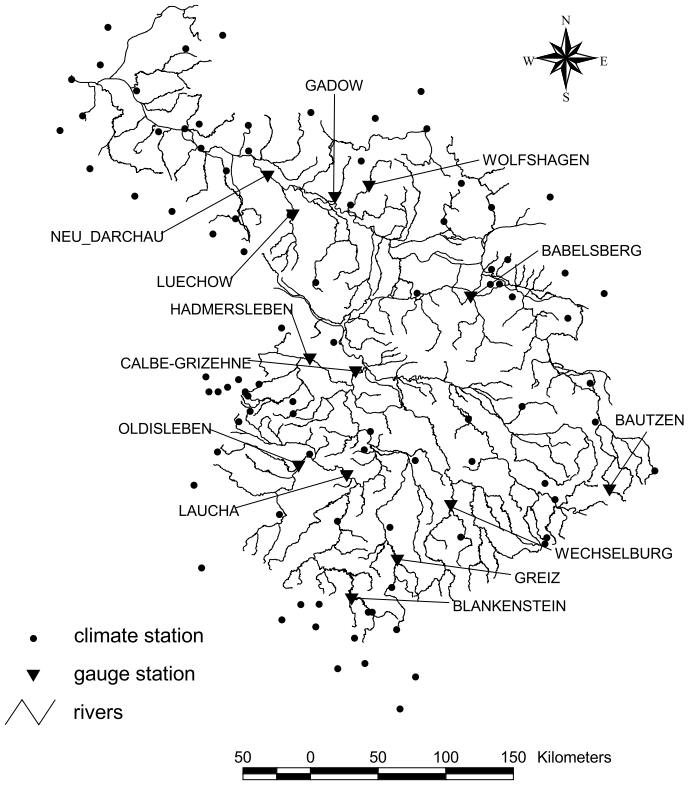

Figure 2.1. The river network of the German part of the Elbe basin, the locations of the gauge stations, where comparisons with the observed river discharge were conducted, and the climate stations.

The northern lowlands are formed by mostly sandy glacial sediments and drained by slowly flowing streams with broad river valleys. The higher sites with deeper water table are covered by sandy, highly permeable soils and predominantly pine forests, the valleys often have loamy soils with very shallow groundwater. Valleys are covered by grassland and forests in areas with shallow groundwater, and arable land elsewhere.

The soils in the loess region, chernozems and luvisols, are mostly loamy and tend to have layers with low water permeability, so that in areas with higher slopes floods are generated, namely in the Saale and the Mulde tributaries. The sediments normally have high field capacities and nutrient supply, and therefore the loess subregion is an area with very intensive agricultural land use.

The soils in the mountains, mainly thin cambisols, are formed by weathering products and redeposited rocky materials. The mountainous areas are often covered by forests and grassland.

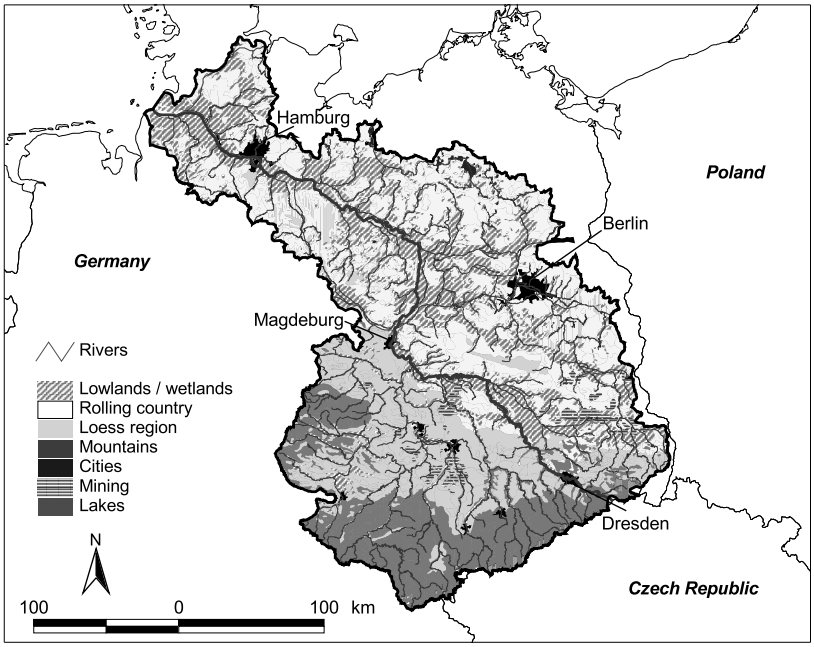

Figure 2.2. The German part of the Elbe river basin.

2.2.3 Input data and data pre-processing

Spatial data

All spatial information (the digital elevation model (DEM), the soil, land use and water table contour maps) were stored on a grid format with 250 m resolution. Subbasin boundaries were provided by the German Federal Environmental Office (UBA) and partly subdivided, using the DEM and the geoinformation system GRASS. The whole Elbe basin was subdivided into 226 subbasins. In addition, 12 mesoscale catchments of the Elbe river basin were selected and modeled separately to get a better understanding of the hydrological behavior of the main subregions of the whole basin. They were disaggregated into 20 - 120 subbasins, depending on their total area. Figure 2.1 shows their location in the basin, and Table 2.1 specifies their statistics like the size and the ratio of the main land use classes.

The land use map was created using the European CORINE land cover map (Dollinger and Strobl, 1996). The original 44 land use classes were reclassified into 15 classes (Krysanova et al., 2000). Of the area modeled, 6.4 % is covered by human settlements and industry, 59.8 % by farmland (52 % cropland and the rest

grassland), 28.7 % by forest (coniferous forests 21.9 %), 4.4 % is open water and wetlands (mainly in the north) and 0.6 % is bare soil (coal mines) and heathland.

Table 2.1. The area and land cover of the subbasins in the Elbe catchment where nested investigations were performed.

catchment	gauge station	settlement [%]	arable [%]	grassland [%]	forest [%]	others [%]	area [km^2]
Spree	Bautzen	9	54	1	33	3	280
Löcknitz	Gadow	2	65	14	19	1	447
Stepenitz	Wolfshagen	3	77	7	12	2	574
Upper Saale	Blankenstein	6	48	13	28	5	1013
Weiße Elster	Greiz	8	55	2	32	3	1236
Jeetze	Luechow	2	62	12	22	2	1347
Nuthe	Babelsberg	5	43	13	36	3	1993
Mulde	Wechselburg	13	47	2	34	4	2091
Bode	Hadmersleben	5	60	5	27	2	2689
Unstrut	Oldisleben	1	69	3	20	7	4174
Saale	Laucha	5	65	3	24	3	6220
Saale	Calbe-Griz.	4	46	4	42	5	23687
Elbe	Neu-Darchau	6	52	8	29	5	80258

Soil information was taken from the soil map of the Federal Republic of Germany (scale 1:1,000,000). The map distinguishes between 72 different soil types. Each soil type has a so called 'leading profile' with up to 8 different layers. Together with the soil map, physical parameters for each layer, like texture classes, porosity, bulk density, humus and organic nitrogen content are provided. Saturated conductivity was estimated for each soil layer using pedotransfer functions. The DEM is a composite of elevation maps with different scales and was resampled to a spatial resolution of 250 m to be compatible with the other spatial information.

In simulations of the whole Elbe basin, the observed flow from the Czech Republic was added to that one calculated by SWIM and then routed through the subbasins to the outlet of the river basin.

Climate data preprocessing

Located in and around the Elbe basin are about 90 stations where climate information is measured, and approximately 400 additional rain gauge stations. The time series from 1961 to 1996 were selected and evaluated. The spatial density

of climate stations in the Elbe basin is relatively low in some areas (see Figure 2.1), and therefore a special investigation was made to select a satisfactory interpolation algorithm. Climate information represents the main forcing data of the model, and investigation of spatial hydrological processes makes sense only if the spatial distribution of the climate data input has a sufficient precision (Haberlandt and Kite, 1998).

Table 2.2. The Nash and Sutcliffe (1970) efficiencies of the cross validation of the interpolated climate input data.

interpolation method	T average	radiation	precipitation
Thiessen polygons	-0.214	-0.046	-0.006
inverse distance	0.241	0.302	0.303
ordinary kriging	0.238	0.399	0.355
external drift kriging	0.715	0.384	0.305

Four interpolation methods were compared: Thiessen Polygons (TP), Inverse Distance (ID), Ordinary Kriging (OK) and External Drift Kriging (EDK) (Haberlandt and Kite, 1998). The advantage of kriging techniques is that the spatial autocorrelation of the data is used to interpolate them (Journel and Huijbregts, 1978), and the advantage of the EDK method is that it is possible to take into account additional data, like the elevation (DEM). The spatial autocorrelation functions γ (called semivariograms) have to be calculated beforehand. They are estimated using experimental semivariograms γ^*:

$$\gamma^* = \frac{1}{2N(h)} \sum_{u_i - u_j = h} \left(Z\left(u_i\right) - Z\left(u_j\right)\right)^2 \tag{2.12}$$

where h is the search distance $[m]$, and $Z(u_i)$ and $Z(u_j)$ are two observations from points u_i and u_j (in our case climate stations) with the distance h. *N(h)* is the number of pairs $[Z(u_i), Z(u_j)]$.

A cross validation was then applied to select the method with the best results, where the Nash and Sutcliffe (1970) efficiency (see Equation 2.14) was the criterion to estimate the quality of the interpolation technique. Table 2.2 lists the climate variable, the interpolation method and results of the cross validation.

It can be seen that the TP method, the standard method used in SWIM and SWAT before, always gives the worst results. In this study the EDK technique was used to interpolate temperature (with the DEM as additional information), and the OK method was used to interpolate radiation and precipitation.

2.2.4 Modelling strategy

First, the model was applied separately to 12 subbasins of the Elbe located in different regions (catchment area from 280 to 23,690 km^2, see Figure 2.1). The hydrological processes were calibrated on a daily time step using the observed river discharge for comparison. A rough non-generic automatic calibration was performed using a Monte Carlo method combined with the Latin Hypercube method (Tarantola, 2000) in order to make sure that all physically meaningful parameter combinations are considered in the modeling procedure. Afterwards, fine-tuning of the model was done by hand. The best 20 results of the automatic calibration for each subregion (mountains, loess area, lowlands) of the Elbe were taken and statistically evaluated applying a cluster analyzes, where the parameter sets of the simulation results were used as independent values to classify them, in order to investigate how typical the parameter sets are for the subregions of the Elbe basin. Besides the initial storage values and the radiation correction factor, the following three parameters were used to calibrate the hydrological processes in the model: the parameter *rcor* to tune river flow routing, the parameter *sccor* to calibrate the saturated soil conductivity and the groundwater reaction factor α to adjust the base flow. The simulated river discharge was compared with the measured discharge for an eight year period. Statistical evaluation of the results was done by analyzing the long-term difference of the observed river discharge Q_{obs} against the simulated one Q_{sim} in percent (the relative difference in discharge or discharge balance):

$$discharge\ balance = \frac{Q_{sim} - Q_{obs}}{Q_{obs}} \cdot 100 \tag{2.13}$$

and calculating the efficiency criteria of Nash and Sutcliffe (1970) for Q_{sim} against Q_{obs} on a daily time step t:

$$efficiency = 1 - \frac{\sum_t \left(Q_{sim_t} - Q_{obs_t}\right)^2}{\sum_t \left(Q_{obs_t} - \overline{Q}_{obs_t}\right)^2} \tag{2.14}$$

The efficiency can vary from minus infinity to 1.

The spatial behavior of the hydrological processes was analyzed using contour maps of the water table and observed time series of groundwater levels. The long-term mean water table in three lowland basins (the Stepenitz basin with an area of 574 km^2, the Löcknitz basin with 447 km^2, and the Nuthe basin with 1993 km^2) was simulated and calibrated.

Based on the calibration results, the hydrology of three selected subbasins and the entire Elbe basin was validated: one subbasin in the lowlands (the Löcknitz basin, gauge station Gadow), one in the loess area (the Mulde basin, gauge station Wechselburg), and one from the mountains (the Upper Saale basin, gauge station Blankenstein). The same three subbasins were used, together with the entire Elbe basin, in parallel in the sensitivity and uncertainty study. The results from the mesoscale catchments were analyzed. Some general patterns were apparent when comparing the values of the calibration factors in the catchments of the main subregions.

Table 2.3. Ranking of the sensitivity of the main calibration parameters to the model results 'discharge balance' and 'efficiency' for the geographic regions in the German Elbe basin.

	Discharge balance			Efficiency		
	Blankenstein (mountains)	Wechselburg (loess)	Gadow (lowlands)	Blankenstein (mountains)	Wechselburg (loess)	Gadow (lowlands)
rad	1	1	1	3	3	3
rcor	4	4	4	1	2	2
sccor	2	2	2	2	1	1
α	3	3	3	4	4	4

It was possible to divide the parameter sets into three main clusters: one set for the lowlands, one for the loess area, and one for the mountains. Based on the information gained from the mesoscale catchments, the parameter sets were taken and used to validate the hydrological processes over the whole Elbe basin.

In parallel, a sensitivity and uncertainty analysis was performed, so that the robustness of the simulated hydrological results could be estimated (see Chapter 2.4).

2.3 Results and discussion

2.3.1 Calibration using river discharge dynamics

The quality of the model results (simulated water balance and river discharge) is comparable with the results of recently published macroscale applications of other models (Abdulla and Lettenmaier, 1997; Nijssen et al., 1997; Kite and Haberlandt, 1999; Krysanova et al., 1999a; Haddeland et al., 2002; Klöcking and Haberlandt, 2002). Figures 2.3 to 2.5 show plots with simulation results of river discharge. The first one is an example from the mountains, the second is a basin in the loess region, and the third from the lowlands. The plots demonstrate a comparison of observed against simulated daily and monthly river discharge.

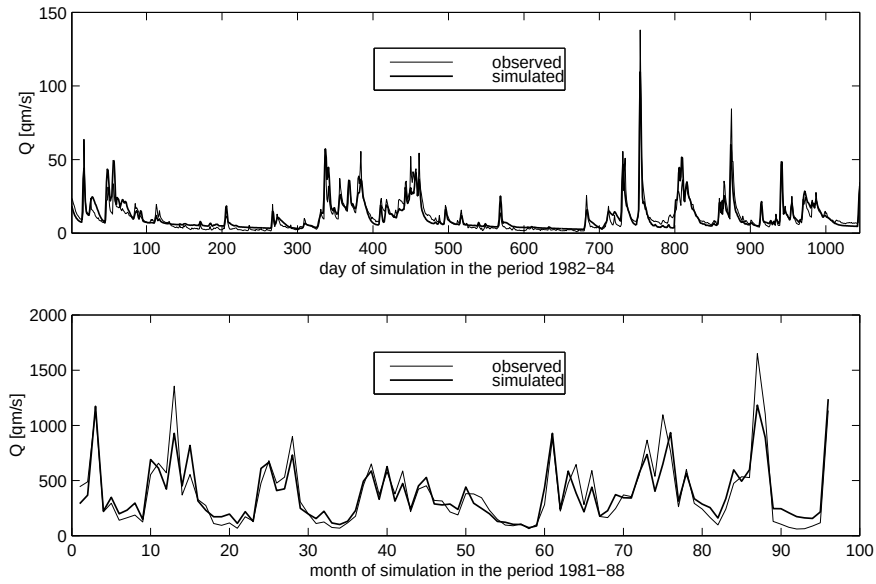

Figure 2.3. River discharge at the gauge station Blankenstein (river Saale, 1,013 km^2, mountains). Upper plot: simulated against observed daily river discharge (1982-84), lower plot: comparison of the monthly discharge (1981-88) in accumulated mean daily runoff (m^3 s^{-1}) per month.

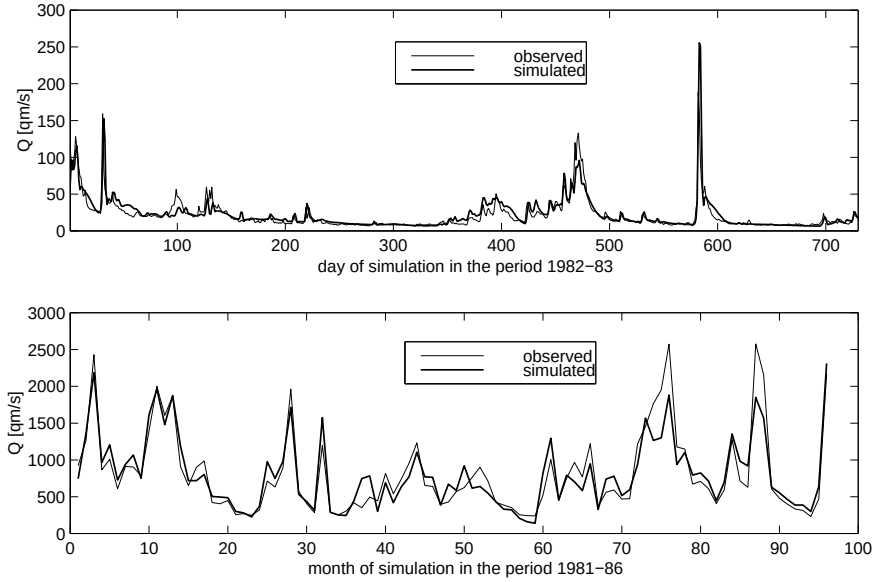

Figure 2.4. River discharge at the gauge station Wechselburg (river Mulde, 2,091 km^2, loess area). Upper plot: simulated against observed daily river discharge (1982-83), lower plot: comparison of the monthly discharge (1981-88) in accumulated mean daily runoff (m^3 s^{-1}) per month.

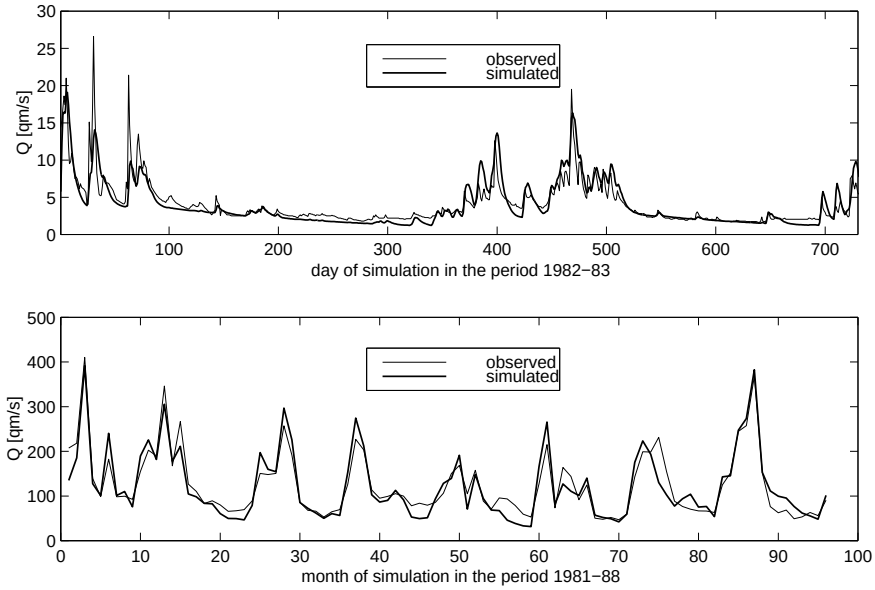

Figure 2.5. River discharge at the gauge station Wolfshagen (river Stepenitz, 574 km^2, lowlands). Upper plot: simulated against observed daily river discharge (1982-83), lower plot: comparison of the monthly discharge (1981-88) in accumulated mean daily runoff (m^3 s^{-1}) per month.

Simulation results are mostly satisfactory. The largest differences occur in

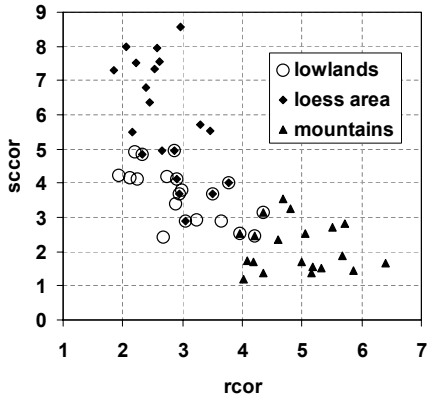

Figure 2.6. The values for saturated soil conductivity correction (*sccor*) and river routing correction (*rcor*) of the best 20 simulations for the subregions in the Elbe basin.

the Stepenitz basin (lowland), and the best fit is achieved in the mountain subbasin, where the relief intensity is high and it is therefore easier to reproduce the hydrological processes. The results of the other mesoscale subbasins confirm the gradient in the results from mountainous to lowland catchments. The most sensitive model parameters were the factor *sccor* to correct the saturated soil conductivity, the factor *rad* to correct radiation and the factor *rcor* to correct river routing (see also the sensitivity study in Chapter 2.4.1 and the ranking of the calibration parameter sensitivity in Table 2.3). Table 2.4 summarizes the results for the total calibration period 1981-88.

Some main patterns were obvious. The first is that the results (efficiency and discharge balance) are scale-independent, they are in the same range for smaller catchments as they are for the larger ones. The next is that the values of the main correction factors were typical for the landscape of the specific subbasins (see Figure 2.6). When applying the cluster analysis on the best 60 results of the automatic calibration (see Chapter 2.2.4), it is possible to divide the parameter sets into one cluster for the mountains, one for the loess area, and one for the lowlands: The routing correction factor *rcor* tends to have lower values for the lowland subbasins (Löcknitz, Stepenitz and Nuthe) than for the mountain catchments (upper Saale, Weiße Elster). The catchments with mainly loess soils (Bode and Unstrut) have high *rcor* and very high *sccor* values. It is obvious that the parameters given in the soil database underestimate the saturated conductivity of

loess sediments. The reason might be that the saturated conductivity of the soil sediments is measured in laboratories. Structures in soil profiles like cracks and macropores, responsible for fast preferential flow, are therefore underestimated without calibration. The factor α to correct the groundwater reaction time was rather insensitive to river discharge and mostly has the same value. In lowland catchments, it was determined using the knowledge gained during the investigation of groundwater dynamics (see Chapter 2.3.2). The calibrated parameters of the entire Elbe basin are very similar to the ones of the lowland catchments. The lowlands cover the largest part of the Elbe basin, and apparently have a prevailing influence on river discharge in the basin.

Table 2.4. The Nash and Sutcliffe (1970) efficiencies of observed against simulated river discharge and the discharge balance for an eight year period (1981-88, *1981-86). The catchments are sorted by their area.

river	gauge station	topography	area [km^2]	efficiency daily	efficiency monthly	discharge balance
Spree	Bauzen	mountains/ loess	280	0.71	0.71	1
Löcknitz	Gadow*	lowlands	447	0.74	0.82	-1
Stepenitz	Wolfshagen	lowlands	574	0.72	0.86	-1
Upper Saale	Blankenstein*	mountains	1013	0.79	0.85	0
Weiße Elster	Greiz	mountains	1236	0.75	0.82	2
Jeetze	Luechow	lowlands	1347	0.65	0.72	1
Nuthe	Babelsberg	lowlands	1993	0.61	0.66	0
Mulde	Wechselburg*	mountains/ loess	2091	0.75	0.87	2
Bode	Hadmersleben	mountains/ loess	2689	0.72	0.81	-1
Unstrut	Oldisleben	mountains/ loess	4174	0.76	0.85	0
Saale	Laucha	mountains/ loess	6220	0.7	0.82	-2
Saale	Calbe - Grizehne	integrates all	23687	0.76	0.87	-1
Elbe	Neu-Darchau*	integrates all	80258	0.89	0.94	-1

2.3.2 Spatial validation using water table dynamics

Another option to validate the hydrological processes, especially in the lowland river basins, was to use contour maps of the water table and time series of observed monthly groundwater levels (Hattermann et al., 2002). First, the simulated mean annual water table depth of all subbasins in the Stepenitz catchment, the Nuthe catchment and the Löcknitz catchment was calibrated using the groundwater reaction factor α (see Equation 2.8). The mean square error of the long-term mean observed against the mean simulated water table depth in all subbasins was 0.08 m^2. The parameter α of the subbasins had values between 0.1 (loamy sediments) and 0.3 (sandy sediments), and this additional information was used to estimate the reaction factors for the total basin. The lowland subbasins with mainly sandy soils received a retention value of 0.25, the subbasins mainly covered by loess a retention value of 0.1.

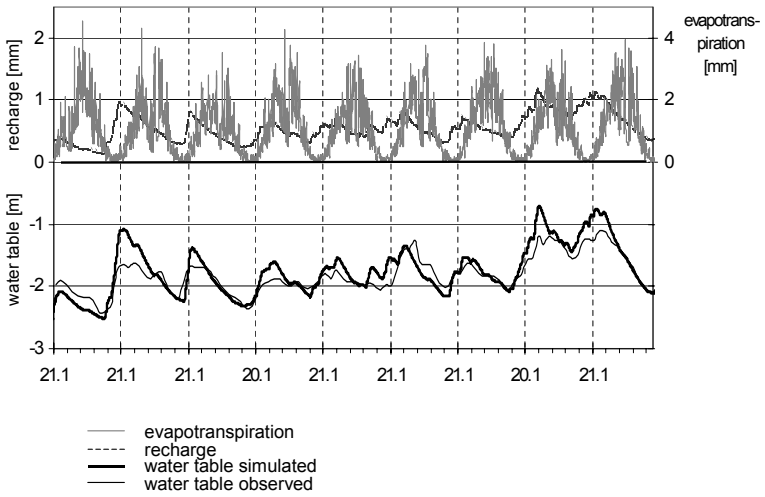

Figure 2.7. The simulated water table, simulated groundwater recharge and simulated evapotranspiration of one subbasin in the Stepenitz river catchment. The observed water table data are from a well located in the subbasin (Wendisch Pribor).

After calibrating the mean water table, the simulated daily water table was compared with the observed monthly time series, without further calibration. Figure 2.7 shows the comparison of the observed water table against the simulated one from a subbasin in the Stepenitz river. The simulated daily water table shows a good fit with the observed monthly values, when considering the amplitude of the curves and the fluctuations. Also shown is the simulated groundwater

recharge and the simulated evapotranspiration during the period. The simulated water table and the recharge have nearly the same dynamics, but the water table curve is smoothed because the water percolates with some delay from the last soil layer into the aquifer. During the winter season, the groundwater balance (recharge - discharge) is positive and the levels increase fast, while during the spring and summer the increasing evapotranspiration is the reason for a negative balance and a relatively smoothed recession curve of groundwater.

2.3.3 Validation for meso- and macroscale catchments

The validation was carried out in three subcatchments of the Elbe (the upper Saale, the Löcknitz, and the Mulde basins) and for the total Elbe basin with a daily time step, over a six year period (1987 - 1992). Table 2.5 summarizes the results.

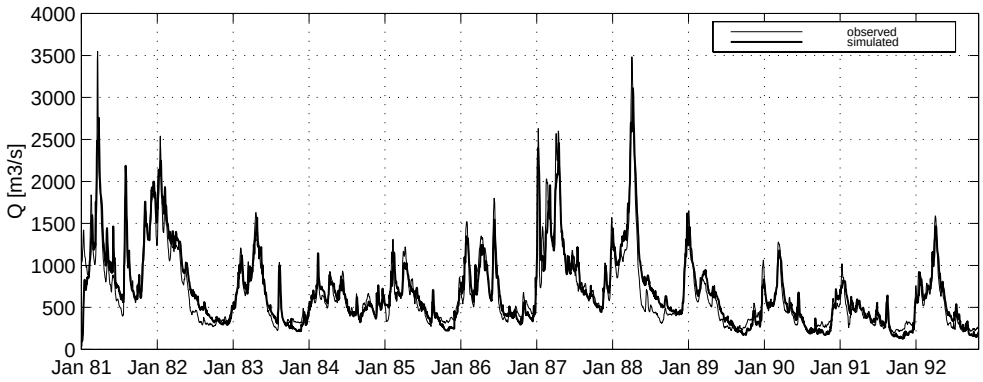

Figure 2.8. The river discharge of the total Elbe basin at Neu Darchau (1981-92). The first part (1981-86) is the calibration period and the second (1987-92) the validation period

Table 2.5. The efficiency criteria for the observed and simulated river discharge of the validation period (1987-92).

river	gauge station	topography	efficiency daily	efficiency monthly	discharge balance
Saale	Blankenstein	mountains	0.81	0.86	4.2
Mulde	Wechselburg	mountains / loess	0.76	0.83	-6.1
Löcknitz	Gadow	lowlands	0.72	0.81	6.6
Elbe	Neu-Darchau	integrates all	0.92	0.94	4.0

The results are between 0.72 and 0.92 for the daily efficiency and 0.81 and 0.94 for the monthly efficiency. Except for the lowland catchment, the discharge balance is positive in all simulations. The highest difference is that for the whole basin with a value of 4.0 %. Occasionally, the validation period has a mean precipitation below average, so that the average river discharge during the calibration period (1981-86) is 728 m^3 s^{-1} against 638 m^3 s^{-1} during the validation period (1987-92). Figure 2.8 presents the comparison of observed and simulated discharge at the outlet of the total Elbe basin, the first six years (1981-86) represent the calibration period, and the next six the validation period (1987-92).

2.4 Sensitivity and uncertainty analysis

In order to get a better understanding of the model behavior and to evaluate the simulated results, the sensitivity of the main input and calibration parameters to model results was tested and an uncertainty analysis performed in parallel to the model validation. Three subbasins of the Elbe, the rivers Upper Saale (mountains, 1013 km^2), Mulde (mountains / loess area, 2091 km^2), Löcknitz (lowlands, 447 km^2), and the total Elbe basin were selected to investigate the sensitivity and uncertainty. The subbasins were chosen because they cover the main subregions of the Elbe basin. The intention of the analysis is to investigate how robust or reliable the results of the hydrological validation are. One objective is to illustrate the sensitivity of the model results to changes in the basic input parameters. Another is to investigate the uncertainty of the model results when applying the model to catchments without observed data in different regions of the Elbe river basin or under similar conditions elsewhere.

The choice of the parameters is specified above in the model description (Chapter 2.2.1), where

- some of the parameters are calibration factors (*sccor* for saturated soil conductivity, *rcor* for river routing, *rad* for radiation, α for groundwater return flow and water table depth). The calibration factors were sampled randomly, within their physically meaningful limits, whereby the parameter limits are site-specific and set based on information gained during the nested model validation (Chapter 2.3).

- some other parameters were chosen to understand the sensitivity of the

model to input data, as provided by the local authorities (*slope* to analyze the influence of the topography), or as taken from tables (*be* and *cnum* to analyze the influence of the biomass energy ratio and the SCS curve number).

The parameters *be*, *rad*, *slope*, and *cnum* were sampled from a normal distribution with a mean of one, and the values were multiplied by the input data of the biomass energy ratio, radiation, slope and SCS curve number, in order to assess the sensitivity of the model results to higher or lower input parameters.

Three hundred parameter sets were generated for each of the four basins using the Latin Hypercube method in order to restrict the number of simulations (Richter et al., 1996). Each parameter set was the input for a four-year simulation run. Two model results were taken into account: the discharge balance and the efficiency criteria after Nash and Sutcliffe (1970) of daily simulated against daily observed discharge (Equation 2.13 and 2.14).

2.4.1 Sensitivity analysis

The sensitivity of model results to the parameters was estimated using the Partial Correlation Coefficients (PCC) of the rank transformed data (the simulation results, Tarantola, 2000). For a sequence of observations, the correlation Cor between the specific input variable Xj (model parameter) and the model output Y (discharge balance and the efficiency) is defined by

$$Cor_{XjY} = \frac{\sum_{i=1}^{m} \left(X_{ij} - \bar{X}_j\right)\left(Y_i - \bar{Y}\right)}{\left[\sum_{i=1}^{m} \left(X_{ij} - \bar{X}_j\right)^2\right]^{1/2} \left[\sum_{i=1}^{m} \left(Y_i - \bar{Y}\right)^2\right]^{1/2}} \tag{2.15}$$

with

$$\bar{Y} = \sum_i Y_i/m, \;\; \bar{X}_j = \sum_i X_{ij}/m, \quad i = 1, ..., m. \tag{2.16}$$

The correlation coefficient provides a measure of linear relationship between Xj and the model output Y.

Figure 2.9 shows the results of the sensitivity analysis. The upper plot illustrates the correlation of the randomly sampled parameters with the discharge balance, the lower one with the efficiency. In all cases, radiation has the highest correlation with the discharge balance, followed by the saturated soil conductiv-

ity, while the other parameters have nearly no influence. The result confirms the well-known fact that a correct reproduction of evapotranspiration dominates the quality of the simulated water balance.

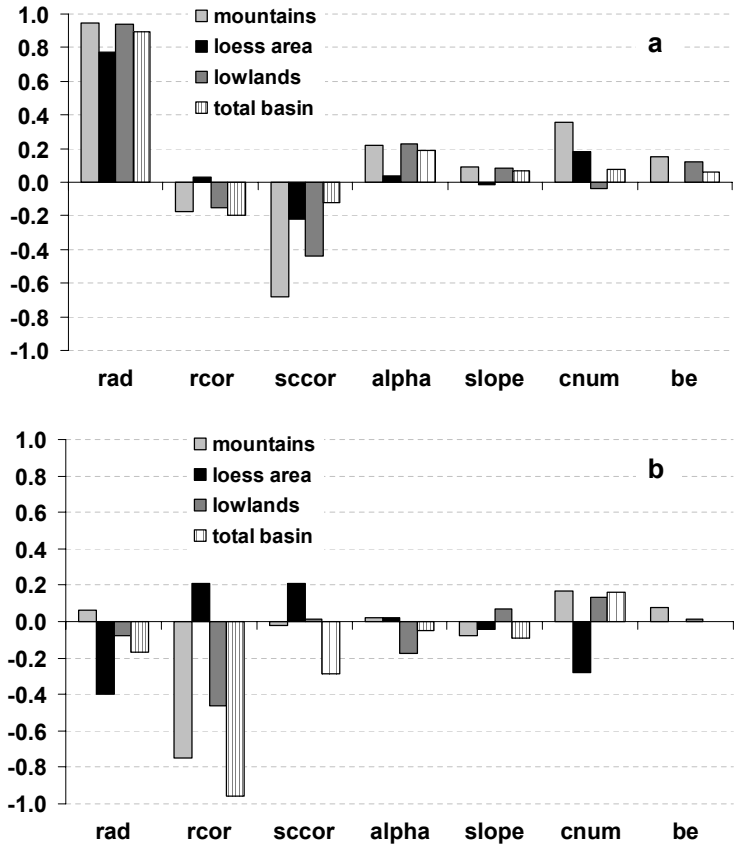

Figure 2.9. The correlation of the model results to the model parameters and input data, based on 300 Monte Carlo simulations, using the Latin Hypercube method (top: sensitivity to water balance, bottom: sensitivity to efficiency).

The correlation of the parameters to the model result 'efficiency' is not so uniform for the different subbasins. The influence of the routing parameter *rcor* is very high for the total basin and the mountainous catchment, relatively high for the lowland basin and relatively low for the catchment from the loess area. This is important, because the efficiency is a criteria to analyze whether the model is able to reproduce the water fluxes dynamically (e.g. the flow regime and generation of floods). Apparently, routing is the most important process in areas with high relief intensity (mountains), whereas in loess basins, having soils with high water holding capacity, also the correct simulation of evapotranspiration has

a relatively high influence on the quality of the dynamic model results. Moreover, the sensitivity of the parameters for the loess area is often in direct opposition to the sensitivity of the other catchments to these parameters (see results of the uncertainty analysis). Striking is the low sensitivity of the model to changes in the parameter for biomass allocation (*be*), because the leaf area index is a function of above ground biomass in SWIM and related to plant transpiration.

2.4.2 Uncertainty analysis

The uncertainty was investigated using histograms of the two criteria efficiency and discharge balance, based on the 300 simulations for every basin as described in Chapter 2.4.1.

Table 2.6. Statistical results of the uncertainty analysis.

Discharge balance	mean	median	90th percent.	75th percent.	25th percent.	10th percent.	min.	max.
Mountains	0.4	0.1	6.7	4.1	-2.7	-5.5	-9.5	14.2
Loess/mount.	8.4	8.0	18.2	13.7	3.7	-1.6	-10.2	30
Lowlands	1.6	1.0	14.7	8.9	-5.1	-9.9	-18.7	32.2
Elbe basin	2.6	1.8	10.7	7.1	-1.7	-4.9	-9.0	21.4

Efficiency	mean	median	90th percent.	75th percent.	25th percent.	10th percent.	min.	max.
Mountains	0.7	0.71	0.77	0.75	0.65	0.6	0.42	0.79
Loess/mount.	0.62	0.63	0.7	0.67	0.59	0.53	0.32	0.77
Lowlands	0.64	0.65	0.72	0.69	0.61	0.57	0.36	0.77
Elbe basin	0.73	0.75	0.86	0.82	0.64	0.57	0.44	0.91

Figure 2.10 shows eight histograms demonstrating the results of the uncertainty analysis. The distribution of the model criteria 'discharge balance' is plotted in the upper part of the figure. The bottom plot illustrates the distribution of the efficiency. Each subplot has four histograms, three for the subbasins from the mountains, the loess area and the lowlands, and one for the total Elbe basin. The

statistical values of the histograms (mean, percentiles, minimum and maximum) are summarized in Table 2.6.

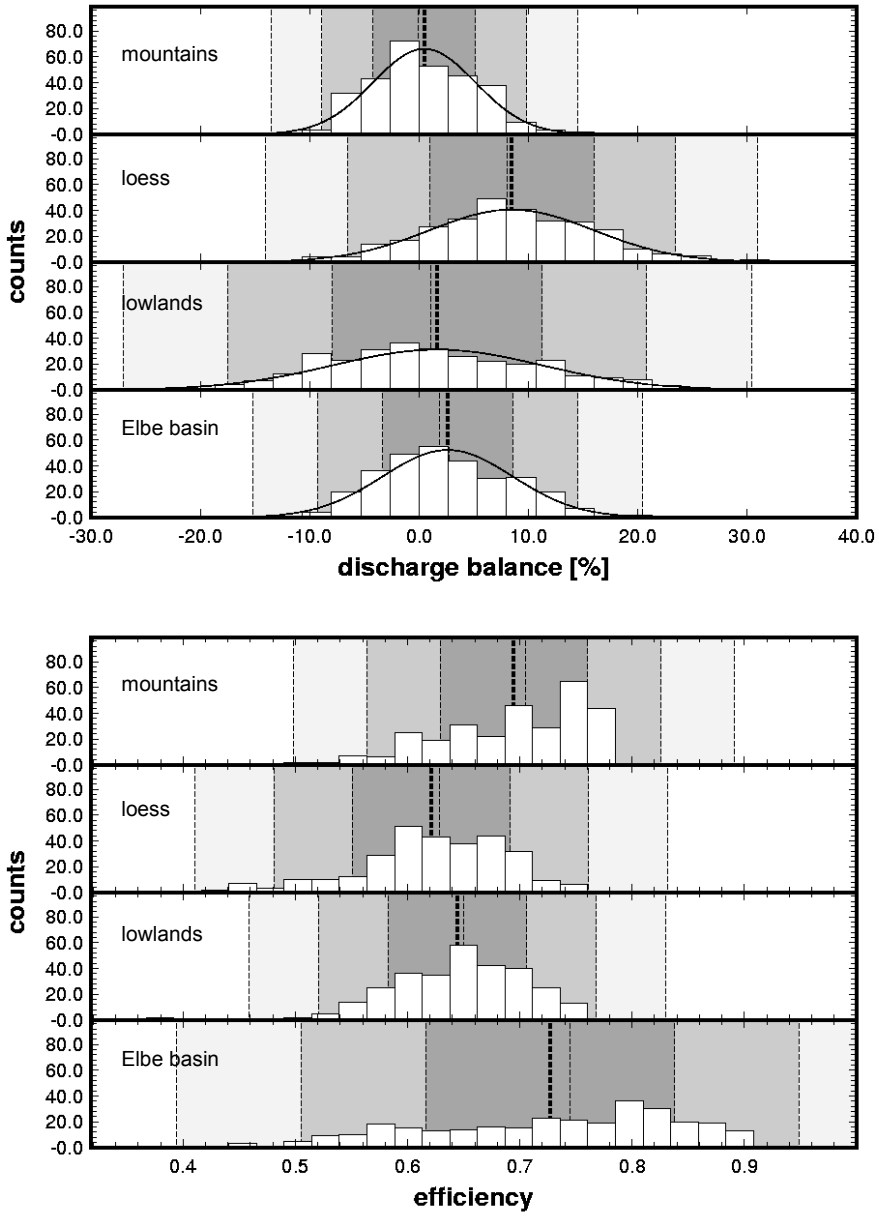

Figure 2.10. The results of the uncertainty analysis. Upper plot: distributions of the model criterion 'discharge balance', based on 300 Monte Carlo simulations, for basins from the mountains, the lowlands, the loess area, and the total basin. Lower plot: distributions of the model criterion 'efficiency'.

The model gives a good reproduction of the water balance, the mean value of 300 simulations is around zero for all catchments except those in the loess area,

where the model tends to overestimate discharge (and, hence, underestimates evapotranspiration) slightly. It was already discussed in Chapter 2.3.1 that the hydraulic parameterization of loess soils involves a lot of uncertainties when the parameters are transferred from lab measurements to the basin scale, so that the inherent heterogeneity of the soils (cracks, macropores, textural characters) cannot be represented in macroscale polygon covers. The sensitivity analysis as well as the uncertainty analysis indicates that there is a high potential to improve the correct representation of loess soils in the soil data base, and therefor also in the model.

The distributions of the efficiency values are presented in the lower plot of Figure 2.10. All values are above 0.3, the mean values above 0.6. The conclusion is that also taking into account the uncertainty in the parameter input, the model reproduces satisfactory the dynamic flow pattern of the river discharge in different basins. The region where the model shows the best performance with the highest efficiencies is that from the mountainous catchment; this is understandable from our previous discussion (Chapter 2.4.1). The lower efficiencies, with higher standard deviation, are obtained for the loess and lowland catchment. This result agrees with the outcome of the model validation, where the nested lowland catchments produced the poorest results, while the validation of the hydrological processes in catchments from the mountains gave the best results. In lowland catchments, the hydrological conditions are often unclear (groundwater flow, ponds, wetlands drainage network) and it is impossible to reproduce them with higher accuracy without detailed information.

The distributions of the total Elbe basin for the discharge balance and for the efficiency are a composite of the results of the nested subbasins above. The simulated discharge is slightly overestimated. The average of the efficiency distribution is better than those in the smaller subbasins but has a high variation (see Table 2.6).

The overall result of the uncertainty analysis is that in macroscale applications of SWIM 90 % of the simulations have an efficiency above 0.53 and an absolute deviation between observed and simulated river discharge lower then 9.9 %. The uncertainty in simulating the hydrological processes in lowland and loess subareas is higher, while the results in mountainous parts of the basin show a robust and stable performance, and are not very sensitive to small changes in the model

parameters.

2.5 Summary and conclusions

The SWIM model has proven to provide good simulation results on a daily time step in terms of river runoff for meso- to macroscale basins (200 - 80,000 km^2) after some model calibration correcting mainly four parameters (the saturated soil conductivity, the river routing factor, global radiation and the groundwater reaction factor). Some general patterns were apparent when comparing the values of the calibration factors in the 12 nested catchments, so that it was possible to divide the parameter sets into three main clusters, one for the lowlands, one for the loess area and one for the mountains. The validation results were better in mountainous catchments (efficiency of daily results 0.75 - 0.79, of monthly ones 0.82 - 0.84) than in lowland basins (0.61 - 0.72 daily efficiency, 0.66 - 0.86 monthly efficiency). It was possible to reproduce also local hydrological processes like water table dynamics inside subbasins, using contour maps of the water table depth and observed groundwater level data. The additional use of water table maps and observed groundwater levels has a high potential to enhance the simulation of spatially distributed hydrological processes, but the investigation is not finished and has to be expanded (Hattermann et al., 2004). This is crucial, because the primary idea of eco-hydrological models like SWIM and SWAT is to simulate processes in subbasins and hydrotopes in addition to river discharge, but they are often validated using exclusively the observed river discharge for comparisons. The river discharge is an integral characteristic of the hydrological processes in the whole basin, but its correct representation by the model does not guarantee the adequacy of the spatial and temporal dynamics of all water components in the basin.

The calibration and validation of the mesoscale subcatchments, covering the main subregions of the Elbe basin, was used to understand the hydrological characteristics in the different parts of the total basin. It was found that the best reproduction of the hydrological processes in the total Elbe basin was possible with a parameter set very similar to the one used for the lowland subbasins. Apparently, the hydrological processes of the lowlands dominate the dynamics of the river flow regime in the Elbe basin.

The sensitivity and uncertainty analyzes show that the model results were robust but more stable in mountainous catchments than in lowland and loess parts of the model area. The most sensitive calibration parameter corresponding to the water balance was the radiation correction factor, indicating that evapotranspiration is the process that dominates long-term water fluxes. Regarding the efficiency, the saturated conductivity correction factor and the routing correction factor were the most sensitive tuning parameters in lowland and loess area model applications, in mountainous catchments only the routing correction factor, indicating that river routing is the crucial process driving the dynamics of river discharge in mountainous areas with high elevation intensity. In lowlands, the percolation of water through the soil layers is more important than in mountains. In order to improve the simulation results in lowlands and in particular in catchments covered by loess soils, more efforts are needed to create better soil maps for macroscale applications.

The sensitivity analysis described in this study is a comprehensive tool to find the important processes in different landscapes, but also to reveal shortcomings in the model concept. For example, we suggest further exploration of the low sensitivity of the model results to changes in the biomass energy ratio (Figure 2.9), where we expected a significant negative correlation instead of the weak positive one.

The overall conclusion of the study is that model applications on the macroscale should always include additional investigations in smaller subbasins to analyze and understand the special characteristics of the subregions where that comprise the entire basin. Different processes play a dominating role in different areas of the basin (like river routing in mountains), where the implementation of additional observations (like groundwater records) in the validation procedure helps to improve the model results.

Acknowledgments

The authors would like to thank all their colleagues at the PIK who contributed to this paper with technical help, particularly Uwe Haberlandt and David Kneis. Part of this work was supported by the German BMBF programme GLOWA (GLObal WAter) Elbe.

ENVIRONMENTAL MODELLING & SOFTWARE 19, 1039–1051 (2004)

Chapter 3

Integrating groundwater dynamics in regional hydrological modeling

Shorttitle: Groundwater Dynamics in Regional Modeling

Keywords: hydrological validation; eco-hydrological model; groundwater dynamics; groundwater module; water level trend.

Hattermann, FF*, Krysanova, V, Wechsung, F, Wattenbach, M
Potsdam Institute for Climate Impact Research
* Full address of the corresponding author:
Dipl.-geoecol. Fred Fokko Hattermann
Global Change and Natural Systems Department
Potsdam Institute for Climate Impact Research
P.O. Box 601203, Telegrafenberg
14412 Potsdam
Germany
Fax: +49 331 288 2600
Tel. +49 331 288 2649
E-mail: fred.hattermann@pik-potsdam.de

Abstract The paper presents an integrated catchment model and a method with which it is possible to analyze local water table dynamics inside subbasins along with river flow on the regional scale. A simple but comprehensive mechanistic groundwater module coupled with the eco-hydrological model SWIM (Soil and Water Integrated Model), which integrates hydrological processes, vegetation, erosion and nutrient dynamics at the watershed scale, was used in the study. The reliability of the model results was tested under well defined boundary conditions by comparing the results with those from a two dimensional numeric groundwater model under steady-state and transient conditions as well as with observed data for two meso-scale basins, using contour maps of the long-term mean water table, observed groundwater level data in wells and observed river discharge. Especially in lowland catchments, where the water table is relatively shallow, the dynamics of river discharge are mainly influenced by changes in groundwater contribution to river flow. However, a correct reproduction of river discharge by hydrological models does not guarantee the adequacy of simulated spatio-temporal dynamics of soil moisture, water fluxes and groundwater in the basin. But even though the primary purpose of distributed hydrological models is to reproduce river discharge and water fluxes in the entire catchment, they are often validated using only the observed river discharge at the basin outlet for comparisons. The additional use of groundwater observations for model validation can serve as a measure to overcome the problem.

The study area is located in the lowland part of the Elbe river basin, which is representative for semi-humid landscapes in Europe, where water availability during the summer season is the main limiting factor for plant growth and crop yields. The importance of adequate reproduction of the groundwater dynamics is illustrated in an investigation of a decreasing trend in regional groundwater level.

3.1 Introduction

A comprehensive process based eco-hydrological model integrating surface and groundwater hydrology is presented (Krysanova et al., 1998; Arnold et al., 1994). The model was used to investigate the dynamics of groundwater in two basin-scale model applications, this being the scale typically used to evaluate the costs,

benefits and risks of changes in water resource management, and to analyze the impacts of climate and land use changes (Arnold et al., 2000). Hydrological models became a common tool to manage river catchments and to evaluate the impacts of human intervention (Abbott and Refsgaard, 1996; Singh, 1995). Consequently, the models have to include all hydrological processes of interest, but they are generally validated by using merely data of observed river discharge at the catchment outlet. It is often assumed that a good reproduction of fluctuations in river discharge implies a good reproduction of soil moisture and other hydrological processes inside the catchments like percolation, plant water uptake, and retention processes in groundwater. But especially in lowland catchments with a shallow water table groundwater plays a crucial role in the hydrological cycle and usually represents the main component in river discharge. Therefore the additional use of groundwater data for model validation makes it possible to have an insight in the local hydrological processes in subbasins. The direct use of groundwater observations has the advantage that the data are mostly commonly available, whereas it is impossible to measure the groundwater contribution to river flow in most practical cases. The objective of treating a river basin as a whole integrating all relevant processes has been identified not only by various national hydrological programs but also by the European Commission and is outlined in the Water Framework Directive (EC, 2000; Querner and van Lanen, 2001). The Water Framework Directive requires that previous, single discipline approaches to manage surface and groundwater resources should be combined in an interdisciplinary scientific framework (Hiscock et al., 2001).

The model used in this study is the eco-hydrological model SWIM (Soil and Water Integrated Model, Krysanova et al. 1998). The model SWIM was chosen, because it is process-based and uses only commonly available data as inputs and can therefore easily be applied at the meso- to macro-scale, where extensive field work to obtain input information is not feasible. It was developed especially for impact studies at the regional and basin scales and includes all relevant hydrological processes, like water percolation, surface runoff, interflow, groundwater recharge, plant water uptake, soil evaporation, and river routing. SWIM is based on two older model developments, the basin scale eco-hydrological model SWAT (Soil and Water Assessment Tool, Arnold et al., 1994) and the nitrogen transport model MATSALU (Krysanova and Luik, 1989). Arnold et al. (1993) first coupled

a simplified groundwater module (Smedema and Rycroft, 1983), allowing groundwater flow and groundwater table heads to be simulated at the subbasin scale, with SWAT to predict monthly surface and base flow. This simplified model is also part of SWIM and was developed further in order to have a better spatial representation of groundwater dynamics and to allow for automatic calibration. The application of a fully distributed physically based three-dimensional hydrological model in the study was impossible because of limits in data availability and computation resources. Besides, in some cases the basic assumptions regarding the boundary conditions have to be simplified (Sophocleous et al., 1999) in order to enable the application of such complex models. Many attempts to overcome this limitations and to reduce the level of complexity of the fully distributed physically based models have been considered, for example to divide the water cycle into vertical and lateral processes (Becker and Braun, 1999; Krysanova et al., 1998, 1999a; Refsgaard and Knudsen, 1996; Bergström, 1995). In some of these process based models, the groundwater component is reduced to a simple linear storage equation, where comparison with observed data is difficult. Other models are coupled with one-dimensional analytical solutions of the Boussinesq Equation for groundwater flow, where data requirements again represent a limiting factor in large-scale applications.

The simplified linear groundwater module presented in this study allows reproduction of the daily groundwater dynamics (water level and discharge) on a meso-scale and can be parameterized using physically meaningful data (Smedema and Rycroft, 1983). If these data are not available, water table fluctuations and at the same time groundwater recharge can be calibrated using only two parameters. The reliability of the simplified model is demonstrated by:

- comparing the model results with those obtained from a numerical solution of the nonlinear Boussinesq Equation (Kinzelbach and Rausch, 1995), using well defined boundary conditions and the same geo-hydrological parameters,
- comparing the model results with observed groundwater data from two meso-scale catchments.

A simulation experiment using the coupled model illustrates the importance of an adequate reproduction of groundwater dynamics in meso-scale model applications. A decreasing trend in groundwater level in a basin is investigated, where

the problem to be solved is hydrologically so complex that the model used should integrate all relevant hydrological processes and water management options like implementation of drainage systems and flow regulation.

3.2 Method and data

3.2.1 The Model

SWIM

The eco-hydrological watershed model SWIM integrates hydrological processes, vegetation, erosion and nutrient dynamics at the basin scale. A three-level scheme of spatial disaggregation from basin to subbasins and to hydrotopes is used. A hydrotope is a set of elementary units in the subbasin, which have the same geographical features like land use, soil type, and average water table depth. Therefore it can be assumed that they behave in a hydrologically uniform way. Water fluxes, plant growth and nitrogen dynamics are calculated for every hydrotope, where up to 60 vertical soil layers can be considered. The outputs from the hydrotopes are aggregated at the subbasin scale. The lateral fluxes are routed over the river network, taking transmission losses into account. A full description of the model can be found in Krysanova et al. (1998, 2000). An extensive hydrological validation of the model in the Elbe basin including sensitivity and uncertainty analyzes is described in Hattermann et al. (2002). In order to understand the structure of the model, the main hydrological processes in SWIM are briefly listed below.

The Priestley and Taylor (1972) or Penman-Monteith (Maidment, 1993) methods are used to estimate the potential evapotranspiration. Soil evaporation and plant transpiration are calculated as functions of leaf area index LAI using the approach of Ritchie (1972). The snowmelt component of SWIM is a simple degree-day equation.

Surface runoff is determined using a modification of the Soil Conservation Service (SCS) curve number technique. Water, which has infiltrated into the soil, percolates through the soil layers using a storage routing technique (Arnold, 1990). The water percolated from the bottom soil layer, which reaches the groundwater table with some delay time, is defined as groundwater recharge (see

Chapter 3.2.1).

Lateral subsurface flow or interflow is calculated simultaneously with percolation using a cinematic storage model. Interflow occurs in a given soil layer, if the soil layer below is saturated. Flow routing in the river network is calculated using the Muskingum flow routing method (Maidment, 1993), where a continuity equation is assumed.

A simplified EPIC approach (Williams et al., 1984) is included in SWIM for simulating arable crops (like wheat, barley, rye, maize, potatoes) and aggregated vegetation types (like e.g.'mixed forest'), using specific parameter values for each crop/vegetation type. The potential increase in biomass is adjusted daily if one of the plant stress factors is less than 1, considering stresses caused by water, nutrients and temperature. The water stress factor is calculated by comparing water supply in soil and water demand, assuming that about 30 % of the total water comes from the top 10 % of the root zone. The approach allows roots to compensate for water deficits in certain layers by using more water in other layers with adequate supply.

The classical groundwater model approach

Groundwater refers to saturated flow below the water table (Kinzelbach and Rausch, 1995). The rate and direction of flow can be expressed as differences in soil water potential (combined gravitational and pressure potential). The classical equation to describe groundwater potential flow is the Boussinesq Equation, which combines two basic laws of groundwater flow, Darcy's Law and the Law of Conservation of Mass (the Continuity Equation). The equation is discussed here briefly, because a numerical solution of the equation is used under well defined physical boundary conditions as a reference to compare its results (steady state and unsteady state) with the results of the simplified groundwater module used in this study. In case of two-dimensional flow these equations are (Sangrey et al., 1984): the Darcy's Law for water flow in porous media:

$$v_x = -k_x \cdot \frac{\delta h}{\delta x}, \; v_y = -k_y \cdot \frac{\delta h}{\delta y}, \tag{3.1}$$

the Continuity Equation for an infinitesimal small control volume:

$$-\nabla \cdot (m \cdot \vec{v}) + q_s = S \cdot \frac{\delta h}{\delta t}, \tag{3.2}$$

and the combination of Equation 3.1 and 3.2, the Boussinesq Equation:

$$-\nabla \cdot (m \cdot k_{xy} \cdot \nabla h) + q_s = S \cdot \frac{\delta h}{\delta t}, \tag{3.3}$$

where v_x and v_y denote the Darcy Velocity in x- and y- direction in $m\ s^{-1}$, k_x and k_y are the permeability in x- and y- direction in $m\ s^{-1}$, h is the height of the phreatic surface above a reference elevation or the piezometric head in m, S is the specific yield in $m^3\ m^{-3}$, q_s is a source term, k_{xy} is the permeability tensor and m is the thickness of the aquifer in m. Equation 3.3 is a second order non-linear partial differential equation and has to be solved numerically.

To derive an analytical solution of the Boussinesq Equation and to overcome the non-linearity, some basic simplifications have to be made, which are known as the Dupuit-Forchheimer assumptions. According to these, for flow in a sloping unconfined aquifer two main assumptions have to be used (Zissis et al., 2001):

1. The streamlines are horizontal and the hydraulic gradient is equal to the absolute slope of the water table.

2. The streamlines are nearly parallel to the sloping impermeable layer.

Numerous analytical solutions of the Boussinesq Equation, which can be applied to agricultural land drainage problems and to modeling the seepage towards unconfined horizontal aquifers, have been presented in the past (Hall and Mönch, 1972; Sangrey et al., 1984; Guo, 1997; Workman et al., 1997; Sloan, 2000; Zissis et al., 2001). These solutions basically need the same amount of geo-hydrologic parameters as the original Boussinesq Equation.

The simplified groundwater model approach

Smedema and Rycroft (1983) followed another approach also based on the Dupuit-Forchheimer assumptions. They derived a linear storage equation to predict the non-steady-state response of groundwater flow to periodic recharge from Hooghoudt (1940)'s steady-state formula, assuming that the variation in return

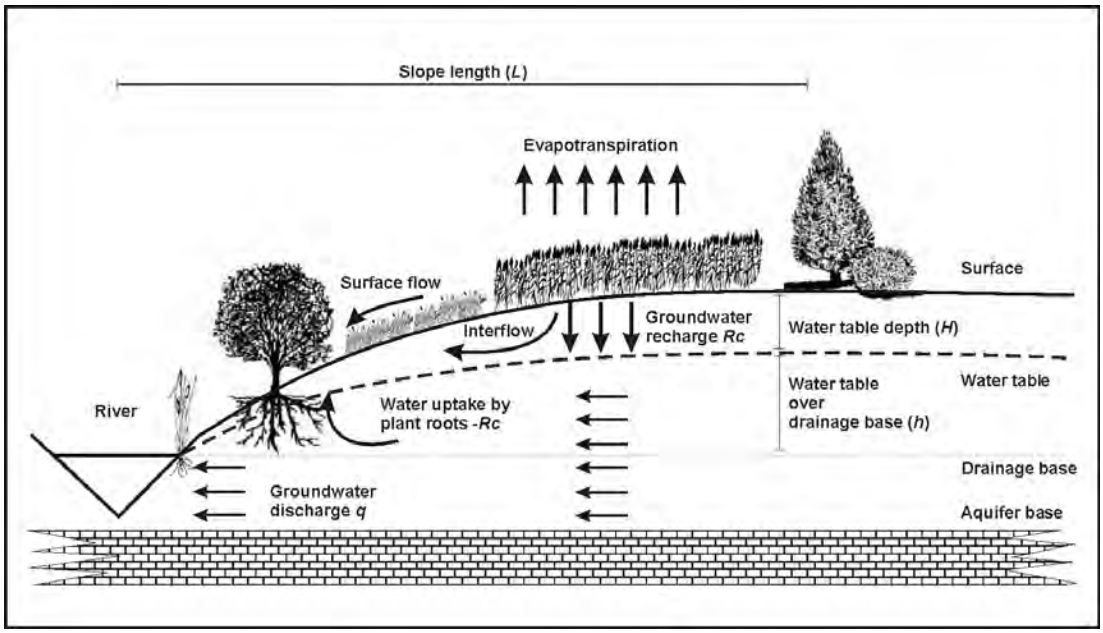

Figure 3.1. Diagram of a cross-section of a model watershed.

flow q in $mm\ d^{-1}$ at time step t is linearly related to the rate of change in water table height h in m (only headlosses in horizontal direction are considered):

$$\frac{dq}{dt} = \frac{8 \cdot T}{L^2} \cdot \frac{dh}{dt}, \tag{3.4}$$

where T is the transmissivity in $m^2\ d^{-1}$ and L the slope length in m (see Figure 3.1).

If the groundwater body is recharged by deep soil percolation or another source (Rc in $mm\ d^{-1}$) and is depleted by drain discharge (q), it follows that the water table will rise when $Rc - q > 0$ and fall when $Rc - q < 0$. The water table fluctuations may be described as (Smedema and Rycroft, 1983):

$$\frac{dh}{dt} = \frac{(Rc - q)}{C \cdot S}. \tag{3.5}$$

S is again the specific yield. From (3.4) and (3.5) it follows that by assuming C = 0.8:

$$\frac{dq}{dt} = \frac{10 \cdot T}{S \cdot L^2} \cdot (Rc - q) = \alpha \cdot (Rc - q), \tag{3.6}$$

so that the change in drain discharge dq/dt is proportional to the excess recharge

Rc-q, with α being the proportionality factor (reaction factor). Integration of Equation 3.6 between the limits q = *qt* (t = *t*) and q = *qt-1* (t = *t-1*) after separation of the variables:

$$\int_{q_{t-1}}^{q} \frac{dq}{(Rc - q)} = \int_{t-1}^{t} \alpha \cdot dt. \tag{3.7}$$

gives

$$\frac{(Rc - q)_t}{(Rc - q)_{t-1}} = e^{(-\alpha \Delta t)} \tag{3.8}$$

Equation 3.8 can be transformed to gain the equation for return flow:

$$q_t = q_{t-1} \cdot e^{(-\alpha \cdot \Delta t)} + Rc_{\Delta t} \cdot \left(1 - e^{(-\alpha \cdot \Delta t)}\right) \tag{3.9}$$

Using the linear relationship between q and h (Equation 3.4), we get:

$$h_t = h_{t-1} \cdot e^{(-\alpha \cdot \Delta t)} + \frac{Rc_{\Delta t}}{0.8 \cdot S \cdot \alpha} \cdot \left(1 - e^{(-\alpha \cdot \Delta t)}\right) \tag{3.10}$$

The equations are scale independent and the spatial unit for which h and q are calculated can be either the hydrotope or the subbasin. In this study, the mean groundwater dynamics were calculated on the subbasin scale and the changes in height *(dh/dt)* where then added to the mean water table $\bar{h}$ of the hydrotopes U in the subbasins:

$$\frac{dh\,(U)}{dt} = \bar{h}(U) + \frac{dh}{dt}. \tag{3.11}$$

the reaction factor α

The factor α is a function of the transmissivity T and the slope length L:

$$\alpha = \frac{10 \cdot T}{S \cdot L^2}. \tag{3.12}$$

Therefore, the reaction factor has a physical meaning (see Equation 3.12), as illustrated by the comparison with the results of the numerically solved Boussinesq Equation (Figure 3.3), where the same geo-hydrological parameters (T, L, S) were used. However, for meso- to macro-scale basins the basic geo-hydrological parameters, namely transmissivity and specific yield, are usually not available. Especially the specific yield is difficult to determine. Arnold et al. (1993) sug-

gested another method to estimate the reaction factor α from field observations: From Equation 3.9, it follows that in periods without recharge *(Rc = 0)*:

$$\alpha = \frac{lnq_{t-1} - lnq_t}{\Delta t}. \tag{3.13}$$

α can be estimated by analyzing the actual response of the stream during time periods of no recharge ($Rc = 0$) and low evapotranspiration. In this study, an extension of this method is suggested. Because of the linear relationship between h and q, it follows that:

$$if \quad \alpha = \frac{lnq_{t-1} - lnq_t}{\Delta t} \quad then \quad \alpha = \frac{lnh_{t-1} - lnh_t}{\Delta t}. \tag{3.14}$$

Based on Equation 3.14, α can be estimated using observations of the groundwater head h directly. The method has the following advantages:

- due to the linear relationship between h and q (Equation 3.4), calibration of h will also improve q,
- the data are mostly commonly available,
- the groundwater monitoring net is usually denser than that for river discharge, especially in areas with shallow water levels, where groundwater is the main component in river discharge,
- it is not necessary to explore time periods without precipitation and direct flow (interflow and surface flow) to derive α, because in contrast to river discharge, fluctuations in groundwater are by definition not influenced by direct flow components,
- the base flow component is determined by a directly interacting process, viz fluctuations in the water table.

The Soil - Aquifer Interface

In areas with deep groundwater tables, water that percolates through the soil zone reaches the saturated horizons with some delay, because it has to percolate through the unsaturated drainage area between the last soil layer and the groundwater head. Different models were developed to estimate the delay time and the

so called 'effective recharge' (Sangrey et al., 1984). Venetis (1969) proposed an exponential decay weighting function to estimate the effective groundwater recharge after drainage through the unsaturated horizons. The equation allows for the representation of the current effective recharge Rc at time step t in terms of the percolate $Rc*$ from the lowest soil layer above the unsaturated drainage area:

$$Rc_t = \left(1.0 - e^{(1.0/\delta)}\right) \cdot Rc_t^* + e^{(1.0/\delta)} \cdot Rc_{t-1}^* \tag{3.15}$$

where δ is the delay time or drainage time of the unsaturated zone between soil and groundwater table. The equation will affect only the timing of the groundwater recharge and therefore the return flow and not the total volume. The delay time can be roughly estimated using the seepage velocity v_s $[m\ s^{-1}]$, normally used under saturated conditions (Maidment, 1993), where $k(\Theta)$ in $m\ s^{-1}$ is the permeability of the unsaturated zone z $[m]$ with the soil water content T in $m^3\ m^{-3}$ and n the number of layers:

$$v_s\left(z\right) = \frac{k\left(\Theta\right) \cdot dz}{S\left(\Theta\right)} \tag{3.16}$$

$$\delta = \sum_{n}^{i=1} v_s\left(z_i\right) \cdot \Delta z_i \tag{3.17}$$

In periods with high recharge and in areas with shallow groundwater, the water table may rise and affect the lower soil zones. The soil is discretized in SWIM vertically into 5 cm layers. Layers *(i, i+1, ...)* that are affected by groundwater are deactivated and the percolate from the layer *i-1* is then defined as groundwater recharge. The layer is reactivated when the water table sinks.

3.2.2 Description of the study area and the data

The northern lowland part of the German Elbe basin, where the model was tested in its two subbasins (the Nuthe, 1993 km^2, and the Stepenitz, 574 km^2, see Figure 3.2), is climatically one of the driest regions in Germany, with mean annual precipitation of about 600 mm per year. Hence, water availability during the summer season is the limiting factor for plant growth. The lowland is formed by mostly sandy glacial sediments and drained by slowly flowing streams with broad river valleys. The upper sites with deep water tables are covered by sandy, highly

permeable soils and mostly pine forests (in the Nuthe river basin), or by arable land on ground moraine with till soils that tend to have layers with lower water permeability (in the Stepenitz river basin). Valleys are covered by loamy alluvial soils with grassland and riparian forests, where the groundwater is very shallow, and arable land elsewhere. During the last two decades, decreasing water levels in rivers and groundwater have been observed (Landesumweltamt Brandenburg 2000 & 2002). The main mean climatic and hydrologic characteristics of the study area are listed in table 3.1.

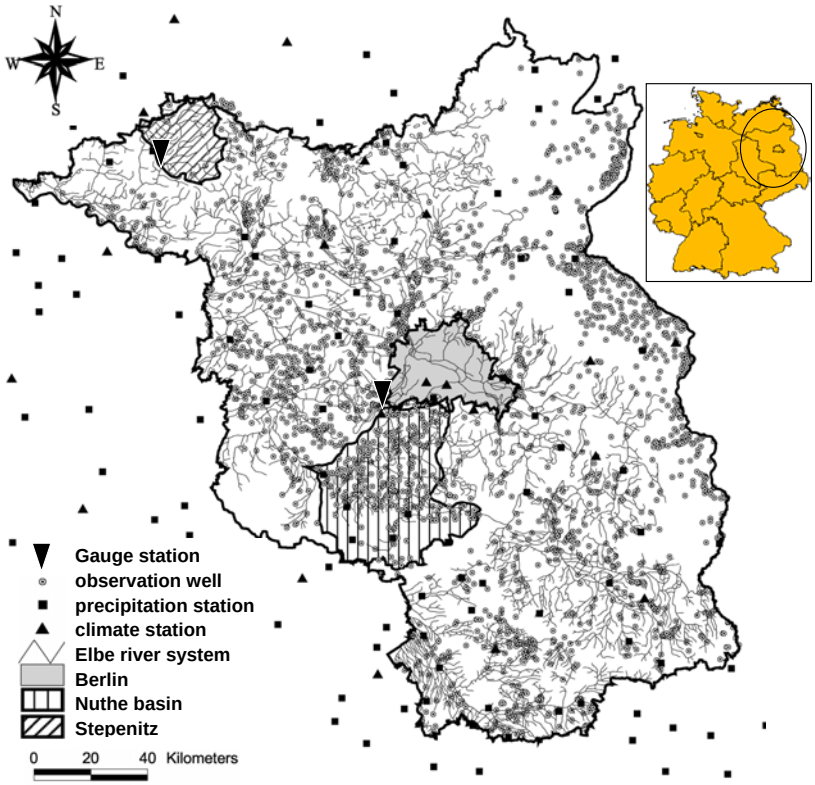

Figure 3.2. The state Brandenburg, the basins under study, the river network of the Elbe basin and the locations of the stations with climate, water level and river discharge observations.

All necessary spatial information to derive the subbasin and hydrotope structure of the basins, the digital elevation model (DEM), the soil map of the Federal Republic of Germany, the land use map and water table contour maps were stored on a grid format with 50 m resolution. The Stepenitz basin was subdivided into 95 and the Nuthe basin into 122 subbasins based on the DEM and the drainage network.

Table 3.1. Long term mean annual precipitation (P), mean annual temperature (T) and river discharge (Q) of the two basins under study.

basin	area [km^2]	P [mm a^{-1}]	T [°C]	Q [m^3 s^{-1}]
Nuthe	1938.0	590.5	8.8	9.1
Stepenitz	584.3	655.5	8.3	2.2

The evapotranspiration module in SWIM requires five different climate parameters to calculate daily potential evapotranspiration (Priestley-Taylor method), infiltration and groundwater recharge: minimum, maximum and average daily temperature, daily radiation and daily precipitation. The data were interpolated using the External Drift Kriging method (Hattermann et al., 2002).

3.2.3 Modeling procedure

River discharge

First, the hydrological processes for the two basins under study were calibrated on a daily time step using the observed river discharge for a period of eight years (1981-88). The period was chosen because the hydrological observations started mostly in the late 1970s. Figure 3.2 shows the map with the river system and locations of the gauging stations. Besides the initial storage values, three parameters were used to calibrate the hydrological processes in the model SWIM: a routing factor, a factor to calibrate saturated soil conductivity and the groundwater reaction factor α. Statistical evaluation of the simulated river discharge was done by analyzing the long-term difference between mean observed discharge in the river $\bar{Q}_{obs}$ against the mean simulated one $\bar{Q}_{sim}$ (the relative difference in discharge or discharge balance):

$$discharge\ balance = \frac{\bar{Q}_{sim} - \bar{Q}_{obs}}{\bar{Q}_{obs}} \cdot 100, \tag{3.18}$$

and calculating the efficiency criteria of Nash & Sutcliffe (1970) for Q_{sim} against Q_{obs} on a daily time step (t):

$$efficiency = 1 - \frac{\sum_t \left(Q_{sim_t} - Q_{obs_t}\right)^2}{\sum_t \left(Q_{obs_t} - \bar{Q}_{obs_t}\right)^2} \tag{3.19}$$

Groundwater dynamics

Contour maps of the mean water table and observed time series of groundwater levels (the locations of the wells are shown in Figure 3.2) were taken as the spatial-temporal information to analyze and adjust the characteristics of the hydrological processes in the subbasins. The calibration process was based on Equation 3.10, where an increase in α (higher transmissivity) results in a decreasing mean water table and vice versa, and a higher specific yield (S) in a smoothed groundwater table fluctuation. The calibration was done automatically using a special pre-processing program in two steps:

1. The first step was to adjust the simulated long term mean water table in subbasins by calibrating the reaction parameter α. During the process of automatic calibration, the mean observed water table per subbasin $\bar{h}_o$ was compared against the mean simulated one $\bar{h}_s$ after each simulation run, and α was then adjusted according to the results.

2. The second step was to calibrate the amplitude of the observed against the simulated water table by fitting the specific yield S.

The resulting spatial distribution of the reaction parameters in the basin is physically meaningful and is correlated to soil transmissivity and slope. The Mean Absolute Error (MAE) and the bias are used to compare the observed versus simulated long term mean water table:

$$MAE = \frac{1}{n} \cdot \sum_{i=1}^{n} \sqrt{\left(\bar{h}_{o_i} - \bar{h}_{s_i}\right)^2} \tag{3.20}$$

$$bias = \frac{1}{n} \cdot \sum_{i=1}^{n} \bar{h}_{o_i} - \bar{h}_{s_i} \tag{3.21}$$

3.3 Results and discussion

3.3.1 Model comparison

A comparison between the non-steady-state reaction of the groundwater head as calculated by Equation 3.10 and the results of a numeric solution of the non-linear Boussinesq Equation was carried out to demonstrate the reliability of the simplified groundwater module (see Figure 3.3).

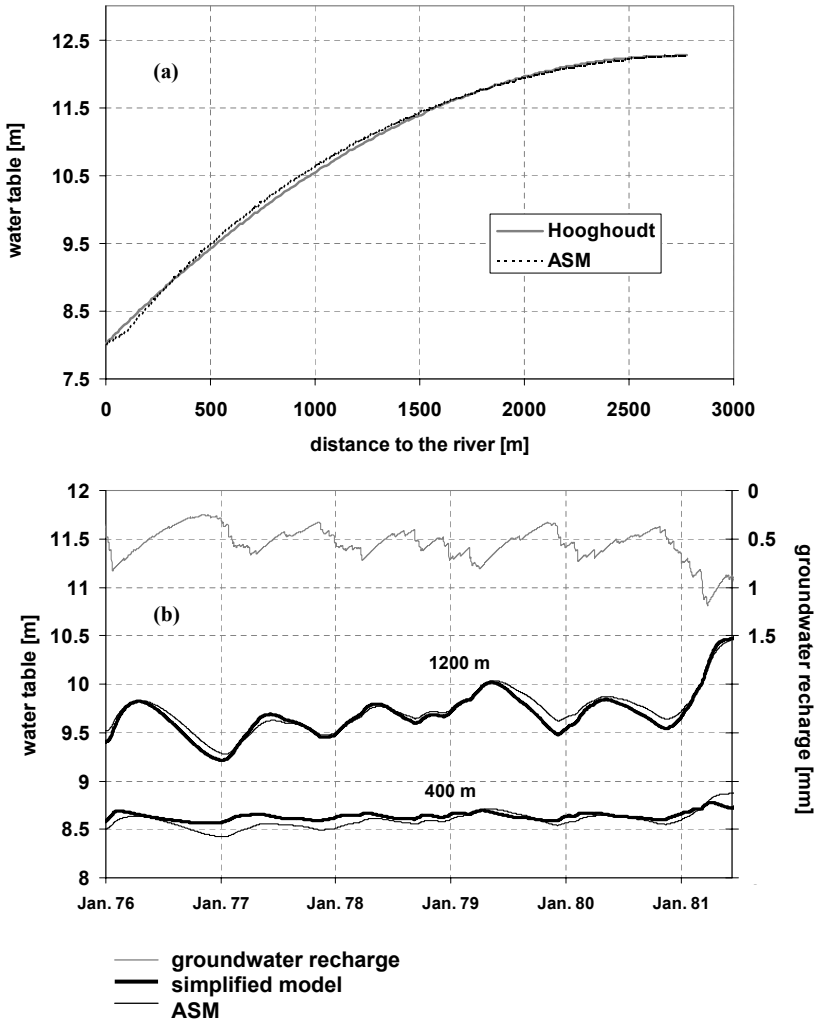

Figure 3.3. Results of the model comparison between the simplified model and the model ASM steady state (a) and unsteady state (b) with q = 0.00036 m s^{-1}, T = 0.001 m^2 s^{-1}, S = 0.05 m^3 m^{-3}.

The ASM finite difference computational scheme (Aquifer Simulation Modell,

Kinzelbach and Rausch, 1995) was applied in the comparison to derive a numeric solution of Equation 3.3, using the Preconditioned Conjugate Gradient Method to solve the fully implicit equation system. The code of ASM was changed for this purpose to be able to accept daily groundwater recharge (Rc), calculated by SWIM, as upper boundary condition. It has to be mentioned, that a mean transmissivity was used in the simplified formula, whereas in the numerical solution the transmissivity varies with time and location. Figure 3.3a shows a comparison of the steady state results of the simplified model and the ASM model, and Figure 3.3b a comparison of the non-steady-state results (two groundwater hydrographs per model calculated at 400 m and 1200 m distance from the river). Thereby, the groundwater recharge in the second example was calculated by SWIM. The comparison of the results obtained by the two approaches shows that there are only relatively slight differences in the simulated water tables. Moderate problems occur under non-steady-state conditions close to the river with low fluctuations in the hydrographs. Both models have the same sensitivity to the hydro-geologic input data. It is worth mentioning that the uncertainty in determining the hydrogeologic parameters and the model input have a much stronger influence on the model results, and the uncertainty in the model outputs caused by the parametric uncertainty is much higher than the variations between the two models.

3.3.2 River discharge

The model performed satisfactory in both case studies. The quality of the model results is comparable to recently published results from similar meso- to macroscale applications of other models in lowland river basins (Hiscock et al., 2001; Dunn and Ferrier, 1999; Stewart et al., 1999; Whitehead et al., 1998). The most sensitive model parameters in the calibration process of river discharge were the factors to correct saturated soil conductivity and river routing. The river discharge was rather insensitive to the reaction factor α. Figures 3.5 and 3.4 show the daily and monthly river discharge of the two basins, and the statistical values of the results are listed in Table 3.2.

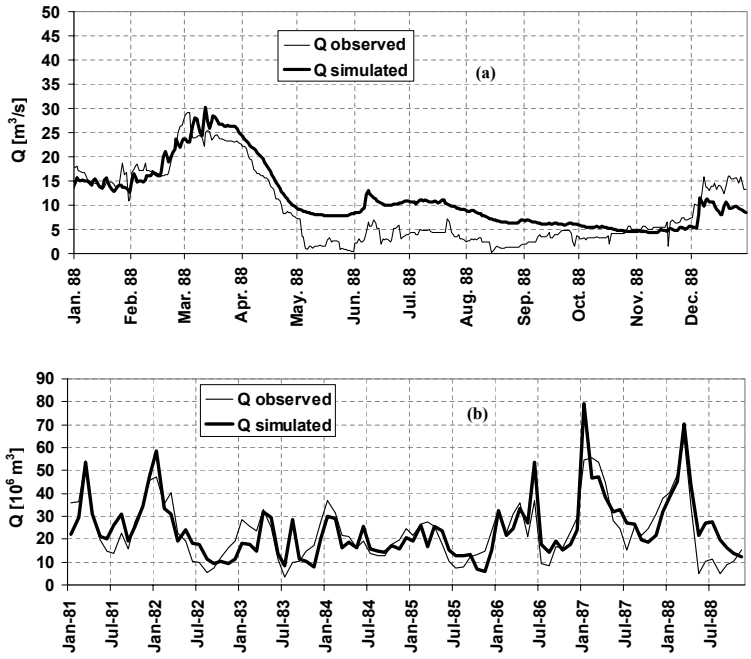

Figure 3.4. The observed and simulated river discharge (Q) for the Nuthe basin, (a) for daily time step and (b) for monthly time step.

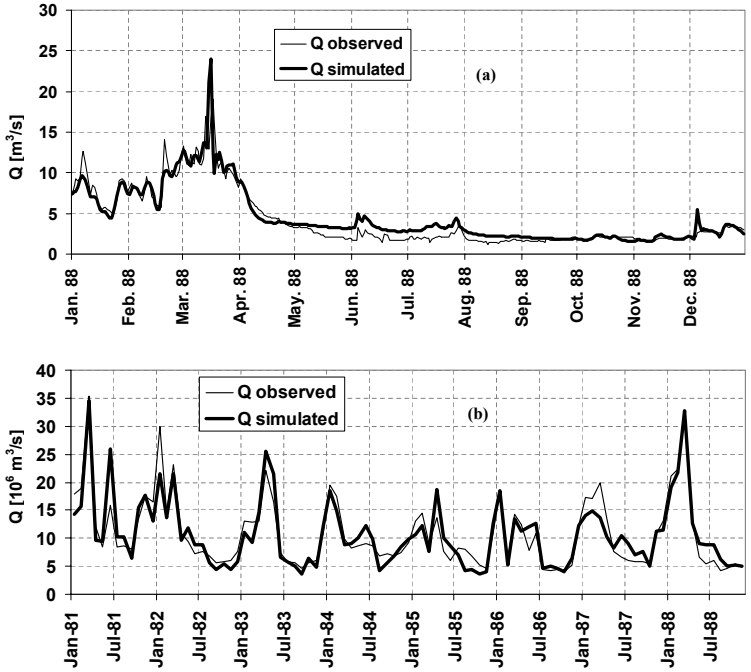

Figure 3.5. The observed and simulated river discharge (Q) for the Stepenitz basin, (a) for daily time step and (b) for monthly time step.

The difference between the observed and simulated river discharge (Equation 3.18) is 0.0 % in the Stepenitz model application and 3.0 % in the Nuthe application for the period 1981 - 1988, indicating that the water balance is correctly calculated by SWIM. The daily efficiency (Equation 3.19) is 0.71 in the Stepenitz and 0.60 in the Nuthe river basin. The hydraulic regime of the Nuthe basin is strongly influenced by water management regulations like drainage systems and weir plants, so that it is difficult to reproduce the hydrograph with higher accuracy. For example, for the Nuthe river hydrograph the summer discharge is overestimated by the model (see Figure 3.4). This can be explained by water abstraction and regulation measures, when a minimum river flow is provided by reservoir management in dry summer periods.

Table 3.2. Results of the hydrological calibration using observed river discharge.

Basin	efficiency daily	efficiency monthly	rel. diff. in discharge [%]
Nuthe	0.60	0.67	3
Stepenitz	0.71	0.84	0

It is worth mentioning that the efficiency was notably higher for other meso- and macro-scale subbasins of the Elbe located in hilly and mountainous areas (Hattermann et al., 2002). The comparison of the observed and simulated groundwater heads in the following section shows that the hydrological dynamics inside the basins are well reproduced.

3.3.3 Water table dynamics

First, the simulated mean annual water table depth of all subbasins in the Stepenitz and Nuthe basins were calibrated automatically as described in Chapter 3.2.3. The mean amplitude of the water table fluctuations in the Stepenitz basin was not calibrated, whereas in the Nuthe basin, the mean simulated amplitude was too high and had to be smoothed by a moderate increase in the value of specific yield. The Mean Absolute Error (Equation 3.20) of the long term mean observed against the mean simulated water table in all subbasins was 0.053 m for the Stepenitz basin, and 0.026 m for the Nuthe basin (see Table 3.3). The

Table 3.3. Results of the water table simulation.

basin	number of subbasins	MAE [m]	bias [m]
Nuthe	122	0.026	0.004
Stepenitz	95	0.053	0.028

groundwater reaction factors of the subbasins had values between 0.1 (loamy sediments) and 0.3 (sandy / loamy sediments). The time dynamics of the simulated water tables in terms of rising and retention periods were not calibrated.

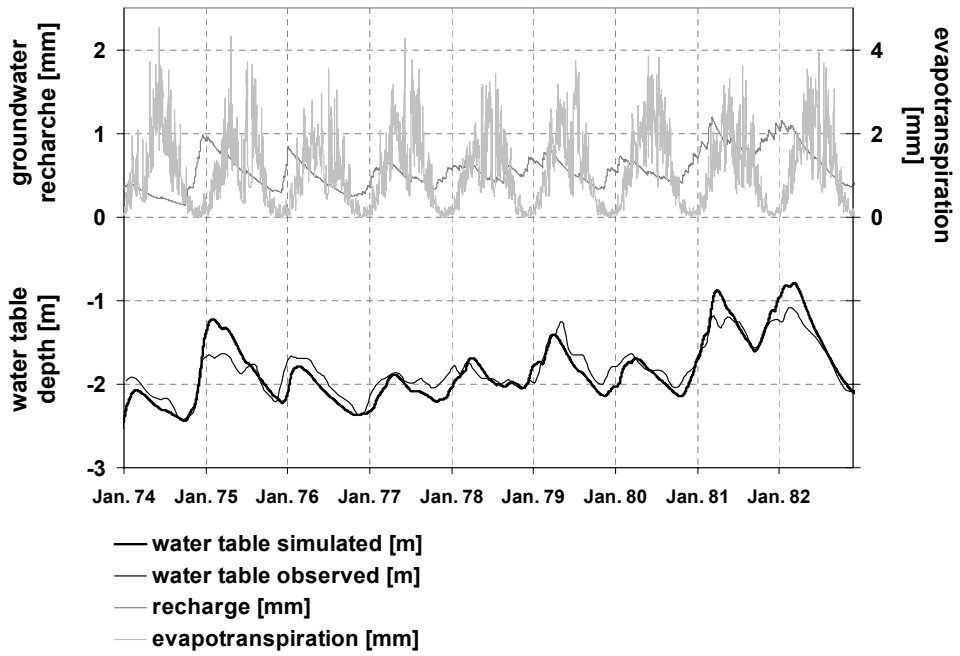

Figure 3.6. The simulated evapotranspiration, groundwater recharge and groundwater table and the observed groundwater table (station Wendisch Priborn, Stepenitz basin).

Figure 3.6 shows the comparison of the observed against that simulated water table for a subbasin in the Stepenitz catchment (the longest observed time series of the basin). The simulated daily water table shows a good fit with the observed data, when the amplitude and retention of the curves are considered. Actual evapotranspiration and groundwater recharge are also included in Figure 3.6 to provide a better understanding of the hydrological processes in the basin. It is obvious that the good reproduction of the water table dynamics also implies that

soil water percolation and groundwater recharge processes have approximately the correct magnitude and time dynamics, because otherwise the amplitude would have a shift in time. Water levels rise during the winter, when plant production and evapotranspiration are low, and they start falling in early spring. In some years, the simulated amplitude of the water level is higher than that observed, where the peaks are very low. The possible reason for that could be that high water levels are prevented by drainage systems for groundwater control.

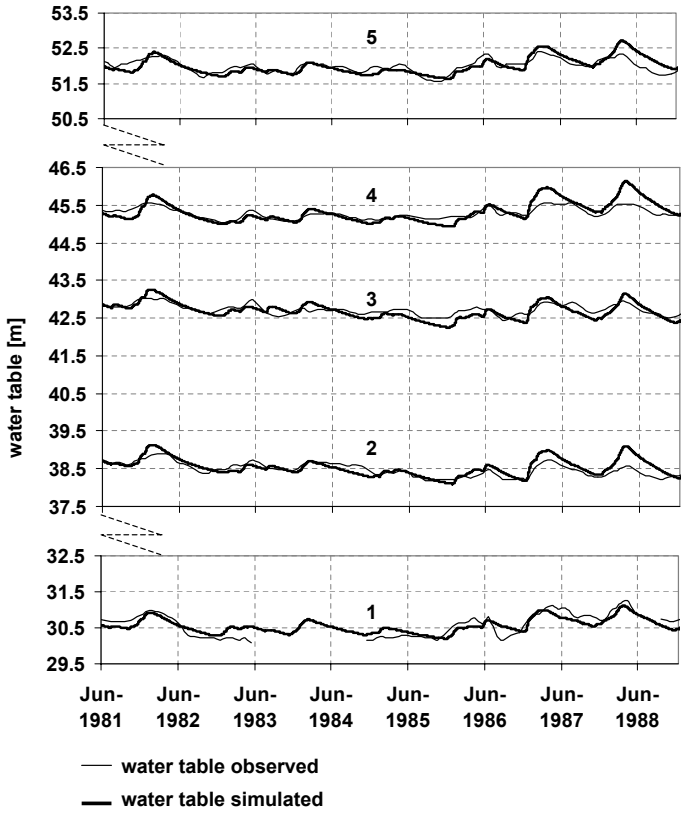

Figure 3.7. Observed and simulated groundwater table (five records from the Nuthe basin).

Figure 3.7 shows a comparison of five observed groundwater table hydrographs from the Nuthe basin with those simulated. The observation wells were selected in order to represent a cross-section through the basin from the lowlands in the north to the hilly area in the south. Well 1 is located next to the outlet of the Nuthe river catchment. Similar to the Stepenitz basin, the curves show a good fit, especially for the early 1980s. The rise of the groundwater level in 1987 and 1988 is slightly overestimated by the model in subbasins 2, 4 and 5. As explained in

Chapter 3.2.2, the natural flow regime in the Nuthe basin is influenced by stream flow control (weir and reservoir management), and especially in the lowland areas the water level is controlled by land drainage.

The simulated groundwater hydrographs are very similar, whereas the observations show more differences. The higher variability in the observed water levels is the result of small-scale heterogeneities in the aquifer and of local precipitation events which are missing in the observed records. An even better fit would be possible by implementing additional management information. However, this was not the objective of the study. On the contrary, the study aimed at showing that a simplified model approach yields satisfactory results using commonly available data without extensive field work and additional data collection. The results shown here demonstrate that an easy handling of the model is very important to obtain physically meaningful and comprehensive results on the meso- to macro-scale. The next section will describe a case study where the coupled model was used to analyze decreasing groundwater tables in the study area.

3.3.4 Water table trends in the north-eastern lowland of the Elbe basin

During the last two decades, falling water tables have been observed over nearly the entire area that is covered by the state of Brandenburg (see Figure 3.2). The question is whether the trend is mainly due to climate change or to a change in the local water management practices. The water table can fall because of human interventions in the water regime, such as increased crop production, implementation of drainage systems, lowering of the drainage base and increased groundwater extraction (Dunn and Ferrier, 1999; Smedema and Rycroft, 1983).

Large parts of the area have very shallow groundwater, and in particular here the water cycle is strongly influenced by water management practices like the installation of drainage systems for groundwater control (Freude, 2001; Landgraf, 2001; Succow, 1996; Borg et al., 1995). The Stepenitz basin was selected as an example to investigate the trend, because the decrease here is especially distinct (see Figure 3.10a).

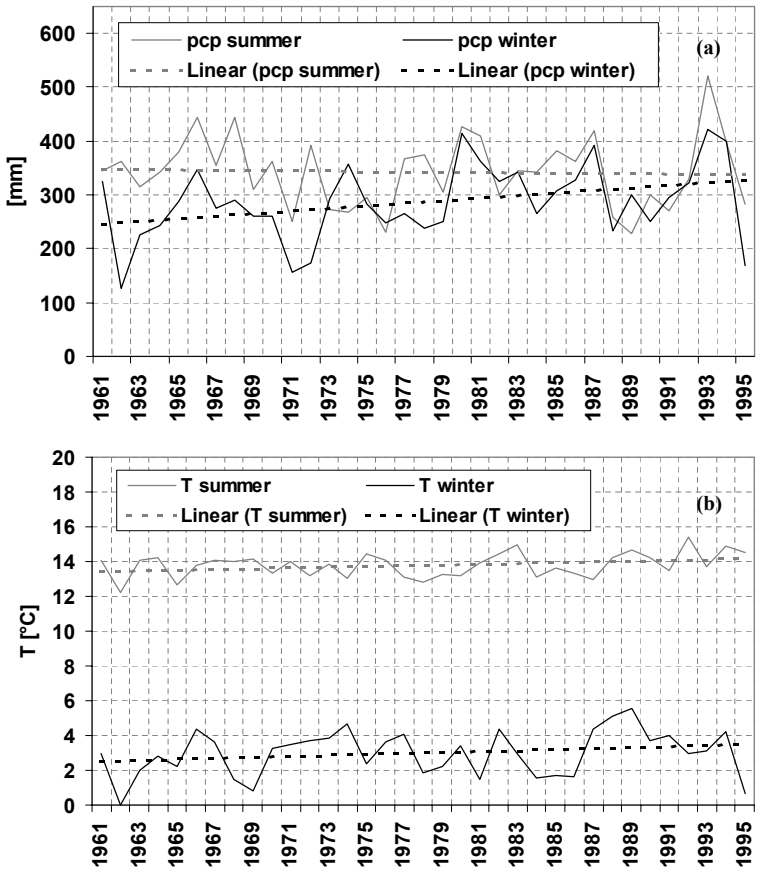

Figure 3.8. Trends in precipitation (a) and temperature (b) in the Stepenitz river basin.

Figure 3.8 shows the trends in the climate variables precipitation (Figure 3.8a) and temperature (Figure 3.8b). The sum of winter precipitation increases from 250 mm in 1961 to 320 mm in 1996, whereas the sum of summer precipitation has no significant trend. The mean winter temperature increase during the same period is about 1 °C, the mean summer temperature increase only about 0.5 °C.

It is difficult to analyze the reasons for the trend statistically because the records of river discharge started in only 1978, and the water table trend just a few years later. The correlation of river discharge and water table trends is therefore vague and unreliable. Precipitation and also temperature increased slightly during recent decades, with a higher increase in both parameters during the winter season. These changes could influence the water cycle in opposite directions. An increase in precipitation would result in rising water tables in an undisturbed water system, while higher temperatures would stimulate a higher

evapotranspiration and falling water tables, though the significance of changes depends on the value of climate parameter change.

SWIM was applied to the Stepenitz river basin to investigate the groundwater trend. The application of a complex model, which integrates all processes of interest, is crucial in this case, due to the non-linear reaction of the water cycle to changes in the climate input and because of the fact that the amount of observations is too limited to enable statistical analysis (e.g. a simple correlation between river discharge and groundwater levels). The first step was to analyze whether SWIM is sensitive to climate trends in respect to the groundwater table. In Figure 3.9, the results of a simulation experiment are demonstrated, where two climate trends were induced by subtracting each year 1 % and 2 % respectively of the observed precipitation. The first result of the experiment is that the groundwater table is falling steadily, and thereby the amplitude of the fluctuations is decreasing. The second is that the water table decline is limited by the drainage base, in our case the river water level. Both results reflect the hydrological processes correctly. Therefore, the groundwater module in SWIM is sensitive to climate change and a decrease in groundwater recharge.

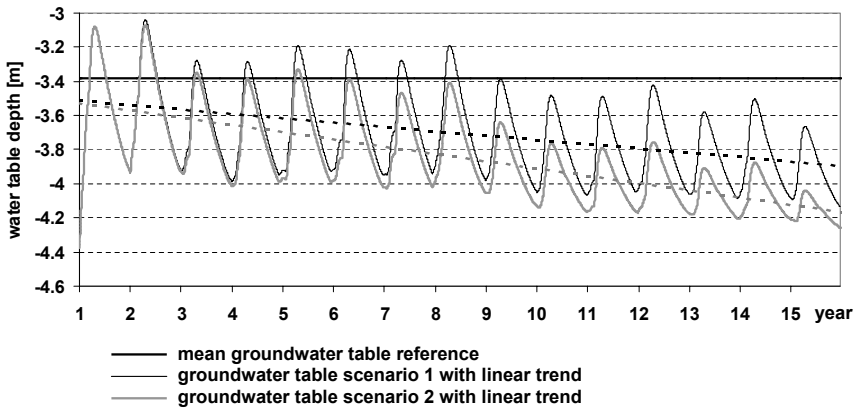

Figure 3.9. Sensitivity of the simplified groundwater module in SWIM to a decreasing trend in precipitation. The daily precipitation was reduced each year by 1 % (scenario 1) or 2 % (scenario 2) respectively.

The second step was to apply SWIM in the Stepenitz basin and to perform a model run with the observed climate data as input. Figure 3.10a shows the comparison between the simulated and observed groundwater levels for the time period January 1974 to December 1996.

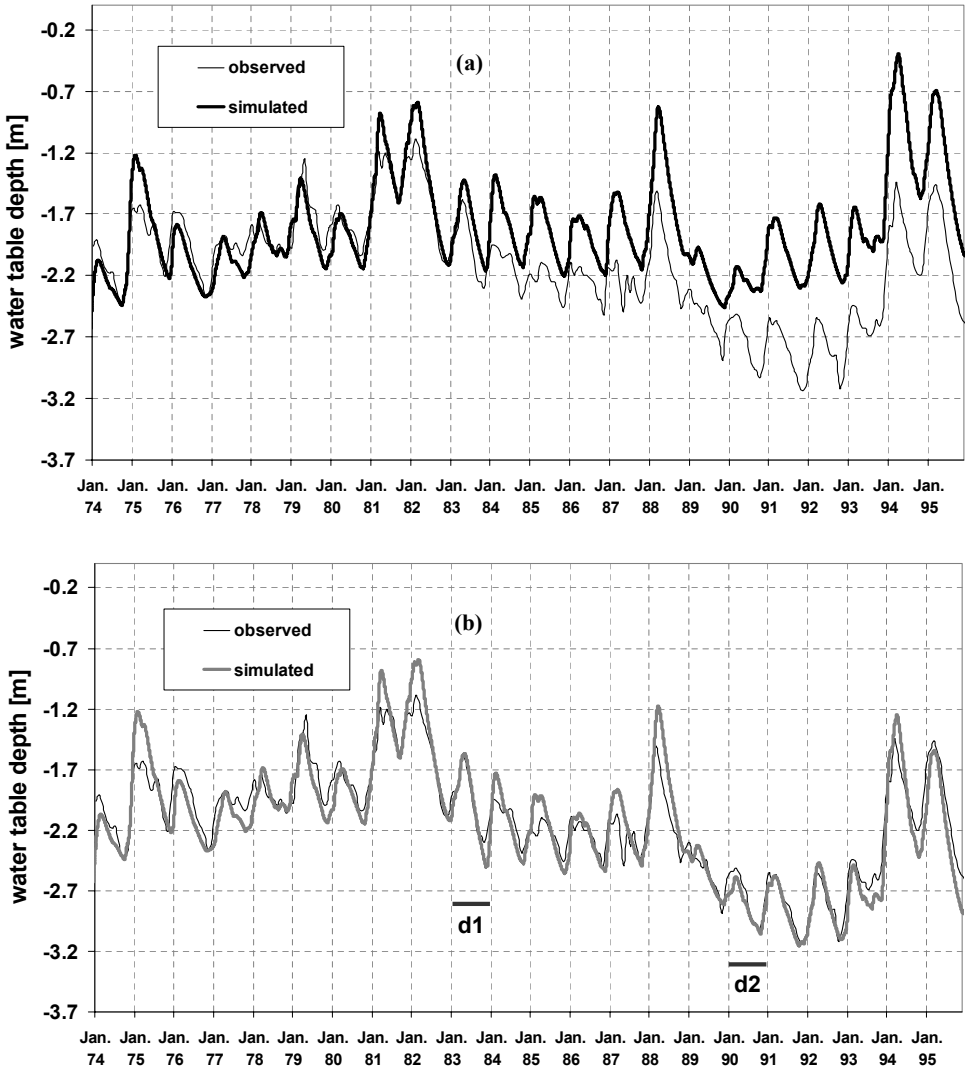

Figure 3.10. The observed and simulated groundwater levels (station Wendisch Priborn). (a) The trend starting from summer 1983 cannot be reproduced taking observed climate data. (b) The groundwater hydrographs agree when the simulation is done assuming a decline in the drainage basis of -0.35 m in the period 1983 - 1984 (**d1**) and of -0.80 m in the period 1990-1991 (**d2**).

During the first ten years until spring 1983, the two hydrographs have approximately the same dynamics and even the same trend to increasing water levels. However during summer 1983 the observed water table declines, while the simulated one has nearly no decreasing trend and remains practically at the same level. A similar pattern can be observed in other subbasins of the Stepenitz catchment. A conclusion is that the trend cannot be caused by climate change,

because in that case also the simulated water level would decrease, as illustrated in the simulation experiment (see Figure 3.9).

A possible reason for the decline could be the extensive melioration and river deepening that took place from the late 1960s in Brandenburg (Succow, 1996) and later also in the Stepenitz river basin. The drainage base was lowered by these two measures. The structural water engineering measures were amplified in the Stepenitz catchment at the beginning of the 1980s (Pietschmann, Brandenburg State Environmental Department, oral communication). Based on this information, the simulation can be extended. Applying the coupled model, it is possible to roughly detect the reason for the water table decline during the early 1980s and the early 1990s. In Figure 3.10b, the observed water table is compared with the simulated one, whereby the simulated water table was calculated assuming a decrease in the drainage base (the river water level) of 0.35 m during the first half of the 1980s and of 0.80 m during the early 1990s. The effect is that the simulated curves again agree with the observed data, even the decline in summer 1989 and the increasing trend in the 1990s is well reproduced.

The range of drawdown of the drainage base is also recorded in other European lowlands with shallow groundwater and human interference and hydrological engineering (Querner and van Lanen, 2001). Consequently, from the analyzes of the climate data and the modeling results it can be concluded that the water table trend is rather induced by engineering measures in the basin, which have led to a decline in the drainage base of the aquifer. The result can also be reproduced and observed in other subbasins of the Stepenitz catchment.

3.4 Summary and conclusions

The study has shown that the additional use of water table maps and observed groundwater levels has a high potential to enhance the simulation of spatially distributed hydrological processes, because a good reproduction of groundwater dynamics implies also a good reproduction of the hydraulic processes in soils in terms of evapotranspiration and percolation. Data availability and computation time limit the application of fully distributed physically based models on the catchment scale creating a demand for simplified model approaches integrating all important hydrological processes and focusing on groundwater dynamics

(Hall and Mönch, 1972; Sangrey et al., 1984; Guo, 1997; Workman et al., 1997; Sloan, 2000; Zissis et al., 2001). The simplified model approach used in this study produced good simulation results in two meso-scale lowland basins with a daily time step in terms of river discharge taking into account that the natural flow regime is strongly influenced by artificial flow regulation. During the calibration of river discharge, only three parameters were modified (saturated soil conductivity, river routing and groundwater reaction). It was also possible to reproduce local hydrological processes such as water table dynamics inside subbasins, using observed groundwater level data and a simplified groundwater module (Smedema and Rycroft, 1983). The adjustment of the mean water table was done automatically on the subbasin scale. The mean long term differences between the mean observed and mean simulated water table were smaller than 0.06 m for all subbasins.

The importance of water level dynamics in basin-scale model applications is demonstrated in a case study, the investigation of a negative trend in regional water tables. The modeling study was applied to analyze whether the trend is the impact of climate change or the impact of local water and groundwater management (like implementation of drainage systems and flow regulation). The conclusion was that the trend was induced by engineering measures in the basin, which led to a decline in the drainage base of the aquifer. The simulation experiment demonstrates the need for physically sound comprehensive groundwater models, which are applicable on a regional catchment scale, where extensive additional field data collection is impossible, and where an easy handling of the model is very important to obtain physically meaningful and comprehensive results.

Acknowledgments

The authors would like to thank all their colleagues at the PIK who contributed to this paper with technical help, particularly Daniel Doktor. Part of this work was supported by the BMBF programme GLOWA (GLObal WAter) Elbe and the Brandenburg State Environmental Agency (LUA Brandenburg).

ECOLOGICAL MODELLING (2005)
(*in print*)

Chapter 4

Integrating wetlands and riparian zones in river basin modeling

Short title: wetlands in river basin modeling

Keywords: Riparian zones; wetlands; water quality; groundwater dynamics; nutrient retention; integrated river basin modeling.

Hattermann[1*], FF, Krysanova[1], V, Habeck[1], A, Bronstert[2], A
[1]Potsdam Institute for Climate Impact Research
[2]University of Potsdam, Institute for Geoecology, Chair for Hydrology and Climatology
* Full address of the corresponding author:
Dipl.-geoecol. Fred Fokko Hattermann
Global Change and Natural Systems Department
Potsdam Institute for Climate Impact Research
P.O. Box 601203, Telegrafenberg
14412 Potsdam
Germany
Fax: +49 331 288 2600
Tel. +49 331 288 2649
E-mail: fred.hattermann@pik-potsdam.de

Abstract Wetlands, and in particular riparian wetlands, represent an interface between the catchment area and the aquatic environment. They control the exchange of water and related chemical fluxes from the upper catchment area to surface waters like streams and lakes. Their influence on water and nutrient balances has been investigated mainly at the patch scale. In this study an attempt was made

- to integrate riparian zones and wetlands into eco-hydrological river basin modeling, and
- to quantify the impacts of riparian wetland processes on water and nutrient fluxes in a meso-scale catchment located in the northeastern German lowland.

The investigation was performed by analyzing hydro-chemical field data and applying the eco-hydrological model SWIM (Soil and Water Integrated Model), which was extended to reproduce the relevant water and nutrient flows and retention processes at the catchment scale in general, and in riparian zones and wetlands in particular. The main extensions introduced in the model were: (1) implementation of daily groundwater table dynamics at the hydrotope level, (2) implementation of water and nutrient uptake by plants from groundwater in riparian zones and wetlands, and (3) assessment of nutrient retention in groundwater and interflow at the catchment scale. The simulation results indicate that wetlands, though they represent relatively small parts of the total catchment area, may have a significant impact on the overall water and nutrient balances of the catchment. The uncertainty of the simulation results is considerably high, with the main sources of uncertainty being the model parameters representing the geo-hydrology and the input data for land use management.

4.1 Introduction

The Water Framework Directive of the European Commission (EC) requires that water bodies in Europe are brought into "a good ecological status" (EC, 2000). Much effort has been made and many improvements carried out, mainly in the implementation of wastewater treatment plants. But these measures only help

to reduce pollution from point sources, whereas the main origin of some important pollutants are diffuse sources like leaching from fertilized cropland and atmospheric deposition.

Riparian zones and wetlands, being an interface between catchments and surface waters, can play an important role in the control of water quantity and water quality of surface water systems in general, and in reduction of diffuse pollution in catchments in particular (Maitre et al., 2003; Lane et al., 2003; Tanner et al., 1999; Dall'O' et al., 2001; Yang et al., 2001; Romero et al., 1999; Bach et al., 1997; Mander et al., 1997; Martin and Reddy, 1997). In wetlands, plant roots may reach the groundwater table and plants can satisfy their nutrient and water demands even during dry periods, while vegetation in higher areas without contact to groundwater has to reduce or stop its transpiration and nutrient uptake (Yang et al., 2001; Tanner, 1996). In addition, sediments in wetlands normally have a higher carbon content because of reduced mineralisation under anoxic conditions. Anoxic conditions and available carbon sources stimulate denitrification in wetlands and riparian zones (Mander et al., 1997).

The effectiveness of wetlands in water and nutrient retention has been the subject of several investigations, mostly at the plot scale or for small watersheds, usually based on an intensive monitoring programme, and including some studies of constructed wetlands (Meuleman et al., 2003; Stottmeister et al., 2003; Lin et al., 2002; Matheson et al., 2002; Bachand and Horne, 1999a,b; Tanner et al., 1999; Mitsch and Mander, 1997). A comprehensive summary of studies on the efficiency of riparian zones in rural catchments is given in Mander and Kull (1997), where the measured denitrification in riparian zones is between 0.16 and 2960 kg ha^{-1} a^{-1}, and vegetation uptake of nitrogen is between 10 and 350 kg ha^{-1} a^{-1}. The large range of the observed values can be explained by the variety of riparian zone types discussed in the studies, which include different kinds of riparian forests and meadows. Their influence at the river basin scale is more difficult to determine (Haag and Kaupenjohann, 2001), because of a lack of comparable detailed and accurate data at this scale. The transferability of the small-scale results to larger river basins is therefore restricted.

modeling studies can help to understand the impact of riparian zones and wetlands on the overall water and nutrient balances in river basins (Krysanova et al., 1998). While simple methods like regression models, export-coefficient

approaches and GIS-based mass balances can roughly estimate the relative significance of different processes and sources (Behrendt and Opitz, 2000; Behrendt and Bachor, 1998; Wendland et al., 1993), more sophisticated dynamical process-based approaches are needed to analyze the role of wetlands processes in catchments. In such models the interrelation of groundwater dynamics, soil moisture, nutrient leaching and retention, plant growth and plant water and nutrient uptake should be considered (Bogena et al., 2003; Singh and Frevert, 2002; Wade et al., 2002; Dall'O' et al., 2001; Bronstert et al., 1997). However, the process-based modeling of water quality in catchments, especially in large-scale river basins, is still a challenge (Horn et al., 2004; Haag and Kaupenjohann, 2001), and integration of riparian zones in catchment modeling is even more challenging because of the complex interactions and feedbacks between hydrology, vegetation and soils in wetlands (Martin and Reddy, 1997; Cirmo and McDonnell, 1997). The feedback effects of hydrological and chemical fluxes (ground-surface water exchange, nitrogen storage and uptake etc.) are of particular interest in ecosystems, where the coupling of different system compartments is important and can not be neglected in a satisfactory description of the governing dynamics of the system (Bronstert et al., 2005). As phosphorous is mainly transported from soil to river via erosion, our study was focused on nitrogen dynamics. Therefore the objectives of this study were:

- to analyze hydro-chemical data on nitrogen dynamics in groundwater and surface water in a meso-scale rural river basin (1938 km^2) located in the northeastern German lowland,
- to find a method for implementation of the relevant eco-hydrological processes in wetlands and riparian zones in meso- and large-scale river basin modeling,
- to quantify the impacts of wetlands on water and nitrogen fluxes in the mentioned river,
- to identify areas in the catchment, which are mainly responsible for river pollution from diffuse sources, and
- to analyze the uncertainty of input data and model parameters related to the model extension.

The model used in the study is the eco-hydrological model SWIM (Soil and Water Integrated Model, Krysanova et al., 1998), which integrates hydrology, vegetation, erosion and nutrient dynamics at the river basin scale. Spatial disaggregation in SWIM has three levels: the basin is subdivided into subbasins, and then the subbasins are subdivided into hydrotopes or hydrotope classes based on uniformity of land use and soil.

By implementing the wetland and riparian zones in SWIM, the technical aim was to find modeling solutions which are physically sound but simple enough to apply at the river basin scale using regionally available data. This is compatible with the overall structure and process representation in SWIM (Krysanova et al., 2000; Krysanova and Becker, 1999). However, the scarcity of field data valid at the regional scale made it necessary to take additional 'soft' information (from literature, expert knowledge) to validate the model, although it was clear that the inherent uncertainty of the data would cause a high degree of uncertainty to be propagated by the model. The uncertainty of the model results generated by the inherent uncertainty in input data and model parameters was analyzed using a comprehensive sensitivity and uncertainty analysis method.

The river basin used to test the model is located in the lowland part of the Elbe river basin, which is representative for semi-humid landscapes in Central and Eastern Europe, where water availability during the summer season is the main limiting factor for plant growth and crop yields. The water and nutrient balances of the catchments are influenced by water and land use management measures such as implementation of drainage systems, lowering of the drainage base and increased groundwater extraction. Extensive parts of the area have very shallow groundwater, and over much of the region water management is regulated through the installation of weirs and gates in the surface waters and drainage systems for groundwater control (Freude, 2001; Landgraf, 2001; Borg et al., 1995).

4.2 Material and methods

4.2.1 The study area and data

The study area is the catchment of the River Nuthe, which drains into the Havel river, a tributary of the Elbe river in northeastern Germany. The catchment area

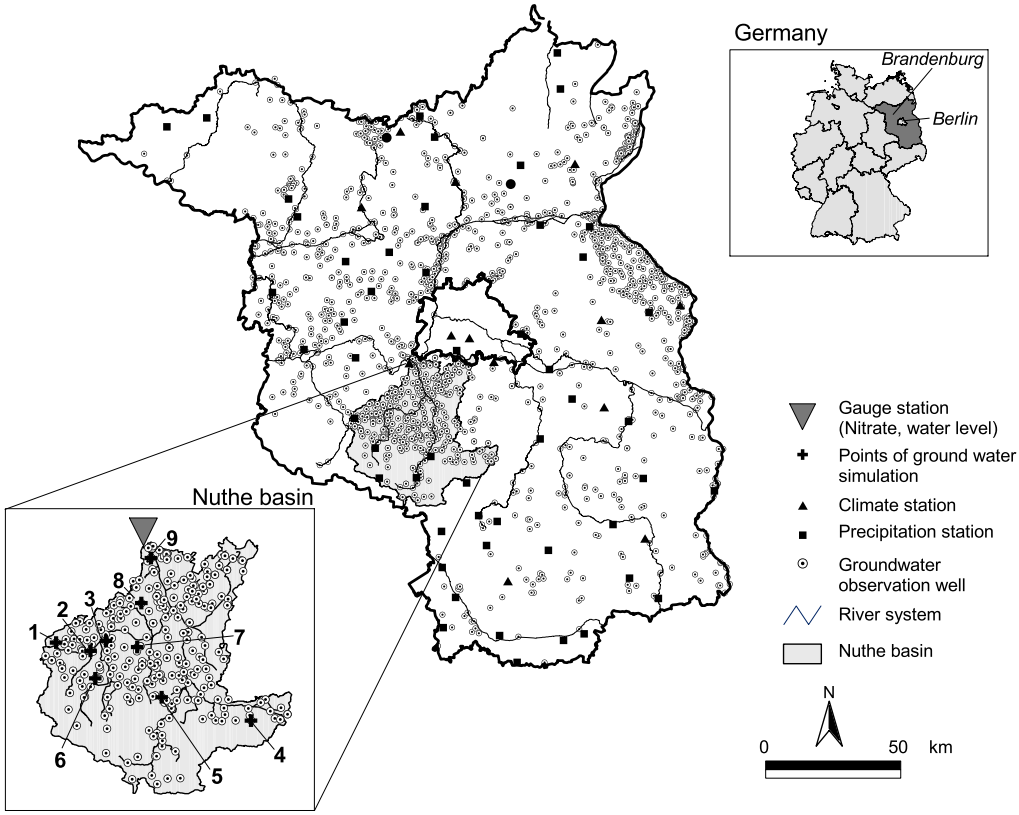

Figure 4.1. The location of the Nuthe basin and the observation points.

of the Nuthe covers 1938 km^2 in a Pleistocene landscape dominated by agricultural land use. The mean annual precipitation is about 600 mm per year (see Table 4.1). Water availability during the summer season is the limiting factor for plant growth, because the area is covered mainly by sandy glacial sediments with low water-holding capacity. The basin is drained by slowly flowing rivers and ditches in broad river valleys. The upper areas with deeper water tables are covered by sandy, highly permeable soils and forests mainly of pine or by arable land on ground moraine with till soils that tend to have layers with lower water permeability. Valleys are covered by loamy alluvial soils with grassland and riparian forests, where the groundwater is very shallow, and arable land elsewhere. Approximately 27 % of the basin area is covered by wetlands, which are regulated by water management measures such as the installation of drainage systems for groundwater control (Freude, 2001; Landgraf, 2001). During the last two

decades, decreasing water levels in rivers and groundwater have been observed (Landesumweltamt, 2000; Herrmann, 2002), caused mainly by human intervention (lowering of drainage depth, melioration, straightening of rivers, etc.). As a result, many wetland ecosystems were drained and altered their hydrological character to dryer conditions, and their restoration by river flow regulation measures is ongoing or planned. The landscape is rural, dominated by farmland and forest, the population density is low (although the basin is adjacent to Berlin), and there is no significant industry (see Figure 4.1 and Table 4.2).

Table 4.1. Long-term mean annual precipitation (P), mean annual temperature (T), river discharge (Q), runoff coefficient (rc), and river nitrate N concentration in the 1980s (C8(N)) and 1990s (C9(N)).

P	T	Q	rc	C8(N)	C9(N)
[mm a^{-1}]	[°C]	[m^3 s^{-1}]	[%]	[mg l^{-1}]	[mg l^{-1}]
590.5	8.8	9.1	21.1	1.84	0.56

All necessary spatial information to derive the subbasin and hydrotope structure of the basin, i.e. the digital elevation model (DEM), the soil map of the State of Brandenburg, the geo-hydrological map (NBL, 1985), the land use map and water table contour map were stored on a grid format with 50 m resolution. This format has been chosen because it is the original spatial resolution of the DEM and the soil map, while the original resolution of the land use information is a grid format of 25 m and the one of the geo-hydrological map only of 1 km. The groundwater contours were produced by averaging the yearly groundwater level of 226 observation wells and interpolation using External Drift Kriging (Akin and Siemes, 1988), whereby the elevation was taken into account as a second variable. The Nuthe basin was subdivided into 122 subbasins based on the DEM and the drainage network.

Table 4.2. Catchment area and land use in the Nuthe basin.

area	settlement	arable land	grassland	forest	other
[km^2]	[%]	[%]	[%]	[%]	[%]
1938	≈ 5	≈ 43	≈ 13	≈ 36	≈ 3

Six climate stations and sixteen precipitation stations are located in and around the basin. Their daily measurements have been interpolated for each subbasin using Inverse Distance techniques. The land use distribution is shown in Table 4.2, the main climatic and hydrologic characteristics of the study area are listed in Table 4.1.

4.2.2 The model SWIM

The eco-hydrological model SWIM is a continuous-time semi-distributed model, which integrates hydrological processes, vegetation, erosion and nutrient dynamics at the river basin scale (Krysanova et al., 1998, 2000, 2001). SWIM was developed on the basis of two previously developed models, SWAT (Soil and Water Assessment Tool, Arnold et al., 1993, 1994) and MATSALU (Krysanova and Luik, 1989). A three-level scheme of lateral spatial disaggregation from basin to subbasins and to hydrotopes is used, where the hydrotopes form the highest disaggregation level. A hydrotope is a set of elementary units in the subbasin, which have the same geographical features like land use and soil type. It can therefore be assumed that they behave hydrologically in a uniform way.

Water fluxes, plant growth and nitrogen dynamics are calculated for every hydrotope, where up to 10 vertical soil layers can be considered. The approach allows the spatial pattern of land use and land use changes to be considered. After reaching the river system, water and nutrients are routed along the river network to the outlet of the catchment.

The simulated hydrological system is conceptualized as having four compartments: the soil surface, the root zone, the shallow aquifer, and the deep aquifer. The water balance for the soil column includes infiltration, surface runoff, evapotranspiration, percolation, and generation of interflow and groundwater recharge. The water balance for the shallow aquifer includes groundwater recharge, capillary rise to the soil profile, lateral flow, and percolation to the deep aquifer.

Plant dynamics are simulated using a simplified EPIC approach (Williams et al., 1984), where the potential increase in biomass is estimated as the product of intercepted energy in terms of solar radiation and a plant-specific parameter converting energy into biomass. Nutrient uptake by plants is estimated using a supply and demand approach. Four stress factors control the plant growth, one for available water, one for optimal temperature and two for available nutrients

(nitrogen and phosphorus).

The nitrogen and phosphorus modules include pools for nitrate nitrogen, active and stable organic nitrogen, organic nitrogen in the plant residue, labile phosphorus, active and stable mineral phosphorus, organic phosphorus, and phosphorus in the plant residue, and the flows of fertilization, input with precipitation, mineralisation, denitrification, plant uptake, leaching to groundwater, losses with surface runoff, interflow and erosion. The model considers two sources of nitrogen mineralisation (Seligman and van Keulen, 1981): the fresh organic nitrogen pool, associated with crop residue, and the active organic nitrogen pool, associated with the soil humus. Organic nitrogen flow between the active and stable pools is described with an equilibrium equation, assuming that the active pool fraction at equilibrium is 0.15. The decomposition rate of residue is a function of the C:N ratio, C:P ratio, temperature, and water content in soil. The mineralisation from the active organic nitrogen is a function of temperature and the water content in soil.

Denitrification occurs only in conditions of oxygen deficit, which usually is associated with a high water content in soil. Denitrification is a microbial process and occurs as a function of soil temperature and carbon content.

The crop is allowed to take nitrogen from any soil layer that has roots, or in the extended version also from groundwater, if the roots have access to it. Uptake starts at the upper layer and proceeds downwards until the daily demand is met or until all nitrogen has been depleted. A full description of the model can be found in Krysanova et al. (1998, 2000). An extensive hydrological validation of the model for the whole Elbe basin including sensitivity and uncertainty analysis of the hydrological processes in lowland is described in Hattermann et al. (2005a). The next section will introduce the further development of the model, which was carried out to implement the wetland module and nutrient retention in the river basin.

4.2.3 Model extensions

The original model SWIM (Krysanova et al., 1998) had no explicit representation of wetlands and riparian zones, and a very simple representation of nutrient retention on the way from soil to river. Therefore, the model had to be extended, and formulations for the reproduction of relevant flow and retention processes in

catchments and especially in wetlands had to be implemented. The developed model concept is transferable to other regions in Europe and beyond, with the limitation that the process formulations are not valid in mountainous areas with rocky or karstic aquifers, where wetlands normally do not play an important role.

For modeling purposes the wetland or riparian zone is defined as a hydrotope with a shallow groundwater table, where plant roots can reach the groundwater. The riparian zone is a type of wetland located along the river. The area covered by wetlands and riparian zones in a river basin is therefore not constant, but varies over the season and between years due to variations of the groundwater table. Though there could be 'stable' wetlands in a basin, they are usually assumed to be 'ephemeral' (depending on current conditions in the catchment). The main changes introduced in the model were:

1. implementation of daily groundwater table dynamics at the hydrotope level (it was previously simulated only at the subbasin level),

2. assessment of nutrient retention in groundwater and interflow at the catchment scale,

3. implementation of water and nutrient uptake by plants from groundwater in riparian zones and wetlands, which is allocated according to the daily water table depth.

Additionally, in the extended version, average water table depth, distance to the next river, and flow concentration time can also be considered by delineating hydrotopes. For nitrogen (mainly nitrate nitrogen) all three pathways from soil to river, i.e. with surface runoff, with interflow and with groundwater discharge, are relevant. The following description will focus on nitrate nitrogen and has therefore to consider all three pathways. Figure 4.2 illustrates the main extensions. Firstly, nitrate nitrogen, which leaves the root zone with interflow and groundwater recharge, is subject to denitrification and plant uptake on the way from the hydrotope to the surface river system. These processes depend on the characteristics of the sediments along the flow path and on the mean residence time of the nutrients in the subsurface (point 1 in Figure 4.2). Secondly, plants in lower parts of the subcatchment are allowed to satisfy their water and nutrient demand also from lateral flows coming from upper parts (point 2 in Figure 4.2). Thirdly, the groundwater table is simulated daily for each hydrotope (point

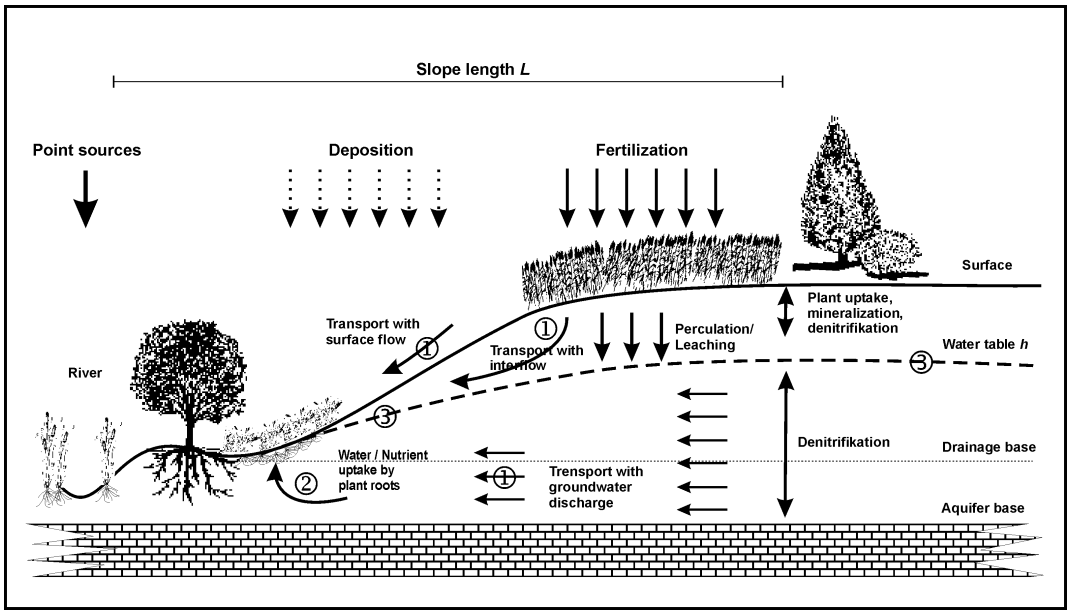

Figure 4.2. Scheme of the main nutrient fluxes in a catchment.

3 in Figure 4.2). This allows us to consider the wetland areas in the model as being variable: the total wetland area in a basin will decrease in dry conditions in summer, and increase in wet periods, when the water table is rising.

The following sections will explain these extensions and the required data pre-processing in more detail. During the work, the aim was to find methods which are physically sound but simple enough to be applicable at the large river basin scale using regionally available data, and to save computation time. The mathematical description below follows these basic aims. If specific subsurface information (permeability, nutrient turnover conditions) are not available, one can also start using first global data from literature, and then regionalize them by calibration.

Groundwater table dynamics

A good reproduction of groundwater dynamics is crucial for the investigation of hydrological processes and nutrient fluxes in wetlands, since the main characteristic of wetlands is their shallow groundwater. The groundwater table dynamics is especially important for processes like root growth, water and nutrient uptake from shallow groundwater by plants, and for saturated overland flow. In the ex-

tended SWIM, the groundwater table is simulated daily for each hydrotope. The model now allows daily and seasonal fluctuations in the groundwater table due to changes in groundwater recharge and plant water uptake from groundwater to be considered, and also makes it possible to account for changes in the wetland area. The groundwater module has been first used in large scale modeling by Arnold et al. (1993) to simulate monthly groundwater discharge at the subbasin level. It has been further developed by Hattermann et al. (2004) to simulate daily groundwater table fluctuations at the hydrotope level.

The extended model considers two cases when calculating groundwater recharge: (1) areas and time periods in which the groundwater table is relatively deep, and plants have no access to groundwater, and (2) areas and time periods with very shallow groundwater accessible to plant roots. SWIM uses an exponential delay function to calculate the effective groundwater recharge Rc after drainage through the unsaturated geologic horizons from the lowest soil layer to the groundwater table (Arnold et al., 1993):

$$Rc_t = \left(1.0 - e^{(1.0/\delta)}\right) \cdot Rc_t^* + e^{(1.0/\delta)} \cdot Rc_{t-1}^* \tag{4.1}$$

where Rc^* is the percolate from the lowest soil layer, and δ is the travel time through the unsaturated horizons between soil and aquifer, a function of sediment permeability and saturation (Hattermann et al., 2004). Soil layers (i, i+1, ...) which are affected by shallow groundwater are deactivated, and the percolate from the layer i-1 is defined as groundwater recharge. The deactivated layers are reactivated when the groundwater table declines. Unsaturated soil depth in a hydrotope becomes variable.

The dynamics of groundwater table and groundwater discharge are calculated following the approach of Smedema and Rycroft (1983). They derived a linear storage equation based on the Dupuit-Forchheimer assumptions to predict the non-steady-state response of groundwater flow to periodic recharge from Hooghoudt (1940)'s steady-state formula, assuming that the variation in return flow q in $mm\ d^{-1}$ at time step t is linearly related to the rate of change in water table height h in m (only headlosses in horizontal direction are considered):

$$\frac{dq}{dt} = \frac{8T}{L^2}\frac{dh}{dt}, \tag{4.2}$$

where T is the transmissivity in $m^2\ d^{-1}$ and L the slope length in m from hydrotope to next surface water (the drainage base, see Figure 4.2). If the groundwater body is recharged by deep soil percolation or another source (Rc in $mm\ d^{-1}$) and is depleted by drain discharge (q), it follows that the water table will rise when $Rc - q > 0$, and fall when $Rc - q < 0$. Then the groundwater table fluctuations may be described as:

$$\frac{dh}{dt} = \frac{Rc - q}{CS}. \tag{4.3}$$

where S is the specific yield in $mm^3\ mm^{-3}$ (the fraction of meso- and macropores). It follows that by assuming that the retention constant $C = 0.8$ (Smedema and Rycroft, 1983), we get:

$$\frac{dq}{dt} = \frac{10T}{SL^2}(Rc - q) = \alpha \cdot (Rc - q), \tag{4.4}$$

so that the change in drain discharge dq/dt is proportional to the excess recharge Rc-q, with α being the proportionality factor (or reaction factor). Equation 4.4 can be transformed to gain the equation for groundwater discharge:

$$q_t = q_{t-1}e^{(-\alpha\Delta t)} + Rc_{\Delta t}\left(1 - e^{(-\alpha\Delta t)}\right). \tag{4.5}$$

Using the linear relationship between q and h (Equation 4.2), we get:

$$h_t = h_{t-1}e^{(-\alpha\Delta t)} + \frac{Rc_{\Delta t}}{0.8S\alpha}\left(1 - e^{(-\alpha\Delta t)}\right). \tag{4.6}$$

The equations are scale independent and the spatial unit for which h and q are calculated is the hydrotope level, using the average distance to the next river L (or the slope length) to vary the fluctuations in groundwater table in a physically sound way (see Equation 4.4). The factor α is a function of the transmissivity T and the slope length L:

$$\alpha = \frac{10 \cdot T}{SL^2}. \tag{4.7}$$

Therefore, the reaction factor has a physical meaning, as was illustrated by a comparison with the results of the numerically solved Boussinesq Equation (Hattermann et al., 2004), where the same geo-hydrological parameters (T, L, S) were used to solve both the equations.

However, two of these parameters, namely transmissivity and specific yield,

are not usually available at the regional scale. Another method is to estimate the reaction factor α from field observations by directly using observations of the groundwater head h. This was done using an automatic calibration algorithm by adjusting T and S in physically sound limits. Parameter α has a time dimension and can be interpreted as the reaction time of the groundwater table and discharge to changes in recharge. The approach also allows better simulation of fluctuations in base flow (where relatively few observations exist) by calibration of fluctuations in groundwater table (where relatively many observations exist), since both equations use the same reaction factor α.

Nutrient retention in subsurface and groundwater

During the subsurface transport of nitrogen from soil column to rivers and lakes, the geo-chemical conditions change from oxidation to reduction, depending on water content, and carbon and oxygen concentration along the pathway. These conditions are site-dependent and can change in SWIM from hydrotope to hydrotope. They are crucial for the intensity of denitrification, which is probably the major process leading to loss of nitrogen from soil during its subsurface transport (Mander and Kull, 1997). The second important parameter influencing denitrification is the residence time of nitrogen in the subsurface, which determines the time period during which nutrients can be subject to denitrification. The time scales considered here are much larger (years and decades) than the time scales for groundwater table dynamics (the reaction time). The equation derived below combines these two parameters, and the derivation of the parameters is described in the next section.

Assuming that a change in the amount of subsurface nitrogen over time (dN/dt) without transformation (denitrification) is determined by nitrogen input N_{in} ($kg\ ha^{-1}$) into the subsurface and nitrogen output N_{out} ($kg\ ha^{-1}$), we get:

$$\frac{dN_t}{dt} = dN_{t,in} - dN_{t,out} \tag{4.8}$$

According to (Wendland et al., 1993), the denitrification of nitrate nitrogen in the subsurface can be approximated in large-scale simulations by using a linear decay equation, where the denitrification rate λ $[d^{-1}]$ is a function of temperature, carbon and available oxygen. Then the change in subsurface nitrogen can be

described as:

$$\frac{dN_t}{dt} = dN_{t,in} - dN_{t,out} - \lambda dN_t \tag{4.9}$$

Assuming in addition that the system is linear, and the actual amount of nitrate nitrogen can be expressed as a function of output dN_{out} and a storage constant or mean residence time K (d):

$$N_t = KN_{t,out}, \tag{4.10}$$

we can substitute N_t by $N_{t,out}$:

$$\frac{dN_{t,out}}{dt} = \frac{dN_{t,in}}{K} - \frac{dN_{t,out}}{K} - \lambda dN_{t,out} = \frac{dN_{t,in}}{K} - \left(\frac{1}{K} + \lambda\right) N_{t,out} \tag{4.11}$$

Therefore, the full retention in a landscape is a function of mean residence time of nitrate N in the subsurface and the denitrification potential (expressed by λ) of its hydrotopes. K has the dimension of time in days d, and the retention constant λ the dimension of d^{-1}. The underlying two basic simplifications of this linear approach are an assumption of a perfect mixture of the water volumes during the subsurface flow path by diffusion and dispersion, and an assumption that K and λ are normally distributed. Equation 4.11 is an inhomogeneous linear function of first order and can be further resolved as:

$$N_{t,out} = N_{\Delta t,in}\frac{1}{1+K\lambda}\left(1 - e^{-\left(\frac{1}{K}+\lambda\right)\Delta t}\right) + N_{t-1,out}e^{-\left(\frac{1}{K}+\lambda\right)\Delta t} \tag{4.12}$$

where K is the mean residence time of water needed to flow from the specific hydrotope to the surface water system, and $[ln(2)/\lambda]$ is the subsurface half-life time of nitrogen typical for the specific geological formation (Wendland et al., 1993). Since SWIM distinguishes between nutrient fluxes with surface flow, interflow and base flow, each having different retention characteristics (residence time, oxygen and carbon content of the sediments), they all can be described by the same Equation 4.12 with the flux-specific parameters.

Water and nutrient uptake by plants from groundwater

Plant uptake of water and nutrients from groundwater is only possible when the plant roots have access to it, and under the condition that water and/or

nutrient demand cannot be satisfied by soil water and nutrient content. The additional uptake is further limited to the amount of water and nutrients flowing through the specific hydrotope. The access of plant roots to groundwater and nutrients in groundwater is controlled by resistance functions (Equations 4.13 - 4.15). The parameter of the resistance function for water uptake was estimated using lysimeter data of Riek et al. (1994) for comparable wetland soils from a neighboring catchment, where GW_{upm} ($mm\ d^{-1}$) is the maximum uptake from groundwater, GW_{upa} ($mm\ d^{-1}$) the actual uptake, h the groundwater table height in m and r_gw the resistance parameter with values from 0 to 1 to adjust the uptake:

$$GW_{upa} = r_{gw} GW_{upm} \quad if\ plant\ root\ length\ >\ water\ table\ depth \tag{4.13}$$

$$GW_{upa} = 0 \quad elsewhere, with \tag{4.14}$$

$$r_{gw} = 0.001h + 1.3 \tag{4.15}$$

The resistance function for nitrogen uptake from groundwater is more simply, because of the lack of detailed data to adjust the relevant processes:

$$Ngw_{upa} = r_n Ngw_{upm} \quad if\ plant\ root\ length\ >\ water\ table\ depth \tag{4.16}$$

$$Ngw_{upa} = 0 \quad otherwise, \tag{4.17}$$

where Ngw_{upa} is the actual N uptake from groundwater, Ngw_{upm} the maximum N uptake, and r_n the resistance parameter, which combines different processes affecting plant uptake of nitrogen. The absolute amount of possible daily uptake per hydrotope is limited to the amount of nutrients flowing through the hydrotope as calculated using the flow accumulation method described in the next section.

Estimation of additional parameters

In order to implement the model extensions, we have to estimate the new model parameters described above. These parameters are important for lateral water flow and nutrient retention, and could be treated as constants having only minor changes over long time periods that can be ignored in the modeling framework. They can be estimated during the data preprocessing using Geoinformation Sys-

tems (GIS) functions like the flow path method and maps of the geo-hydrology and groundwater contours. The flow path method calculates, for each cell, the least-accumulative-cost distance over a cost surface (groundwater contour map) from a source cell or a set of source cells (the hydrotopes) while accounting for surface distance and horizontal and vertical cost factors (e.g. travel times per horizontal unit, see Equation 4.19).

The distance L to the next river (used in Equation 4.7) was calculated following the gradient in groundwater table to the next river or lake:

$$L = \sum_{i=1}^{n} dz_i \tag{4.18}$$

with dz in m being the size of a spatial unit z and n the number of spatial units flowed through. The mean residence time K in days (used in Equation 4.12) is a function of permeability, porosity, real flow path and gradient in groundwater table for subsurface flow and the gradient in topography and Manning's roughness for surface flow. It can be calculated using the seepage velocity ν_s $(m\ d^{-1})$ (Maidment, 1993):

$$\nu_s(z) = \frac{-k \cdot J(z)}{S} \tag{4.19}$$

$$K = \sum_{i=1}^{n} \frac{d(z_i)}{\nu_s(z_i)} \tag{4.20}$$

where k in $m\ d^{-1}$ is the hydraulic conductivity of the spatial unit z, J the dimensionless hydraulic gradient, and S the specific yield.

The mean denitrification λ (used in Equation 4.12) has been calibrated using values taken from Wendland et al. (1993) for the Elbe region as initial values. Additional calibration was necessary because of the lack of detailed information about the parameters necessary to calculate λ (redox potential and carbon concentration of the catchment sediments). Generally, the sediments in the Nuthe basin have high pyrite concentrations and therefore good denitrification conditions, with a half-life time of nitrate of between 1 and 3 years (Wendland et al., 1993), which corresponds to λ values of between $6{\cdot}10^{-4}$ d^{-1} and $2{\cdot}10^{-3}$ d^{-1}.

The maximum uptake was calculated using the flow accumulation method which calculates the amount of substances (e.g. nutrients, sediments) flowing through a spatial unit of the catchment following the groundwater gradient. The

proportion of the long-term average nutrient discharge per wetland hydrotope to the long-term total nutrient discharge in wetlands gives the share of the possible daily uptake by plant roots per hydrotope as defined by Equation 4.16.

It is assumed that the values discussed above have only small changes in time but no increasing or decreasing trend (steady state conditions over a long time period). This is certainly true for geo-hydrological parameters like porosity and permeability, which can only change over geological time scales, but fluctuations in the groundwater table and therefore the gradient in groundwater have more pronounced dynamics. However, the changes in groundwater gradient are normally very small and the mean residence time of groundwater flow is very large (e.g. on average 40 years in our study area), therefore the small reversible changes in groundwater gradient are negligible. In addition, these parameters affect only the steepness of the recession curve of groundwater table and nutrient concentration, but the actual values are calculated by SWIM on a daily time step based on groundwater recharge and nutrient leaching from soil. Following this assumption, calculation of the relevant retention parameters for lateral flow during the data preprocessing allows computation time to be saved while considering the fundamental hydrological processes in a physically sound way.

4.3 Results and discussion

4.3.1 Hydrology

The first step of the modeling procedure was to adjust the groundwater fluctuations at the hydrotope level. This was done by comparing the simulated mean annual water table of the subbasins in the Nuthe catchment against the observed mean annual water table. The calibration was done automatically by changing the transmissivity in a physically sound range, based on the geo-hydrological information (between 10 m d^{-1} for the layers having low transmissivity and 60 m d^{-1} for the layers with high transmissivity (see NBL, 1985; Wendland et al., 1993). After adjusting the transmissivity, it was found that the simulated daily amplitude of groundwater table changes was too high for several hydrotopes. The groundwater dynamics were corrected by a moderate increase in the value of specific yield, whereby the range of specific yield is about 3 % for the layers with low and about 20 % for the layers with high porosity (NBL, 1985). The Mean Absolute Error

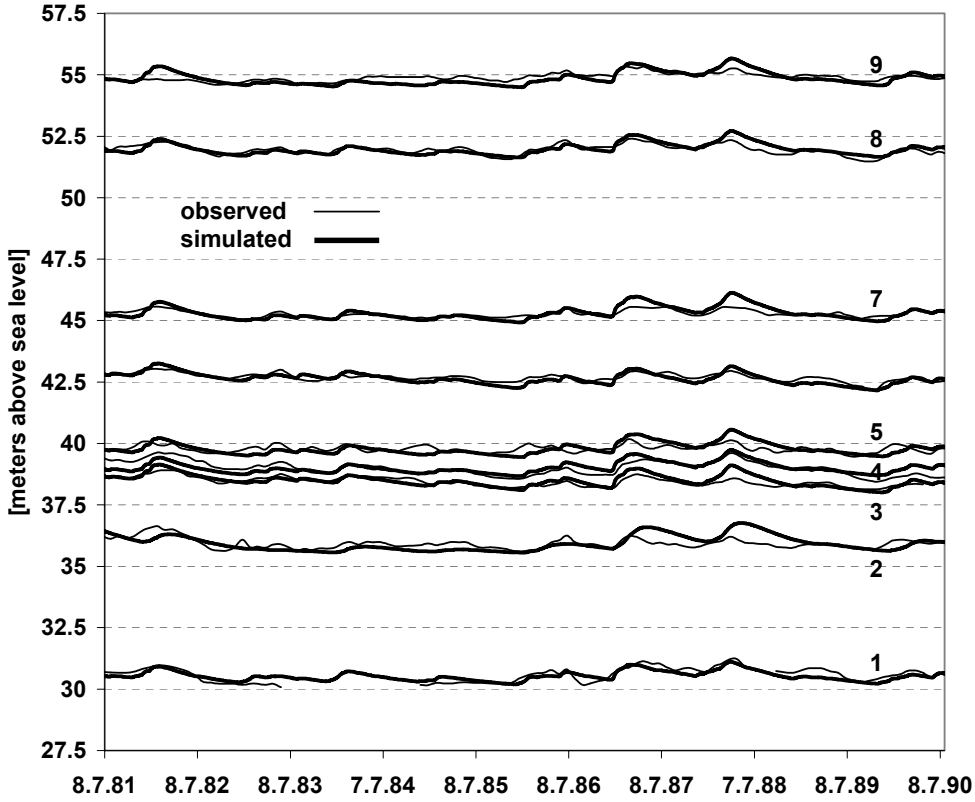

Figure 4.3. Comparison of observed and simulated groundwater table for nine observation wells in the Nuthe basin (locations are shown in Figure 4.1).

of the observed long-term mean against the mean simulated water table in all subbasins was 0.026 m. The dynamics of the simulated water tables in terms of rising and retention periods were not calibrated. The amplitudes are smaller close to the river system and become larger with increasing distance from the drainage base.

A comparison of observed and simulated groundwater levels for nine points is depicted in Figure 4.3. The locations of the observation wells were selected in order to represent a cross section through the basin from the lowland in the north to the hilly area in the south. Well 1 is located close to the outlet of the Nuthe river catchment. The curves show a good fit, especially for the early 1980s. However, the rise of the groundwater level in 1987 and 1988 is slightly overestimated by the model in subbasins 2, 7, 8 and 9. As explained earlier, the

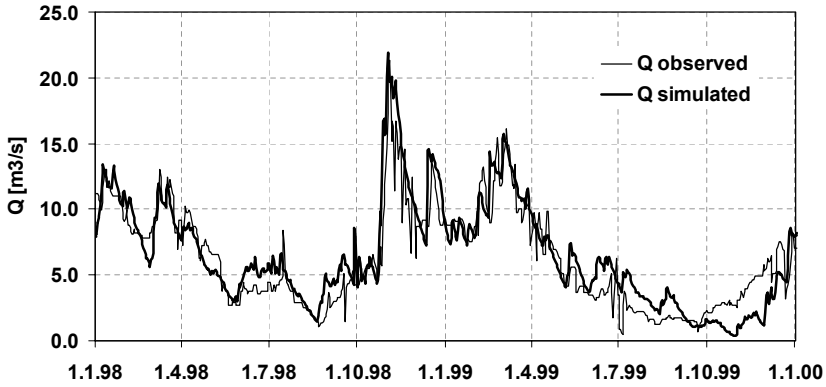

Figure 4.4. Comparison of the observed and simulated daily river flow (Babelsberg gauge) using the new module.

flow regime in the Nuthe basin is regulated by weirs and gates, and especially in the lowland areas the water level is controlled by land drainage. These small-scale regulations are not considered in the model. Notable is also that the simulated groundwater hydrographs are very similar, whereas the observations show more differences. The higher variability in the observed water levels is presumably the result of small-scale heterogeneities in the aquifer and of local precipitation events, which are missing in the observed records. A better fit would be possible by considering more accurate small-scale data and also additional management information. However, this was not the objective of the study. On the contrary, the study aimed at showing that a simplified model approach provides satisfactory results using commonly available data. The simulation results confirm that the introduced groundwater module in SWIM is able to reproduce the observed water table dynamics in the basin satisfactorily enough to serve as the lower boundary condition for plant water and nutrient uptake.

The long-term difference between the observed and simulated runoff is +1.0 % for the calibration period 1981 - 1988, and +6.0 % for the validation period 1989 - 2000, indicating that the water balance is correctly calculated by SWIM with some problems in the validation period. The daily Nash and Sutcliffe efficiency (Nash and Sutcliffe, 1970) is 0.7 for the calibration period and 0.54 for the validation period. Figure 4.4 shows a comparison of the observed and simulated river discharge at the outlet of the basin for 1998 - 1999. Unrecorded small-scale water management and regulation measures of the natural river flow regime in the basin make it difficult to reproduce the hydrograph with higher accuracy. It

is remarkable that the summer discharge in some years is overestimated by the model (compare with Figure 4.4). This can be explained by unrecorded water abstraction for irrigation and by flow regulation measures aimed at maintaining a minimum river level in dry summers through ponding so that the river flow is interrupted and the river discharge decreases. Unrecorded water abstractions may also explain the model's overestimation of river discharge in the validation period, which was significantly dryer than the calibration period. According to simulation results, the additional plant water uptake from groundwater by plants in wetlands with groundwater contact during dry periods is up to 350 mm a^{-1} (less in wet years). At the basin scale, and specifically in the Nuthe basin, this additional water uptake contributes about 12 % of the total evapotranspiration and leads to about 49 % lower contribution to river runoff (for the time period 1990 & 2000). Despite the inherent uncertainty and difficulties of validation, this model outcome underlines the significant impact of a relatively small area (about 27 % of the total basin area, depending on the water table depth) on the water balance of the total catchment, especially in lowland basins with shallow groundwater table, and the importance of taking these processes into account.

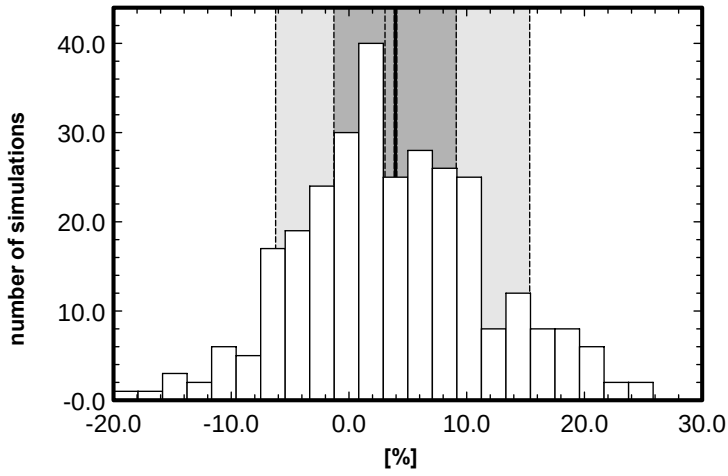

Figure 4.5. Uncertainty of the simulated water balance in the basin (the long-term difference between simulated and observed discharge: dark gray - 50 % of the simulations are included; light grey - 90 % are included).

The uncertainty of the model results is relatively high because of high uncertainty in the input data (soil parametrization, geo-hydrology, topology etc.), and the unrecorded water management measures. This is illustrated in Figure 4.5,

where the uncertainty of the water balance (in terms of the difference between the long-term simulated and observed river runoff) is plotted. The uncertainty analysis is based on a conditioned Monte Carlo simulation using the Latin Hypercube method (Richter et al., 1996; Tarantola, 2000). The analysis took into account 20 parameters responsible for different aspects of the input data (e.g. soil conductivity, maximum leaf area index), and describing different hydrological processes in the model (surface runoff, residence time), and 8 parameters responsible for nitrate uptake and retention. 300 simulations have been carried out, whereby the variation of the 28 parameters was allowed within their physically plausible range (see Annex B).

4.3.2 Nitrogen dynamics

Nitrogen input in arable soils of the Nuthe basin considered in the model consists of fertilizer applications (about 150 kg ha^{-1} a^{-1} for winter wheat, 120 kg ha^{-1} a^{-1} of that in the form of mineral fertilizers), atmospheric deposition (about 25 kg ha^{-1} a^{-1}), and plant residue decompositions after harvesting. Information on crop rotations and scheduling and amounts of fertilizers in the basin was taken from regional statistics. The nitrate N concentration in the Nuthe river during the 1980s was strongly influenced by point sources (municipal waste water and even direct discharge of liquid manure into surface water) and sewage filtration fields in restricted areas (Scheytt et al., 2000; Werner and Wodsack, 1994). The existing records for this period are vague and incomplete, therefore our simulations were performed for the 1990s (see comparison in Figure 4.6), when the impact of point sources was limited due to the improvements of waste water treatment and other measures (see Table 4.1). The sewage fields were in full operation until 1988-89.

The comparison in Figure 4.6a shows that the periodicity and amplitude of the observed values is mostly well reproduced by SWIM, although there are some differences. Better reproduction is however practically impossible because of the imprecise nature of information on crop rotations, fertilisation regime, etc., as well as the absence of information on flow regulation by dams and weirs and the influence of drainage systems. The mean residence time of nitrate N fluxes with groundwater for the whole basin estimated using GIS and Equation 4.20 is 41 years, with a maximum of approximately 400 years. The values are in good agreement with other estimates (Behrendt et al., 2002), where the nutrient loads

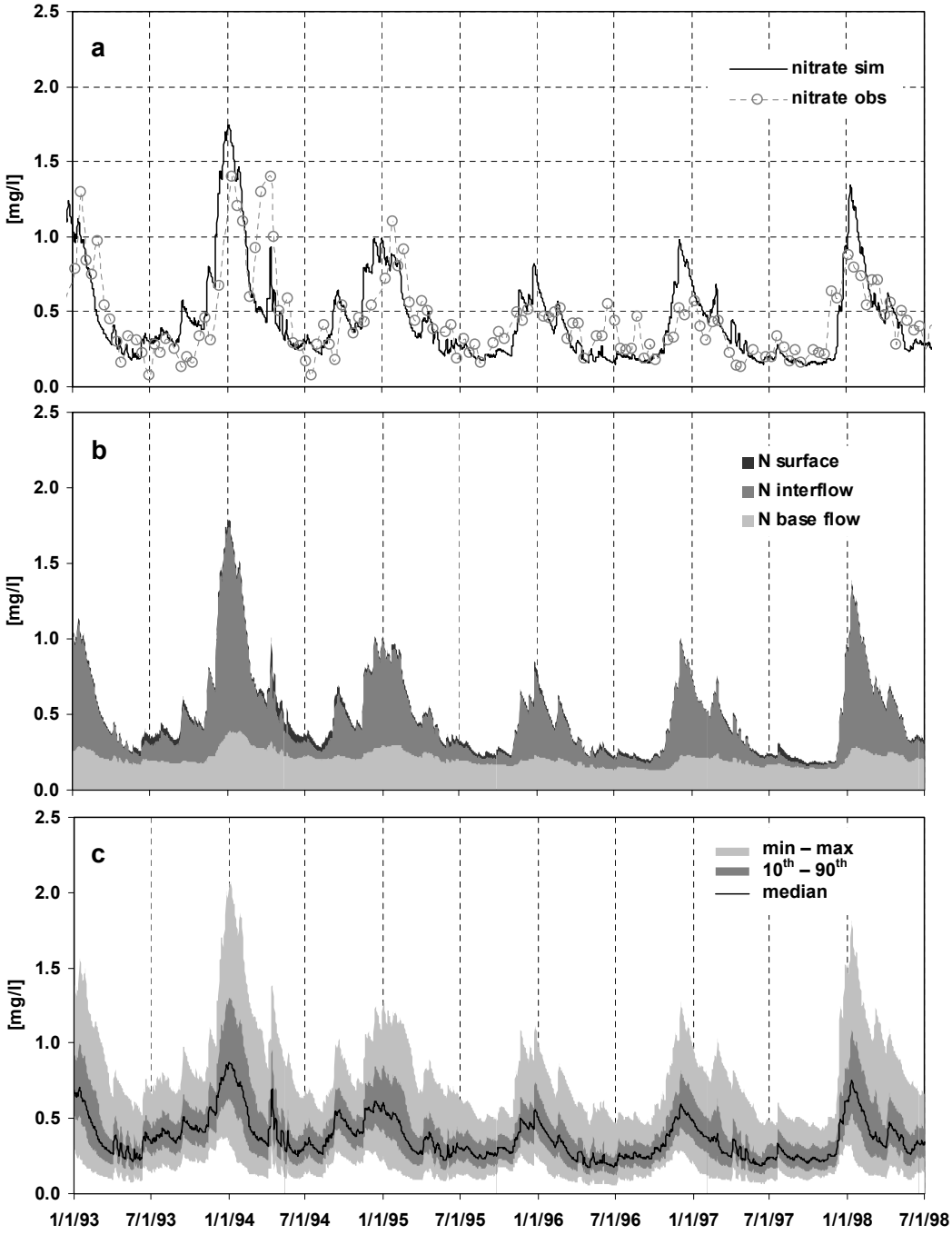

Figure 4.6. Simulated and observed nitrate N concentrations in the Nuthe river (a), nitrate N coming with different pathways (with surface runoff, interflow and baseflow) (b), and the uncertainty of the simulated results (c) (Babelsberg gauge).

and retention in the lowland catchments of the Elbe basin were evaluated. The calibrated value for the parameter of denitrification in groundwater λ is 0.003 d^{-1}, which means that the half-life time of nitrate in groundwater is 231 days.

Figure 4.6b gives an overview of nitrate N pathways to the river outlet. One can see that the baseflow flux of N prevails in summer, whereas the winter (high water period) peaks are formed by a high interflow N concentration and a baseflow flux of N. Although groundwater recharge is the dominant water flow generation process and nutrient transport component in the Nuthe basin, only about 50 % of the nitrate N in the river outlet is transported with the base flow. The reasons are the high denitrification rate, and the long residence time in the aquifer. The base flow component is smoothed, with some small peaks which are generated by riparian hydrotopes located close to the river and having a shorter residence time. Nitrate N transported by interflow shows a greater dynamic, mainly due to shorter residence times. The nitrate retention rate in the groundwater of the Nuthe catchment is 99 % ± 1 % and in interflow 96 % ± 2.5 %, in other words in total about 99 % of the nitrate leaching to groundwater and about 96 % of nitrate transported by interflow is denitrificated during the flow to the subsurface water system. The result for the total nitrate retention in the Nuthe basin is supported by Behrendt et al. (2002) as well as by a simple balance equation taking into account inputs by fertilisation and deposition and annual river load. These retention values are the spatio-temporal average values for the total Nuthe basin, which may vary from year to year and from site to site. They do not mirror the spatial heterogeneity in the basin as it is considered in the new model concept, where hydrotopes located close to the surface waters contribute much more to the river nitrate load due to the shorter residence time of water than hydrotopes located further away (see also Figure 4.8d-f).

Figure 4.6c shows the uncertainty of the simulation results (expressed as the 90 % confidence interval around the calibrated values, based on 300 simulations with varying parameters). The uncertainty was estimated using the same methodology as for the water balance, but including 8 more parameters describing the mean residence times and retention parameters for the different flow components. It is obvious that the uncertainty in the simulated nutrient fluxes is high, with an asymmetrical distribution around the median. The uncertainty is higher for peaks than for lower concentrations, indicating that the model is able

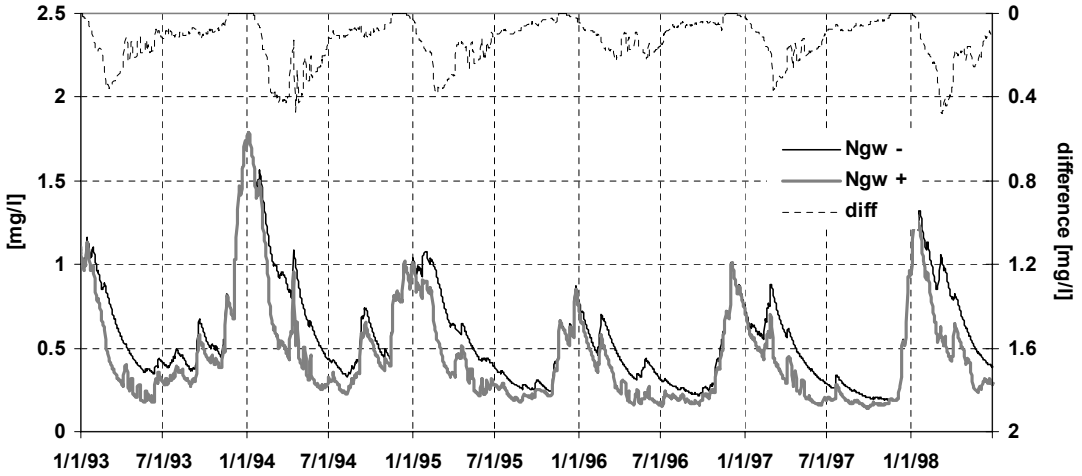

Figure 4.7. Comparison of simulated and observed nitrate N concentration with and without plant water uptake from groundwater.

to predict satisfactorily the base flow component (the long-run behaviour), but has problems in reproducing correctly the short-run behaviour, where the model parameterisation is crucial. It is therefore likely that the model would have difficulties to simulate the peak concentrations without observed data for calibration and accurate management data, for example under scenario conditions or in ungauged basins. However the model performance in dry periods is more reliable.

Figure 4.7 illustrates the impact of the model extension described in Section 4.2.3, when additional nitrate N uptake by plants from groundwater is considered in riparian zones and wetlands. The differences are the highest during the summer season, when plant N demand is high and can therefore not be satisfied only by N in soil water. The differences become negligible by the late autumn. The long-term decrease in annual river nitrate N load due to additional plant uptake from groundwater is about 21 %.

Figure 4.8 shows six maps demonstrating nitrate N dynamics in the Nuthe basin: nitrate N input by fertilisation and atmospheric deposition, leaching from soil layers by groundwater recharge and interflow, plant uptake from soil, plant uptake of nitrate N from groundwater, and nitrate fluxes generated at a specific site that actually reach the surface water system by base flow and direct flow (surface and interflow) in kg ha^{-1} a^{-1}.

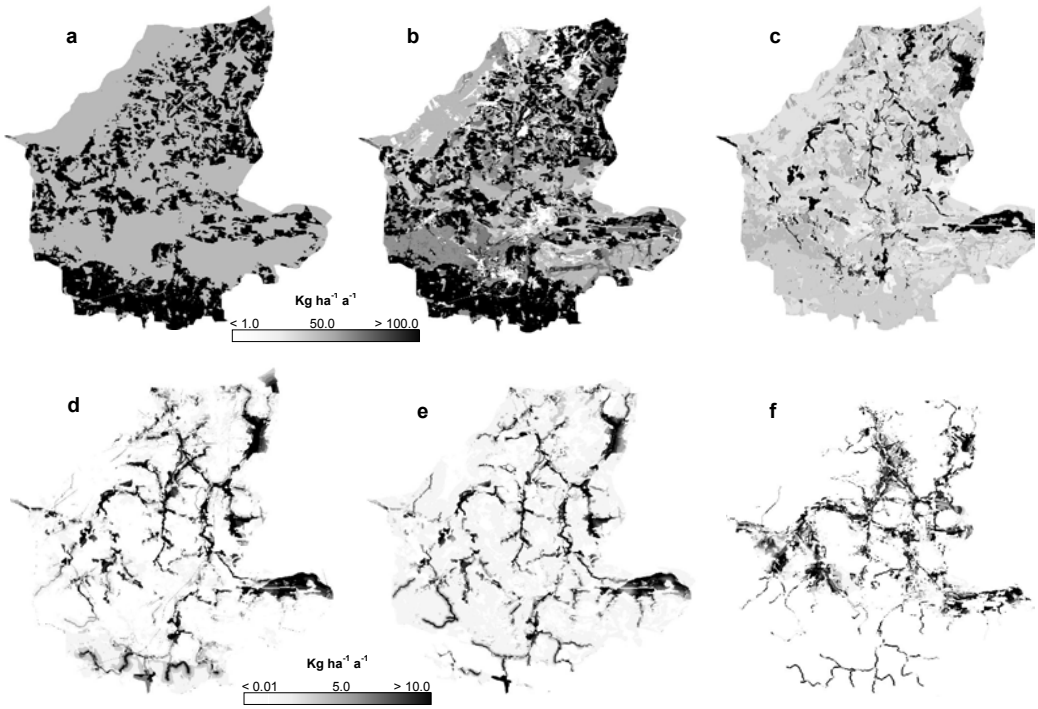

Figure 4.8. Nitrate N dynamics in the Nuthe basin: nitrate N input by fertilisation and atmospheric deposition (a), nitrate N leaching from soil columns by groundwater recharge and interflow (b), plant uptake of nitrate N (c), nitrate N flux from a specific site to the river transported by interflow and surface flow taking into account retention (d), nitrate N flux from a specific site to the river transported by base flow taking into account retention (e), plant uptake of nitrate N from groundwater in wetlands and riparian zones (f).

Figure 4.8b allows detection of areas responsible for groundwater pollution, maps 4.8e and 4.8f indicate areas responsible for the pollution of river water. For example, the till soils in the southern part of the catchment generate high amounts of nitrate N leaching, which are then transported by interflow to the river system, whereas transport by groundwater is negligible in this area. Generally, areas located closer to surface waters contribute more to the river nitrate load than areas further away, due to the shorter transport time and therefore lower denitrification intensity. The amount of additional plant nitrate N uptake from groundwater in wetlands is not particularly high compared with the total plant N uptake (up to 160 kg ha^{-1} a^{-1}). The additional nitrate N uptake is about 1 % of the total N uptake, however this leads to a reduction of the total river nitrate N load of about 22 %. The reason for this is that the additional uptake

happens mostly in riparian areas close to the surface water system, where the largest part of the nitrate N transported from upper parts of the catchment is already denitrified.

4.4 Conclusions

Using the extended model, which includes representation of retention and riparian processes in the catchment, it was possible to analyze the impacts of wetlands and riparian zones on water and nitrogen dynamics, and to reproduce the spatial heterogeneity of water and nitrate retention in the Nuthe basin. The spatial scale considered (about 2000 km^2) is relevant for water management planning and for the implementation of the Water Framework Directive. The aim was thereby to find modeling solutions which are physically sound but simple enough to be applied at the river basin scale using regionally available data.

The reliability of the model results was tested using the contour maps of the long-term mean water table, observed groundwater level data and observed river discharge and nitrogen concentrations. Additional small-scale validations were carried out in a parallel study by comparing the simulated results with observations from lysimeter experiments (Post et al., 2005), and under well-defined boundary conditions by comparing the SWIM results with those from a two-dimensional numeric groundwater model under steady-state and transient conditions. Since the accuracy of the regionally available input data (soils, geo-hydrology, land use, crop rotations, application of fertilizer) is rather poor, special attention was paid to the assessment of uncertainty propagated by the model.

The model structure allows the fundamental processes relevant for water and nutrient flows and retention in catchments to be considered, with a focus on wetlands and riparian zones. The model results and especially the small-scale spatial distribution of nutrient fluxes could be improved by using more accurate data on crop rotations and fertilizer application regimes. The results show that riparian zones and wetlands are important buffer systems influencing the water balance and are able to reduce eutrophication in surface waters. The riparian zones, although relatively small subareas of the total catchment area, have a significant impact on the water and nutrient balances in the catchment. For the Nuthe basin in the period 1990 - 2000 the additional evapotranspiration was about

12 % (of the total evapotranspiration in the whole catchment), and additional nitrate uptake was about 1 % (of the total nitrate uptake in the whole catchment), leading to a decrease in river discharge of about 49 %, and to a decrease in annual river nitrate load of about 22 %, although the results are associated with high uncertainty. The impact of riparian wetlands is so significant because they are at the interface between upper catchment areas and surface water systems, with the transported nutrients from arable fields passing through them on their way to the river, and because these areas have a connection to groundwater. The larger part of nitrogen applied as fertilisers or mineralised in soil is volatilised during the subsurface passage, and a notable part of the remaining nitrate concentration is taken up by plant roots located in riparian zones.

The restoration and management of wetlands therefore has high priority in the control of non-point source pollution of surface waters. However, the impact on the local water balance has to be considered in the river basin planning process. Only about 24 % of the annual rainfall in the Nuthe basin reaches the basin outlet in terms of river discharge (Table 4.1), and small changes in evapotranspiration have a large influence on the total amount of river flow. The restoration of wetlands will lead to increased water losses by evapotranspiration, crucial in a region where river discharge during the summer season is only possible by water regulation through dams and weirs, and where a trend towards lower annual precipitation has been observed during the last decades. It follows that water managers have to find a balance between water quality and water quantity aspects in the process of river basin planning and management.

Acknowledgments

The authors would like to thank all their colleagues at PIK who contributed to this paper with technical help. Part of this work was supported by the German BMBF programme GLOWA (GLObal WAter) Elbe and the Brandenburg State Environmental Agency (LUA Brandenburg).

HYDROLOGICAL SCIENCES-JOURNAL DES SCIENCES HYDROLOGIQUES (2005)
(*submitted*)

Chapter 5

Assessing uncertainty of water availability in a Central European river basin (Elbe) under climate change

Shorttitle: uncertainty of water availability under climate change

Keywords: Climate change impacts, climate change uncertainty, climate downscaling, regional hydrological modeling, crop yields.

Hattermann*, FF, Krysanova, V, Post, J, Gerstengarbe, FW, Werner, PC, Wechsung, F
Potsdam Institute for Climate Impact Research
* Full address of the corresponding author:
Dipl.-geoecol. Fred Fokko Hattermann
Global Change and Natural Systems Department
Potsdam Institute for Climate Impact Research
P.O. Box 601203, Telegrafenberg
14412 Potsdam
Germany
Fax: +49 331 288 2600
Tel. +49 331 288 2649
E-mail: fred.hattermann@pik-potsdam.de

Abstract The Elbe region is representative of humid to semi-humid landscapes in Central Europe, where water availability during the summer season is the limiting factor for plant growth and crop yields, especially in the loess areas with high crop productivity, where the annual precipitation is lower than 500 mm. This study tries to assess the reliability of water supply in the German part of the Elbe river basin for the next 50 years, a time-scale relevant for the implementation of water and land use management plans. A global scenario of climate and agro-economic change has been regionalized to generate transient climate forcing data and land use boundary conditions for an eco-hydrological model integrating hydrology, nutrient transport and vegetation growth at the catchment scale. The model is used to transform the climate and land use changes into altered evapotranspiration, groundwater recharge, crop yields and river discharge. Particular emphasis was given to assessing the significance of the impacts on the hydrology, taking into account in the analysis the inherent uncertainty of the regional climate change as well as the uncertainty in the results of the model which is used to assess the impacts.

One climate anomaly of the region is that both the observed and the projected trend in precipitation differ from the anticipated global trend. The average trend of the regional climate change scenario indicates a decrease in mean annual precipitation up to 2055 of about 1.5 %, but with high uncertainty (covering the range from -15.3 % to +14.8 %), and a less uncertain increase in temperature of approximately 1.4 K. The relatively small change in precipitation in conjunction with the change in temperature leads to severe impacts on groundwater recharge and river flow. Increasing temperature induces longer vegetation periods, and the seasonality of the flow regime changes towards longer low flow spells in summer. The uncertainty of the trend is particularly high in regions where the change is the highest. The concluding result of the study is that natural environment and communities in parts of Central Europe will have considerably lower water resources under scenario conditions.

5.1 Introduction

Major advances have been made in atmospheric modeling and in the understanding of climate processes and climate change (IPCC, Part I, 2001). The increase

in global surface temperature leads to higher evapotranspiration rates and higher amounts of atmospheric water vapor, and an increase in precipitation is likely to affect large areas in the tropics and at higher latitudes. Increased climate variability is already being observed, although there are still large uncertainties about the causal connection to climate change (IPCC, Part I, 2001). The impacts are wide ranging, but the relevance for water and land management and terrestrial ecosystems, where climate is one of the most dominant boundary conditions, is obvious and profound (Kabat et al., 2002). Floods, droughts and other extreme events add to the problems water managers face from population growth, urbanization and land use changes (Kundzewicz et al., 2002). Measures that enhance both ecological and human social resilience in vulnerable settings are, accordingly, crucial for mitigating the growing risk of climate change and climate-related disasters. Nevertheless, typically the implications of climate variability and climate change have not been considered in current water and agriculture policy and decision-making frameworks.

There have been numerous studies on the potential impacts of climate change on water resources and agriculture over the last decade (for example (Bronstert et al., 2002; Menzel and Burger, 2002; Chiew and McMahon, 2002; Eckhardt and Ulbrich, 2003); a review on climate change, climate models and water resources management can be found in (Varis et al., 2004). However, in most studies the climate change impact was investigated for the hydrological regime, land use and agriculture separately, applying different and incompatible tools, and without addressing the possible feedbacks and inherent uncertainty of the results (Bronstert, 2004). This study tries therefore to

- develop and apply a transient climate and land use change scenario which is consistent in terms of its climate and socio-economic boundary conditions, and takes feedbacks into account.
- investigate and quantify the climate and land use change impact on water resources in a region where the per capita water supply is very low, and where the water availability is the main constraint for vegetation growth and crop yields.
- quantify the uncertainty of water resources availability.

The uncertainty induced by the climate change scenario has to be considered

because the climate system of the earth, of which human activities are one part, is highly nonlinear and hence future trends are hard to predict (Manning, 2003). To tackle this problem, the Intergovernmental Panel on Climate Change (IPCC) defined several scenarios of future developments in order to investigate their impacts on the earth system (IPCC, Part II, 2001). One tool that is widely used to analyze the impacts of these scenarios on the climate are global circulation models (GCMs). However, GCMs are designed to work on the global-scale and are unable to reproduce the small scale variability of climate characteristics in space and time due to their coarse spatial resolution and to the uncertainty of their results at time-scales of days and for variables such as radiation (clouds) and precipitation (Wilby et al., 1999). This is crucial, because floods and droughts are generated at the scale of river basins. In addition, the regional climate trends may differ from the global trend (Varis et al., 2004). For example, the assumption of increasing precipitation in future does not apply to all areas of the earth. Due to possible changes in circulation pattern and local orographic conditions the amount of precipitation will most likely even decrease in some regions in future, e.g. in parts of Central and Eastern Europe (Werner and Gerstengarbe, 1997). For this reason this study takes into account regional characteristics, using climate forcing data produced by a statistical downscaling method to disaggregate the GCM simulation output to the regional catchment scale (Gerstengarbe and Werner, 2005).

Although the downscaling process helps to tune the global climate change scenario to the regional climate characteristics, uncertainty remains. Nevertheless, investigations of future climate change impacts have up to now mostly considered a climate scenario as a new boundary condition and applied it as input in hydro-environmental modeling as if were observed (hard) data (Christensen et al., 2004; Limbrick et al., 2000). To overcome this problem, the regional climate scenario applied in this study is based on a conditioned Monte Carlo simulation, such that the set of future climate realizations covers the possible range of climate change under scenario conditions in the Elbe region. Special attention was given to two scenario realizations: one is based on the observed precipitation change for the period 1951-2000 and is the most reliable climate extrapolation for the total basin, and the second is the most reliable extrapolation for the Magdeburg climate station, located in the center of the loess region, the area having the

highest agricultural productivity.

The second boundary condition subject to global change and important for the water balance of a landscape is the local land use pattern (Fohrer, 2002). The land use scenario used in this study has been derived assuming that changes will mainly affect agriculture. Both the anticipated trend in global agricultural economics and the trend for crop yields under climate change were integrated in develop of the land use scenario, with feedbacks between climate change and vegetation growth being taken into account to assure consistency in the climate and land use scenario. The description of the methodology to derive the land use scenario and the illustration of climate change impacts on crop yields are the topic of a complementary article (Wechsung et al., 2005b). A brief introduction to the scenario generation and the associated model setup is given in section 5.2.1.

The eco-hydrological model used to analyze the impacts of changes in climate and land use on hydrology and crop yields is the model SWIM (Soil and Water Integrating Model, Krysanova et al., 1998). It was chosen because it combines all major eco-hydrological processes at the meso- to macroscale, which are important for land use and climate change impact studies, such as hydrology, vegetation, erosion and nutrient dynamics (Bronstert et al., 2005). The approach allows simulation of all interrelated processes within a single model framework using regionally available data. SWIM was validated in the Elbe river basin for the reference period (1951-2000) and has proven to be able to reproduce the observed hydrological characteristics as well as the regional crop yields (Hattermann et al., 2005a; Krysanova and Becker, 1999). SWIM is used to propagate the inherent uncertainty in water supply under climate change caused by the uncertainty in the climate input data (the regionalized GCM output), whereby SWIM transforms the change in climate into altered hydrological quantities. The results are statistically analyzed and compared against the results of the reference period as well as results of relevant studies recently published.

5.2 Material and methods

5.2.1 The modeling strategy

The aim of the project was to assess the reliability of water supply and crop yields in the German Elbe river basin for the next 50 years, whereby this study focuses on changes in water resources. It was decided to use a scenario where the driving forces, climate as well as land use changes, are consistent and based on the same IPCC story-line. The GCM simulation run selected to apply in the study was produced by the coupled atmosphere-ocean model ECHAM4-OPYC3 (Röckner et al., 1999), which was driven by the IPCC SRES emission scenario A1. This section will give a brief description of the modeling procedure applied to develop the regional scenario, which was the basis for the estimation of the water supply and crop yields under global change in the study area.

The regional climate change scenario was derived using the statistical downscaling model STAR (STAtistisches Regionalmodel, Werner and Gerstengarbe (1997) (1 in Figure 5.1), based on the assumption that the most reliable result of GCM model simulations is the trend in temperature. Long-term transient time series of the possible future climate (2000 - 2055) were calculated in such a way that they reflect the temperature changes calculated by the GCM in the given scenario as well as the observed regional climate pattern. The IPCC temperature scenario selected gives a rather moderate temperature increase of approximately 1.4 K up to 2050. The anticipated scenario increase in temperature can be - due to the robustness of the temperature signal with only small differences of temperature increase in the different IPCC scenarios up to 2050 - regarded as representative for the model region and different scenarios (Gerstengarbe and Werner, 2005).

The stochastic character of the possible climate change in the region was taken into account in the scenario derivation by incorporating a conditioned Monte Carlo approach in the downscaling process and producing 100 realizations. They cover the possible range of climate change under various scenario conditions in the German Elbe basin. Due to the method used each of the realizations maintains the basic statistical characteristics, in this case consistency in frequency distribution, annual and inter-annual variability and persistence of the main climate characteristics. The results were tested by comparing the values for the reference

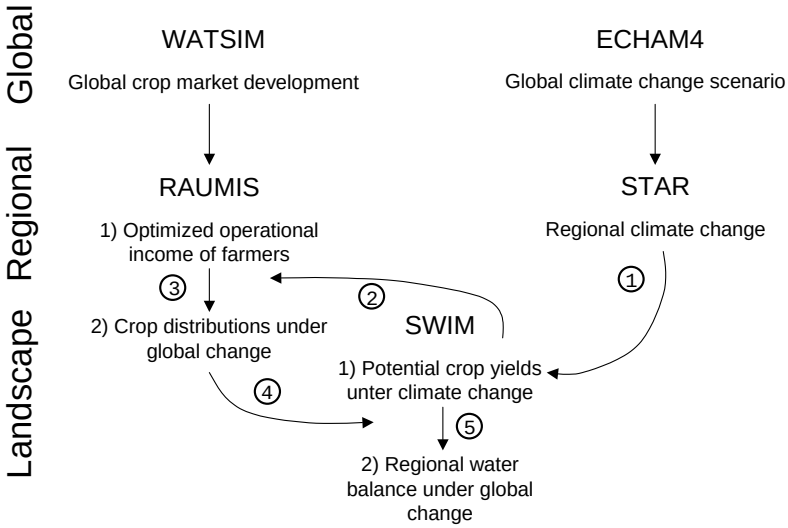

Figure 5.1. Flow chart of the modeling procedure.

period and the scenario period. Afterwards, the most probable realizations were determined by comparison with the observed trend in the reference period. For further details about the regional climate model STAR and the development of the regional climate scenario see Gerstengarbe and Werner (2005).

The next step was to derive a land use change scenario consistent with the socio-economic story-line of the regional climate change scenario. This was done based on the assumption that land use changes in the Elbe basin will mainly affect arable land. Following this assumption, the eco-hydrological model SWIM was used to calculate potential crop yields under climate change for the nine main crops cultivated in the study area (point 1 in Figure 5.1). The climate change scenario taken was the most probable variant of the 100 scenario realizations produced by STAR. The crop yield simulation included a fertilization effect of a continuously increasing atmospheric carbon concentration from 346 ppm to 456 ppm (Wechsung et al., 2005a). The results represented one input for the regional agro-economic model RAUMIS (Regionales Agrar- und Umweltinformationssystem für Deutschland, Henrichsmeyer et al., 1996). They were used by RAUMIS to optimize the potential operational income of farmers in the study area under climate change and to calculate corresponding county specific crop distributions (land use scenario variant A) (2 in Figure 5.1). The second input was given by global crop market conditions as defined by the underlying IPCC storyline and

produced by the global agro-economic model WATSIM (von Lampe 1999). This input was used by RAUMIS to optimize the potential operational income of farmers under socio-economic change in a second land use scenario (land use scenario variant B). The spatial aggregation level of the simulations is the administrative level of counties. For more information about the models WATSIM and RAUMIS and the development of the land use scenario see (Henrichsmeyer et al., 1996).

The county-specific crop distributions derived by RAUMIS had to be transformed into crop rotations for each spatial element considered in the eco-hydrological model SWIM (3 in Figure 5.1), which are much smaller than the average county area, and which are not defined by administrative boundaries but delineated on the basis of information about the environmental characteristics of the basin (the so called hydrotopes, see next section). A crop generator was developed and implemented in SWIM to disaggregate the county-specific crop distributions and to calculate crop rotations for each hydrotope under the constraint that the simulated crop distributions in the catchment agree each year with the county statistics (Wechsung et al., 2005b). This was done for seven soil fertility classes, whereby the commercially more valuable crops with generally higher nutrient and water demand were allocated to areas with fertile soils and vice versa, as recorded in the local crop statistics.

The final step was to transform the regional climate and land use change into altered hydrological quantities (5 in Figure 5.1). This was done by running SWIM 100 times, each time forced by another realization of the climate change scenario, and with the land use scenarios as spatial boundary condition. For technical reasons (modeling performance) and considerations of quality assurance, this procedure was performed automatically. The climate (observed and 100 realizations) and land use data were stored in a database, and an interface has been developed which organizes the data exchange between data base and eco-hydrological model, the preprocessing of the climate data (selection from the database, interpolation of the data and transformation into the input format of the eco-hydrological model) and the land use data, the 100 runs of the eco-hydrological model and the post-processing of the results (aggregation and statistical analysis). The automation simplifies the problem analysis and error detection and allows a fast repetition and reproduction of each single step of the modeling procedure.

5.2.2 The SWIM model

The SWIM model integrates the relevant hydrological processes to investigate the impacts of climate changes like water percolation, surface runoff, interflow, groundwater recharge, plant water uptake, soil evaporation, and river routing. SWIM is based on two older model developments, the basin scale eco-hydrological model SWAT (Soil and Water Assessment Tool, Arnold et al., 1994), and the regional model MATSALU (Krysanova and Luik, 1989). A three-level scheme of spatial disaggregation from basin to subbasins and to hydrotopes is used. A hydrotope is a set of elementary units in the subbasin which have the same geographical features like land use, soil type, and average water table depth. Therefore it can be assumed that they behave in a hydrologically uniform way. Water fluxes, plant growth and nitrogen dynamics are calculated for every hydrotope on a daily time step, where up to 10 vertical soil layers can be considered. The outputs from the hydrotopes are aggregated at the subbasin scale, taking water and nutrient retention into account. The lateral fluxes are routed over the river network, considering transmission losses. A comprehensive description of the model can be found in Krysanova et al. (1998, 2000). An extensive hydrological validation of the model in the Elbe basin including sensitivity and uncertainty analysis is described in Hattermann et al. (2005a). In order to illustrate the structure of the model, the main hydrological processes in SWIM are briefly listed below and shown in Figure 5.2.

The Priestley and Taylor (1972) method is used to estimate the potential evapotranspiration. Soil evaporation and plant transpiration are calculated as functions of leaf area index LAI using the approach of Ritchie (1972). The snowmelt component of SWIM is a simple degree-day equation.

Surface runoff is determined using a modification of the Soil Conservation Service (SCS) curve number technique. Water which has infiltrated into the soil, percolates through the soil layers using a storage routing technique (Arnold, 1990). The water percolated from the bottom soil layer, which reaches the groundwater table with some delay time, is defined as groundwater recharge.

Lateral subsurface flow or interflow is calculated simultaneously with percolation using a kinematic storage model. Interflow occurs in a given soil layer, if the soil layer below is saturated. Flow routing in the river network is calculated using the Muskingum flow routing method (Maidment, 1993), where a continuity

equation is assumed.

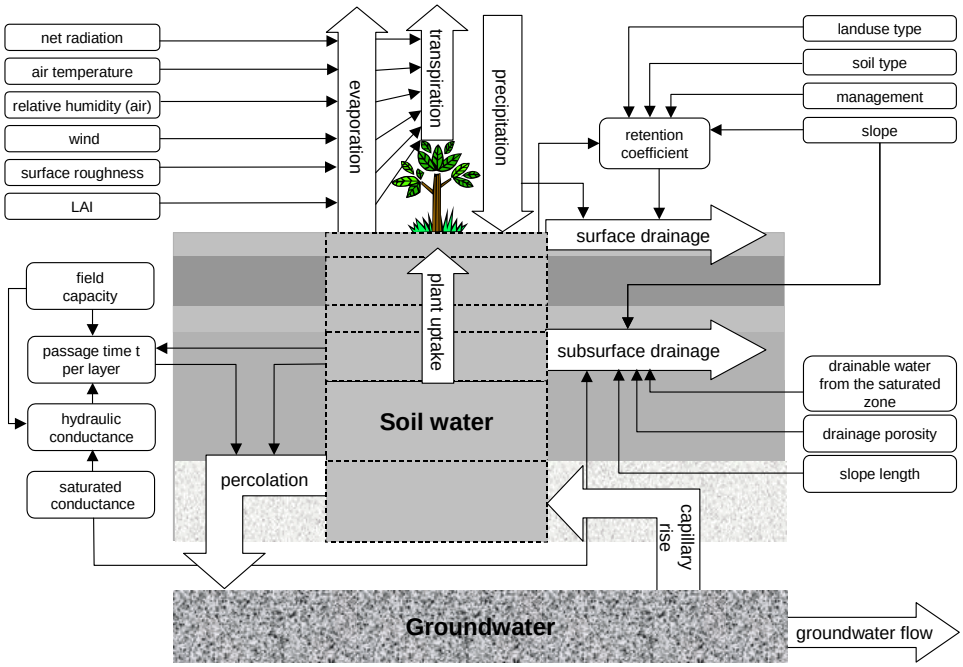

Figure 5.2. The hydrological processes of the SWIM model including the parameter demand.

The equations for groundwater flow and groundwater table depth were derived from Smedema and Rycroft (1983), assuming that the variation in return flow is linearly related to the rate of change in water table height. A simplified EPIC approach (Williams et al., 1984) is included in SWIM for simulating arable crops (like wheat, barley, rye, maize, potatoes) and aggregated vegetation types (e.g. 'mixed forest'), using specific parameter values for each crop/vegetation type. The potential increase in biomass is adjusted daily if one of the plant stress factors is less than 1, considering stresses caused by water, nutrients and temperature. The water stress factor is calculated by comparing water supply in soil and water demand, assuming that about 30 % of the total water comes from the top 10 % of the root zone. The approach allows roots to compensate for water deficits in certain layers by using more water in other layers with adequate supply.

5.2.3 The basin under study

The Elbe river is the most easterly of the large rivers that flow into the North Sea. The total Elbe basin has a catchment area of 148,268 km^2. The German part of the Elbe, where the model was applied, covers 80,256 km^2 from the Czech border to Neu Darchau, the most downstream gauge station not influenced by the tide of the North Sea (see Figure 5.3), and an additional 16,148 km^2 in the inter-tidal zone or drained by rivers influenced by the tide. The total length of the Elbe river is 1092 km; 728 km of that is in Germany. About 52 % of the catchment area are covered by arable land, 29 % by forest, 6 % by settlements and industry and 5 % by lakes, mining pits and other land use forms.

The Elbe and its estuaries are regulated by 273 dams for flood protection and freshwater supply. Despite flood protection measures, several extreme floods occurred during the last few decades in the region, culminating in the disastrous August 2002 flood in the Elbe basin. The flood was caused by a low pressure system called Vb ("five b"), a circulation pattern that is known to produce heavy and intensive rainfall in Central Europe (Becker and Grünewald, 2003).

Climatically, the Elbe basin is one of the driest regions in Germany, with mean annual precipitation below 500 mm in the lee of the Harz mountains (western part of the basin), where the loess plains with high agricultural productivity are located. The long-term mean annual precipitation over the whole basin is 659 mm in the period 1951-2000 (corrected), and the long-term mean discharge at the estuary is 877 m^3 s^{-1} with an average inflow from the Czech Republic of 315 m^3 s^{-1} (ATV-DVWK, 2000). The per capita water supply is only 680 m^3 a^{-1}, one of the lowest in Europe. The average per capita water supply in Germany is ca. 2200 m^3 a^{-1}, with approximately 1370 m^3 a^{-1} in the Rhine basin and 4300 m^3 a^{-1} in the German Danube basin (Stanners and Bourdeau, 1995). The per capita water demand in Germany is 495 m^3 a^{-1}, about 14 % of it being for public freshwater supply.

Over the last two decades, decreasing water levels in rivers and groundwater have been observed in the lowland parts of the basin. Groundwater recharge, especially, is extremely sensitive to changing conditions of climate and land use, since it represents the residual of the water balance (Hattermann et al., 2004).

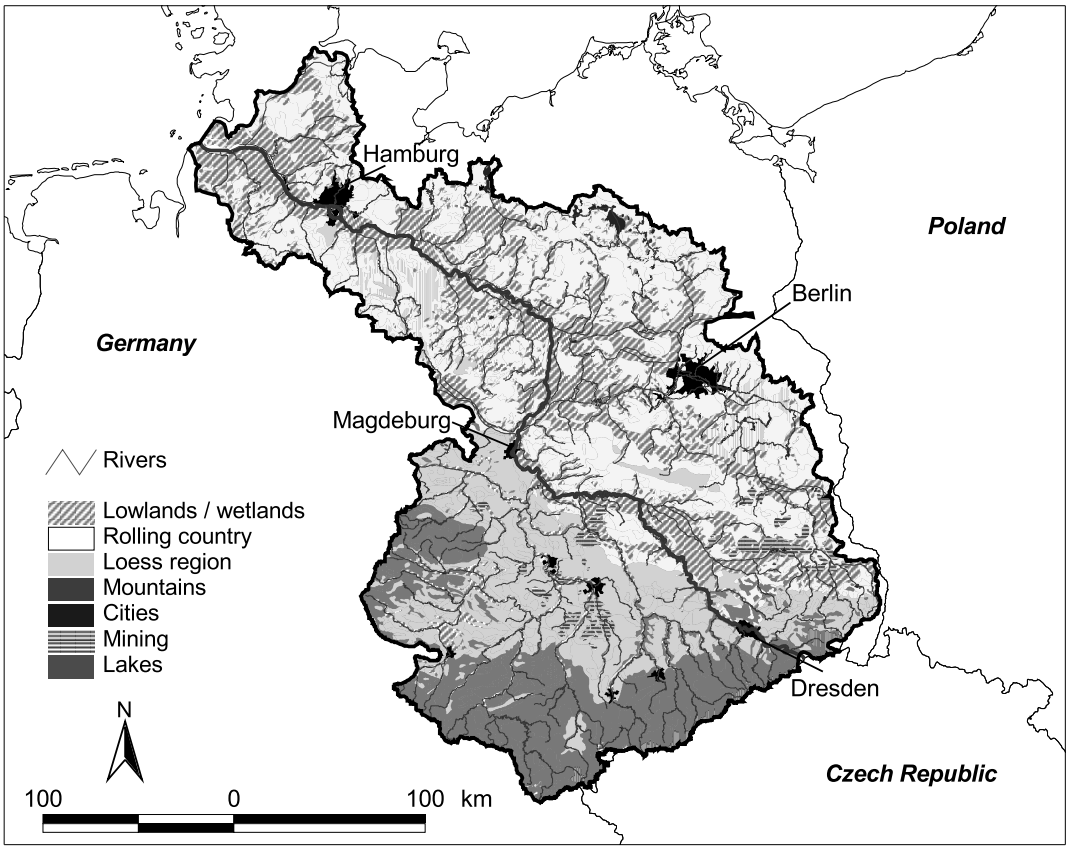

Figure 5.3. The German part of the Elbe basin.

Hydrologically, the area can be subdivided into three main subregions (see Figure 5.3): (1) the mountainous area in the south, approximately 20 % of the total area, (2) the hilly mountain foreland, predominantly covered by loess soils (approximately 28 %), and (3) the undulating northern lowlands, approximately 52 % of the total area (see Figure 5.3).

The northern lowlands are formed by mostly sandy glacial sediments and drained by slowly flowing streams with broad river valleys. They have a low agricultural productivity and water holding capacity. The soils in the loess region, chernozems and luvisols, are mostly loamy and tend to have layers with low water permeability, so that in areas with higher slopes floods are generated, namely in the Saale and the Mulde tributaries. The sediments normally have high field capacities and nutrient supply, and therefore the loess subregion is an area with very intensive agricultural land use. The soils in the mountains, mainly thin

cambisols, are formed by weathering products and redeposited rocky materials. The mountainous areas are often covered by forests and grassland.

5.2.4 Input data and data pre-processing

Spatial data

Subbasin boundaries were provided by the German Federal Environmental Office (UBA) and partly subdivided into 262 subbasins, using a digital elevation model (DEM) and a geoinformation system (GRASS). In addition, 12 mesoscale catchments of the Elbe river basin were selected and modeled separately to get a better understanding of the hydrological behavior of the main subregions of the whole basin. They were disaggregated into 20 - 120 subbasins, depending on their total catchment area (Hattermann et al., 2005a).

The land use map was created using the European CORINE land cover map (Dollinger and Strobl, 1996). The original 44 land use classes were reclassified into 15 classes (Krysanova et al., 2000).

Soil information was taken from the soil map of the Federal Republic of Germany (scale 1:1,000,000). The map distinguishes between 72 different soil types. Each soil type has up to 8 different layers. Together with the soil map, physical parameters for each layer like saturated conductivity, texture classes, porosity, bulk density, humus and organic nitrogen content are provided.

In order to validate the model results with observed runoff data during the reference period, the observed flow from the Czech Republic (gauge Schöna) was added to the one calculated by SWIM and then routed through the subbasins to the outlet of the river basin.

Observed climate data

There are 84 stations located in and around the Elbe basin where climate information is measured, and 285 additional rain gauge stations. Before 1950, the time series are partly incomplete or interrupted. Therefore, continuous time series from 1951 to 2000 have been taken for trend analysis and model validation. The period 1951 to 2000 is referred to as the reference period. Table 5.1 summarizes the climate characteristics of the main geographical regions in the basin, the mountainous area, the loess area and the northern lowlands (see Figure 5.3).

Table 5.1. The observed mean annual temperature and precipitation (uncorrected station observations) in the German Elbe basin for the period 1951-2000.

	temperature [K]			precipitation [mm]		
	summer	winter	average	summer	winter	annual
mountains	13.4	1.9	7.7	413	327	737
loess region	14.6	2.95	8.8	344	249	591
lowland	14.4	2.92	8.7	341	266	607
total Elbe basin	14.2	2.8	8.6	350	264	616

The values indicate that the amount of precipitation is higher during the summer period than during the winter. The loess plains, where the agricultural production is the highest in the Elbe catchment due to the fertility of the soils, have the lowest annual precipitation.

The observed trend in the Elbe basin differs from the global trend because of local orographic conditions, where the Elbe basin is in the lee of the Harz mountains (the west of the basin). During the reference period, more westerly wind circulation pattern have been recorded over the Elbe basin (Gerstengarbe and Werner, 2005). The climate during the period 1951 to 2000 shows a non-linear pattern (Table 5.2). The trend in precipitation indicates a decrease in summer precipitation of about 46 mm and an increase in winter precipitation of about 50 mm. The increase in temperature of 0.8 K for the summer season is lower than the increase of 1.4 K for the winter season. These trends are important for plant growth and river discharge, because the summer season is the period, when the plant water demand and hence evapotranspiration are high and as a result river discharge is low. The increase in temperature and the decrease in precipitation during the vegetation period result in longer periods of water stress for the vegetation in the basin. On the other hand, the winter is the season where the groundwater reservoir recharges, and the increase in winter precipitation results in higher infiltration rates and after percolation to an increase in groundwater recharge, which can partly balance the decrease during the summer season.

A special investigation was made to select a satisfactory interpolation algorithm for the climate data (Hattermann et al., 2005a). It was found that the

Table 5.2. The observed change in temperature and precipitation (uncorrected station observations) in the German Elbe basin from 1951 to 2000.

	temperature [K]			precipitation [mm]		
	summer	winter	average	summer	winter	annual
mountains	0.8	1.3	1.1	-31	65	32
loess region	0.7	1.4	1.0	-49	45	-6
lowland	0.8	1.4	1.1	-51	56	-6
total Elbe basin	0.8	1.4	1.1	-46	50	4

most accurate results were achieved using geostatistical techniques, but comparable results were obtained using an inverse distance technique (ID) and taking the DEM as an additional information for the interpolation. The ID technique was applied in the study because it is much faster than geostatistical methods and able to compute long time series for many realizations in an appropriate time. Daily precipitation was corrected using the empirical method developed by Richter (1995), where the underestimation of observed precipitation is adjusted by monthly changing weighting factors.

5.3 Results and discussion

5.3.1 Reference period

Climate downscaling

Observed climate data of the period 1951 to 2000 were chosen to validate the regional climate model STAR (Gerstengarbe and Werner, 2005). The validation criterion was that the stability of the main statistical characteristics of the regional climate (variability, frequency distribution, annual cycle, persistence) had to be maintained. A set of 100 realizations of the climate for this period was generated. By comparison of the climate statistics of the individual realizations with the observed trend in climate it was found that the median trend in precipitation of the 100 variants has the highest correlation with the observed trend for the integral of the total basin (see Table 5.2), and realization 32 has the highest correlation with the observed climate data for the climate station Magdeburg (see

Figure 5.3), which is in the center of the German Elbe basin and representative for the loess area, where the agricultural productivity is the highest. Statistically, realization 32 has a much lower average annual precipitation than the median of the whole set of 100 realizations.

Hydrology

The eco-hydrological model was first adjusted to the hydrological processes in the Elbe basin using a multi-objective, multi-site and multi-scale validation (see Hattermann et al., 2005a). The model was tested in 12 subbasins located in different regions of the German Elbe basin with catchment areas from 280 to 23,690 km^2 (multi-site calibration). The experiences gained in these nested studies were used to validate the hydrological processes of the model for the entire basin (multi-scale calibration). The calibration was done on a daily time step using records of observed river discharge and groundwater table dynamics for comparison (multi-objective calibration).

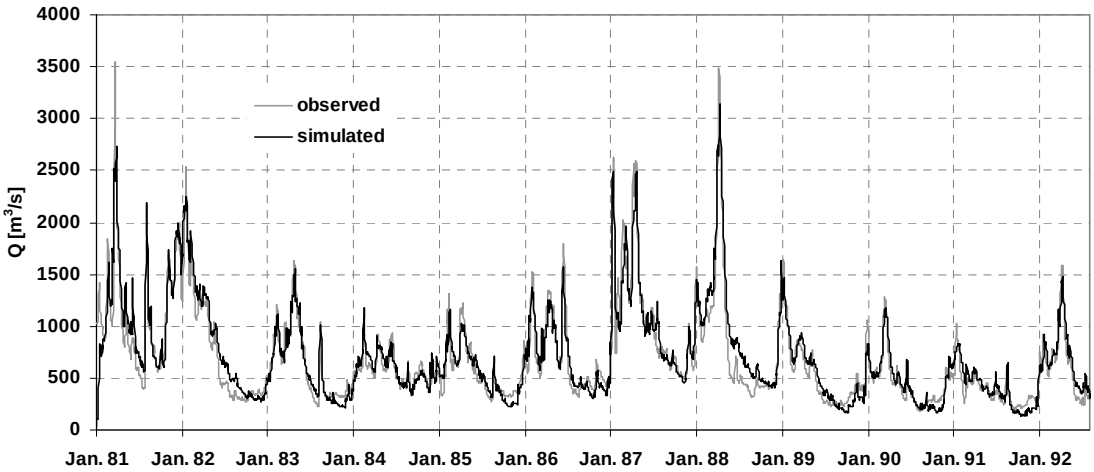

Figure 5.4. Comparison of the simulated and observed river discharge of the Elbe basin (Neu-Darchau, catchment area 86,000 km^2) (Hattermann et al., 2005a).

A non-generic automatic calibration was performed using a Latin Hypercube method (Tarantola, 2000) to make sure that all physically meaningful parameter combinations were considered in the modeling procedure. The same method was applied to analyze the model sensitivity and to quantify the uncertainty of the simulation results. Afterwards, fine-tuning of the model was done by

Table 5.3. The long-term differences between simulated and observed river discharge for the validation period of typical subregions in the Elbe basin and the uncertainty of the results expressed by the 10th and 90th percentiles of 300 simulations using different model parameter combinations (Hattermann et al., 2005a).

river	topography	mean discharge balance [%]	10th percentile [%]	90th percentile [%]
Saale	mountains	4.2	-5.5	6.7
Mulde	mountains / loess	-6.1	-10.6	18.2
Löcknitz	lowlands	1.6	-9.9	14.7
Elbe	integrates all	2.7	-4.9	10.7

hand. The simulated river discharge was compared with the measured discharge for a twelve year period (calibration period 1981-86, validation period 1987-92). Statistical evaluation of the results was done by analysing the long-term difference of the observed river discharge against the simulated one in percent (the relative difference in discharge or 'water balance') and calculating the efficiency criteria of Nash and Sutcliffe (1970) for the daily river flow.

The spatial behavior of the hydrological processes was analyzed using contour maps of the water table and observed time series of daily groundwater level dynamics.

Figure 5.4 shows a comparison of observed against simulated river discharge for the entire Elbe river basin, Table 5.3 summarizes the statistical results of the long term difference between simulated and observed river discharge for the reference period. It is visible that the uncertainty of the results, expressed by the percentiles of the 300 simulations, is relatively high in the loess areas and the lowland part of the basin, and relatively low in the mountainous part of the basin. The overall result is that the SWIM model tends to overestimate river runoff or underestimate actual evapotranspiration slightly. 80 % of the simulations for the entire Elbe basin (gauge Neu Darchau) have a long term difference of observed and simulated river runoff of between -4.9 % and +10.7 %. The quality of the model simulations is comparable with the results of recently published macroscale applications of other models (Abdulla and Lettenmaier, 1997; Nijssen et al., 1997; Kite and Haberlandt, 1999; Krysanova et al., 1999b;

Haddeland et al., 2002; Klöcking and Haberlandt, 2002; Wood et al., 2004).

5.3.2 Scenario period

Climate

The trend of climate change under scenario conditions and the range of the 100 variants is shown in Table 5.4. As already discussed in the section about the climate input data, the observed trend of precipitation in the Elbe river basin differs from the global trend due to the regional orography (the Harz mountains in the west of the basin) and an increase in westerly wind circulation patterns. It is assumed that this trend will continue into the future, and as a result also the slightly negative trend in precipitation. Due to the uncertainties in the changes in regional climate, the possible range of change in annual precipitation is between approximately -80 mm and +70 mm (Table 5.4).

Table 5.4. The scenario trend in temperature and precipitation for the entire German Elbe basin (difference of the average 1961-90 and 2051-55).

	temperature [K]			precipitation [mm]		
	summer	winter	average	summer	winter	sum
lowland	1.7	1	1.5	6.4 (-43.3; 72.5) *	-8 (-22.5; 0.9) *	-1.7 (-73.4; 65.8) *
loess region	1.7	1	1.5	11.5 (-39.58; 102.45) *	-16.6 (-34.7; -12.5) *	-5.1 (-74.3; 90.1) *
mountains	1.7	1	1.5	2.3 (-42.6; 109.0) *	-18.9 (-27.7; -5.9) *	-16.6 (-70.3; 103.1) *
total Elbe basin	1.7	1	1.5	5.9 (-42.5; 84.2) *	-11.5 (-25.7; -2.8) *	-5.6 (-68.2; 81.5) *

*Range of change between the driest and the wettest climate scenario variant.

The range of possible change in precipitation as an integral over the entire

basin is shown in Figure 5.6, where also the average annual precipitation during the reference period is included for comparison. It becomes obvious that realization 32, the variant that has the highest correlation with the observed trend in the loess region, is a much drier variant than the median of the set of realizations, where only a slight decrease in precipitation can be found. A trend analysis reveals that the trend in precipitation is only significant for the two driest realizations (with a 90 % confidence), one of which is realization 32. The analysis of the trend in hydrological quantities simulated with the climate change scenario as input discussed later shows that a relatively small and insignificant trend in climate can result in significant trends in groundwater recharge and river flow.

Land use

The eco-hydrological model estimated a decrease in crop yields under climate change of approximately 11 % to 15 % as a basin wide average for different C3-cereals and no significant change in the productivity of C4 plants like maize. The comparison included simulation results at the hydrotope level simulated by SWIM, which were validated using the available statistical data for the period 1996-99 as the reference period, and the simulation results for the scenario period 2051-55. These results vary regionally (see Figure 5.5). Areas in the lee of the Harz mountains which are affected by a more significant decrease in precipitation suffer more, areas in the northwest and in the south, where precipitation has an increasing trend, have a higher productivity under climate change, due in part to the fertilizing effect of higher CO_2 concentrations.

On the basis of these results, the agro-economic model RAUMIS calculated new crop distributions for the counties in the German Elbe basin, assuming that local farmers optimize their operational income under climate change. The main land use changes are in areas, where cost-effective crop cultivation would become impossible under altered climate conditions, because of the low fertility and water-holding capacity of the local soils and / or the decrease in precipitation. These areas become fallow land in the land use scenario. The result is that if climate change alone is considered (land use scenario variant A), this would induce only a small shift from agricultural land to fallow land (a decrease in cropland area of approximately 0.9 %), with the shares of the different crops cultivated in the area remaining relatively stable. The changes are more pronounced when

the liberalization of global crop markets is considered in the second land use scenario (land use scenario variant B): The share of fallow land of the total crop area becomes approximately 29.8 % (beforehand lower than 7.0 %), the share of winter wheat drops from 26.4 % to 21.7 %, and that of maize drops from 7.0 % to 2.0 % (see Figure 5.5).

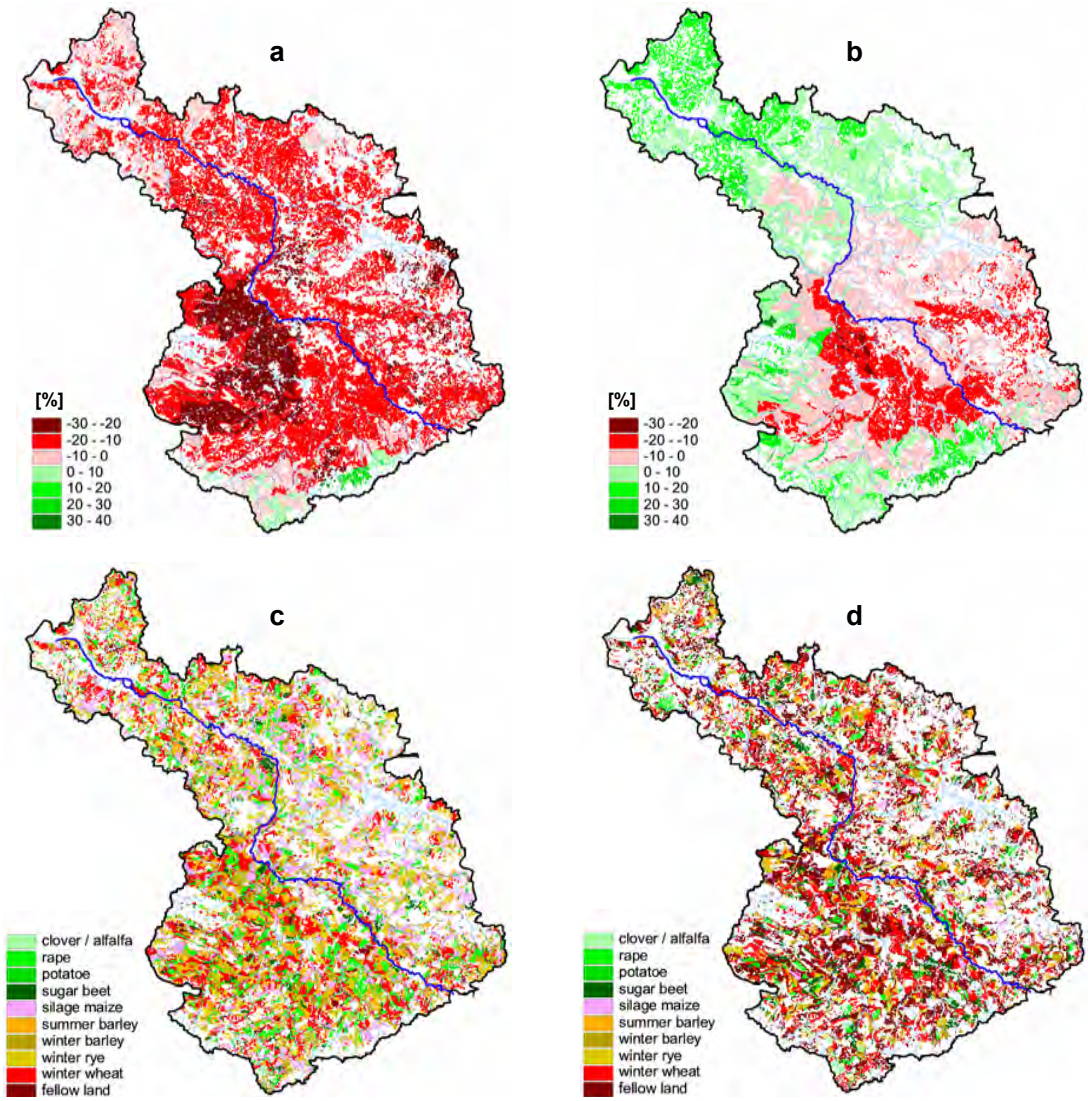

Figure 5.5. The change in potential crop yields (reference period 1996-99 against scenario period 2051-55) for winter wheat (a) and silage maize (b) and the crop distributions for one year in the reference period (c) and in the scenario period (d) (land use scenario variant B).

Land use scenario variant A is the basis for the assessment of the impacts of

a possible climate change on the water resources in the German Elbe river basin reported in this study. The main changes in hydrological quantities caused by the change in land use calculated with land use scenario B as boundary condition (under current climate) would be an increase in evapotranspiration of approximately 7.7 % and a decrease of groundwater recharge of approximately 14.3 %, assuming that a cover crop is cultivated in time periods without main crops. The aim of this study was to have a land use scenario consistent with the climate scenario to quantify the impacts of global change on the water balance in the German part of the Elbe basin. The further investigation of the land use scenarios has to be the task of future research.

Hydrology

The analysis of the impacts of climate change on the hydrology in the German Elbe basin was performed by comparing the hydrological processes in the period 1961-1990 against the period 2051-2055. The hydrological decade 1961-1990 is referred to as the reference period, the period 2051-2055 as the climate change or scenario period. The climate change period is shorter than the reference period because the annual precipitation during the scenario period has a relatively steady decrease (see Figure 5.7). Averaging over a longer time period would conceal the problems for water users arising from water shortage at the end of the planning period. The relevance of the length of the scenario period which was selected for comparison against the reference period is illustrated in Table 5.5, where a longer scenario period was additionally chosen to calculate the possible changes in hydrological quantities.

The uncertainty of the results is expressed by confidence intervals indicating the range of possible changes. The first part discusses the annual changes in precipitation, evapotranspiration, direct runoff (surface runoff and interflow) and base flow, which are generated in the German Elbe. They provide a first overview of the total changes and the uncertainty of the results. The next results discussed are changes in daily runoff generation and daily river discharge. They are used to illustrate changes in the intra-annual characteristics of the flow regime in terms of low flow and flooding periods. The last results presented are maps of precipitation and groundwater recharge to analyze sub-regional differences in the trend of climate change and their impacts on hydrology.

Annual characteristics

The daily water fluxes simulated by SWIM were aggregated to average annual values of the entire basin for the reference period and the 100 climate change realizations of the scenario period (Figures 5.6a-d). The histograms illustrate the possible range of changes of the main components of the water cycle (precipitation, evapotranspiration, direct runoff and groundwater recharge). The distribution of the ten year average of the 100 realizations 2051-55, the mean, average and 10th, 25th, 75th and 90th percentiles, and the average of the reference period 1961-90 are included for comparison. The results for the realization 32 are indicated by a dashed line. The mean annual precipitation of the 100 scenario realizations is slightly lower than in the reference period (1.5 %, see Figure 5.6a). Added to the increase in evapotranspiration under increasing temperatures (approximately 7.0 %), this will already lead to a relatively strong decrease in groundwater recharge by 22 % and in river discharge by 15 %, significantly out of the range of the uncertainty of the model performance reported in Table 5.3. However, due to the higher uncertainty in future, 41 % of the variants have a higher annual precipitation than in the reference period.

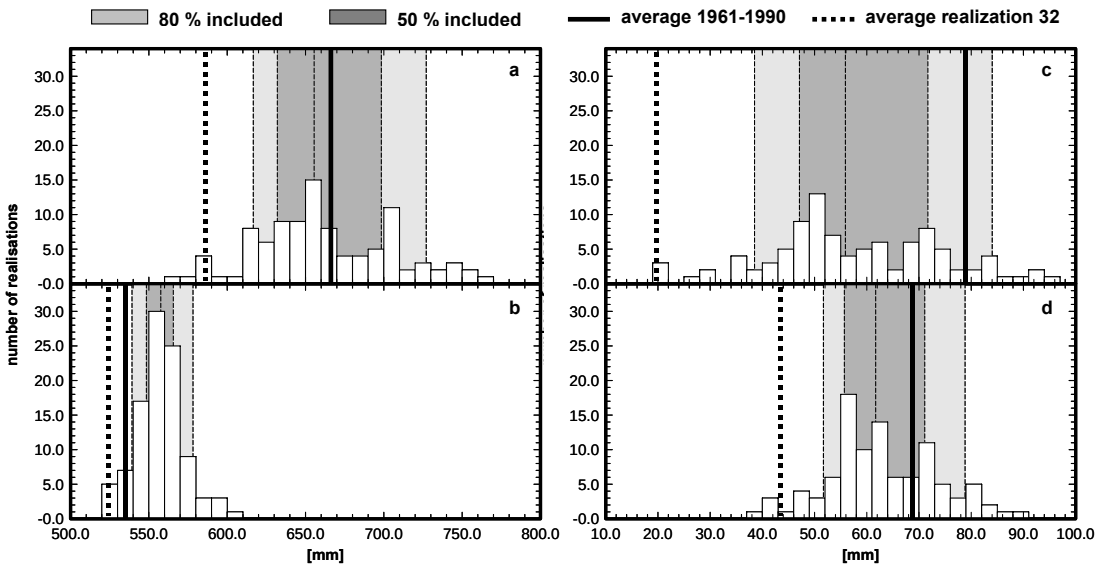

Figure 5.6. The distribution of the ten year average 2051-55 of the 100 variants, their median and 10th, 25th, 75th and 90th percentiles, and the median of the reference period 1961-90 (a: precipitation, b: evapotranspiration, c: groundwater recharge, d: direct runoff)

5.3 Results and discussion

Despite lower precipitation in average, evapotranspiration will slightly increase in future (Figure 5.6b). Evapotranspiration is a function of energy input and water availability. Higher annual temperatures under scenario conditions stimulate plant growth and evapotranspiration. Plants start growing earlier in spring, and the vegetation period extends into the late autumn (see also Figure 5.9). Both effects result in increasing transpiration, and as a logical result 99 % of the scenario variants have a higher evapotranspiration than in the reference period. Surface runoff is on average lower in the future period, although the climate change realizations with higher precipitation lead to higher direct runoff (interflow and surface flow) in 31 % of the simulations (Figure 5.6c). The largest impacts of climate change are on groundwater recharge, where also the range (uncertainty) of the results is the highest (Figure 5.6d). Groundwater recharge - the residual of the local water balance - is very sensitive to changes in precipitation and temperature (evapotranspiration). This is mirrored in the scenario results, where in 87 % of the scenario variants a decrease in groundwater recharge can be recorded. Table 5.5 summarizes the results for the total basin.

Table 5.5. The range of possible changes in the hydrological cycle under climate change. Shown are the changes for the driest, median and wettest climate change variant (difference in % of the average 1961-90 (reference) and 2051-55), and the number of scenario variants which have a decrease in the corresponding hydrological component.

	reference	dry* [%]	median* [%]	wet* [%]	drier variants
precipitation	665.07	-15.3 (-12.0)	-1.5 (-0.5)	14.8 (8.8)	59
act. evapotr.	522.34	0.0 (3.5)	6.8 (6.4)	14.9 (11.8)	1
dir. flow	68.22	-44.2 (-31.7)	-11.2 (-6.2)	32.7 (9.1)	69
gw recharge	78.75	-75.0 (-69.8)	-28.5 (-22.0)	50.2 (-10.3)	87

*In brackets are the differences of the reference period 1961-90 and 2046-55.

The changes induced by scenario realization 32 are more pronounced than for the average climate change realization: During the period 2051-55, the annual precipitation of realization 32 is the second lowest of the 100 variants (13.8 % lower than in the reference period). Evapotranspiration would increase slightly by 1.9 %, direct runoff would be 37.1 % lower and groundwater recharge 75.0 % lower. The total runoff generation and therefore also the river discharge generated in the German Elbe catchments would be 57.6 % lower.

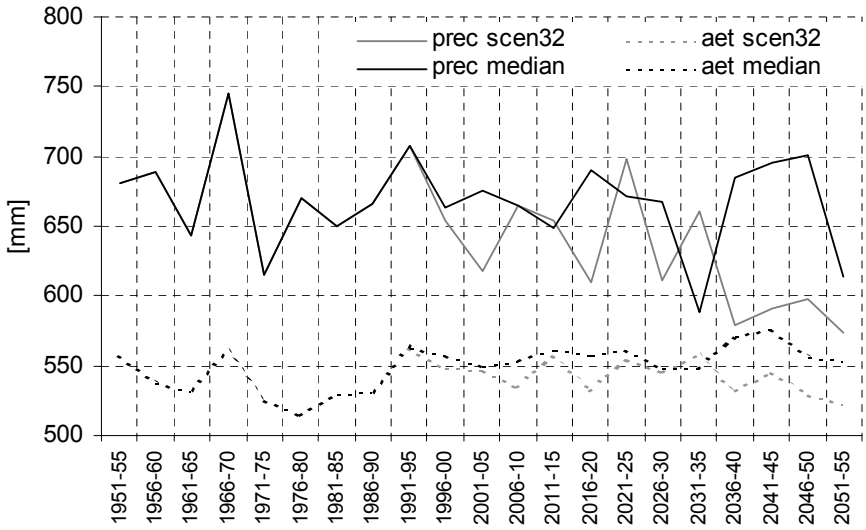

Figure 5.7. Trend in precipitation and evapotranspiration 1951-2055.

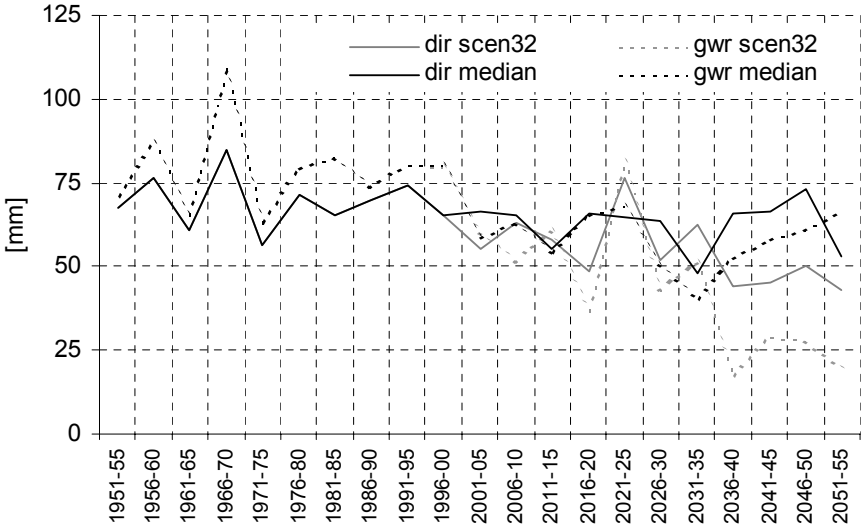

Figure 5.8. Trend in direct runoff and groundwater recharge 1951-2055.

Figures 5.7 and 5.8 show the transient trend of the hydrological quantities for the median of the 100 realizations and realization 32 in five year steps, starting in the reference period: remarkable is that the precipitation at the end of the scenario period of variant 32 is only 12.7 % higher than the actual evapotranspiration (Figure 5.7). This leads to a moderate decrease in direct runoff and a more pronounced decrease in groundwater recharge (Figure 5.8). While the amount of annual groundwater recharge is higher than the amount of direct runoff in the observation period, this pattern changes during the scenario period. These effects are more pronounced when taking realization 32 as input than for the median climate realization. The impacts of the change on runoff generation in the intra-annual river flow dynamics are discussed in the next section.

The annual change in hydrology is significant only for the driest realizations. While only two climate realizations show a significant trend in precipitation, 14 of the realizations have a significant trend in evapotranspiration, also 14 a significant trend in groundwater recharge and 11 a significant trend in river runoff. The effects are not necessarily combined: realization 32, for example, has a strong and significant trend in precipitation, but not in evapotranspiration, where the possible increase in evapotranspiration due to the increase in temperature is limited by the water (precipitation) available, and thus reduces the trend signal.

Daily dynamics

A comparison of typical seasonal dynamics of evapotranspiration, direct runoff (surface runoff and interflow), and groundwater recharge in the reference and scenario periods is depicted in Figure 5.9 as an average for the total basin. Two years (1965 and 2055) whose annual precipitation was closest to the average annual precipitation for the periods 1960-1990 and 2051-2055 were chosen as representative for the comparison. As one can see, summer evapotranspiration is lower under scenario conditions, though the values above 2 mm d^{-1} appear earlier. The sum of direct runoff and groundwater recharge is also lower, the latter even starts to become negative during the scenario period due to capillary rise in summer, when plants in wetland areas satisfy their additional water demand from groundwater (see Figure 5.10 and also Figure 5.12).

Figure shows the daily river discharge of the 100 realizations at the Neu-Darchau gauge, averaged for the reference period 1961-90 and the scenario period

2051-55. One main result is that the average discharge under scenario conditions is in 80 % of the variants lower for the scenario period than during the reference period. In addition, the annual flow regime under climate change is different from the one under reference conditions: due to higher temperatures, the vegetation season extends into the late autumn, and as a result the river water level rises more slowly at the end of the summer.

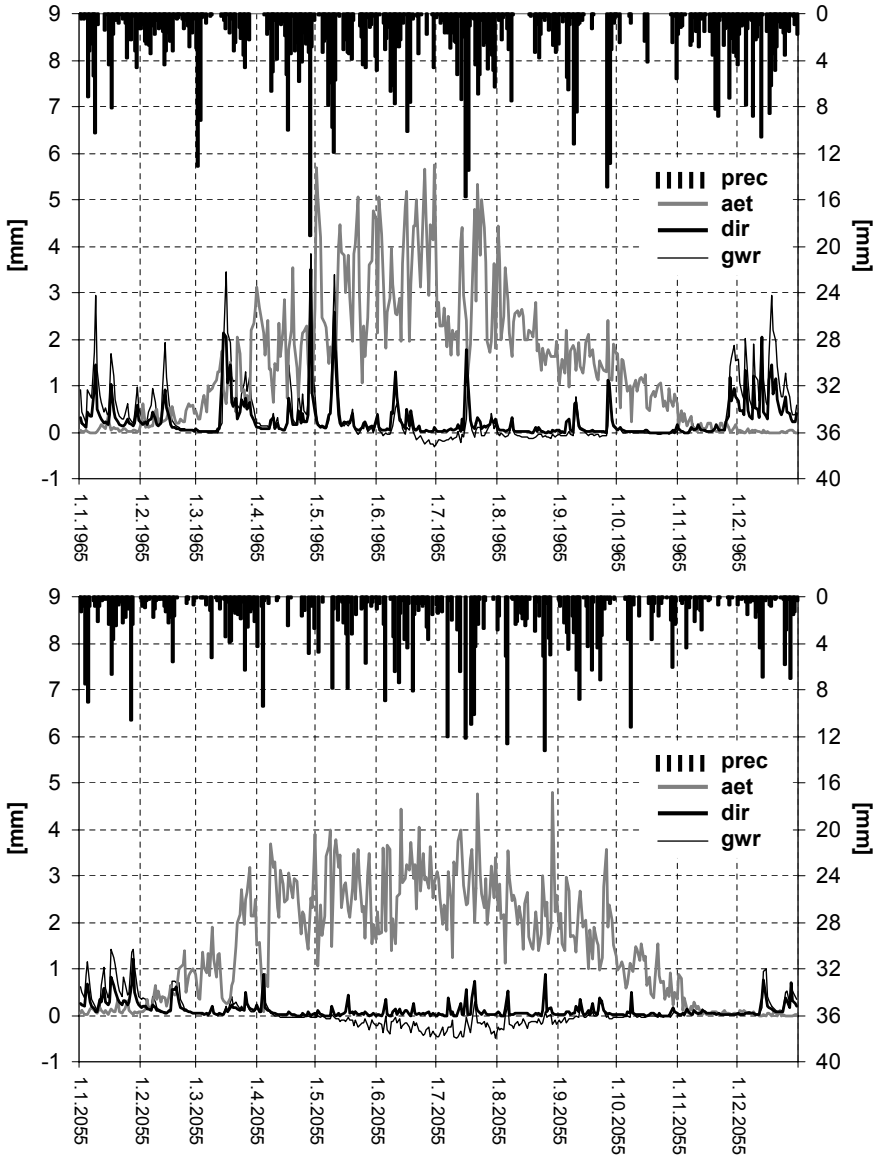

Figure 5.9. Daily runoff generation as an integral for the total German Elbe basin (top: 1965, bottom: 2055; prec = precipitation, aet = actual evapotranspiration, dir = surface runoff + interflow, gwr = groundwater recharge).

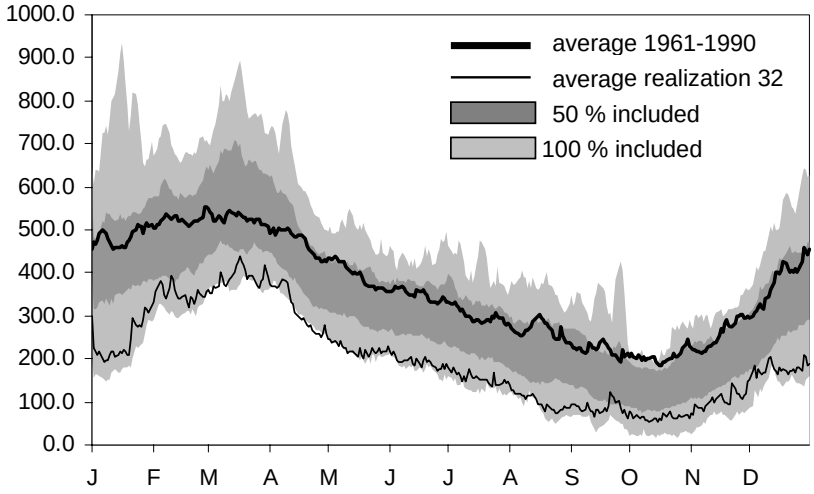

Figure 5.10. Ten-year average daily water discharge at gauge station Neu-Darchau for the reference period and under scenario conditions.

More and more pronounced low water situations can be observed in late summer and early fall. Floods are generated in early spring in the reference period, stimulated by snow melt. But due to higher temperatures, the runoff retention of snow will be lower under climate change, and the period 2051-55 shows the highest flood events during January. The consequence for water resources management is that longer periods with low discharge as well as severe flood events in early winter have to be taken into account in the planning process.

Sub-regional impacts

Figures 5.11 and 5.12 illustrate the regional changes in precipitation and groundwater recharge (comparison of reference period against scenario variant 32), while Figures 5.11d and 5.12d show the uncertainty of the results expressed by the coefficient of variability. The overall pattern is that rainfall will decrease in the northern part, while the southern part of the basin shows areas with increasing and areas with deceasing annual precipitation. This latter result is supported by Menzel and Burger (2002), who used a different statistical downscaling method to generate a climate scenario for the Mulde catchment located in the southern part of the German Elbe basin. The trend in groundwater recharge follows this general pattern with large decreases in areas with decreased annual precipitation.

Noticeable again is that the relatively small change in precipitation has a

relatively high impact on groundwater recharge (as already discussed for the annual changes in precipitation and groundwater recharge). The areas where the local annual groundwater recharge is negative due to plant water uptake from groundwater (red areas in Figures 5.12a and 5.12b) become larger under scenario conditions.

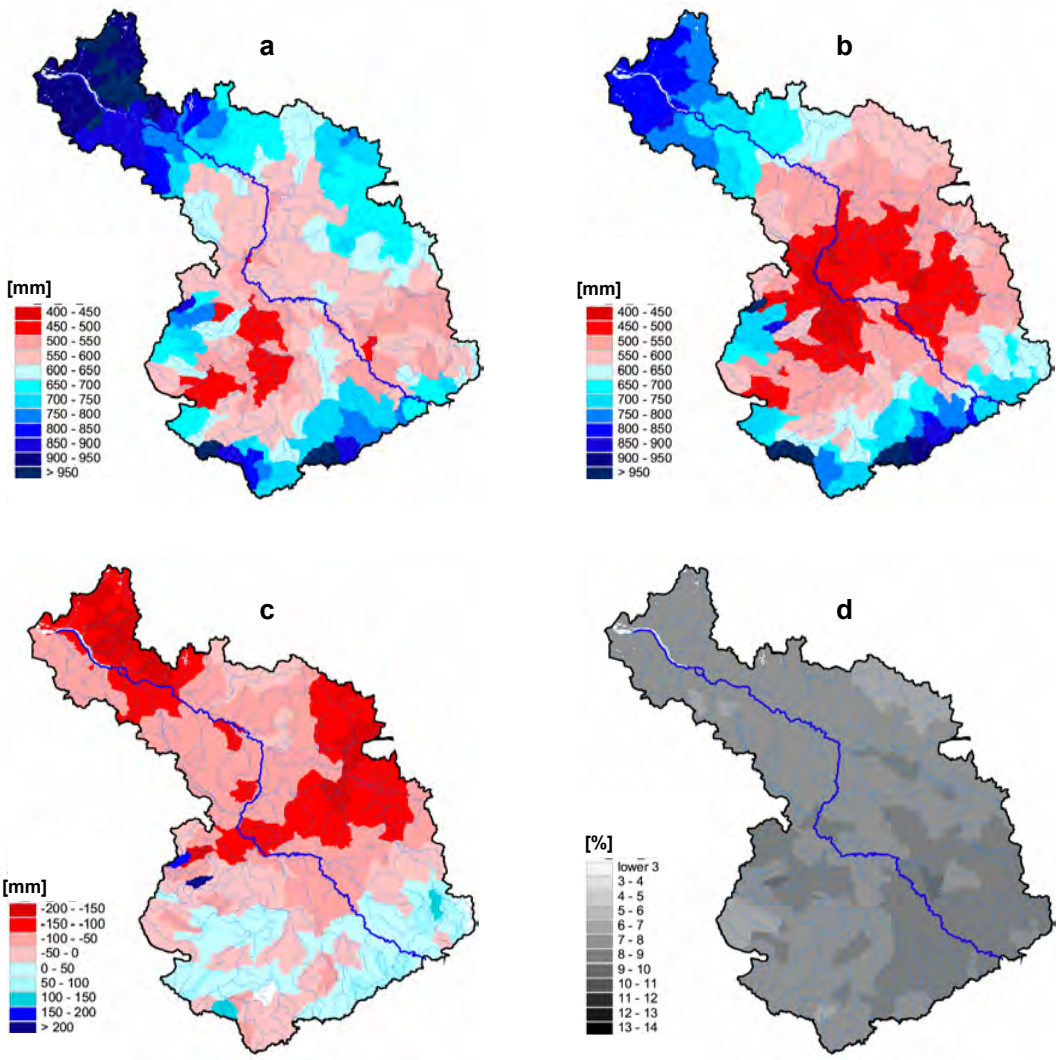

Figure 5.11. The mean annual precipitation 1961-90 (a) and 2051-55 (b), the change in precipitation (c) and the coefficient of variability in % (d).

The greatest relative changes occur in the lee region of the Harz mountains, where also the change in precipitation is the highest. These are the areas where, due to the high water holding capacity of the loess soils, groundwater recharge is

very low also during the reference period.

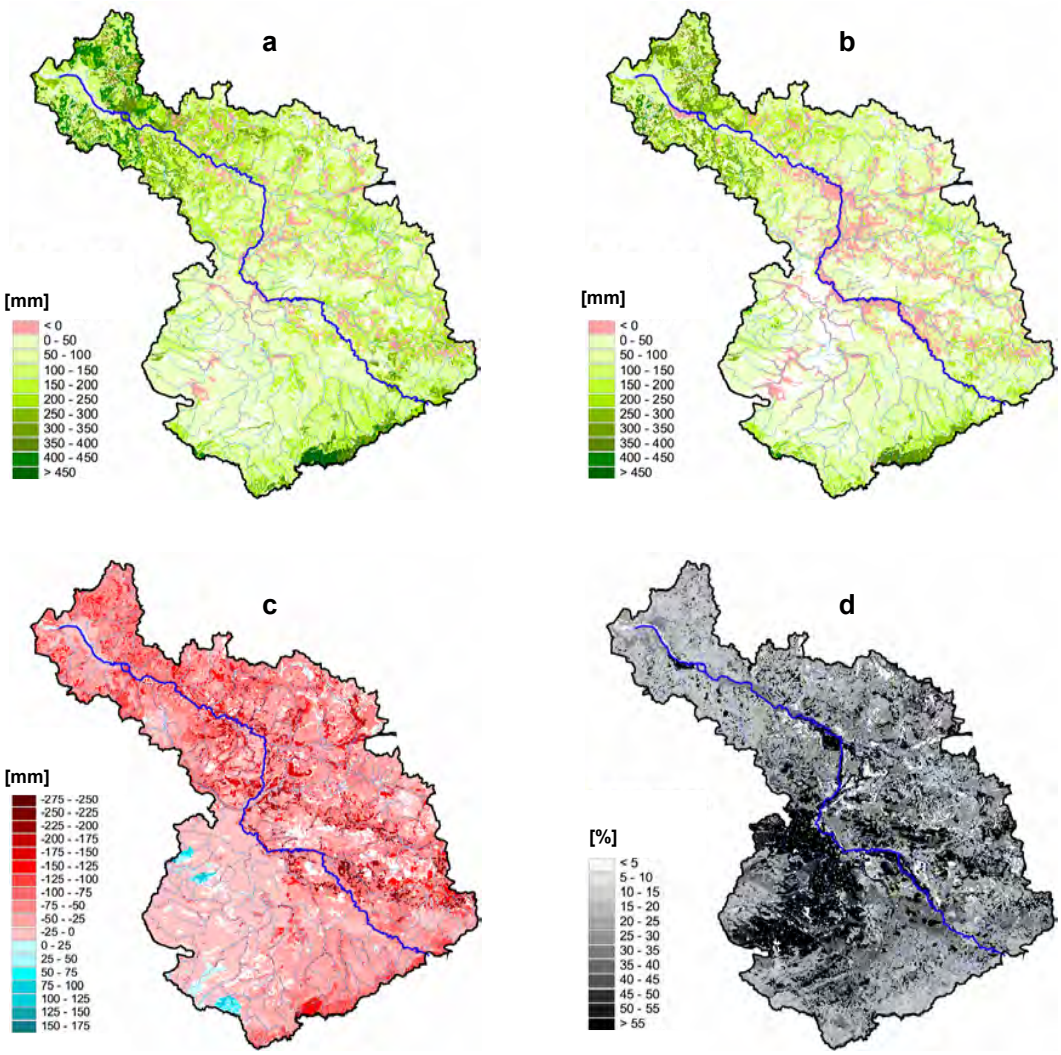

Figure 5.12. The mean annual groundwater recharge 1961-90 (a) and 2051-55 (b), the change in recharge (c) and the coefficient of variability in % (d).

The uncertainties in precipitation expressed by the coefficient of variability of the 100 variants are the highest in the lee of the Harz mountains, and the same is visible for groundwater recharge, with a spatial focus in the loess plains (see Figure 5.12). The highest uncertainties in groundwater recharge occur in areas where the total annual amount of recharge during the reference period has been small anyway. Small changes in precipitation have a great impact on recharge in these areas, and a coefficient of variability of maximum 14 % for precipitation in

these areas results in a coefficient of more than 50 % for groundwater recharge.

5.4 Summary and conclusions

The methodology presented in this study allows us to assess the uncertainty of water supply under global change, taking into account the most important drivers, land use and climate, and allowing consideration of feedbacks between trend in climate and its impact on land use.

The overall result is that both the natural environment and society in the catchments of the German Elbe basin face severe changes in water availability and river flow regimes, although the results are associated with high uncertainty. The trend in temperature of 1.4 K in the period 2001-2055 will stimulate plant growth and lead to a prolongation of the vegetation period. As a result plant transpiration will intensify in early spring and continue into late autumn. This will influence the river flow regime, where river water levels will rise later in early winter and recede earlier in spring. More and longer low water intervals can be observed in late summer and early fall. The increase in evapotranspiration will have the highest impacts on groundwater recharge, the residual of the local water balance, which is very sensitive to changes in water supply.

While the trend in temperature and therefore also the trend in evapotranspiration and the change of the river flow regime are relatively certain, much more uncertainty exists about the trends in groundwater recharge, direct runoff and river discharge and in the strength of the trends. Of the total set of 100 climate change realizations, 59 show a decrease in precipitation and 99 an increase in evapotranspiration, this results in 69 of the variants in a decrease in direct runoff (surface runoff and interflow), in 87 in a decrease in groundwater recharge and in 80 in a decrease in river runoff. The results show a strong spatial heterogeneity. The median trend in precipitation of the 100 scenario realizations indicates only a small decrease of precipitation by 1.5 % (with a range from -15.3 % to +14.8 %). Added to the increase in evapotranspiration under increasing temperatures, even this will lead to a relatively strong decrease in groundwater recharge of 22 % and river discharge by 15 %. This change is out of the range of uncertainty of the eco-hydrological model‘s performance. The most reliable trend in precipitation for the loess plains, where the soils have the highest fertility, will result in a more pro-

nounced decrease of precipitation and consequently also a much stronger impact on groundwater recharge and river flow. Under these conditions, direct runoff will fall by about 37 %, groundwater recharge by about 75 %, and river runoff by about 58 %. The impacts on hydrological components are directly correlated with a change in water resources, where the per capita amount of annual water supply generated originally in the German Elbe basin would decrease by 15 % in the moderate scenario variant, which is the best extrapolation of the observed trend (the median change in precipitation). The result is even more severe when we consider that 80 % of the freshwater for human water supply is taken from groundwater, where the decrease is more pronounced.

The study shows that a relatively small and insignificant change in precipitation in combination with a more significant increase in temperatures can result in severe and significant changes in hydrological variables, in particular in river flow and groundwater recharge. The uncertainty of the results induced by the uncertainty in the development of the regional climate change and propagated by the eco-hydrological model is much higher than the uncertainty generated by the performance of the eco-hydrological model itself.

The impacts of the anticipated land use change on the water balance in the Elbe basin are not significant when climate change alone is the reason for the land use change (land use scenario variant A). The impacts become more severe when global socio-economic changes are also considered in the land use scenario (land use scenario variant B). Here, the management of land use becomes very important (Niehoff et al., 2002; Fohrer et al., 2005), for example the types of land cover which will replace agriculture (e.g. grassland, forests or settlements).

Acknowledgments

The authors would like to thank all their colleagues at the Potsdam Institute for Climate Impact Research (PIK) who contributed to this paper with technical help. Part of this work was supported by the German BMBF program GLOWA (GLObal WAter) Elbe.

Chapter 6

Summary and key findings

The scope of the study is integrated river basin modeling in the Elbe basin to improve the understanding of environmental changes in the past and to investigate possible impacts of climate and land use change in the future. Special emphasis is placed on the spatial heterogeneity in the basin, especially on processes in wetlands and riparian zones.

Until now, model applications at the large scale ($A_{E0} \approx$ 10,000 km^2) were mostly limited to the investigation of a single variable such as the water cycle or crop yields (Varis et al., 2004). Studies integrating different features of the river basin in a dynamic mode (like hydrology and vegetation processes) including feedbacks, small-scale spatial heterogeneity and temporal variability, have been mostly restricted to the small- and mesoscale ($A_{E0} \approx$ 1-10,000 km^2).

The German part of the Elbe river basin belongs to the macroscale ($A_{E0} \approx$ 100,000 km^2). It is clear that the environmental problems in the basin discussed in Section 1.3.2 can only be described by a model which integrates all the important eco-hydrological processes, such as water, nutrient fluxes and vegetation growth in combination with water and land use management, and by considering the spatial heterogeneity typical for the basin (Bronstert et al., 2005; Horn et al., 2004). To cover these detailed spatial characteristics of the Elbe basin, it was decided to use a process based semi-distributed model, adopting state-of-the-art modeling techniques derived at the mesoscale, and to develop and evaluate new modeling approaches for large scale applications. In the process of the large-scale implementation it was necessary to develop three new modules and a number of new modeling tools. The new modules are for:

- retention processes in the subsurface and in wetlands and riparian zones, considering groundwater table dynamics at the hydrotope level and the residence time of nutrients and the nutrient turn-over,
- crop generation to reproduce the yearly changing spatial pattern of crops close to the real crop distribution in the basin, and
- interpolation of climate data.

Comprehensive modeling approaches were developed and applied for:

- model calibration and validation,
- sensitivity analysis and uncertainty propagation,
- interfaces to climate and agro-economic models, and
- development of projections into the future taking into account feedbacks between climate and land use changes when deriving the land use scenario.

Finally, the model was applied:

- over 12 different subbasins nested in the Elbe catchment and for the entire German part of the Elbe basin, to investigate the regional hydrological processes and crop yields typical for the different landscapes in the basin,
- in a subbasin in the northern central part of the Elbe basin to investigate decreasing water tables,
- to analyze and quantify the impact of retention processes in wetlands, riparian zones and groundwater on water quality and river discharge in a subbasin close to Berlin, and
- to investigate the possible changes in hydrology and crop yields under global change (in terms of climate and agro-economic changes) in the whole German part of the Elbe basin.

The following sections give a brief summary of the main objectives and results of the four papers, followed by a critical discussion of the model developments presented in the paper section and the results of the simulation experiments.

6.1 Validation of the SWIM model for hydrological processes at the macroscale

The objective of the first article was to validate the model SWIM for the hydrological processes at the macroscale in the Elbe basin taking account of the inherent spatial heterogeneity in the catchment. It is commonly agreed that a comprehensive model validation, including sensitivity and uncertainty analysis, has to be the fundamental first step when applying a model. The question is thereby whether the model is able to accurately enough reproduce the response of the system under investigation to external and internal pressures, which are changing its state, in our case the response of the hydrological processes in a catchment to changes in land use and climate.

To apply the model SWIM at the macroscale and to have a satisfactory model representation of the important eco-hydrological processes in the basin, it was necessary a) to develop the model further by incorporating a simplified representation of the groundwater dynamics and evapotranspiration in wetlands, b) to have advanced techniques for climate interpolation and c) to include new routines to consider the inflow from the Czech part of the basin and to have a model output of river discharge at different subbasin outlets separately for base flow and direct flow. Besides, new approaches for sensitivity and uncertainty analysis and model validation have been developed and applied to investigate the model performance under different environmental conditions.

The improved model is able to simulate river runoff for 12 meso- to macroscale basins (200 - 20,000 km^2) nested in the Elbe basin, and for the whole German part of the Elbe basin, in good agreement with observed data. Model calibration corrects mainly three parameters (the saturated soil conductivity, the river routing coefficient and the groundwater reaction factor). The nested subbasins were selected to be representative of the major subregions of the Elbe basin (see Figure 1.9). Some general patterns were apparent when comparing the values of the calibration factors in the 12 nested catchments, so that it was possible to divide the parameter sets into three main clusters representing the main landscapes in the basin: one for the lowlands, one for the loess area and one for the mountains. Validation results were generally better in mountainous catchments (efficiency after Nash and Sutcliffe (1970) is 0.75 - 0.79 with daily time steps, and

Table 6.1. Comparison of the vertical flow processes simulated by SWIM and the values taken from the Hydrological Atlas of Germany (Leibundgut and Kern, 1999). Shown are average values for the German part of the Elbe basin.

	simuated [mm]	Hydrological Atlas [mm]
precipitation	687	695
evapotranspiration	526	518
direct runoff	77	89
groundwater recharge	95	88

0.82 - 0.84 with monthly time steps) than in lowland basins (0.61 - 0.72 and 0.66 - 0.86, correspondingly). The model sensitivity and uncertainty analysis revealed a systematic overestimation of evapotranspiration in loess areas, probably due to rather poor parameterization of loess soils. The lower uncertainty in mountainous areas can also be explained by the natural river networks, which are far more regulated in lowland areas. Uncertainty in the discharge balance (simulated minus observed discharge) for the Elbe at Neu Darchau was within a range of -4.9 % and +10.7 % in 80 % of the simulations (see Chapter 2.4.2).

The quality of the simulation results is also confirmed by a comparison with the values of the recently updated version of the Hydrological Atlas of Germany (Leibundgut and Kern, 1999), where the flow components are within the same range (see 6.1).

Additionally, the model was able to reproduce local hydrological processes like groundwater table dynamics inside three subbasins, where groundwater data were available. This was shown using contour maps of the water table depth and observed groundwater level data.

Using the experience gained by the calibration and validation of the nested subcatchments, it was possible to validate SWIM for the whole basin considering the hydrological processes in the different landscapes. The most important information from the nested investigations was that wetlands should be included in the model set-up: The daily and monthly efficiency of simulated and observed river discharge was 0.90 and 0.91 for the model set-up without the wetland extension, and 0.92 and 0.94 for the model set-up with the wetland module implemented. The change is more pronounced for the long term difference of simulated minus

observed river discharge, which dropped from 9.7 % to 4 % with the wetland module included. Figure 7.2 shows the difference in river runoff with and without the extended model. The best reproduction of the hydrological processes in the whole Elbe basin was achieved with a parameter set very similar to that used for the lowland subbasins. Apparently, hydrological processes of the lowlands dominate the dynamics of the river flow regime in the Elbe basin.

The sensitivity and uncertainty analysis shows that the model results were robust in all regions but more stable in mountainous catchments than in lowland and loess parts of the model area. Regarding model efficiency (Nash and Sutcliffe, 1970), the saturated conductivity and the routing correction factors were the most sensitive tuning parameters in lowland and loess area model applications. The routing correction factor was the most sensitive in mountainous catchments, indicating that river routing is the crucial process driving the dynamics of river discharge in mountainous areas with high elevation gradient. In lowland, the percolation of water through the soil layers is more important than in mountains. In order to improve the simulation results in lowlands and in particular in catchments covered by loess soils, the resolution and parameterization of the soil map should be further improved.

An important result of the study is that model applications on the macroscale should always include additional investigations in smaller subbasins to analyze and understand the special characteristics of the subregions. The quality of the results confirms that after validation the model can be applied to investigate the environmental changes in the Elbe basin.

6.2 Implementation of groundwater dynamics at the hydrotope level

The validation of SWIM for the entire German part of the Elbe basin has shown that an improved spatial representation of the hydrological processes inside the subbasins in terms of groundwater dynamics is helpful to improve the model performance especially in lowland and for low flow periods. In addition, groundwater fluctuations are triggered by soil water percolation, and observations of the local water table dynamics can be used to validate the model indirectly for the hydrological processes at the hydrotope level. Implementation of groundwater

dynamics at the hydrotope level is also necessary, because they are very important for wetland processes, which are further discussed in the next chapter. The objective of the second article was therefore a) to modify SWIM so that daily groundwater fluctuations can be reproduced at the hydrotope level in regional applications of the model, b) to incorporate a direct interaction of groundwater and soil profile in the areas with shallow groundwater where it can reach soil layers, and c) to test the model in two different lowland subbasins in the Elbe catchment (the Nuthe and the Stepenitz), where data on groundwater table dynamics were available. Besides, a new approach was developed to calibrate the simulated groundwater fluctuations.

The results presented in Chapter 3.3.3 show that the SWIM model was, after modification, able to reproduce the groundwater table dynamics in the studied basins. This is shown in three steps. Firstly the groundwater fluctuations simulated by the modified SWIM were compared under well defined boundary conditions with those simulated using a numerical groundwater model. Differences were minor and much smaller than those induced by the model parameter uncertainty.

A second step was to apply SWIM over two mesoscale lowland basins and to compare the simulated groundwater table fluctuations against the observation. By using the automatic calibration method and variation of two parameters, namely permeability and effective porosity of the aquifer, it was possible to adjust the simulated water table against to that observed: The Mean Absolute Error of the long term mean observed against mean simulated water table in all subbasins was 0.053 m for the Stepenitz basin, and 0.026 m for the Nuthe basin (see Chapter 3.3.3).

The third step was to apply the model to investigate the observed trend in the groundwater table in the state of Brandenburg, which has decreased in parts of the region by approximately 0.5 m to 1.0 m over last decades. Using SWIM with the extended groundwater module it was demonstrated that the decrease of the groundwater table in the case study region cannot be explained by climate variability in the area, rather by a decrease in the drainage base during recent decades (human intervention). Available information from literature and oral communication confirmed that the intensive melioration measures in the region (implementation of drainage systems to regulate the groundwater table and of

weirs to control the water level of the surface waters) are the main reason for the observed decrease in groundwater table.

6.3 Integration of retention processes in groundwater, wetlands and riparian zones in the SWIM model

The third paper deals with nitrate retention processes in groundwater, riparian zones and wetlands, considering the residence time and turn-over of nutrients at the hydrotope level. These processes are very important because they control the diffuse nutrient inputs into rivers and lakes, which are still considerably high, while the input from point sources has decreased after the basin-wide implementation of better sewage treatment (especially building new plants and improving technology in the old ones since 1990). The relevance of processes in riparian zones and wetlands for the water and nutrient balance of river basins is twofold: a) they represent an interface between the upper catchment area and surface waters, where lateral flows of water and nutrients pass through and are partly retained, and b) they have shallow groundwater, where plant roots can reach the saturated zone enabling vegetation to satisfy their demand by accessing water and nutrients from groundwater, especially during periods of shortage in the unsaturated soil horizon. The research objective was to quantify the impact of nitrate retention processes in the subsurface, wetlands and riparian zones on the water quality and river discharge, and to calculate the residence time of nitrate in the subsurface, especially in groundwater. Since the original SWIM model had only a very simple representation of retention processes in the subsurface and no representation of wetland processes, a wetland module was developed based on the implementation of groundwater dynamics described in the previous section, to represent a) the mean residence time and the turn-over of nitrate in the subsurface, b) the nitrate retention in the riparian zone and wetlands, and c) the uptake of water and nitrate by plants if the plant roots have access to groundwater (see Chapter 4.2.3).

The results shown in the Chapter 4.3 illustrate the ability of the extended model to represent the processes relevant for water and nitrate flow and retention

in catchments with special focus on wetlands and riparian zones. A relatively small fraction of the total catchment area has a high impact on the water and nitrate balance in the whole catchment (leading e.g. to a decrease in annual river discharge of about 49 % at the basin outlet and to an decrease in annual river nitrate load of about 22 % in this catchment), although the results are associated with a high uncertainty, mainly due to the rather low reliability of the regionally available input data (soils, geo-hydrology, land use, crop rotations, application of fertilizer).

The impact of wetlands and riparian zones is so significant because they are at the interface between catchment and river systems, and have specific conditions (access to groundwater and good conditions for denitrification). In addition, the majority of the nutrient input in the catchment has been retained before reaching the wetland and riparian zone (e.g. by plant uptake and nutrient turn-over in the soil zone and in groundwater), and a relatively large part of the remainder is taken up by plant roots located in a relatively small area of the total catchment.

6.4 Assessing uncertainty of water availability and crop yields in a Central-European river basin under climate change

The aim of the study was to assess the reliability of water supply and crop yields in the German part of the Elbe basin under global change taking into account the uncertainty of the future climate. The scenario period of the study is 2000-2055, a time scale relevant for the implementation of water and land use management plans. The intention was to mirror the possible range of climate and land use change in the Elbe basin in the model experiments and simulation results, and thereby to apply scenarios where the underlying assumptions regarding the driving forces for climate and land use change are consistent, and to consider feedbacks between land use and climate change.

The experience gained in the previous publications was accumulated to have a satisfactory model representation of the study area, but additional developments and model adjustments were necessary a) to wrap the model in a framework for automatic pre-processing of the climate data for the 100 realizations of the

climate scenario, model simulation and statistical post-processing of the simulation results, b) to derive land use change scenarios consistent with the climate scenario, and c) to generate crop rotations and distributions taking into account the input information of the agricultural agencies for the reference and of the scenario conditions for the scenario period (Chapter 5.2.1).

The methodology presented in this study allows to assess the uncertainty of water supply under global change considering the most important drivers, land use and climate, whereby feedbacks between trend in climate and its impact on land use can be taken into account.

The overall result is that nature as well as society in the German part of the Elbe basin are confronted with severe changes in water availability and river flow regimes, although the results are associated with a high uncertainty (see Chapter 5.3.2). The rise in temperature of 1.4 K in the period 2001-2055 will stimulate plant growth and lead to a prolongation of the vegetation period. As a result, plant transpiration will intensify in early spring and continue into late autumn.

This will influence the river flow regime, and the rise of the river water level will be later in late autumn and the recession earlier in spring. More frequent and prolonged periods of low water levels can be observed in late summer and early fall. Increases in evapotranspiration will have the highest impacts on groundwater recharge, which is very sensitive to changes in water supply. Figure 6.1 summarizes the results. While the trend in temperature and therefore also the trend in evapotranspiration and the related change of the river flow regime are relatively certain, much more uncertainty exists with the trends in precipitation, groundwater recharge, direct runoff and river discharge and the strength of these trends. Of the total set of 100 climate scenario realizations, 59 show a decrease in precipitation and 99 an increase in evapotranspiration (when comparing the periods 1961-90 and 2051-55). As a result, 69 realizations lead to a decrease in direct runoff (surface runoff and interflow), 87 to a decrease in groundwater recharge, and 80 to a decrease in river runoff. The results have a strong spatial heterogeneity. The median trend in precipitation of the 100 scenario realizations indicates only a small decrease of precipitation by 1.5 % (the range of the realizations is from -15.3 % to +14.9 %). Added to an increase in evapotranspiration under warmer conditions, this would lead to a relatively large decrease in groundwater recharge by 22.5 % and river discharge by 15.5 %. This change is out of the range

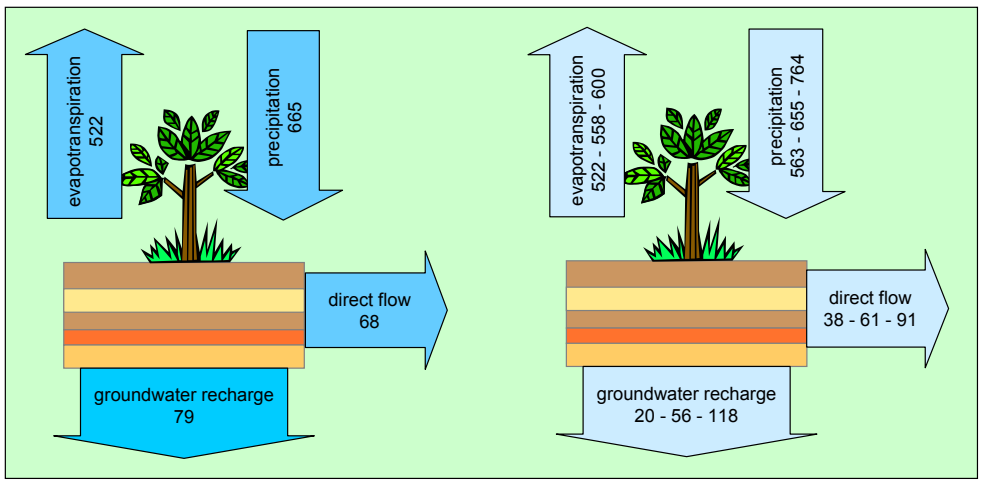

Figure 6.1. Summary of the impacts of a climate change on the water cycle in the German part of the Elbe basin; left: average values for the reference period 1961-1990 in mm, right: average values for the scenario period 2051-2055 in mm for the driest, median and wettest realization of the climate scenario.

of uncertainty of the eco-hydrological model performance (see Chapter 2.4.2).

Impacts on hydrological components are directly correlated with a change in water resources, where the per capita annual water supply generated in the German part of the Elbe basin would decrease by 15 % in the moderate scenario realization, which is the median of the 100 realizations (the median change in precipitation). The result is even more severe when considering that currently 80 % of freshwater used for human water demand is taken from groundwater, where the decrease is most pronounced.

Another result of the decrease in precipitation is that also crop yields show a decreasing trend, whereby the changes are higher for C3-crops like wheat, barley and rye (-12 % to -15 %), and less pronounced for the C4-plant maize (-1 %), which benefits more from the increase in temperature than the C3-cereals. The changes in crop distributions caused by the climate change is minor, but becomes important when also global agro-economic changes are taken into account (Chapter 5.3.2). This more pronounced change has a significant impact on the water cycle in the Elbe basin, with a decrease in evapotranspiration (approximately 8 %) and an increase in flow generation (approximately 14 %). Here, the management of land use becomes very important, for example the types of land cover which will replace agriculture (e.g. grassland, forests or settlements).

Chapter 7

Discussion and conclusions

This study illustrates the vulnerability of the water balance in the German part of the Elbe basin to changes in precipitation and temperature. The Elbe basin has the second lowest water availability of the large rivers in Central Europe (see Stanners and Bourdeau, 1995), and according to model results, it is most likely that the observed trend to lower water availability (Gerstengarbe and Werner, 2005) will continue into the future. Small changes in the drivers (precipitation, temperature) will have a large impact on the water cycle (Chapter 5.3.2, Hattermann et al., 2005c). The decrease of annual precipitation will be more pronounced in the lee of the Harz mountains and the central parts of the basin, while the climate scenario gives increasing amounts of precipitation in the northwest and the south of the basin. The change in the central part of the basin is so important because this is the region where the precipitation is already the lowest in the catchment, but where the soils have the highest fertility. It has to be mentioned that the center of the German part of the Elbe basin is also the area where the variability of the future precipitation across the scenario realizations and hence the uncertainty of the simulation results is the highest (see Chapter 5.3.2), making it difficult to plan and implement long-term adaptive land use strategies.

The ecosystems in the basin will have to adapt to dryer conditions over large parts of the basin. This can lead to losses in biodiversity (Schröter et al., 2005) and crop yields (Chapter 5.3.2), and the local water managers and farmers will have to find adapted water and land use management options. Possible strategies for adaptation are to build reservoirs as buffers during droughts and structural

changes in land use, especially in agriculture (Kabat et al., 2004; Fohrer, 2002).

In the study, only arable land is subject to land use change (approximately 52 % of the area of the German part of the Elbe basin) (Chapter 5). The areas, which will become set-aside under scenario conditions, will be maintained as farm land. These areas are considered as extensive meadow in the model, which has lower water demand and as a result lower evapotranspiration than arable land. Two land use scenarios consistent with the climate change scenario are investigated in the study: The first includes only climate change as a driving force to derive new crop distributions in the basin, the second considers also global agro-economic pressures. Under the first land use scenario, the crop distriubtions will have only a very small change. The second will lead to more pronounced changes in crop distributions with an increase of set-aside from approximately 7 % to approximately 29 % (see Figure 5.5), and as a result of the increase of set-aside, evapotranspiration will decrease by approximately 8 % and river runoff increase by approximately 14 % (see Chapter 5.3.2). This is within the range of change induced by the climate change.

It has to be mentioned that the scope of the study, considering land use scenarios, was to investigate and present a methodology to develop consistent land use and climate scenarios, rather than to explore the large variety of possible changes in land use management. This is clearly a topic for future research: One challenge is for example to take into account altered soil parameters to describe the soil properties of fallow land, which are different from arable land (Fohrer et al., 2005; Frede et al., 2002). A possible land use change, which has to be included in future investigations, is afforestation, where fallow land becomes brush land and forest (Wattenbach et al., 2005). First model experiments show that under such conditions evapotranspiration will increase in the German part of the Elbe basin and hence accelerate the pressure on the water resources in the catchment induced by the possible climate change.

Another task for future research related to the investigations of water resources in the Elbe basin is to include the Czech part of the basin in the model, because although the simulations for the German part of the Elbe river basin indicate a strong decrease in water availability and river discharge, it is unclear as to whether this result is representative for the entire basin including the Czech part. Observations of precipitation in the southern part of the Elbe basin and

observed river discharge indicate that an increase of precipitation in the Czech part may balance the decrease in the central part of the basin. However, the increase in temperature will also affect the Czech part of the basin and result in an intensification of evapotranspiration and decrease of river discharge.

Results shown in Chapter (4.3) (Hattermann et al., 2005b) illustrate the influence of wetlands and riparian zones on the water and nutrient cycle in the basin. The actual evapotranspiration in this areas reaches the potential evapotranspiration. This is important, because wetland restoration measures are ongoing or planned for the conservation of valuable wildlife habitats and for the future development of tourist attractions, but with possibly unfavorable consequences for the local water balance, because an increase of the wetland area will lead to higher annual evapotranspiration and a decrease in river discharge. One such example is the Spree subbasin of the Elbe, where the the Spreewald biosphere reserve is located, one of the largest wetland areas in Germany, but where the per capita water availability is only 280 m^3 a^{-1} (Wechsung et al., 2005a).

On the other hand, retention processes in groundwater, wetlands and riparian zones have a high potential to reduce the nutrient concentrations of rivers and lakes, because they are located at the interface between catchment area and surface water bodies, where they are controlling the diffuse nutrient inputs (Mander et al., 1997). This is illustrated in the Nuthe subbasin with nitrate as an example (Chapter 4.3.2). The relatively high retention of nitrate in the Nuthe basin is partly due to the long residence time of water in the subsurface (about 40 years in the Nuthe basin) with good conditions for denitrification (lignite in the subsurface), and partly because of the plant uptake of nitrate in the wetlands and riparian zones. Although the Nuthe basin is in a way an extreme example because of the high proportion of wetlands in the total catchment area, it is representative for large regions in Central Europe (approximately 50 % of the German part of the Elbe basin are located in lowland areas). The long residence time of nitrate in the subsurface in the Elbe basin may be one reason for the still high nitrate concentrations observed in other subbaisns of the Elbe and in the Elbe discharge. Here, the different conditions for denitrification in groundwater play a key role (Wendland et al., 1993). The results are in good agreement with Behrendt et al. (1999), who investigated the nutrient loads of the river basins in Germany.

The investigations have been done using the eco-hydrological model SWIM,

which has been embedded in a model framework of climate and agro-economic models (see Chapter 5.2.1, Hattermann et al., 2005c). An integrated modeling description of all relevant water and nutrient flow processes and including management options was necessary because of the numerous interactions and feedbacks between land use, vegetation, climate and hydrological processes, which are so complex that they can only be analyzed in a formalized way using computer models (see Bronstert et al., 2005). The advantage of having a computer based model description of the Elbe basin is the possibility to easily investigate and analyze different climate and socio-economic scenarios, to quantify their impacts on the environment in the basin and find management solutions to mitigate the impacts.

However, the predictive capacity of models is generally limited because of the often low quality (and quantity) of the available input data, uncertain model parameters and due to structural shortcomings of the models (Singh and Frevert, 2002). It is therefore the responsibility of the modeler to communicate and illustrate these limitations and to do everything possible to improve the quality of the model outputs (Refsgaard et al., 1996). This brings us back to the four points requested by Bronstert (2004) and mentioned in the introduction, where the new challenges in hydrological modeling in the context of climate and land use changes are discussed:

1. *The standard calibration methods of hydrological models need to be adjusted or extended to have an adequate representation of altered internal dynamics of the hydrological system if the boundary conditions change. The calibration process should be multi-criteria and multi-site.* This has been done when the SWIM model was validated for the hydrological processes in the German part of the Elbe basin first for different subbasins nested in the catchment to investigate the relevant processes in different landscapes of the model area, for subbasins with different catchment area to investigate scaling effects, and using not only observations of river discharge, but also groundwater dynamics and regional crop yields for comparison.

2. *The development of the scenario of changed boundary conditions should be done considering feedbacks to derive consistent scenarios for land use and climate changes.* Simulation results presented in this study have been derived assuming the same IPCC scenario for the development of land use

(agriculture) and climate change. The feedbacks of climate change on land use are considered when at first the potential crop yields under climate change are simulated by SWIM and afterwards transferred to the agro-economic model to form the input for producing a scenario of changed agricultural land use, which is consistent with the climate scenario and following the same IPCC storyline.

3. *The uncertainty in data, parameters and model processes propagated by the model has to be quantified and, what is new, also the uncertainty in the scenario conditions.* The estimation of uncertainty in the model results, for the validation as well as for the scenario period, has been consequently considered during each modeling step of the study. It was found that the average range of change of the hydrological quantities induced by climate change is larger than the uncertainty of the simulation results because of model parameter and input data uncertainty.

4. *It is necessary and important to adjust the climate or land use scenarios for extremes such as floods or droughts.* This has been done for droughts and low flow conditions, since the study aimed at the investigation of long term changes in water supply and crop yields under scenario conditions, and not at the investigation of flood risk.

Not explicitly mentioned in the list above but implicitly part of point 1, where it is said that *an adequate representation of altered internal dynamics of the hydrological system is needed*, is the fact that it might be necessary to extend and improve the model concept and the model structure to adapt it to the scientific question and the modeling problem of the study by implementing additional processes in the model code. This has to be done considering the complexity of the modeling task and the data and model parameter availability. The new methods, which have been implemented in the SWIM model during the study, are physically based and applicable at large spatial scales, assuming some simplifications (e.g. regarding the geometry of the subsurface flow), which are acceptable in regional modeling (see Chapters 3.2.1 and 4.2.3).

Shortcomings in the model concept of SWIM and in the available input data could be identified because the model was first tested and validated for the eco-hydrological processes in nested catchments located in the most important sub-

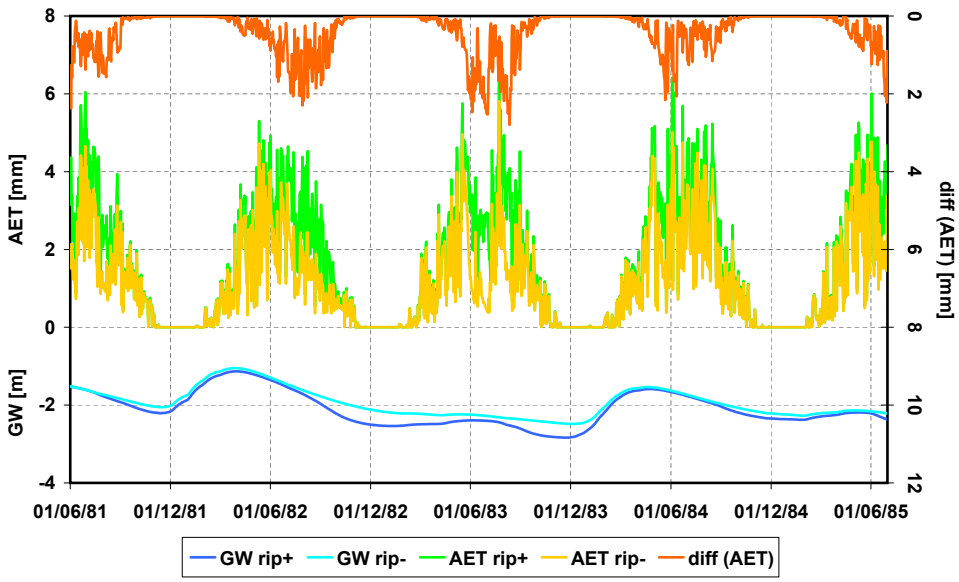

Figure 7.1. Effects of additional plant uptake of water in wetlands in one example hydrotope (GW = groundwater table, AET = actual evapotranspiration, rip- = without additional uptake, rip+ = with additional uptake, diff (AET) = difference in evapotranspiration with and without additional plant uptake).

regions of the basin, and because different criteria were taken into account in the validation process, like river discharge in connection with groundwater dynamics, but also comparisons of crop yields. The first simulation experiments during this study revealed for example an underestimation of evapotranspiration in lowlands (see Figure 7.1). Hence the model overestimated river discharge during the summer period. This is crucial because more and longer lasting droughts and low flow events are expected in the future. The problem was solved by implementing hydrological processes in wetlands and riparian zones in the model, as discussed in Chapter 4, which are especially important for evapotranspiration during the summer period and during droughts, but also for nutrient retention. The results shown in Figure 7.2 are in a plausible range, when comparing them with results of other modeling studies (Becker et al., 2003) and with field scale observations in wetland areas (Meuleman et al., 2003).

An additional advantage of the developed method is that it takes the residence time of nutrients in the subsurface into account, whereby the nutrient turn-over is simulated at a daily time step. This is new in large scale model applications, where the aim is to simulate the nutrient loads coming from the catchment area

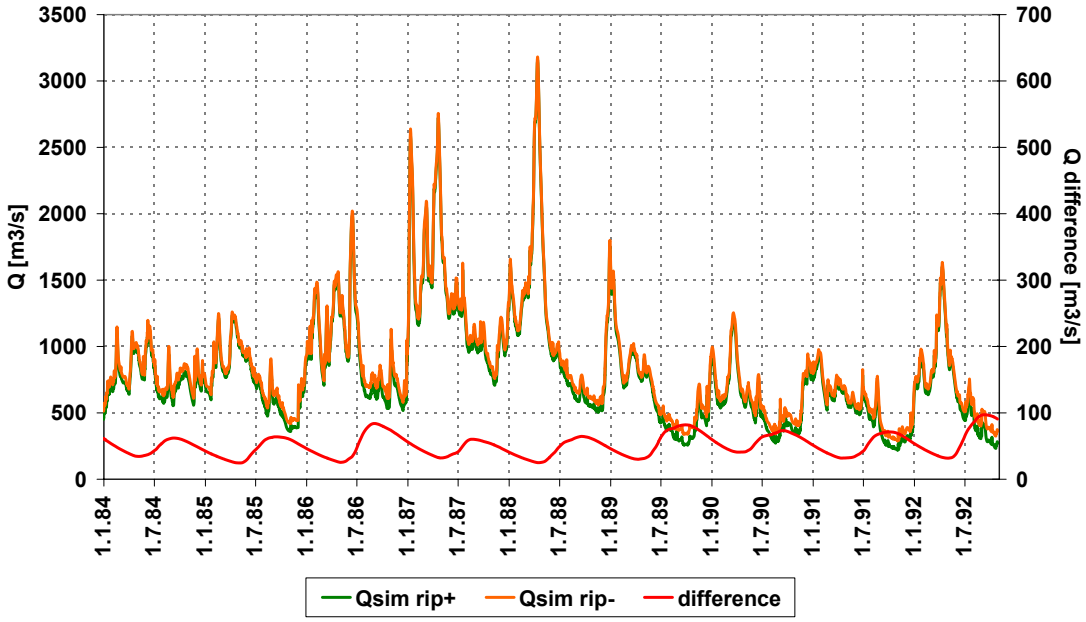

Figure 7.2. Simulation of river discharge at gauge Neu Darchau with (rip+) and without (rip-) implementation of wetland processes in the model concept, and the difference.

into the surface waters. Normally, the nutrient concentrations in groundwater discharge are considered as being constant (Arnold et al., 1994), or the model assumes a balanced nutrient cycle over long time periods (e.g.five years), where the retention in a catchment is simply the input (from point and diffuse sources) minus the output (the river loads), where different flow paths might be considered (Behrendt et al., 2002). The next step has to be to apply the extended model to the entire Elbe basin to investigate changes in the nutrient balance of the whole catchment in the past and under scenario conditions.

Another example, where model applications in nested subbasins helped to validate the model, are problems with the parameterization of loess soils, which have been found when applying SWIM over nested subbasins located in the loess area, and when the model sensitivity to different model parameters is investigated (see Chapter 2.4 and 4.3.2).

A necessary development to improve the spatial distribution of climate input data was the improvement of the interpolation technique used by SWIM. The technique originally implemented was the method of Thiessen polygons. This method gives sufficiently good results for small scale applications, where the

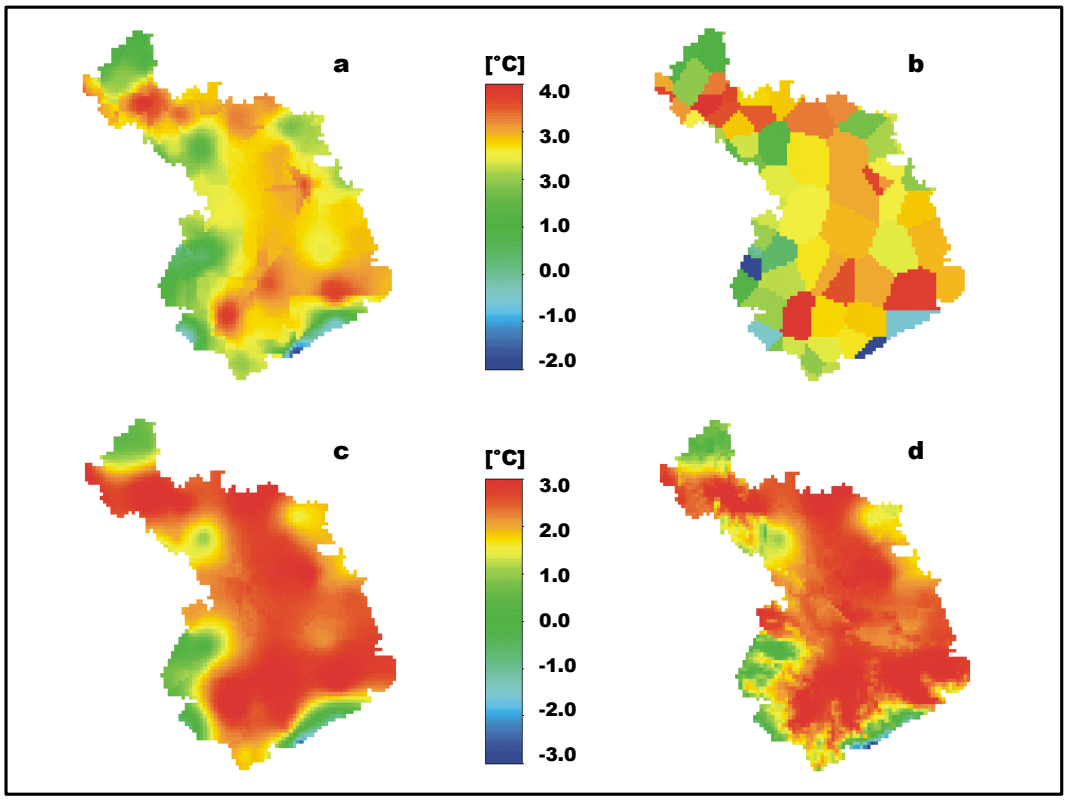

Figure 7.3. Comparison of four interpolation techniques to calculate the climate boundary conditions (here mean daily temperature) for the SWIM model (a: Inverse Distance; b: Thiessen Polygons; c: Ordinary Kriging; d: External Drift Kriging using the elevation map as a secondary variable for interpolation) (see Hattermann et al. (2005a) in Chapter 2.2.3).

density of climate stations is high, or at the plot scale with only one station. In and around the German part of the Elbe basin 89 climate and 280 precipitation stations with long time climate records are available, but the spatial density of the stations is very inhomogeneous (lower in lowland areas). The application of the method of Thiessen polygons, which does not account for landscape features, would lead to an artificial and unrealistic spatial pattern of climate variables with hard straight line borders between two polygons (see Figure 7.3). The geo-statistical and inverse-distance methods introduced and applied in this study give a more realistic picture of the spatial variability of the climate input data, as shown by a cross validation using the observed climate information of the 369 weather stations applied in the study (see Table 2.2 in Chapter 2.2.3).

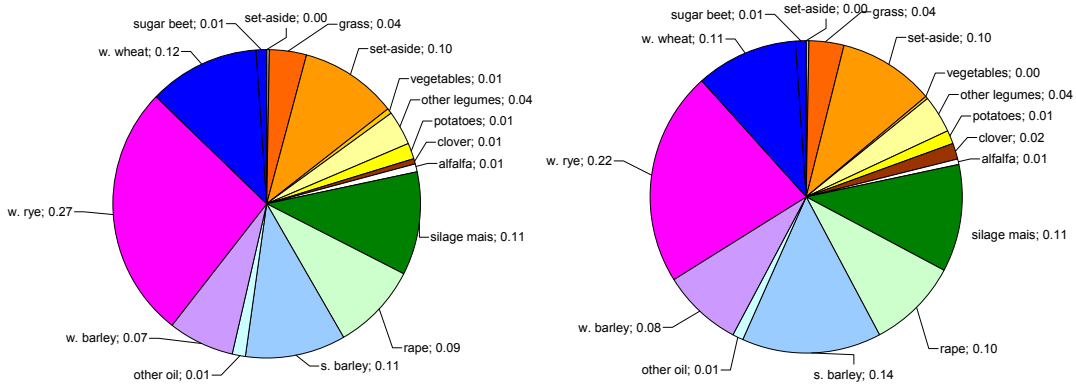

(a) Statistics (b) Simulation

Figure 7.4. Use of arable crop land in the German part of the Elbe basin: a) taken from statistics b) after reallocation applying the crop allocation algorithm.

A difficult task was to derive a land use scenario consistent with the regional climate scenario. This was done, as mentioned before, by assuming that land use changes in the Elbe basin will mainly affect arable land, and that the arable land, which will be set aside under scenario conditions, will not be afforested. A crop generator has been developed to regionalize the land use scenario delivered by the agro-economic group, which serves as an interface between agricultural land use statistics and the hydrotope module in SWIM (see Wechsung et al., 2005b). State-of-the-art investigations of climate change impacts on water and nutrient fluxes normally do not account for daily plant growth dynamics and in particular do not consider crop rotations and crop distributions in the catchment under study (Varis et al., 2004). But, as illustrated in Chapter 5.3.2, the distribution of different crops (like summer and winter crops, grains and foliate plants) might be important for the basin-wide water balance, a feedback that has to be taken into account in the model (Bronstert et al., 2005; Fohrer, 2002).

Generally, it is important to mention that it is impossible to integrate all features and characteristics of a landscape in a single model framework. It is rather the responsibility of the modeler to find adequate model solutions during the model set-up, which consider the relevant flow and retention processes and the important management options. This has to be done without overloading the model framework by including features and processes, which are not important but need additional expert experience, input data and model parameters. Here, a careful analysis of the available data (climate, hydrology, soils, vegetation, geo-

chemistry) and a comprehensive sensitivity investigation will help to identify an appropriate model concept and problems in the model structure (Abbott and Refsgaard, 1996).

Summarizing the discussion it can be concluded that the integrated model presented in the study is a very valuable tool to support water and land use managers, decision makers and environmental agencies to find sustainable solutions in the very sensitive problem field of environmental protection versus socio-economic development and human water demand. However, additional studies have to be performed to include the Czech part of the Elbe basin in the model, to analyze the impact of riparian zones and wetlands on the water quality of the whole Elbe river basin and to investigate additional land use scenarios taking into account possible changes in soil properties.

Bibliography

M. B. Abbott and J. C. Refsgaard. *Distributed hydrological modeling*. Kluwer Academic Publishers, Dordrecht, Boston, London, 1996.

F. A. Abdulla and D. P. Lettenmaier. Development of regional parameter estimation equations for a macroscale hydrologic model. *Journal of Hydrology*, 197(1-4):230–257, 1997.

H. Akin and H. Siemes. *Praktische Geostatistik*. Berlin, Heidelberg, 1988.

J. Andersen, J. C. Refsgaard, and K. H. Jensen. Distributed hydrological modelling of the Senegal river basin – model construction and validation. *Journal of Hydrology*, 247(3-4):200–214, 2001.

J. G. Arnold. ROTO - a continuous water and sediment routing model. *ASCE Proceedings Of the Watershed Management Symposium*, pages 480–488, 1990.

J. G. Arnold, P. M. Allen, and G. Bernhardt. A comprehensive surface-groundwater flow model. *Journal of Hydrology*, 142(1-4):47–69, 1993.

J. G. Arnold, R. S. Muttiah, R. Srinivasan, and P. M. Allen. Regional estimation of base flow and groundwater recharge in the Upper Mississippi river basin. *Journal of Hydrology*, 227(1-4):21–40, 2000.

J. G. Arnold, J. R. Williams, R. Srinivasan, K. W. King, and R. H. Griggs. *SWAT, Soil and Water Assessment Tool*. USDA, Agriculture Research Service, Grassland, Soil and Water Research Laboratory, Temple, Texas, 1994.

ATV-DVWK. Die Elbe und ihre Nebenflüsse. Belastung und Trends, Bewertung, Perspektiven. Technical report, Deutsche Vereinigung für Wasserwirtschaft, Abwasser und Abfall e. V., Hennef, 2000.

M. Bach, J. Fabis, and H.-G. Frede. Filterwirkung von Uferstreifen für Stoffeinträge in Gewässer in unterschiedlichen Landschaftsräumen. Band1. Technical report, DVWK 28, 1997.

P. A. M. Bachand and A. J. Horne. Denitrification in constructed free-water surface wetlands: I. Very high nitrate removal rates in a macrocosm study. *Ecological Engineering*, 14(1-2):9–15, 1999a.

P. A. M. Bachand and A. J. Horne. Denitrification in constructed free-water surface wetlands: II. Effects of vegetation and temperature. *Ecological Engineering*, 14(1-2):17–32, 1999b.

A. Becker and P. Braun. Disaggregation, aggregation and spatial scaling in hydrological modelling. *Journal of Hydrology*, 217(3-4):239–252, 1999.

A. Becker and U. Grünewald. Flood Risk in Central Europe. *Science*, 300: 1098–1099, 2003.

A. Becker, B. Klöcking, W. Lahmer, and B. Pfützner. The hydrological modelling system ArcEgmo. In V. P. Singh, editor, *Handbook of hydrology*. 2003.

H. Behrendt and A. Bachor. Point and diffuse load of nutrients to the Baltic Sea by river basins of North East Germany (Mecklenburg-Vorpommern). *Water Science and Technology*, 38(10):147–155, 1998.

H. Behrendt, P. Huber, D. Opitz, O. Schmoll, G. Scholz, and R. übe. Nährstoffbilanzierung der Flußgebiete Deutschlands. Technical report, Umweltbundesamt, 1999.

H. Behrendt and D. Opitz. Retention of nutrients in river systems: dependence on specific runoff and hydraulic load. *Hydrobiologia*, 410:111 – 122, 2000.

H. Behrendt, D. Opitz, and O. Schmoll. *Stoffeinträge in die Gewässer des Landes Brandenburg*, volume 68 of *Fachbeiträge des Landesumweltamtes*. 2002.

S. Bergström. The HBV model. In V. P. Singh, editor, *Computer Models of Watershed Hydrology*, pages 443–476. Water Resources Publications, Littleton, Colorado, USA, 1995.

BIBLIOGRAPHY

S. Bergström and L. P. Graham. On the scale problem in hydrological modelling. *Journal of Hydrology*, 211(1-4):253–265, 1998.

K. Beven. TOPMODEL: A critique. *Hydrological Processes*, 11(9):1069–1085, 1997.

H. Bogena, B. Diekkrüger, K. Klingel, K. Jantos, and J. Thein. Analysing and modelling solute and sediment transport in the catchment of the Wahnbach River. *Physics and Chemistry of the Earth*, 28(6-7):227–237, 2003.

H.-R. Borg, C. Dalchow, H. Kächele, H.-P. Piorr, and K.-O. Wenkel. *Agrarlandschaftswandel in Nordost-Deutschland*. Ernst & Sohn, Berlin, 1995.

A. Bronstert. Probleme, Grenzen und Herausforderungen der hydrologischen Modellierung: Wasserhaushalt und Abfluss. *BfG*, 2003.

A. Bronstert. Rainfall-runoff modelling for assessing impacts of climate and land-use change. *Hydrological processes*, 18(3):567–570, 2004.

A. Bronstert, J. Carrera, P. Kabat, and S. Lütkemeier. *Coupled Models for the Hydrological Cycle - Integrating Atmosphere, Biosphere, and Pedosphere*. Springer, Berlin, Heidelberg, New York, 2005.

A. Bronstert, V. Krysanova, A. Schröder, A. Becker, and H.-R. Bork. *Modellierung des Wasser- und Stofftransportes in großen Einzugsgebieten*, volume 43 of *PIK Report*. Potsdam Institute for Climate Impact Research, Potsdam, 1997.

A. Bronstert, D. Niehoff, and G. Burger. Effects of climate and land-use change on storm runoff generation: present knowledge and modelling capabilities. *Hydrological Processes*, 16(2):509–529, 2002.

F. H. S. Chiew and T. A. McMahon. Modelling the impacts of climate change on Australian streamflow. *Hydrological Processes*, 16(6):1235–1245, 2002.

N. S. Christensen, A. W. Wood, N. Voisin, D. P. Lettenmaier, and R. N. Palmer. The effects of climate change on the hydrology and water resources of the Colorado river basin. *Climatic Change*, 62:337–363, 2004.

C. P. Cirmo and J. J. McDonnell. Linking the hydrologic and biogeochemical controls of nitrogen transport in near-stream zones of temperate-forested catchments: a review. *Journal of Hydrology*, 199(1-2):88–120, 1997.

S. M. Cuddy and C. Gandolfi. Editorial. In S. M. Cuddy and C. Gandolfi, editors, *Integrated assessment and decision support*, volume 19, pages 989–990. Environmental Modelling and Software Society, 2004.

M. Dall'O', W. Kluge, and F. Bartels. FEUWAnet: a multi-box water level and lateral exchange model for riparian wetlands. *Journal of Hydrology*, 250(1-4): 40–62, 2001.

O. Dassau. GRASS GIS 6.0 Handbuch. Technical report, Hannover, 2005.

F. Dollinger and J. Strobl. *Angewandte Geographische Informationsverarbeitung VIII, Heft 24*. Salzburger Geographische Materialien, Salzburg, 1996.

S. M. Dunn and R. C. Ferrier. Natural flow in managed catchments: a case study of a modelling approach. *Water Resources Research*, 33(3):621–630, 1999.

EC. Establishing a framework for community action in the field of water policy. Directive 2000/60/EC of the European Parliament and of the Council of 23 October 2000. Brussels, 2000.

K. Eckhardt and U. Ulbrich. Potential impacts of climate change on groundwater recharge and streamflow in a central European low mountain range. *Journal of Hydrology*, 284(1-4):244–252, 2003.

N. Fohrer. *River basin research and management: influence of land cover, land use and soil surface conditions on hydrological processes and water balance of catchments*, volume 27. Physics and Chemistry of the Earth, 2002.

N. Fohrer, S. Haverkamp, and H.-G. Frede. Assessment of the effects of land use patterns on hydrologic landscape functions. *Hydrololgical Processes*, 19(3): 659–672, 2005.

H.-G. Frede, M. Bach, N. Fohrer, and L. Breuer. Interdisciplinary modeling and the significance of soil functions. *Journal of Plant Nutrition and Soil Science*, 165(4):460–467, 2002.

BIBLIOGRAPHY

M. Freude. *Landschaftswasserhaushalt in Brandenburg: Situationsanalyse und Ausblick*. SPD Brandenburg, 2001. Dokumentation der SPD Veranstaltung "Landschaftswasserhaushalt".

H. Gehrels and N. E Peters. Impact of Human Activity on Groundwater Dynamics. *International Association of Hydrological Sciences*, 2001.

F. W. Gerstengarbe and P. C. Werner. Simulationsergebnisse des regionalen Klimamodells STAR. In Wechsung F., A. Becker, and P. Gräfe, editors, *Integrierte Analyse der Auswirkungen des globalen Wandels auf Wasser, Umwelt und Gesellschaft im Elbegebiet*, volume Report 95. Potsdam Institute for Climate Impact Research, Potsdam, 2005.

A. Güntner, S. Uhlenbrook, J. Seibert, and C. Leibundgut. Multi-criterial validation of TOPMODEL in a mountainous catchment. *Hydrological Processes*, 13(11):1603–1620, 1999.

W. Guo. Transient groundwater flow between reservoirs and water-table aquifers. *Journal of Hydrology*, 195(1-4):370–384, 1997.

D. Haag and M. Kaupenjohann. Landscape fate of nitrate fluxes and emissions in Central Europe - A critical review of concepts, data, and models for transport and retention. *Agriculture, Ecosystems and Environment*, 86:1 – 21, 2001.

U. Haberlandt and G. W. Kite. Estimation of daily space-time precipitation series for macroscale hydrological modelling. *Hydrological Processes*, 12(9): 1419–1432, 1998.

F. Habets, J. Noilhan, C. Golaz, J. P. Goutorbe, P. Lacarrere, E. Leblois, E. Ledoux, E. Martin, C. Ottle, and D. Vidal-Madjar. The ISBA surface scheme in a macroscale hydrological model applied to the Hapex-Mobilhy area - Part II: Simulation of streamflows and annual water budget. *Journal of Hydrology*, 217(1-2):97–118, 1999a.

F. Habets, J. Noilhan, C. Golaz, J. P. Goutorbe, P. Lacarrere, E. Martin, C. Ottle, and D. Vidal-Madjar. The ISBA surface scheme in a macroscale hydrological model applied to the Hapex-Mobilhy area - Part I: Model and database. *Journal of Hydrology*, 217(1-2):75–96, 1999b.

I. Haddeland, B. V. Matheussen, and D. P. Lettenmaier. Influence of spatial resolution on simulated streamflow in a macroscale hydrologic model. *Water Resources Research*, 38(7), 2002.

F. R. Hall and A. F. Mönch. Application of the convolution equation to stream-aquifer relationships. *Water Resources Research*, 8(2):487–493, 1972.

F. F. Hattermann, V. Krysanova, F. Wechsung, and M. Wattenbach. Multiscale and multicriterial hydrological validation of the ecohydrological model SWIM. In A. Rizzoli, E., and A. J. Jakeman, editors, *Integrated assessment and decision support*, volume 1, pages 281–286. Environmental Modelling and Software Society, 2002. Proceedings of the 1st biennial meeting.

F. F. Hattermann, V. Krysanova, F. Wechsung, and M. Wattenbach. Integrating groundwater dynamics in regional hydrological modelling. *Environmental Modelling & Software*, 19(11):1039–1051, 2004.

F. F. Hattermann, M. Wattenbach, V. Krysanova, and F. Wechsung. Runoff simulations on the macroscale with the ecohydrological model SWIM in the Elbe catchment - validation and uncertainty analysis. *Hydrological Processes*, 19:693–714, 2005a.

F. F. Hattermann, V. Krysanova, A. Habeck, and A. Bronstert. Integrating wetlands and riparian zones in river basin modelling. *Ecological Modelling*, 2005b. in print.

F. F. Hattermann, V. Krysanova, J. Post, F. W. Gerstengarbe, P. C. Werner, and F. Wechsung. Assessing uncertainty of water availability in a Central-European river basin (Elbe) under climate change. *IAHS International Association of Hydrological Sciences*, 2005c. submitted.

W. C. C. Henrichsmeyer, W. Löhe, M. Meudt, R. Sander, F. von Sothen, F. Isermeyer, A. Schefski, K.-H. Schleef, E. Neander, F. Fasterding, B. Helmcke, M. Neumann, H. Nieberg, D. Manegold, and T. Meier. Entwicklung eines gesamtdeutschen Agrarsektormodells (RAUMIS96). Endbericht zum Kooperationsprojekt. Technical report, Bundeslandwirtschaftsministerium, 1996.

B. Herrmann. Bericht 2002 des Landesumweltamtes. Technical report, Landesumweltamt Brandenburg, 2002.

K. M. Hiscock, D. H. Lister, R. R. Boar, and F. M. L. Green. An integrated assessment of long-term changes in the hydrology of three lowland rivers in eastern England. *Journal of Environmental Management*, 61:195–214, 2001.

S. B. Hooghoudt. Bijdrage tot de kennis van enige natuurkundige grootheden van de grond. *Versl. Landbouwkd. Onderz.*, 46(14):515–707, 1940.

A. L. Horn, F. J. Rueda, G. Hörmann, and N. Fohrer. Implementing river water quality modelling issues in mesoscale watershed models for water policy demands - an overview on current concepts, deficits, and future tasks. *Physics and Chemistry of the Earth*, 29(11-12):725–737, 2004.

IKSE. Zahlentafeln der physikalischen, chemischen und biologischen Parameter des internationalen Messprogrammes der IKSE. Technical report, Magdeburg, 2001.

IPCC, Part I. Climate Change 2001: The Scientific Basis. Contributions of Working Group I to the Third Assessment Report of the Intergovernmental Panel on Climate Change. Technical report, Cambridge University Press, 2001.

IPCC, Part II. Climate Change 2001: Impacts, Adaptation and Vulnerability. Contributions of Working Group II to the Third Assessment Report of the Intergovernmental Panel on Climate Change. Technical report, Cambridge University Press, 2001.

A. G. Journel and C. J. Huijbregts. *Mining geostatistics*. Academic Press, London, 1978.

P. Kabat, M. Claussen, A. P. Dirmeyer, J. H. C. Gash, L. B. de Guenni, M. Meybeck, R. A. Pielke, C. J. Vörösmarty, R. W. A. Hutjes, and S. Lüttkemeier. *Vegetation, Water, Humans and the Climate - A New Perspective of an Interactive System*. IGBP. Springer, Heidelberg, 2004.

P. Kabat, R. E. Schulze, M. E. Hellmuth, and J. A. Veraart, editors. *Coping with Impacts of Climate Variability and Climate Change in Water Management: A Scoping Paper*. Wageningen, 2002.

K. W. King, J. G. Arnold, and R. L. Bingner. Comparison of Green-Ampt and curve number methods on Goodwin Creek Watershes using SWAT. *American Society of Agricultural Engineers*, 4:919–925, 1999.

W. Kinzelbach and R. Rausch. *Grundwassermodellierung - Eine Einführung mit Übungen*. Gebrüder Bornträger, Berlin, Stuttgart, 1995.

G. W. Kite and U. Haberlandt. Atmospheric model data for macroscale hydrology. *Journal of Hydrology*, 217(3-4):303–313, 1999.

B. Klöcking and U. Haberlandt. Impact of land use changes on water dynamics - a case study in temperate meso- and macroscale river basins. *Physics and Chemestry of the Earth*, 27:619–629, 2002.

V. Klemes. Operational testing of hydrological simulation models. *Hydrological Sciences Journal*, 31:13–24, 1986.

W. G. Knisel. CREAMS: A field scale model for chemicals, runoff and erosion from agricultural management systems. Technical report, 1980.

V. Krysanova and A. Becker. Integrated modelling of hydrological processes and nutrient dynamics at the river basin scale. *Hydrobiologia*, 410:131–138, 1999.

V. Krysanova, A. Bronstert, and D.-I. Müller-Wohlfeil. Modelling river discharge for large drainage basins: from lumped to distributed approach. *Hydrological Sciences-Journal-des Sciences Hydrologiques*, 44(2):313–331, 1999a.

V. Krysanova, U. Haberlandt, H. Österle, and F. F. Hattermann. Effects of natural and anthropogenic factors on nitrogen fluxes in agricultural soils: a modelling study in the Saale River basin (central Europe). In *Impact of Human Activity on Groundwater Dynamics*, volume 269, pages 331–338. IAHS, 2001.

V. Krysanova, F. F. Hattermann, and F. Wechung. Development of the ecohydrological model SWIM for regional impact studies and vulnerability assessment. In N. Fohrer and J. Arnold, editors, *Regional Assessment of Climate and Management Impacts Using the SWAT Hydrological Model*, volume 19, pages 693–714. Hydrological Processes, 2005a.

V. Krysanova, Z. B. Kundzewicz, I. Pinkswar, Habeck A., and F. F. Hattermann. Regional socio-economic and environmental changes in Central and Eastern Europe and their impacts on water resources. *Water Resources Management*, 2005b. submitted.

V. Krysanova and H. Luik. *Simulation Modelling of a System Watershed-River-Sea Bay*. Valgus, Tallinn, Russia, 1989.

V. Krysanova, A. Meiner, J. Roosaare, and A. Vasilyev. Simulation modelling of the coastal waters pollution from agricultural watershed. *Ecological Modelling*, 49(1-2):7–29, 1989.

V. Krysanova, D.-I. Müller-Wohlfeil, and A. Becker. Development and test of a spatially distributed hydrological/water quality model for mesoscale watersheds. *Ecological Modelling*, 106(2-3):261–289, 1998.

V. Krysanova, F. Wechsung, J. Arnold, R. Srinivasan, and J. Williams. PIK Report Nr. 69 "SWIM (Soil and Water Integrated Model), User Manual". Potsdam, 2000.

V. Krysanova, F. Wechsung, A. Becker, W. Poschenrieder, and J. Gräfe. Mesoscale ecohydrological modeling to analyse regional effects of climate change. *Environmental modeling and Assessment*, pages 259–271, 1999b.

W. Z. Kundzewicz, S. Budhakooncharoen, A. Bronstert, H. Hoff, D. Lettenmaier, L. Menzel, and R. Schulze. Coping with variability and change: Floods and droughts. *Natural Resourses Forum*, 26:263–274, 2002.

Landesumweltamt. Flächendeckende Modellierung von Wasserhaushaltsgrößen für das Land Brandenburg. Technical Report Band 27, Landesumweltamt Brandenburg, 2000.

L. Landgraf. Tätigkeitsbericht der Projektgruppe "Landschaftswasserhaushalt". SPD Brandenburg, 2001. Dokumentation der SPD Veranstaltung "Landschaftswasserhaushalt".

R. R. Lane, H. S. Mashriqui, G. P. Kemp, J. W. Day, J. N. Day, and A. Hamilton. Potential nitrate removal from a river diversion into a Mississippi delta forested wetland. *Ecological Engineering*, 20(3):237–249, 2003.

C. Leibundgut and F.-J. Kern. Hydrologischer Atlas von Deutschland. *DVWK Hydrobrief*, 4, 1999.

R. A. Leonard, W. G. Knisel, and D. A. Still. GLEAMS: Groundwater loading effects on agricultural management systems. *Trans. ASAE*, 30(5):1403–1428, 1987.

K. J. Limbrick, P. G. Whitehead, D. Butterfield, and N. Reynard. Assessing the potential impacts of various climate change scenarios on the hydrological regime of the River Kennet at Theale, Berkshire, south-central England, UK: an application and evaluation of the new semi-distributed model, INCA. *The Science of The Total Environment*, 251-252:539–555, 2000.

Y.-F. Lin, S.-R. Jing, T.-W. Wang, and D.-Y. Lee. Effects of macrophytes and external carbon sources on nitrate removal from groundwater in constructed wetlands. *Environmental Pollution*, 119(3):413–420, 2002.

D. R. Maidment. *Handbook of Hydrology*. McGraw-Hill Inc., New York, 1993.

V. Maitre, A.-C. Cosandey, E. Desagher, and A. Parriaux. Effectiveness of groundwater nitrate removal in a river riparian area: the importance of hydrogeological conditions. *Journal of Hydrology*, 278(1-4):76–93, 2003.

U. Mander and A. Kull. Climate change research: Evaluation and policy implications. In S. Zverver, R. S. van Rompaey, M. T. J. Kok, and M. M. Berk, editors, *Studies in environmental sciences*, volume 65, pages 95–97. Elsevier, 1997.

U. Mander, V. Kuusemets, K. Lohmus, and T. Mauring. Efficiency and dimensioning of riparian buffer zones in agricultural catchments. *Ecological Engineering*, 8(4):299–324, 1997.

M. Manning. The difficulty of communicating uncertainty - An editorial comment. *climatic change*, 61:9–16, 2003.

J. F. Martin and K. R. Reddy. Interaction and spatial distribution of wetland nitrogen processes. *Ecological Modelling*, 105(1):1–21, 1997.

F. E. Matheson, M. L. Nguyen, A. B. Cooper, T. P. Burt, and D. C. Bull. Fate of 15N-nitrate in unplanted, planted and harvested riparian wetland soil microcosms. *Ecological Engineering*, 19(4):249–264, 2002.

W. Mauser and S. Schädlich. Modelling the spatial distribution of evapotranspiration on different scales using remote sensing data. *Journal of Hydrology*, 212-213:250–267, 1998.

L. Menzel and G. Burger. Climate change scenarios and runoff response in the Mulde catchment (Southern Elbe, Germany). *Journal of Hydrology*, 267(1-2): 53–64, 2002.

A. F. M. Meuleman, R. van Logtestijn, G. B. J. Rijs, and J. T. A. Verhoeven. Water and mass budgets of a vertical-flow constructed wetland used for wastewater treatment. *Ecological Engineering*, 20(1):31–44, 2003.

W. J. Mitsch and U. Mander. Remediation of ecosystems damaged by environmental contamination: Applications of ecological engineering and ecosystem restoration in Central and Eastern Europe. *Ecological Engineering*, 8(4):247–254, 1997.

M. Monsi and T. Saeki. Über den Lichtfaktor in den Pflanzengesellschaften und seine Bedeutung für die Stoffproduktion. *Japan Journal for Botanic*, 14:22–52, 1953.

J. L. Monteith. Climate and the efficiency of crop production in Britain. *Phil. Trans. Res. Soc.*, 281:277–329, 1977.

J. E. Nash and J. V. Sutcliffe. River flow forecasting through conceptual models part I – A discussion of principles. *Journal of Hydrology*, 10(3):282–290, 1970.

NBL. Karte der Hydrologischen Einheiten der DDR, 1985.

D. Niehoff, U. Fritsch, and A. Bronstert. Land-use impacts on storm-runoff generation: scenarios of land-use change and simulation of hydrological response in a meso-scale catchment in SW-Germany. *Journal of Hydrology*, 267(1-2): 80–93, 2002.

B. Nijssen, D. P. Lettenmaier, X. Liang, S. W. Wetzel, and E. F. Wood. Streamflow simulation for continental-scale river basins. *Water Resources Research*, 33(4):711–724, 1997.

OECD. OECD Core Set. Corps central de l'OCDE: Environmental Indicators. Indicateurs d'environnement. Technical report, Organisation for Economic Cooperation and Development, 1994.

C. Pahl-Wostl. The Implications of Complexity for Integrated Resources Management. In C. Pahl-Wostl, S. Schmidt, and T. Jakeman, editors, *Complexity and Integrated Resources Management*. International Environmental Modelling and Software Society, Osnabrück, Germany, 2005. KeyNote Paper.

C. Pahl-Wostl, T. Downing, P. Kabat, P. Magnuszewski, J. Meigh, M. Schlüter, J. Sendzimir, and S. Werners. Transitions to Adaptive Water Management: The NeWater Project. *Water Policy*, 2005. Submitted.

J. Post, A. Habeck, F. F. Hattermann, V. Krysanova, F. Wechsung, and F. Suckow. Evaluation of water and nutrient dynamics in soil-crop systems using the eco-hydrological catchment model SWIM (Soil and Water Integrated Model). 2005. submitted.

C. H. B. Priestley and R. J. Taylor. On the assessment of surface heat flux and evaporation using large scale parameters. *Monthly Weather Review*, 100:81–92, 1972.

V. Quaschning, N. Geuder, and W. Ortmanns. Vergleich und Bewertung verschiedener Verfahren zur Solarstrahlungsbestimmung. *13. Internationales Sonnenforum Berlin*, 2002.

E. P. Querner and H. A. J. van Lanen. Impact assessment of drought mitigation measures in two adjacent Dutch basins using simulation modelling. *Journal of Hydrology*, 252(1-4):51–64, 2001.

E. Röckner, L. Bengtsson, J. Feichter, J. Lelieveld, and H. Rodhe. Transient climate change simulations with a coupled atmosphere-ocean GCM including the tropospheric sulfur cycle. *Journal of Climate*, 12(10):3004–3032, 1999.

J. C. Refsgaard and J. Knudsen. Operational validation and intercomparison of different types of hydrological models. *Water Resources Research*, 32(7): 2189–2202, 1996.

J. C. Refsgaard and B. Storm. MIKE SHE. In V. P. Singh, editor, *Computer Models of Watershed Hydrology*, pages 443–476. Water Resources Publications, Littleton, Colorado, USA, 1995.

J. C. Refsgaard, B. Storm, and M. B. Abbott. *Construction, calibration and validation of hydrological models*. Kluwer, Dordrecht, 1996.

D. Richter. Ergebnisse methodischer Untersuchungen zur Korrektur des systematischen Messfehlers des Hellmann-Niederschlagsmessers. *Berichte des Deutschen Wetterdienstes*, 194, 1995.

O. Richter, B. Diekkrüger, and P. Nörtersheuser. *Environmental Fate Modeling of Pesticides. From the Laboratory to the Field Scale*. Weinheim, New York, Basel, Cambridge, Tokyo, 1996.

W. Riek, G. Wessolek, and A. von Lührte. Wasserhaushalt-Zuwachsverhalten von Kiefern und Eichen im Raum Berlin. Technical report, TU Berlin, Institut für Ökologie, Berlin, 1994. DFG-Endbericht.

J. T. Ritchie. A model for predicting evaporation from a row crop with incomplete cover. *Water Resource Research*, 8:1204–1213, 1972.

J. A. Romero, F. A. Comin, and C. Garcia. Restored wetlands as filters to remove nitrogen. *Chemosphere*, 39(2):323–332, 1999.

D. A. Sangrey, K. Harrop-Williams, and J. A. Klaiber. Predicting Ground-Water Response To Precipitation. *Journal of geotechnical engineering*, pages 957–975, 1984.

T. Scheytt, S. Grams, and M. Asbrand. Grundwasserströmung und -beschaffenheit unter dem Einfluss 100-jähriger Rieselfeldwirtschaft. *Wasser und Boden*, 52:15 – 22, 2000.

D. Schröter, W. Cramer, R. Leemans, I. C. Prentice, M. B. Araújo, N. W. Arnell, A. Bondeau, H. Bugmann, T. R. Carter, C. A. Garcia, A. C. de la Vega-Leinert,

M. Erhard, F. Ewert, M. Glendining, J. I. House, S. Kankaanpää, R. J. T. Klein, S. Lavorel, M. Lindner, M. J. Metzger, J. Meyer, T. D. Mitchell, I. Reginster, M. Rounsevell, S. Sabaté, S. Sitch, B. Smith, J. Smith, P. Smith, M. T. Sykes, K. Thonicke, W. Thuiller, G. Tuck, S. Zaehle, and B. Zierl. Ecosystem Service Supply and Human Vulnerability to Global Change in Europe. *Science*, 2005. Accepted pending revisions.

N. G. Seligman and H. van Keulen. PAPRAN: A simulation model of annual pasture production limited by rainfall and nitrogen. Simulation of Nitrogen Behaviour of Soil-Plant Systems, pages 192–221, Wageningen, 1981.

P. S. Singh. *Computer Models of Watershed Hydrology*. Water Resources Publications, Littleton, Colorado, USA, 1995.

V. P. Singh and D. K. Frevert. *Mathematical Models of Large Watershed Hydrology*. Water Resources Publications, Littleton, Colorado, USA, 2002.

P. G. Sloan, I. D. Morre, G. B. Coltharp, and J. D. Eigel. Modeling surface and subsurface stormflow on steeply-sloping forested watersheds. Technical Report 142, Water Resources Inst. Univ. Kentucky, 1983.

W. T. Sloan. A physics-based function for modelling transient groundwater discharge at the watershed scale. *Water Resources Research*, 36(1):225–241, 2000.

L. K. Smedema and D. W. Rycroft. *Land Drainage - Planning and Design of Agricultural Drainage Systems*, volume 376. Cornell University Press, Ithaca, New York, 1983.

R. Soncini-Sessa. *Integrated modeling and participatory decision making in practice: The Verbano project*. Mc Graw Hill, Milan, 2004. In Italian, English forthcoming with Elsevier.

M. A. Sophocleous, J. K. Kölliker, R. S. Govindaraju, T. Birdie, S. R. Ramireddygari, and S. P. Perkins. Integrated numerical modeling for basin-wide water management: The case of the Rattlesnake Creek basin in south-central Kansas. *Journal of Hydrology*, 214(1-4):179–196, 1999.

D. Stanners and P. Bourdeau. Europe's Environment: the Dobris Assessment. Technical report, European Environment Agency, Office for Official Publications of the European Communities, 1995.

M. D. Stewart, P. D. Bates, M. G. Anderson, D. A. Price, and T. P. Burt. Modelling floods in hydrologically complex lowland river reaches. *Journal of Hydrology*, 223(1-2):85–106, 1999.

U. Stottmeister, A. Wiessner, P. Kuschk, U. Kappelmeyer, M. Kastner, O. Bederski, R. A. Muller, and H. Moormann. Effects of plants and microorganisms in constructed wetlands for wastewater treatment. *Biotechnology Advances*, 22 (1-2):93–117, 2003.

M. Succow. Nutzen und zukünftige Nutzbarkeit von Niedermoorstandorten. In *"Ökologietage Brandenburg"*, volume 11 of *Studien u. Tagungsberichte*, pages 59–67. Landesumweltamt Brandenburg, 1996.

TAC, editor. *Integrated Water Resources Management*. Global Water Partnership Technical Advisory Committee (TAC), Stockholm, Sweden, 2000.

C. C. Tanner. Plants for constructed wetland treatment systems - A comparison of the growth and nutrient uptake of eight emergent species. *Ecological Engineering*, 7(1):59–83, 1996.

C. C. Tanner, J. D'Eugenio, G. B. McBride, J. P. S. Sukias, and K. Thompson. Effect of water level fluctuation on nitrogen removal from constructed wetland mesocosms. *Ecological Engineering*, 12(1-2):67–92, 1999.

S. Tarantola. SimLab 1.1, Reference Manual. 2000.

UBA. Environmental Policy: Water Resources Management in Germany. Technical report, Federal Ministry for the Environment, Nature Conservation and Nuclear Safety, 2001.

UNCSD. Commission on Sustainable Development: Indicators of Sustainable Development Framework and Methodologies. Technical report, United Nations, 1996.

USDA. The SCS curve number method. *National Engineering Handbook, Hydrological Section 4*, 1972.

USDA. AGNPS 2001 Output Processor Model (version 1.0). *National Sedimentation Laboratory, USA*, 2001.

E. van Beek, M. E. Hellmuth, R. E. Schulze, and E. Stakhiv. Coping with Climate Variability and Climate Change in Water Resources. In P. Kabat, R. E. Schulze, M. E. Hellmuth, and J. A. Veraart, editors, *Coping with Impacts of Climate Variability and Climate Change in Water Management: A Scoping Paper*. International Secretariat of the Dialogue on Water and Climate, Wageningen, 2002.

O. Varis, T. Kajander, and R. Lemmelä. Climate change and water: from climate models to water resources management and vice versa. *Climatic change*, 66: 321–344, 2004.

C. Venetis. A Study of the Recession of Unconfined Aquifers. *Bull. Internat. Assoc. of Sci. Hydrology*, 14(4):119–125, 1969.

A. J. Wade, P. G. Whitehead, and L. C. M. O'Shea. The prediction and management of aquatic nitrogen pollution across Europe: an introduction to the Intregrated Nitrogen in European Catchments project (INCA). *Hydrology and Earth System Sciences*, 6(3):299–313, 2002.

O. Wagenbreth and W. Steiner. *Geologische Streifzüge - Landschaft und Erdgeschichte zwischen Kap Arkona und Fichtelgebirge*. Deutscher Verlag für Grundstoffindustie, Leipzig, 2002.

M. Wattenbach, F. F. Hattermann, R. Weng, F. Wechsung, V. Krysanova, and F. Badeck. A simplified approach to implement forest eco-hydrological properties in regional hydrological modelling. *Ecological Modelling*, 187(1):40–59, 2005.

F. Wechsung, A. Becker, and P. Gräfe, editors. *Global Water Elbe (GLOWA-Elbe) Status Report*, volume 95. Potsdam Institute for Climate Impact Research, Potsdam, 2005a.

F. Wechsung, F. F. Hattermann, J. Post, H. Gömann, P. Kreins, and V. Krysanova. Algorithm for the generation of spatial crop cover patterns on

arable land and its application in a modelling framework for accessing hydrological impacts of land use and climate change in the Elbe river basin. 2005b. submitted.

F. Wendland, H. Albert, M. Bach, and R. Schmidt. *Atlas zum Nitratstrom in der Bundesrepublik Deutschland*. Springer-Verlag, Berlin, 1993.

P. C. Werner and F. W. Gerstengarbe. Proposal for the development of climate scenarios. *Climate Research*, 8:171–182, 1997.

W. Werner and H. P. Wodsack. *Stickstoff- und Phosphoreintrag in die Fließgewässer Deutschlands unter besonderer Berücksichtigung des Eintragsgeschehens im Lockersteinbereich der ehemaligen DDR*, volume 22 of *Agrarspectrum*. DLG-Verlag, Frankfurt am Main, 1994.

P. G. Whitehead, E. J. Wilson, D. Butterfield, and K. Seed. A semi-distributed integrated flow and nitrogen model for multi source assessment in catchments (INCA): Part II - application to large river basins in south Wales and eastern England. *The Science of the Total Environment*, 210/211:559–583, 1998.

R. L. Wilby, L. E. Hay, and G. H. Leavesley. A comparison of downscaled and raw GCM output: implications for climate change scenarios in the San Juan River basin, Colorado. *Journal of Hydrology*, 225(1-2):67–91, 1999.

J. R. Williams, K. G. Renard, and P. T. Dyke. EPIC - a new model for assessing erosion's effect on soil productivity. *Journal of Soil and Water Conservation*, 38(5):381–383, 1984.

A. W. Wood, L. R. Leung, V. Sridhar, and D. P. Lettenmaier. Hydrologic implications of dynamical and statistical approaches to downscaling climate model outputs. *Climatic Change*, 62:189–216, 2004.

S. R. Workman, S. E. Serrano, and K. Liberty. Development and application of an analytical model of stream-aquifer interaction. *Journal of Hydrology*, 200 (1-4):149–163, 1997.

L. Yang, H.-T. Chang, and M.-N. L. Huang. Nutrient removal in gravel- and soil-based wetland microcosms with and without vegetation. *Ecological Engineering*, 18(1):91–105, 2001.

T. S. Zissis, I. S. Teloglou, and G. A. Terzidis. Response of a sloping aquifer to constant replenishment and to stream varying water level. *Journal of Hydrology*, 243(3-4):180–191, 2001.

Part I

Appendix

List of Figures

1.1 Average precipitation 1951-2003 and trend in precipitation 1951-2003. . . . 7
1.2 Result of a questionnaire compiled in the framework of the German GLOWA Elbe project (Wechsung et al., 2005a) and the EC NEWATER project (Pahl-Wostl et al., 2005). The answers have been weighted according to the importance indicated by the water experts. . . . 8
1.3 Processes included in the model SWIM on the hydrotope level and the feedbacks. . . . 10
1.4 Aggregation, disaggregation and layers of information in hydrological modeling . . . 13
1.5 Flow generation processes considered in SWIM. . . . 14
1.6 The hydrological processes (blue) of the model SWIM including the parameter demand (yellow). . . . 16
1.7 The vegetation module in SWIM and its parameter demand. . . . 20
1.8 The nitrogen module in SWIM with the parameters demanded in yellow, which are partly taken from tables and partly simulated by SWIM (see Krysanova et al., 2000). . . . 23
1.9 Subbasins and gauge stations (right) in the German part of the Elbe basin. . . . 26
1.10 Land use and soils in the German part of the Elbe basin. . . . 27
1.11 The main natural landscapes in the German part of the Elbe basin and the Elbe river. . . . 28
1.12 Water related problems in the Elbe basin. . . . 31
1.13 Discharge frequency distributions for subsequent 20 year averages starting in 1904 for the Elbe river flow at gauge Neu Darchau. . . . 32

1.14 Comparison of the average annual concentrations of major nutrients (nitrate N and orthophosphate P) in the Elbe. 33

2.1 The river network of the German part of the Elbe basin, the locations of the gauge stations, where comparisons with the observed river discharge were conducted, and the climate stations. 44
2.2 The German part of the Elbe river basin. 45
2.3 River discharge at the gauge station Blankenstein. 51
2.4 River discharge at the gauge station Wechselburg. 52
2.5 River discharge at the gauge station Wolfshagen. 52
2.6 The values for saturated soil conductivity correction (*sccor*) and river routing correction (*rcor*) of the best 20 simulations for the subregions in the Elbe basin. 53
2.7 The simulated water table, simulated groundwater recharge and simulated evapotranspiration of one subbasin in the Stepenitz river catchment. The observed water table data are from a well located in the subbasin (Wendisch Pribor). 55
2.8 The river discharge of the total Elbe basin at Neu Darchau (1981-92). The first part (1981-86) is the calibration period and the second (1987-92) the validation period 56
2.9 The correlation of the model results to the model parameters and input data. 59
2.10 The results of the uncertainty analysis. Upper plot: distributions of the model criterion 'discharge balance'. Lower plot: distributions of the model criterion 'efficiency'. 61

3.1 Diagram of a cross-section of a model watershed. 72
3.2 The state Brandenburg, the basins under study, the river network of the Elbe basin and the locations of the stations with climate, water level and river discharge observations. 76
3.3 Results of the model comparison between the simplified model and the model ASM steady state (a) and unsteady state (b). 79
3.4 The observed and simulated river discharge (Q) for the Nuthe basin, (a) for daily time step and (b) for monthly time step. . . . 81

LIST OF FIGURES

3.5 The observed and simulated river discharge (Q) for the Stepenitz basin, (a) for daily time step and (b) for monthly time step. . . . 81

3.6 The simulated evapotranspiration, groundwater recharge and groundwater table and the observed groundwater table (station Wendisch Priborn, Stepenitz basin). . . . 83

3.7 Observed and simulated groundwater table (five records from the Nuthe basin). . . . 84

3.8 Trends in precipitation (a) and temperature (b) in the Stepenitz river basin. . . . 86

3.9 Sensitivity of the simplified groundwater module in SWIM to a decreasing trend in precipitation. . . . 87

3.10 The observed and simulated groundwater levels (station Wendisch Priborn). . . . 88

4.1 The location of the Nuthe basin and the observation points. . . . 96

4.2 Scheme of the main nutrient fluxes in a catchment. . . . 101

4.3 Comparison of observed and simulated groundwater table for nine observation wells in the Nuthe basin. . . . 109

4.4 Comparison of the observed and simulated daily river flow (Babelsberg gauge) using the new module. . . . 110

4.5 Uncertainty of the simulated water balance in the basin. . . . 111

4.6 Simulated and observed nitrate N concentrations in the Nuthe river (a), nitrate N coming with different pathways (with surface runoff, interflow and baseflow) (b), and the uncertainty of the simulated results (c) (Babelsberg gauge). . . . 113

4.7 Comparison of simulated and observed nitrate N concentration with and without plant water uptake from groundwater. . . . 115

4.8 Nitrate N dynamics in the Nuthe basin. . . . 116

5.1 Flow chart of the modeling procedure. . . . 125

5.2 The hydrological processes of the SWIM model including the parameter demand. . . . 128

5.3 The German part of the Elbe basin. . . . 130

5.4 Comparison of the simulated and observed river discharge of the Elbe basin (Neu-Darchau, catchment area 86,000 km^2) (Hattermann et al., 2005a). 134
5.5 The change in potential crop yields (reference period 1996-99 against scenario period 2051-55) for winter wheat (a) and silage maize (b) and the crop distributions for one year in the reference period (c) and in the scenario period (d) (land use scenario variant B). . . . 138
5.6 The distribution of the ten year average 2051-55 of the 100 variants, their median and 10th, 25th, 75th and 90th percentiles, and the median of the reference period 1961-90 (a: precipitation, b: evapotranspiration, c: groundwater recharge, d: direct runoff) . . 140
5.7 Trend in precipitation and evapotranspiration 1951-2055. 142
5.8 Trend in direct runoff and groundwater recharge 1951-2055. . . . 142
5.9 Daily runoff generation as an integral for the total German Elbe basin. 144
5.10 Ten-year average daily water discharge at gauge station Neu-Darchau for the reference period and under scenario conditions. 145
5.11 The mean annual precipitation 1961-90 (a) and 2051-55 (b), the change in precipitation (c) and the coefficient of variability in % (d). 146
5.12 The mean annual groundwater recharge 1961-90 (a) and 2051-55 (b), the change in recharge (c) and the coefficient of variability in % (d). 147

6.1 Summary of the impacts of a climate change on the water cycle in the German part of the Elbe basin. 160

7.1 Effects of additional plant uptake of water in wetlands in one example hydrotope. 166
7.2 Simulation of river discharge at gauge Neu Darchau with (rip+) and without (rip-) implementation of wetland processes in the model concept, and the difference. 167
7.3 Comparison of four interpolation techniques to calculate the climate boundary conditions. 168
7.4 Use of arable crop land in the German part of the Elbe basin. . . 169

List of Tables

2.1 The area and land cover of the subbasins in the Elbe catchment where nested investigations were performed. 47

2.2 The Nash and Sutcliffe (1970) efficiencies of the cross validation of the interpolated climate input data. 48

2.3 Ranking of the sensitivity of the main calibration parameters to the model results 'discharge balance' and 'efficiency' for the geographic regions in the German Elbe basin. 50

2.4 The Nash and Sutcliffe (1970) efficiencies of observed against simulated river discharge and the discharge balance for an eight year period (1981-88, *1981-86). The catchments are sorted by their area. 54

2.5 The efficiency criteria for the observed and simulated river discharge of the validation period (1987-92). 56

2.6 Statistical results of the uncertainty analysis. 60

3.1 Long term mean annual precipitation (P), mean annual temperature (T) and river discharge (Q) of the two basins under study. . . 76

3.2 Results of the hydrological calibration using observed river discharge. 82

3.3 Results of the water table simulation. 83

4.1 Long-term mean annual precipitation (P), mean annual temperature (T), river discharge (Q), runoff coefficient (rc), and river nitrate N concentration in the 1980s (C8(N)) and 1990s (C9(N)). 97

4.2 Catchment area and land use in the Nuthe basin. 98

5.1 The observed mean annual temperature and precipitation (uncorrected station observations) in the German Elbe basin for the period 1951-2000. 132
5.2 The observed change in temperature and precipitation (uncorrected station observations) in the German Elbe basin from 1951 to 2000. 133
5.3 The long-term differences between simulated and observed river discharge for the validation period of typical subregions in the Elbe basin and the uncertainty of the results expressed by the 10th and 90th percentiles of 300 simulations using different model parameter combinations (Hattermann et al., 2005a). 135
5.4 The scenario trend in temperature and precipitation for the entire German Elbe basin (difference of the average 1961-90 and 2051-55). 136
5.5 The range of possible changes in the hydrological cycle under climate change. Shown are the changes for the driest, median and wettest climate change variant (difference in % of the average 1961-90 (reference) and 2051-55), and the number of scenario variants which have a decrease in the corresponding hydrological component. 141

6.1 Comparison of the vertical flow processes simulated by SWIM and the values taken from the Hydrological Atlas of Germany (Leibundgut and Kern, 1999). Shown are average values for the German part of the Elbe basin. 154

A.1 List of variables, description and units. IX
A.1 List of variables, description and units. X
A.1 List of variables, description and units. XI
A.1 List of variables, description and units. XII

B.1 Parameter distributions XIII
B.1 Parameter distributions XIV
B.1 Parameter distributions XV

C.1 Land use classes used in SWIM. XVII

Part II

Appendix

Appendix A

List of variables.

Table A.1. List of variables, description and units.

variable	description	units
α	reaction factor	d
AN_{fr}	active organic nitrogen pool fraction	(-)
AN_{or}	readily mineralizable organic nitrogen	kg ha^{-1}
AN_{sflow}	organic nitrogen flow	kg ha^{-1}
β	shape parameter	(-)
B_{ag}	above ground biomass	kg ha^{-1}
B_e	plant specific biomass-energy ratio	kg ha^{-1} d^{-1}
B_{n1-3}	plant specific parameter for nitrogen concentration in plant biomass at different growth stages	(-)
C_N	SCS curfe number	(-)
C_N	exponential function of C:N ratio	(-)
$Corr$	particial correlation coefficient	(-)
C_P	exponential function of C:P ratio	(-)
D_{hun}	accumulated heat unit index per day	(-)
D_{max}	plant specific fraction of the growing season before LAI starts declining	0-1
δ	slope of the saturated vapour pressure	kPa C^{-1}
δ	delay time	d
E_P	potential evapotranspiration	mm d^{-1}

Table A.1. List of variables, description and units.

variable	description	units
F_C	tabulated field capacity	mm
GW_{upa}	actual water uptake by plants from groundwater	mm d^{-1}
GW_{upm}	maximum water uptake by plants from groundwater	mm d^{-1}
H	latent heat of vaporization	MJ kg^{-1}
h	groundwater table height	m
I_{hun}	heat unit index	0-1
K	residence time of groundwater	d
$K(\Theta)$	hydraulic conductivity	mm h^{-1}
K_R	storage time constant (river routing)	d^{-1}
K_S	saturated conductivity	mm h^{-1}
$k_x,\ k_y$	hydraulic conductivity in x and y direction	m d^{-1}
λ	denitrification rate	d^{-1}
L	slope length	m
LAI	leaf area index	m^2 m^{-2}
LAI_{max}	plant specific maximum LAI	m^2 m^{-2}
m	thickness of the aquifer	m
MAE	Mean Absolute Error	(-)
ν	psychrometer constant	kPa C^{-1}
ν	experimental semivariogram	(-)
N_{aom}	mineralization rate for the active organic pool	kg ha^{-1} d^{-1}
NC_{as}	rate of nitrogen flow	(-)
N_{dpl}	daily plant nitrogen demand	kg ha^{-1} d^{-1}
N_{dec}	nitrogen decomposition rate	kg ha^{-1} d^{-1}
Ngw_{upa}	actual nitate uptake by plants from groundwater	kg ha^{-1} d^{-1}
Ngw_{upm}	maximum nitrate uptake by plants from groundwater	kg ha^{-1} d^{-1}
N_{hun}	humus rate constant for nitrogen	0.0003 d^{-1}
N_{in}	nitrate input through leaching	kg ha^{-1} d^{-1}

Table A.1. List of variables, description and units.

variable	description	units
N_{out}	nitrate output by lateral transport	kg ha^{-1} d^{-1}
N_S	nitrate in subsurface	kg ha^{-1}
P	precipitation	mm d^{-1}
P_{ar}	photosynthetic active solar radiation	MJ m $^{-2}$
P_b	accumulated biomass	kg ha^{-1}
P_{CN}	optimal nitrogen concentration in plant biomass	kg ha^{-1}
P_{erc}	percolation	mm d^{-1}
P_{hun}	number of potential heat unit for maturing	(-)
Q	surface runoff	mm d^{-1}
q	groundwater return flow	mm d^{-1}
Q_{i_t}	inflow rate in river reach	m^3 s^{-1}
Q_{o_t}	outflow rate from river reach	m^3 s^{-1}
Q_{obs}	river discharge observed	m^3 s^{-1}
Q_{sim}	river discharge simulated	m^3 s^{-1}
Ra	net radiation	MJ m^{-2}
Rc	groundwater recharge	mm d^{-1}
r_{gw}	groundwater uptake resistance	(-)
r_n	nitrate uptake resistence	(-)
S	specific yield	m^3 m^{-3}
SCS	soil conservation service	(-)
SN_{or}	stable organic nitrogen	kg ha^{-1}
S_{p1}	slope parameter for nitrogen concentration in plant biomass	(-)
S_{p2}	slope parameter for nitrogen concentration in plant biomass	(-)
S_R	water volume in river reach	m^3
S_X	retention coefficient	(mm)
T	hydraulic transmissivity	m^2 d^{-1}
T_b	plant specific base temperature	$^\circ C$
T_f	function of soil temperature	(-)
T_{max}	maximum daily temperature	°C

Table A.1. List of variables, description and units.

variable	description	units
T_{min}	minimum daily temperature	°C
T_T	travel time through soil layer	h
U_L	soil water content at saturation	%
v_s	sepage velocity	m s^{-1}
$v_x,\ v_y$	darcy velocity in x and y direction	m s^{-1}
W_f	relation of soil water to field capacity	(-)
W_S	soil water content	%
X	dimentionless weighting factor (river routing)	(-)
$Z(u)$	observation at point u	(-)

Appendix B

Parameter distributions.

Table B.1. Parameter distributions

parameter	impact	distribution	Values *
roc2	river routing - factor	triangular	α =1, β=6, γ=20
roc4	river routing - factor	triangular	α=4, β=12, γ=30
chanman	factor to perturbate Manning coefficient for channel flow	normal	N≈(0, 0.15)
chanslope	factor to perturbate channel slope	normal	N≈(0, 0.15)
soildepth	factor to perturbate the maximum soil depth	normal	N≈(0, 0.15)
fc	factor to perturbate the field capacity	normal	N≈(0, 0.15)
sccor	factor to correct soil conductivity	uniform	min=1, max=4
cnum	factor to calculate the amount of surface runoff	uniform	min=0.1, max=0.3
cnum1	factor to perturbate model parameter 1 for curve number method	normal	N≈(0, 0.15)

Table B.1. Parameter distributions

parameter	impact	distribution	Values *
cnum3	factor to perturbate model parameter 2 for curve number method	normal	N≈(0, 0.15)
abf	linear storage alpha factor for groundwater discharge	uniform	min=0.05, max=0.7
delay	factor to perturbate the delay time (soil -> groundwater)	normal	N≈(0, 0.15)
basinslope	factor to perturbate the channel slope in subbasins	normal	N≈(0, 0.15)
basinman	factor to perturbate the channel conductivity in subbasins	normal	N≈(0, 0.15)
LAI	factor to perturbate the leaf area index	normal	N≈(0, 0.15)
be	factor to perturbate biomass efficiency ratio	normal	N≈(0, 0.15)
root	factor to perturbate the maximum root depth	normal	N≈(0, 0.15)
tempbas	factor to perturbate the base temperature for plant growth	normal	N≈(0, 0.15)
snow	factor to calculate the snowmelt rate	uniform	min=3, max=5
albedo	factor to perturbate the albedo	normal	N≈(0, 0.15)

Table B.1. Parameter distributions

parameter	impact	distribution	Values *
transNsur	factor to pertubate nitrate N half life time of surface runoff	normal	N≈(0, 0.15)
transNssf	factor to pertubate nitrate N half-life time of interflow	normal	N≈(0, 0.15)
transPerc	factor to pertubate nitrate N half-life time of groundwater	normal	N≈(0, 0.15)
retenNsur	factor to pertubate residence time of surface water	normal	N≈(0, 0.15)
retenNssf	factor to pertubate residence time of inferflow	normal	N≈(0, 0.15)
retenNperc	factor to pertubate residence time of groundwater	normal	N≈(0, 0.15)
accN	factor to pertubate the accumulated N flow per hydrotope	normal	N≈(0, 0.15)
mixN	factor to pertubate the mixing of concentrations during the aquifer passage	normal	N≈(0, 0.15)

* a, ß, and *lambda* indicate minimum, average and maximum values of the triangle distribution, N≈(0, 0.15) describes a normal distribution with mean equals 0.0 and a standard deviation of 0.15, min and max are the minimum and maximum values of a uniform distribution. The normal distributions have a truncation below 0.001 and larger than 0.999.

Appendix C

Land use classes.

Table C.1. Land use classes used in SWIM.

land use class	description
1	water
2	settlement
3	industry
4	road
5	cropland
6	set-aside
7	grassland, extensive use (meadow)
8	grassland, intensive use (pasture)
9	forest mixed
10	forest evergreen
11	forest deciduous
12	wetland nonforested
13	wetland forested
14	heather (grass + brushland)
15	bare soil

Erklärung

Hiermit erkläre ich, dass die Arbeit an keiner anderen Hochschule eingereicht sowie selbstständig und nur mit den angegebenen Mitteln angefertigt wurde.

Potsdam, den 04.09.2005 (Fred Fokko Hattermann)